CHAPTER 2

SITE CHARACTERISTICS

TABLE OF CONTENTS

CHAPTER 2

SITE CHARACTERISTICS

TABLE OF CONTENTS

LIST OF TABLES

LIST OF TABLES

LIST OF TABLES

LIST OF TABLES

LIST OF TABLES

LIST OF FIGURES

LIST OF FIGURES

LIST OF FIGURES

LIST OF FIGURES

ACRONYMS AND ABBREVIATIONS

Acronym/Abbreviation	Definition
/yr	per year
°C	degrees Celsius
°F	degrees Fahrenheit
°N	degrees north (latitude)
°W	degrees west (longitude)
10 CFR	Title 10 of the Code of Federal Regulations
χ/Q	relative atmospheric concentration
ac.	acre
ac-ft	acre-feet
ACI	American Concrete Institute
AFCCC	Air Force Combat Climatology Center
ALOHA	Area Locations and Hazardous Atmospheres
ANSI/ANS	American National Standards Institute/American Nuclear Society
ANSS	Advanced National Seismic System
APO	Federal Aviation Administration Office of Aviation Policy and Plans

ACRONYMS AND ABBREVIATIONS

Acronym/Abbreviation	Definition
AQTESOLV	Advanced Aquifer Test Analysis Software
ASCE	American Society of Civil Engineers
ASHRAE	American Society of Heating, Refrigerating and Air-Conditioning Engineers, Inc.
ASOS	automated surface observing station
ATADS	Air Traffic Activity System
AWOS	automated weather observing station
bgs	below ground surface
BLEVE	boiling liquid expansion vapor explosion
Btu/hr-ft^2	British thermal units per hour per square foot
CAAS	criticality accident alarm system
CEUS-SSC	Central Eastern United States-Seismic Source Characterization
CFR	Code of Federal Regulations
cfs	cubic feet per second
CGIAR-CSI	Consultative Group on International Agricultural Research-Consortium for Spatial Information
Clim-20	Climatography of the United States No. 20

ACRONYMS AND ABBREVIATIONS

Acronym/Abbreviation	Definition
cm	centimeter
cm/yr	centimeters per year
CONUS	continental United States
COOP	(National Oceanic and Atmospheric Administration) cooperative observing station
csm/in.	cubic feet per second per square mile per inch
DBT	dry bulb temperature
deg	degrees
DNR	Department of Natural Resources
DOA	Wisconsin Department of Administration
DOE	U.S. Department of Energy
DOT	Wisconsin Department of Transportation
DPC	Dairyland Power Cooperative
E	east
E[M]	expected moment magnitude
EDS	Environmental Data Service
ENE	east-northeast

ACRONYMS AND ABBREVIATIONS

Acronym/Abbreviation	Definition
EPRI	Electric Power Research Institute
ERPG	Emergency Response Planning Guideline
ESE	east-southeast
ESRI	company name - not an acronym
EW	east-west (direction)
F_a	site coefficient for 0.2 second period
FAA	Federal Aviation Administration
FDT	Fire Dynamics Tools
FEMA	Federal Emergency Management Agency
FSIMS	Flight Standards Information Management System
FSTR	facility structure
ft.	foot
ft./day	feet per day
ft./sec	feet per second
ft^3	cubic feet
F_v	site coefficient for 1-second period

ACRONYMS AND ABBREVIATIONS

Acronym/Abbreviation	Definition
g	gravitational acceleration
Ga	billion years
GIA	glacial isostatic adjustment
GIS	geographic information system
GMPE	ground motion prediction equations
GPS	Global Positioning System
ha	hectares
Hwy	highway
I-90/39	Interstate 90/39
IAEA	International Atomic Energy Agency
IBC	International Building Code
IDLH	immediately dangerous to life and health
in.	inch
in. Hg	inches of mercury
in./yr	inches per year

ACRONYMS AND ABBREVIATIONS

Acronym/Abbreviation	Definition
ISMCS	international station meteorological climate summary
IU	irradiation unit
JFD	joint frequency distribution
k	hydraulic conductivity
kg	kilogram
kg/m^2	kilograms per square meter
KJVL	meteorological station identifier for Janesville, Wisconsin
km	kilometer
KMLI	meteorological station identifier for Moline, Illinois
KMSN	meteorological station identifier for Madison, Wisconsin
kPa	kilopascal
kPag	kilopascal gauge
KRFD	meteorological station identifier for Rockford, Illinois

ACRONYMS AND ABBREVIATIONS

Acronym/Abbreviation	Definition
KSPI	meteorological station identifier for Springfield, Illinois
kW/m^2	kilowatts per square meter
lb.	pound
lb/ft^2	pounds per square foot
LCD	local climatological data
LEL	lower explosive limit
LL	liquid limit
M	moment magnitude
m	meter
m/day	meters per day
m/s	meters per second
m^3	cubic meters
m^3/sec	cubic meters per second
Ma	million years
mb	body-wave magnitude
MCE	maximum considered earthquake

ACRONYMS AND ABBREVIATIONS

Acronym/Abbreviation	Definition
MCR	Mid-Continent Rift
MCWB	mean coincident wet bulb temperature
M_{fa}	body-wave magnitude calculated from earthquake felt area
mi.	mile
$mi.^2$	square miles
min	minute
MLRA	Major Land Resource Area
mm/yr	millimeters per year
MMI	Modified Mercalli Intensity
mph	miles per hour
MSL	above mean sea level
N	north
N-values	standard penetrometer test blow counts
NAAQS	National Ambient Air Quality Standard
NAMAG	North American Magnetic Anomaly Group
NAVD 88	North American Vertical Datum of 1988

ACRONYMS AND ABBREVIATIONS

Acronym/Abbreviation	Definition
NCDC	National Climatic Data Center
NCEER	National Center for Earthquake Engineering Research
NE	northeast
NEIC	National Earthquake Information Center
NEID	National Earthquake Intensity Database
NGDC	National Geophysical Data Center
NIOSH	National Institute for Occupational Safety and Health
NLSI	National Lightning Safety Institute
NNE	north-northeast
NNW	north-northwest
NOAA	National Oceanic and Atmospheric Administration
NPS	National Park Service
NRC	U.S. Nuclear Regulatory Commission
NS	north-south (direction)
NW	northwest

ACRONYMS AND ABBREVIATIONS

Acronym/Abbreviation	Definition
OBE	operating basis earthquake
PAC	Protective Action Criteria
PDE	Preliminary Determination of Epicenters Catalog
PGA	peak ground acceleration
PL	plastic limit
PMF	probable maximum flood
PMH	probable maximum hurricane
PMP	probable maximum precipitation
PMT	probable maximum tsunami
PMWS	probable maximum wind storm
ppb	parts per billion
PSHA	probabilistic seismic hazard analysis
psid	pounds per square inch differential pressure
psig	pounds per square inch gauge
RCA	radiologically controlled area
RCGIS	Rock County Geographic Information System

ACRONYMS AND ABBREVIATIONS

Acronym/Abbreviation	Definition
RDS	radioactive drain system
RMSE	root mean square error
S	south
S_1	maximum considered earthquake 1-second spectral response acceleration
Sa	spectral acceleration
SCL	Saint Charles Lineament
SCS	Soil Conservation Service
S_{D1}	design spectral response acceleration coefficient at 1-second period
S_{DS}	design spectral response acceleration coefficient at short periods
SE	southeast
sec.	second
SH 11	State Highway 11
SH 26	State Highway 26
S_{M1}	maximum considered earthquake spectral response for 1-second period modified for soil Site Class

ACRONYMS AND ABBREVIATIONS

Acronym/Abbreviation	Definition
S_{MS}	maximum considered earthquake spectral response for 0.2 seconds modified for soil Site Class
SPT	standard penetrometer test
sq. km	square kilometer
sq. mi	square mile
SRP	Standard Review Plan
S_s	maximum considered earthquake 0.2 second spectral acceleration
SSE	south-southeast
SSW	south-southwest
SW	southwest
SWRA	Southern Wisconsin Regional Airport
TAF	Terminal Area Forecast
T_L	long-period transition period
TNT	trinitrotoluene
TPS	tritium purification system
TSV	target solution vessel

ACRONYMS AND ABBREVIATIONS

Acronym/Abbreviation	Definition
UBC	Uniform Building Code
UEL	upper explosive limit
US 14	U.S. Highway 14
US 51	U.S. Highway 51
USACE	U.S. Army Corps of Engineers
USAF	U.S. Air Force
USCB	U.S. Census Bureau
USDA	U.S. Department of Agriculture
USDA SCS	U.S. Department of Agriculture Soil Conservation Service
USDOC	U.S. Department of Commerce
USEPA	U.S. Environmental Protection Agency
USGS	U.S. Geological Survey
USHIS	U.S. Earthquakes
USMC	U.S. Marine Corps
USN	U.S. Navy
UTC	Universal Time, Coordinated

ACRONYMS AND ABBREVIATIONS

Acronym/Abbreviation	Definition
W	west
WBAN	Weather Bureau Army Navy
WBT	wet bulb temperature
WDNR	Wisconsin Department of Natural Resources
WGNHS	Wisconsin Geological and Natural History Survey
WNW	west-northwest
WSW	west-southwest
yd.	yard
yr	year

CHAPTER 2 – SITE CHARACTERISTICS

2.1 GEOGRAPHY AND DEMOGRAPHY

2.1.1 SITE LOCATION AND DESCRIPTION

This subsection describes the location and important features of the SHINE site.

2.1.1.1 Specification and Location

The SHINE site is located on previously undeveloped property in the City of Janesville, Rock County, Wisconsin. Figure 2.1-1 shows the location of the site in the state, county, and city.

The site boundary encompasses approximately 91 acres (36.8 hectares) of land. All safety-related structures are located within a square area located near the center of the property to maximize the distance to the site boundary. The center point of this safety-related area has the following coordinates:

Latitude and Longitude (degrees, minutes, seconds)

Latitude: 42º 37’ 26.8”
Longitude: 89º 01’ 29.7”

Universal Transverse Mercator Coordinates, Zone 16T (meters [m])

Northing: 4721061N
Easting: 333946E

Wisconsin State Plane Coordinates – Zone 4803 South

Northing: 69801.619N
Easting: 679992.268E

The SHINE site is located on the south side of the City of Janesville corporate boundaries, and the densely populated parts of the city are more than 1 mile (mi.) (1.6 kilometers [km]) to the north. Figure 2.1-2 shows prominent natural and man-made features in the vicinity of the project site. The distance and direction from the center point of the safety-related area to major nearby features are as follows:

- U.S. Highway 51 (US 51): <0.1 mi. (<0.2 km) west
- Southern Wisconsin Regional Airport: 0.4 mi. (0.6 km) west
- Union Pacific Railroad: 1.7 mi. (2.7 km) northeast
- Rock River: 1.9 mi. (3.1 km) west
- Interstate 39/90 (I-39/I-90): 2.1 mi. (3.4 km) east

2.1.1.2 Boundary and Zone Area Maps

Highways, railways, and waterways that traverse or are in close proximity to the SHINE site are shown in Figure 2.1-2. This figure and all figures referenced in this section have an arrow indicating true north.

Figure 2.1-3 shows the boundaries and zones applicable to the project site. The square area near the center of the site shows the location and size of the operations boundary in accordance with American National Standards Institute/American Nuclear Society (ANSI/ANS) 15.16-2015 (ANSI/ANS, 2015). All safety-related structures, systems, and components of the SHINE facility are located in this central area. The Emergency Planning Zone is encompassed by the operations boundary in accordance with the Emergency Plan.

The site boundary corresponds to the property line around the perimeter of the SHINE site in accordance with ANSI/ANS-15.16-2015. The owner controlled area is the area within the site boundary in accordance with 10 CFR 20.1003. The area directly under the facility operating license is delineated by the site boundary.

Figure 2.1-2 shows the topography within the vicinity of the SHINE site. The finished site grade elevation is approximately 825 feet (ft.) (251.46 m) North American Vertical Datum of 1988 (NAVD 88). The project site and adjacent ground within a radius of approximately 1 mi. (1.6 km) is roughly flat. Within a 5 mi. (8 km) radius from the SHINE site, topographic elevations range from approximately 750 ft. (228.6 m) NAVD 88 along the Rock River, to approximately 950 ft. (290 m) NAVD 88 to the east of the site (USGS, 1980). Therefore, the topography within a 5 mi. (8 km) radius ranges from approximately 75 ft. (22.9 m) below to approximately 125 ft. (38.1 m) above the SHINE site grade elevation.

The tallest building on the SHINE site is the main production facility, which at its highest point is approximately 57 ft. (17.4 m) above the site grade level. The main production facility has an adjacent free-standing exhaust stack that is at 67 ft. (20.4 m) above the site grade level. Eight buildings higher than 67 ft. (20.4 m) above ground level have been identified within 5 mi. (8 km) of the project site. These are listed in Table 2.1-1. These buildings are greater than 3.8 mi. (6.1 km) north or northeast of the SHINE site. Given their distance from the site, none of these buildings are expected to affect diffusion or dispersion of airborne effluents.

The distance from a release point to the site boundary in each of the 16 compass directions is provided in Table 2.1-2. Distances are calculated from a circle (radius of 70 m) that envelopes the radiologically controlled area (RCA) of the main production facility, since a release point could be anywhere in the RCA.

2.1.2 POPULATION DISTRIBUTION

This subsection describes the population distribution within 8 km (5.0 mi.) of the center point of the safety-related area at the SHINE site. The information includes estimates of the resident and transient populations for the most recent census year (2010) and projections of the resident and transient populations for the years 2019, 2024, and 2051.

Estimates and projections of resident and transient populations around the project site are divided into five distance bands, represented as concentric circles at 0 to 1 km (0 to 0.6 mi.), 1 to 2 km (0.6 to 1.2 mi.), 2 to 4 km (1.2 to 2.5 mi.), 4 to 6 km (2.5 to 3.7 mi.), and 6 to 8 km (3.7 to 5.0 mi.) from the center point of the safety-related area. For each distance band the resident population was estimated using U.S. Census Bureau (USCB) 2017 census data. The transient population was estimated using the best available data for major employers, schools, recreation areas, medical facilities, and lodging facilities. Transient population was obtained in 2012 and has been updated where new or different information was available, and is assumed to represent 2019 population levels.

The future resident and transient population growth in each distance/direction segment was projected using specific growth rates that depend on whether the segment is located in the City of Janesville, in the City of Beloit, or in other parts of Rock County. The specific growth rates used in these areas are explained in the following paragraphs.

The Wisconsin Department of Administration (DOA) provides state and county population projections that were developed by the DOA in December 2013 (DOA, 2013). The DOA calculated future population growth rates using the cohort-component method, which involves the review of recent historical patterns to determine age- and sex-specific rates of fertility, mortality, and migration. The estimated 2010 resident in each distance segment that is located entirely outside of the city boundaries was increased by 0.534 percent each year from 2011 through 2020, by 0.587 percent each year from 2021 through 2030, and by 0.193 percent each year from 2031 through 2051.

The City of Janesville Comprehensive Plan, adopted March 9, 2009 (City of Janesville, 2009), presents projections of the city's future population calculated using several possible population growth rates. The Comprehensive Plan states that the growth rate identified as "15-Year Rate Projection (Compounded)" is considered the most reasonable basis for estimating the city's future population. According to the Comprehensive Plan, this growth rate was calculated by determining the average annual rate of growth of the city population over the 15 year period from 1990 to 2005, resulting in an average growth rate of 1.15 percent per year. This growth rate was used to project future populations for the areas around the SHINE site that are within the City of Janesville corporate boundaries. The estimated 2010 resident population in each distance/direction segment that is located partially or entirely within the city boundaries was increased by 1.15 percent each year from 2011 through 2051.

The City of Beloit Comprehensive Plan, adopted March 17, 2008 and updated November 5, 2018 (City of Beloit, 2018), presents projections of the city's future population from 2017 to 2035. The 2018 Comprehensive Plan update provides population projections based on the DOA population projections for 2017, 2020, 2025, and 2030. The DOA population projections for the City of Beloit for 2010 to 2040 were used to estimate growth rates from 2035 to 2051. The estimated 2017 population of Beloit increased 1.54 percent each year from 2017 through 2020, by 0.399 percent each year from 2021 through 2025, by 0.33 percent each year from 2026 through 2030, by 0.096 percent each year from 2031 through 2035 and by -0.136 percent each year from 2036 through 2051.

The following subsections describe the resident and transient population distribution surrounding the SHINE site.

2.1.2.1 Resident Population

The permanent residence nearest to the SHINE site was identified through field reconnaissance and examination of aerial photographs. The nearest permanent residence is a house located approximately 0.50 mi. (0.80 km) northwest of the center point of the safety-related area. There are permanent residences in two other directions that are only slightly farther from the center point: a house located approximately 0.54 mi. (0.86 km) north-northwest of the center point and a house located approximately 0.59 mi. (0.94 km) south-southwest of the center point. The approximate distances between the center point of the SHINE safety-related area and the nearest residences in the 16 compass directions are provided in Table 2.1-3.

The 2019 resident population within the 1 km (0.6 mi.) and 2 km (1.2 mi.) concentric circles was estimated based on the number of occupied houses (as identified through field reconnaissance in 2012 and examination of aerial photographs from 2017) and the average number of people per household (as reported by the USCB in 2017). USCB data indicate that Rock County has an average of 2.45 people per household (USCB, 2017). Therefore, the 2019 resident population was estimated by multiplying the number of occupied houses by 2.45 people per house and rounding to the nearest whole number. The estimate was then extrapolated to the years 2019, 2024, and 2051 using the population projection methodologies described above. The total 2019 resident population estimated in this manner is 101 people at a distance of 0 to 1 km (0 to 0.6 mi.) from the SHINE center point, and 210 people at a distance of 1 to 2 km (0.6 to 1.2 mi.) for 2019. These population estimates are shown in Table 2.1-4 along with the estimates for other distances and years.

USCB 2010 census block and tract data (USCB, 2012) was used to estimate the resident population within the 4 km (2.5 mi.), 6 km (3.7 mi.), and 8 km (5.0 mi.) distance bands. For each segment formed by the distance bands, the percentage of each census tract's land area that falls, either partially or entirely, within that segment was calculated using the geographic information system (GIS) software known as ArcMap9.3.1 (ESRI, 2019). The equivalent proportion of each census tract's population was then assigned to that segment. If portions of two or more census tracts fall within the same segment, the proportional population estimates for the census tracts were summed to obtain the population estimate for that segment.

Using the population projection methodologies described above, the 2010 resident population estimates within the distance bands were extrapolated to the years 2019, 2024, and 2051. Table 2.1-4 shows the total projected resident population for these years within the distance bands, and Figures 2.1-4 through 2.1-6 show the population projections for these years divided into the distance bands.

2.1.2.2 Transient Population

In addition to the permanent residents around the project site, there are people who enter this area temporarily for activities such as employment, education, recreation, medical care, and lodging. These transient populations are estimated based on data obtained from publicly available sources of employment and population data, such as from local officials and government agency websites for major employers, schools, recreation areas, medical facilities, and lodging facilities within 8 km (5.0 mi.) of the center point of the safety-related area.

Table 2.1-5 lists the major employers identified within 8 km (5.0 mi.) of the SHINE center point, the direction and distance band within which each employer is located, and the best available estimate of the total number of people employed at that location. People using the Southern Wisconsin Regional Airport in Janesville were included in the Table 2.1-5. The transient population at the airport are employees of the Southern Wisconsin Regional Airport, employees of various companies at the Southern Wisconsin Regional Airport, passengers, or crew. Based on information provided by the airport, an average of 560 passengers and crew fly into or out of the airport each day, and 100 employees of various companies are on-site. None of these companies are considered major employers in the area.

Most airport buildings, including the terminal, restaurant, and pilots lounge, are located at the southwestern corner of the airport, which is between 1 and 2 km (0.6 and 1.2 mi.) from the SHINE center point in the southwest directional sector. Therefore, passengers, crew, and most

employees were assumed to be in this location. However, there a few buildings with a small number of employees near the eastern edge of the airport, which is within 1 km (0.6 mi.) of the SHINE center point in the west-southwest sector. This location was assumed for 15 percent of the employees.

Table 2.1-6 lists the schools identified within 8 km (5.0 mi.) of the SHINE center point, the direction and distance band within which each school is located, and the best available estimate of the total number of students at that location. Table 2.1-7 lists the recreation areas identified within 8 km (5.0 mi.) of the SHINE center point, the direction and distance band within which each area is located, and the best available estimate of the average number of daily visitors at that location. Table 2.1-8 lists the medical facilities (hospitals and nursing homes) identified within 8 km (5.0 mi.) of the SHINE center point, the direction and distance band within which each facility is located, and the best available estimate of the total in-patient capacity (number of beds) at that location. Table 2.1-9 lists the lodging facilities (hotels and motels) identified within 8 km (5.0 mi.) of the SHINE center point, the direction and distance band within which each facility is located, and the best available estimate of the lodging capacity (number of rooms) at that location. The transient population estimates shown in Tables 2.1-5 through 2.1-9 were obtained in 2011 and updated in 2019 where new information was available.

In order to obtain a more accurate representation of the transient population around the project site, Tables 2.1-5 through 2.1-9 also include values that are weighted according to the length of time people could be expected to stay at each facility, assuming typical use patterns for the particular type of facility. Therefore, the estimates for employers and schools (Tables 2.1-5 and 2.1-6) were multiplied by a weighting factor of 0.27, which assumes that each employee or student is present at the facility 9 hours per day and 5 days per week. The estimates for recreation areas (Table 2.1-7) were multiplied by a weighting factor of 0.33, which assumes that each daily visitor is present at the recreation area 8 hours per day. The estimates for medical facilities (Table 2.1-8) were not multiplied by any weighting factor, effectively assuming that each bed at each facility is occupied 24 hours per day and 7 days per week. The estimates for lodging facilities (Table 2.1-9) were not multiplied by any weighting factor, effectively assuming that each room at each facility is occupied 24 hours per day and 7 days per week.

The weighted 2019 transient population estimates calculated for each type of facility in each distance band are summarized in Table 2.1-10.

Table 2.1-1 – Approximate Distance between the SHINE Site and the Nearest Buildings Taller than 67 ft. within 5 mi. (8 km) of the SHINE Site

Facility	Direction	Height (ft.)	Distance from Site Center to Facility (mi.)
SSM St. Mary's Health	NE	79	3.8
One Parker Place	N	98	4.0
Prospect 101	N	84	4.0
Janesville City Hall	N	96	4.0
Rock County Courthouse	N	85	4.1
Janesville Garden Apartments	N	77	4.2
Mercy Hospital	N	93	4.4
W.W. Grainger Corporate Office	NE	90	4.5

Table 2.1-2 – Shortest Distance between Release Point and the Site Boundary in each of the 16 Compass Directions

Direction	Distance from Release Point to Site Boundary (ft)
N	761.79
NNE	776.51
NE	943.49
ENE	772.85
E	755.96
ESE	777.88
SE	788.03
SSE	782.17
S	790.32
SSW	794.91
SW	793.89
WSW	1013.04
W	1031.77
WNW	845.74
NW	815.62
NNW	786.62

Table 2.1-3 – Approximate Distance between the SHINE Site Center and the Nearest Residence in each of the 16 Compass Directions

Direction	Distance from Site Center to Nearest Residence (mi)
N	0.66
NNE	0.76
NE	0.90
ENE	0.78
E	0.71
ESE	0.73
SE	0.95
SSE	>1.24*
S	>1.24*
SSW	0.59
SW	>1.24*
WSW	>1.24*
W	0.86
WNW	0.77
NW	0.50
NNW	0.54

*No occupied residence within 2 km (1.24 mi) of the site center.

Table 2.1-4 – Resident Population Distribution within 8 Km (5 Mi.) of the SHINE Site

	Distance Band (km)					
Year	**0-1**	**1-2**	**2-4**	**4-6**	**6-8**	**Total 0-8**
2019	101	210	10,454	12,613	29,289	52,667
2024	107	221	11,045	13,287	30,861	55,521
2051	146	296	14,795	17,418	40,139	72,795

Table 2.1-5 – Transient Population Data for Major Employers within 8 Km (5 Mi.) of the SHINE Site

Name of Facility	Directional Sector	Distance Band (km)	Employment
Dollar General Distribution Center	NE	0 to 1	400
Southern Wisconsin Regional Airport	SW	0 to 1	15
Southern Wisconsin Regional Airport	SW	1 to 2	645
Seneca Foods Corporation	N	2 to 4	700
Blackhawk Technical College Janesville Central Campus	SSE	2 to 4	517
Simmons	N	2 to 4	359
Janesville School District	N	4 to 6	1,515
J. P. Cullen & Sons	NNE	6 to 8	350
Blain Supply Co.	NE	6 to 8	490
City of Janesville	N	6 to 8	436
Rock County	N	6 to 8	1,189
Dean Health System	N	6 to 8	447
SSI Technologies Inc.	NNE	6 to 8	560
Mercy Health System Mercy Hospital and Trauma Center	N	6 to 8	2,635
Amtec Corporation	NE	6 to 8	300
W.W. Grainger	NE	6 to 8	910
Total	-	-	11,468
Weighted Total	-	-	3,096

References:

Rock County Wisconsin Economic Development Alliance, 2019.

Table 2.1-6 – Transient Population Data for Schools within 8 Km (5 Mi.) of the SHINE Site (Sheet 1 of 2)

Name of Facility	Directional Sector	Distance Band (km)	Enrollment
Blackhawk Technical College Janesville Aviation Center	SW	1 to 2	34
Rock County Christian School	SSW	2 to 4	107
Jackson Elementary School	N	2 to 4	319
Lincoln Elementary School	NNW	2 to 4	368
Edison Middle School	NNW	2 to 4	583
Oakhill Christian School	NNW	2 to 4	75
Blackhawk Technical College Janesville Central Campus	SSE	2 to 4	3,408
University of Wisconsin Rock County Center	NW	2 to 4	1,303
Headstart Janesville	N	4 to 6	127
Janesville's Montessori	NNW	4 to 6	100
Van Buren Elementary School	NNW	4 to 6	386
Wisconsin Center for the Blind and Visually Impaired	NNW	4 to 6	75
Wilson Elementary School	N	4 to 6	263
St. John Vianney Catholic School	NNE	4 to 6	368
Rock River Charter School	N	6 to 8	211
St. Mary School	N	6 to 8	227
J.A. Craig High School	NNE	6 to 8	1,688
St. Paul's Lutheran Church and School	N	6 to 8	361
Roosevelt Elementary School	N	6 to 8	368
Adams Elementary School	N	6 to 8	312
St. William Catholic School	NNW	6 to 8	219
Madison Elementary School	NNW	6 to 8	447
Franklin Middle School	NNW	6 to 8	638
Washington Elementary School	NNW	6 to 8	335
Parker High School	NNW	6 to 8	1,311
Powers Elementary	S	6 to 8	385

Table 2.1-6 – Transient Population Data for Schools within 8 Km (5 Mi.) of the SHINE Site (Sheet 2 of 2)

Name of Facility	Directional Sector	Distance Band (km)	Enrollment
Turner Middle School	S	6 to 8	365
Turner High School	S	6 to 8	451
Total	-	-	14,834
Weighted Total			4,005

References:

Greatschools, 2019
Schooltree, 2019
WDPI, 2018

Table 2.1-7 – Transient Population Data for Recreation Areas within 8 Km (5 Mi.) of the SHINE Site
(Sheet 1 of 3)

Name of Facility	Directional Sector	Distance Band (km)	Daily Visitors
Airport Park	NW	0 to 1	6
Glen Erin Golf Club	SW	1 to 2	60
Prairie Knoll Park and Dog Exercise Area	NNW	1 to 2	40
Burbank Park	N	2 to 4	10
Southgate Park	NNW	2 to 4	5
Happy Hollow Park	SSW	2 to 4	5
Happy Hollow Boat Launch	SSW	2 to 4	1
Valley Park	NW	2 to 4	5
Pershing Park	NW	4 to 6	5
Marquette Park	N	4 to 6	5
Loch Lommond Park	W	4 to 6	5
Rushmore Park	NNW	4 to 6	1
Lustig Park and Disc Golf Course	NNW	4 to 6	40
LaPrairie Park, Pistol Range, and Trap Range	NNE	4 to 6	20
Jeffris Park and Dawson Softball Fields	N	4 to 6	25
Monterey Park and Monterey Stadium	N	4 to 6	75
Afton Road Boat Launch	NNW	4 to 6	2
Lions Park, Beach, and Rotary Gardens	NNE	4 to 6	75
Lions Park Boat Launch	NNE	4 to 6	5
Kiwanis Pond Boat Launch	NNE	4 to 6	5

Table 2.1-7 – Transient Population Data for Recreation Areas within 8 Km (5 Mi.) of the SHINE Site
(Sheet 2 of 3)

Name of Facility	Directional Sector	Distance Band (km)	Daily Visitors
Fourth Ward Park	N	4 to 6	15
Peace Park	NNW	4 to 6	40
Rockport Park	NNW	4 to 6	50
Rock River Park	SSW	4 to 6	20
Vista Park	N	4 to 6	5
Blackhawk Golf Course	NNE	4 to 6	55
Courthouse Park	N	4 to 6	25
Jefferson Park	N	6 to 8	10
Bond Park	NNW	6 to 8	20
Palmer Park	NNE	6 to 8	200
Parker Park	N	6 to 8	1
Washington Park	N	6 to 8	5
Waveland Park	NNW	6 to 8	5
Ruger Park	NNE	6 to 8	5
Adams Park	N	6 to 8	5
Traxler Park	N	6 to 8	125
Traxler Park Central Boat Launch	N	6 to 8	10
Traxler Park North Boat Launch	N	6 to 8	10
Hampshire Park	NNE	6 to 8	5
Huron Park	NNE	6 to 8	5
Big Hill Memorial Park	SSW	6 to 8	50
Rock County Fairgrounds	N	6 to 8	300

Table 2.1-7 – Transient Population Data for Recreation Areas within 8 Km (5 Mi.) of the SHINE Site
(Sheet 3 of 3)

Name of Facility	Directional Sector	Distance Band (km)	Daily Visitors
Prairie Park	N	6 to 8	5
Total	-	-	1366
Weighted Total	-	-	451

References:
City of Beloit, 2006.
City of Janesville, 2008.

Table 2.1-8 – Transient Population Data for Medical Facilities within 8 Km (5 Mi.) of the SHINE Site
(Sheet 1 of 2)

Name of Facility	Directional Sector	Distance Band (km)	Capacity
Dupont	N	2 to 4	7
Kellogg	N	2 to 4	8
Kandu Industries (services for people with disabilities)	N	2 to 4	40
Rock Valley Community Programs (Caravilla Education and Rehab Center)	SSE	2 to 4	115
Lee Lane	NNW	2 to 4	6
Fillmore	N	2 to 4	3
REM Grant	NNW	2 to 4	3
Riverfront Inc. Afton House	WNW	2 to 4	4
Cedar Crest Waterford Place Apartments	NW	4 to 6	107
Cedar Crest Assisted Living	NW	4 to 6	68
Riverfront Inc. Center House	N	4 to 6	4
Red Road House	N	4 to 6	4
REM Jonathon	NNW	6 to 8	6
Mercy Health System Mercy Hospital and Trauma Center	N	6 to 8	244
REM Bond	NNW	6 to 8	4
Cozy Lil Acre Inc	NNW	6 to 8	12
REM Cantebury	NNE	6 to 8	6
Riverside Terrace	S	6 to 8	45
SSM Health St. Mary’s Hospital-Janesville	NE	6 to 8	50
Oak Park Place	NNE	6 to 8	86
Beechwood	NNW	6 to 8	7
Oakhill Adult Family Home	NNW	6 to 8	4

Table 2.1-8 – Transient Population Data for Medical Facilities within 8 Km (5 Mi.) of the SHINE Site
(Sheet 2 of 2)

Name of Facility	Directional Sector	Distance Band (km)	Capacity
Total	-	-	833
Weighted Total	-	-	833

References:
Mercy Health System, 2011.
Wisconsin Department of Health Services, 2019.

Table 2.1-9 – Transient Population Data for Lodging Facilities within 8 Km (5 Mi.) of the SHINE Site

Name of Facility	Directional Sector	Distance Band (km)	Capacity
Northern Town Motel	N	4 to 6	13
Cobblestone Hotel & Suites	N	4 to 6	53
Lannon Stone Motel	NNE	6 to 8	29
Baymont Inn	NNE	6 to 8	105
Total	-	-	200
Weighted Total	-	-	200

References:

Janesville Area Convention & Visitors Bureau, 2011.
Janesville Area Convention & Visitors Bureau, 2019.

Table 2.1-10 – Weighted Transient Population Distribution within 8 Km (5 Mi.) of the SHINE Site

2019 Population Estimate by Source

Distance Band (km)	Major Employers	Schools	Recreation Areas	Medical Facilities	Lodging	Totals
0-1	112	0	2	0	0	114
1-2	174	9	33	0	0	216
2-4	426	1,664	9	186	0	2,285
4-6	409	356	156	183	66	1,170
6-8	1,976	1,976	251	464	134	4,801
0-8	3,097	4,005	451	833	200	8,586

Figure 2.1-1 – SHINE Site Location

Figure 2.1-2 – Topography and Prominent Features in Site Area

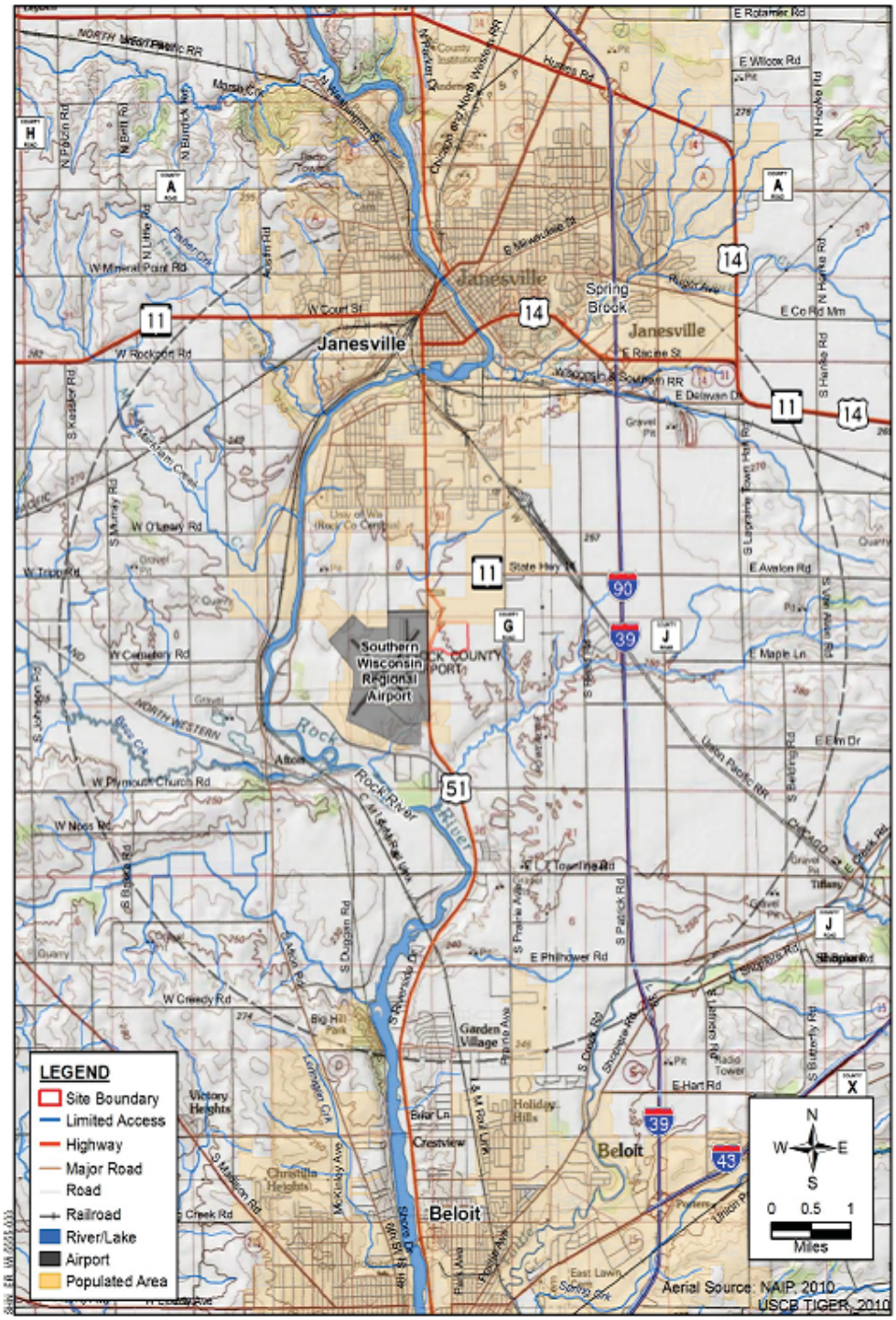

Figure 2.1-3 – Boundary and Zones Associated with the Facility

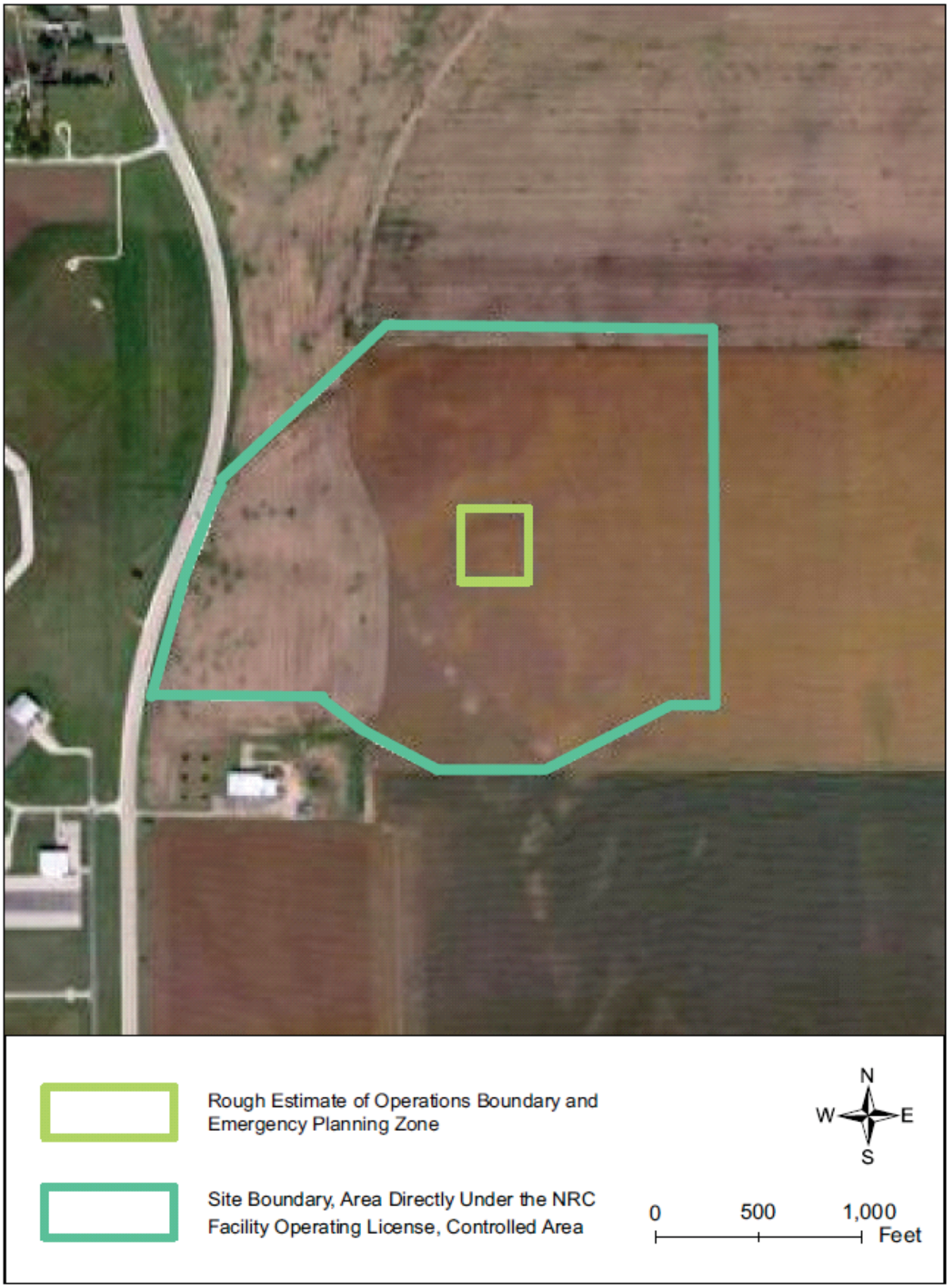

Figure 2.1-4 – Resident Population Distribution – 2019

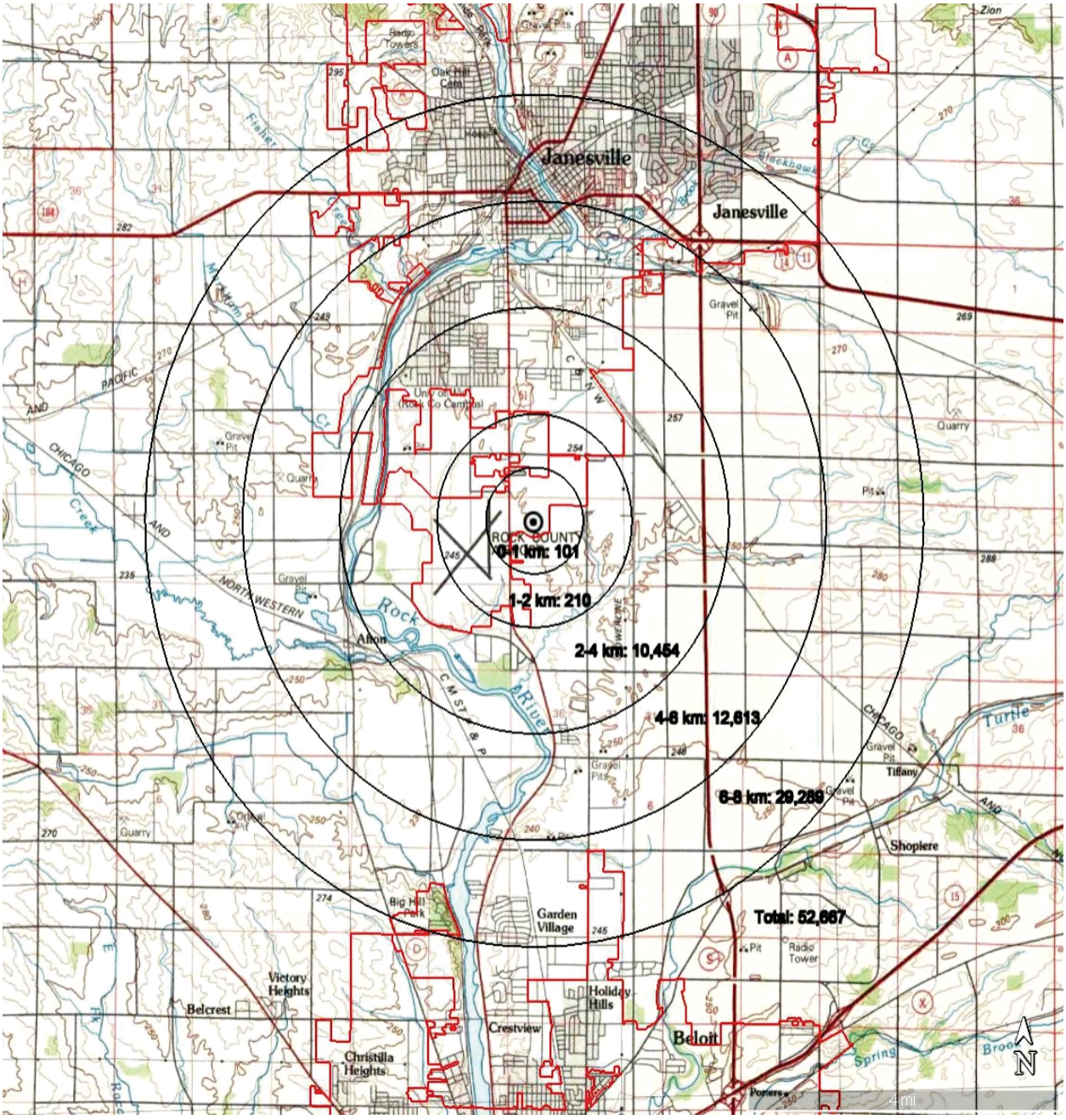

Figure 2.1-5 – Resident Population Distribution – 2024

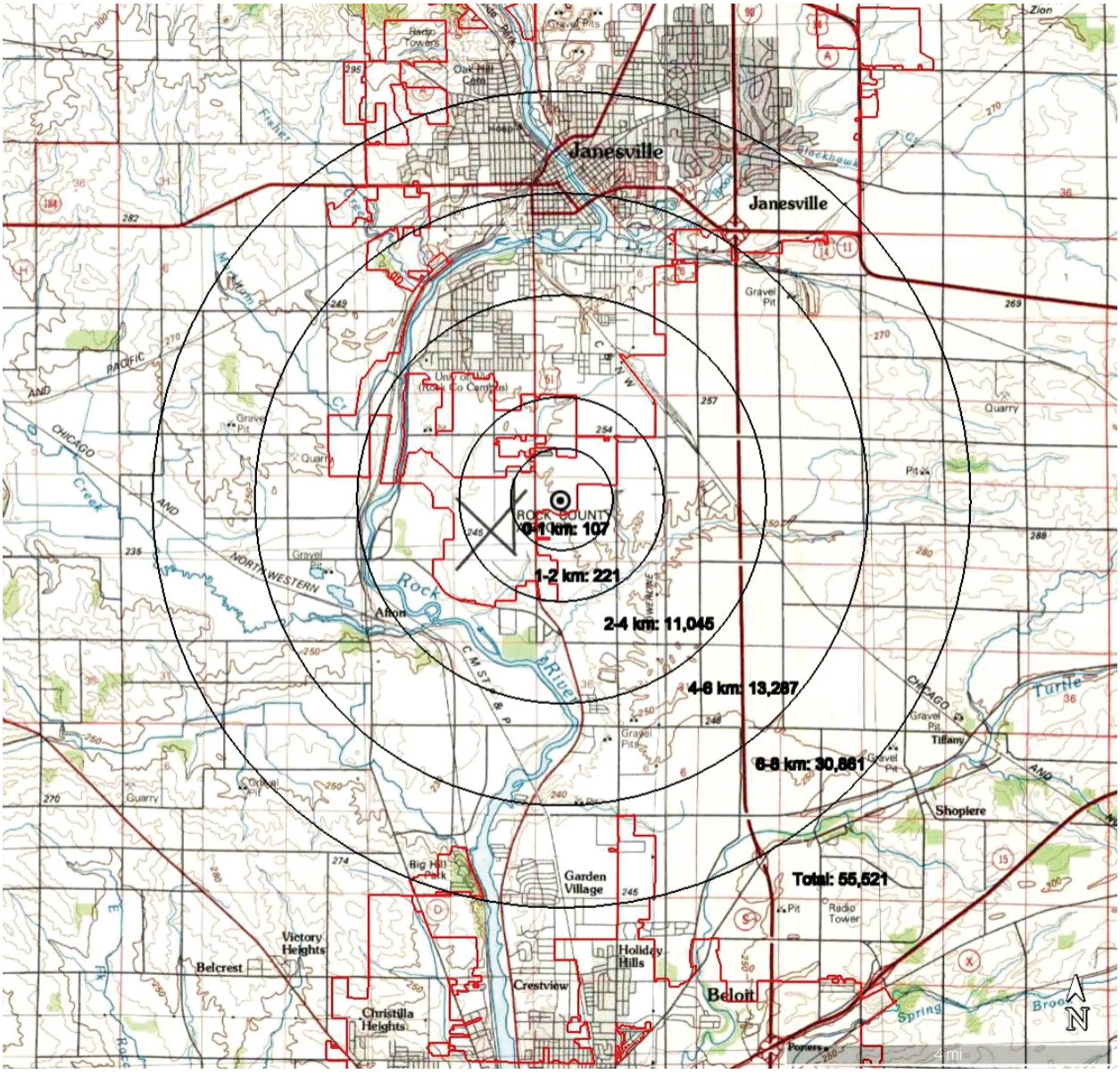

Figure 2.1-6 – Resident Population Distribution – 2051

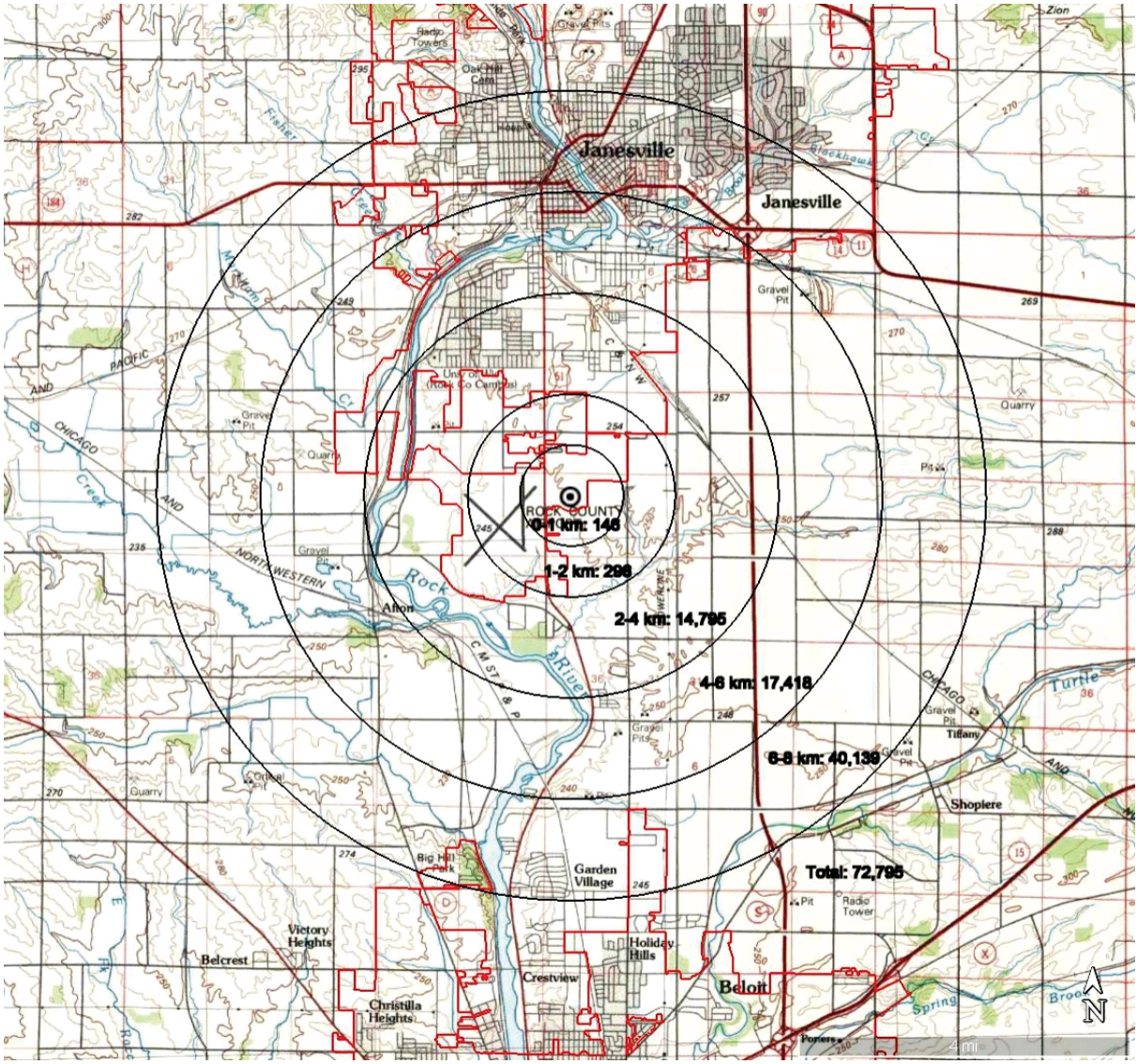

2.2 NEARBY INDUSTRIAL, TRANSPORTATION, AND MILITARY FACILITIES

This section identifies and evaluates present and projected future industrial, transportation, and military installations and operations in the area around the site. NUREG-1537, Part 1, Guidelines for Preparing and Reviewing Applications for Licensing of Non-Power Reactors, Format and Content, states that all facilities and activities within 8 kilometers (km) (5 miles [mi.]) of the facility should be considered (USNRC, 1996). This section identifies all facilities and activities within 8 km (5 mi.) of the boundaries of the safety-related area. This ensures that all facilities and activities within 8 km (5 mi.) of any of the IUs are considered in the evaluation of potential hazards. In addition, facilities and activities at greater distances are considered as appropriate to their significance.

2.2.1 LOCATIONS AND ROUTES

An investigation of industrial, transportation, and military facilities within 8 km (5 mi.) of the site was performed. The U.S. Environmental Protection Agency's Envirofacts Database was initially used to identify potential facilities within 8 km (5 mi.). The Wisconsin Emergency Management Agency supplied Tier II Chemical Inventory Reports for facilities in Janesville and Beloit, Wisconsin that submitted a 2010 report (Wisconsin Emergency Management, 2011). The facilities identified through the above sources were also verified through field reconnaissance. Field reconnaissance consisted of driving major public roads within an 8 km (5 mi.) radius of the site and noting the location of industrial and transportation facilities and their relevant features (e.g., chemical storage tanks). Information on future industrial growth was obtained from local community comprehensive plans (City of Beloit, 2018, City of Janesville, 2009). The Director of Economic Development for the City of Janesville was also contacted in regard to future industrial growth (City of Janesville, 2012).

The following significant facilities were identified within 8 km (5 mi.) of the site:

- Industrial Facilities
  - Abitec Corporation
  - Crop Production Services
  - Evonik Goldschmidt Corporation
  - Janesville Jet Center
  - School District of Beloit Turner
  - United Parcel Service
  - Dollar General Distribution Center
- Pipelines
  - Alliant Energy Natural Gas pipelines
  - ANR Natural Gas pipeline
- Waterways
  - Rock River
- Highways
  - Interstate I-90/39
  - U.S. Highway 51 (US 51)
  - U.S. Highway 14 (US 14)
  - Wisconsin State Highway 11 (SH 11)
  - Wisconsin State Highway 26 (SH 26)

- Railroads
  - Union Pacific Railroad
  - Canadian Pacific Railroad
  - Wisconsin & Southern Railroad
- Airports and Heliports
  - Southern Wisconsin Regional Airport
  - Omniflight Helicopters Heliport
  - Mercy Hospital Heliport
  - St. Mary's Janesville Hospital Heliport
- Airways
  - Low Altitude Airway V9-177
  - Low Altitude Airway V63
  - Jetway Route J90
  - Low Altitude Airway V177
  - Low Altitude Airway V216

In addition, an investigation of industrial, military, and transportation facilities beyond 8 km (5 mi.) from the site identified the following transportation facilities and routes for further evaluation:

- Airports and Heliports
  - Beloit Memorial Hospital Heliport
  - Hacklander Airport
  - Melin Farms Airport
  - Archie's Seaplane Base
  - Beloit Airport
  - Miller Airport
- Airways
  - Low Altitude Airway V228
  - Low Altitude Airway V24-97
  - Low Altitude Airway V9-63-128
  - Low Altitude Airway V246
  - Low Altitude Airway V24
  - Low Altitude Airway V97
  - Jetway Route J105
  - Jetway Route J84-94
  - Jetway Route J100-128
  - Jetway Route J30
  - Jetway Route J16-36
  - Jetway Route J89-101

Table 2.2-1 shows the significant industrial facilities within 8 km (5 mi.) of the site and Table 2.2-2 shows pipelines within 8 km (5 mi.) of the site. Table 2.2-3 shows airports and heliports within 16 km (10 mi.) of the site and Table 2.2-4 shows federal airways within 16 km (10 mi.) of the site. Figure 2.2-1 shows the location of industrial and transportation facilities, with the exception of airways, identified within 8 km (5 mi.) of the site. Figure 2.2-2 illustrates the location of airports, heliports, and airway routes identified within 10 mi. of the site.

2.2.1.1 Descriptions

Descriptions of the industrial and transportation facilities, with the exception of airports and airways, identified within 8 km (5 mi.) of the site are provided in the following subsections. Airports and airways are described in Subsection 2.2.2.

2.2.1.1.1 Industrial Facilities

Seven nearby industrial facilities are identified in Subsection 2.2.1. Table 2.2-1 provides a concise description of these facilities, including their primary functions and major products.

In addition, a detailed analysis of the potential hazards to the facility due to chemical storage both on and off the site is presented in Subsection 2.2.3.

2.2.1.1.2 Pipelines

Several natural gas distribution pipelines are located within 8 km (5 mi.) of the site, as depicted in Figure 2.2-1. Available information about these pipelines is provided in Table 2.2-2 and summarized below.

Alliant Energy operates two main natural gas pipelines near the site. The closest main pipeline is located approximately 2.6 mi. (4.2 km) east of the site at the nearest approach. The other pipeline is located 2.8 mi. (4.5 km) south of the site at the nearest approach. The closest feeder line is a [ ]^{SRI} natural gas feeder line that is located just west of US 51 (Alliant Energy, 2012). ANR Natural Gas operates a natural gas distribution pipeline approximately 3.6 mi. (5.8 km) northeast of the site at the nearest approach.

2.2.1.1.3 Description of Waterways

The Rock River is located approximately 1.7 mi. (2.7 km) west of the site at the nearest approach. The water level of the river is too low to allow for navigation of any watercraft other than recreational watercraft.

2.2.1.1.4 Highways

US 51, a north-south highway, runs directly west of the site. Currently, the site can only be accessed from US 51 and the closest approach to the facility safety-related area is 0.22 mi.

Other highways within 8 km (5 mi.) of the site are I-90/39, US 14, SH 11, and SH 26. The closest approach of I-90/39 is approximately 2.1 mi. (3.4 km) to the east. The closest approach of US 14 is approximately 3.3 mi. (5.3 km) to the north. The closest approach of SH 11 is approximately 0.6 mi. (1.0 km) to the north. The closest approach of SH 26 is 4.1 mi. (6.6 km) to the north.

Information is not available about the materials transported on the roads in the vicinity of the site; therefore, Tier III reports for industrial facilities within 8 km (5 mi.) of the site were reviewed to determine chemicals that may be transported on nearby roads. The Wisconsin Department of Transportation guide for truckers (Wisconsin DOT, 2007) provided the maximum allowable tonnage a truck could carry on Wisconsin highways. Table 2.2-5 summarizes the chemicals that are present at the industrial facilities that could pose a hazard when transported. In addition, bounding chemicals that were not identified as being used within 8 km (5 mi.) of the facility, but

are known to be significantly hazardous, such as hydrogen, were analyzed as potentially traveling on I-90/39. These chemicals are shown in Table 2.2-5. A detailed analysis of the potential impacts of hazardous chemical transportation on the facility is provided in Subsection 2.2.3.

2.2.1.1.5 Railroads

There are three railroad lines located within 8 km (5 mi.) of the site. The railroads transport hazardous and non-hazardous material (Rock County, 2012). A single railroad tank car has a maximum capacity of 30,000 gallons.

The Union Pacific line, approximately 1.4 mi. (2.3 km) east of the site, is the nearest railroad line to the site. The Canadian Pacific line is located on the west bank of the Rock River and its closest approach to the site is approximately 2.0 mi. (3.2 km) to the west. The Wisconsin & Southern Railroad Company is located on the west bank of the Rock River and its closest approach to the site is approximately 2.7 mi. (4.3 km) to the north. The chemicals transported on the nearest railroad are analyzed in Subsection 2.2.3.

2.2.1.1.6 Projections of Industrial Growth

Overall, a small percentage of Rock County is industrial, with the majority of industries in the larger cities of Janesville and Beloit. The only planned industrial growth identified within 8 km (5 mi.) of the site is expansion of the Alliant Energy generation facility and the construction of a new pet food processing plant. The generation facility operations are not expected to grow significantly. The cumulative impacts of these projects and activities have been evaluated and result in small to moderate impact to land use and visual resources, air quality and noise, geologic environment, water resources, ecological resources, historical and cultural resources, socioeconomic environment, human health, waste management, and environmental justice. The Janesville and Beloit Comprehensive Plans do not provide details of any planned industrial growth (City of Beloit, 2012; City of Janesville, 2009).

2.2.2 AIR TRAFFIC

2.2.2.1 Airports

Table 2.2-3 provides a list of airports within 10 mi. (16 km) of the site. Four airports or heliports are within 5 mi. (8 km) and six airports or heliports are between 5 mi. (8 km) and 10 mi. (16 km) of the site. The majority of the airport/heliports have only sporadic activity. Figure 2.2-2 identifies the airports within 10 mi. (16 km) of the facility.

2.2.2.2 Airways

There are 10 low altitude airways and one jetway located within 10 mi. (16 km) of the facility (distance from the center of the facility to the nearest edge of the airway). These airways are identified in Table 2.2-4. NUREG-1537, Part 1, states that "Factors such as frequency and type of aircraft movement, flight patterns, local meteorology, and topography should be considered…" (USNRC, 1996). However, the document does not provide a screening criterion for the distance of the airways from the facility. Therefore, NUREG-0800, Standard Review Plan for the Review of Safety Analysis for Nuclear Power Plants (SRP), Section 3.5.1.6, Aircraft Hazards, was used to provide guidance in evaluating airways near the facility (USNRC, 2010). For airways where the

outer edge of the airway is greater than two statute miles from the facility, SRP Section 3.5.1.6 allows the airway to be screened out with no further evaluation. Three low altitude airways and the one jetway located within 10 mi. (16 km) of the facility were identified as having an edge of the airway within two statute miles of the facility (see Table 2.2-4). The hazards associated with these airways are evaluated in Subsection 2.2.2.5.1. Figure 2.2-2 identifies the centerline of federal airways within 10 mi. (16 km) of the facility.

2.2.2.3 Military Airports and Training Routes

NUREG-1537, Part 1, does not provide screening criteria for military training routes (USNRC, 1996). SRP Section 3.5.1.6, SRP Acceptance Criteria Item 1.B, determines the hazard to be below a probability of 1E-7 if the site is at a distance greater than 5 mi. from the edge of the training route (USNRC, 2010). There are no military airports or training routes located within 10 mi. (16 km) of the facility. The closest military training route is SR771. The centerline of this training route is greater than 25 mi. (40 km) from the facility. This distance is greater than the 5 mi. (8 km) screening criteria in SRP Section 3.5.1.6, and therefore is not evaluated further.

2.2.2.4 Approach and Holding Patterns near the Facility

Three airports have holding patterns near the facility. Table 2.2-6 provides a list of holding patterns in the vicinity of the facility.

NUREG-1537, Part 1, does not provide screening criteria for approach and holding patterns (USNRC, 1996). SRP Section 3.5.1.6, SRP Acceptance Criteria Item 1.C, determines the hazard may be screened out if the site is at a distance greater than 2 statute miles from the nearest edge of an approach or holding pattern (USNRC, 2010).

The distance from the edge of each holding pattern to the facility is greater than the 2 mi. screening criterion in SRP Section 3.5.1.6. This hazard screens out, and no further evaluation is performed on approach or holding patterns.

2.2.2.5 Evaluation of the Aircraft Hazard

2.2.2.5.1 Evaluation of Airways

The U.S. Department of Energy (DOE) provides a method for estimating the probability per year of an aircraft crashing into the facility. The methodology is outlined in DOE Standard DOE-STD-3014-96 (DOE, 2006) and utilizes crash rates for non-airport operations. The non-airport crash impact frequency evaluation is determined from using the following "four factor formula" (DOE, 2006):

$$F_j = N_j \times P_j \times f_j(x, y) \times A_j \qquad \text{(Equation 2.2-1)}$$

Where:

- F_j is the crash impact frequency
- j is each type of aircraft suggested in the DOE Standard
- N_jP_j is the expected number of in-flight crashes per year

- $f_j(x,y)$ is the probability, given a crash, that the crash occurs in a 1-square mile area surrounding the facility
- A_j is the effective plant area

Tables B-14 and B-15 of DOE-STD-3014-96 (DOE, 2006) provide $N_jP_jf_j$ values for general aviation aircraft, air carriers, air taxis, and small military aircraft applicable for specific DOE sites. Tables B-14 and B-15 of DOE-STD-3014-96 (DOE, 2006) also provide crash probabilities for unspecified locations in the continental United States (CONUS), and Table B-43 of DOE-STD-3014-96 (DOE, 2006) provides a generic crash frequency for helicopters. Therefore, CONUS maximum values and generic helicopter values are used for the facility and are provided in Table 2.2-7 (DOE, 2006).

The effective plant area (A_j) for the safety-related structures of the facility depends on the length, width, and height of the facility, as well as the aircraft's wingspan, skid distance, and impact angle as explained below (DOE, 2006):

$$A_j = A_f + A_s \qquad \text{(Equation 2.2-2)}$$

Where

$$A_f = (W_{sj} + R) \times H \times cot(\varphi)_j + \frac{2 \times L \times w \times W_{sj}}{R} + L + w: \qquad \text{(Equation 2.2-3)}$$

And:

$$A_s = (W_{sj} + R)\ x\ S_j \qquad \text{(Equation 2.2-4)}$$

Where:

- A_f is the effective fly-in area
- A_s is the effective skid area
- W_{sj} is the aircraft wingspan (Table 2.2-7)
- R is the length of the diagonal of the facility = $\sqrt{(L^2 + W^2)}$
- H is the facility height
- $cot\varphi$ is the mean of the cotangent of the aircraft impact angle (Table 2.2-7)
- L is the length of facility, facility-specific
- W is the width of facility, facility-specific
- S_j is the aircraft skid distance (mean value) (Table 2.2-7)

The total effective area (Aj) for the safety-related structure facility was calculated. Dimensions of the production facility used in the analysis include a length of 212 feet (ft.)-6 inches (in.), a width of 158 ft.-2 in., and a height of 56 ft.-0 in. Plan and elevation views of the main production facility structure (FSTR) are provided in Figure 1.3-1 and Figure 1.3-2.

The calculated effective area for the five aircraft types is provided in Table 2.2-8.

The crash impact probabilities for small non-military aircraft (i.e., general aviation and air taxi), large non-military aircraft (i.e., air carriers), and military aircraft (i.e., small aircraft and helicopter) from airways are provided in Table 2.2-9.

The N2PS structure is not considered in the evaluation of the aircraft hazard. An aircraft impact into the N2PS structure would not be expected to result in a loss of off-site power because the N2PS structure is located along the east wall of the FSTR while the off-site electrical power source is routed along the south and west walls of the FSTR. An aircraft impact into portions of the FSTR that would interrupt the supply of off-site power would not impact the N2PS structure, and the N2PS would remain operational.

2.2.2.5.2 Evaluation of Airports

Airport screening criteria are obtained from NUREG-1537, Part 1, Section 2.2.2, which directs that an airport can be screened out from probabilistic evaluation depending on the number of operations per year in relation to its distance from the site (USNRC, 1996). Factors such as frequency and type of aircraft movement are considered for airports at distances within 8 km. For airports located between 8 and 16 km from the site, airports can be screened out if they have less than 200 x d^2 aircraft movements per year, where d is the distance in km. For private airports within this distance where operations are classified as sporadic, the Southern Wisconsin Regional Airport (SWRA) and infrequent nature of operation is used to consider the hazard acceptable.

The SWRA and three heliports are within 5 mi. (8 km) of the facility. A probabilistic hazard analysis was performed for SWRA. The three heliports within 5 mi. (8 km) screened out as they have sporadic air activity and their evaluation would be bounded by the evaluation performed for SWRA.

The airports and heliports between 5 mi. (8 km) and 10 mi. (16 km) from the facility were screened out based on their annual operations being less than the screening criteria. Based on this screening criteria, only the SWRA is evaluated for the potential hazard posed by aircraft.

SRP Section 3.5.1.6 (USNRC, 2010) provides a method for estimating the probability of an aircraft crashing into the site from the operations at nearby airports. The probability per year of an aircraft crashing into the site due to airport operations at nearby airports is:

$$P_A = \sum_{i=1}^{L} \sum_{j=1}^{M} C_j N_{ij} A_j \qquad \text{(Equation 2.2-5)}$$

Where:

- P_A is the probability of crash per year
- L is the number of flight trajectories affecting the site
- M is the number of different types of aircraft
- C_j is the probability per square mile of a crash per aircraft movement, for the jth aircraft
- N_{ij} is the number (per year) of movements by the jth aircraft along the ith flight path
- A_j is the effective plant area (in square miles) for the jth aircraft

The calculated effective area for the five aircraft types is provided in Table 2.2-8.

The total operations at the SWRA used in the evaluation of the airport are based on the Federal Aviation Administration (FAA) Office of Aviation Policy and Plans (APO) Terminal Area Forecast

Detail Report issued February 2019 (USDOT, 2019a). The maximum number of operations at the airport for each type of aircraft are listed in Table 2.2-10. The operations include both itinerant and local operations. The values provided in Table 2.2-10 are obtained from the maximum forecasted number of operations from 2019 through 2045 for non-military aircraft. A historical average of military operations from 1990 through 2018 is used to calculate crash impact probabilities from military operations. The historical average of military operations is greater than the forecasted values provided in the Terminal Area Forecast Detail Report and therefore is a more conservative value to use.

Based on communication with the SWRA and the Janesville Air Traffic Control Tower, the operations on each runway, by type of aircraft, are provided in Table 2.2-11. The distance from the end of each runway to the facility center point is provided in Table 2.2-12. The probability of a crash by aircraft type and in relation to distance from the site is provided in Table 2.2-13.

The total crash impact probabilities for small non-military aircraft (i.e., general aviation itinerant operations, local civil operations, and air taxi itinerant operations), large non-military aircraft (i.e., air carriers), and military aircraft (i.e., small aircraft and helicopter) from airports are provided in Table 2.2-9, including consideration of effects from increased traffic due to future potential air shows (see Subsection 2.2.2.5.3).

2.2.2.5.3 Evaluation of Non-Frequent Airport Events

The SWRA has infrequently held air shows and aviation events at their facility. FAA Order 8900.1 (Volume 3, Chapter 6, Section 1) describes aviation events to “include air shows, closed course air races, parachute demonstration jumps, balloon meets, and fly-ins conducted before an invited assembly of persons, for which the FAA issues a Certificate of Waiver or Authorization” (USDOT, 2007). An FAA Certificate of Waiver or Authorization permit temporary relief from certain designated low altitude aviation regulations but “under conditions ensuring the equivalent level of safety”. During air shows, the ingress and egress routes are confined to an aerobatic box which is clearly defined. The aerobatic box is required to be sterile per the FAA regulations.

The FAA National Aviation Events specialists have committed to consider the safety of the facility when granting waivers for future air shows. The aviation event specialists assert that if the facility were not in the aerobatic box or within the ingress or egress routes defined for the planes performing at the air shows, the risk to the facility would be reduced similar to the risk due to normal flight operations in the vicinity.

To conservatively address increased traffic from future air shows, flight and display data was taken from a larger air show held at the nearby Chicago Rockford International Airport. The Rockford Airfest was a two-day event with an estimated attendance of 130,000 spectators. The 2011 Rockford AirFest included more than 50 static display aircraft, consisting of an assortment of commercial aircraft and current and historical military aircraft of various sizes. Assuming that each aircraft flew into and out of the airport, 50 static display aircraft would result in 100 operations. The 2014 Rockford AirFest included 14 aerial performances, each act typically consisting of one or more small commercial or military aircraft, for an estimated 50 total aircraft participating in aerial performances. It was conservatively estimated that each of these 50 aerial performance aircraft:

1) landed at the airport the day before the air show;
2) took off from the airport to perform in their act twice;

3) landed at the airport after their act was complete, for each of two performances; and
4) took off from the airport to leave after the air show was over.

Therefore, the addition of a future airshow at the SWRA could add an estimated 400 operations, or flights, either into or out of the SWRA. These additional 400 operations are added to the hazard evaluation to address the increased activity due to air shows. The classification of each of these operations (e.g., air carriers and military) were based on the aircraft on display at the 2014 Rockford Airfest.

Table 2.2-3 lists the number of operations in 2018 at the SWRA as 37,674, and a projected number of operations in 2045 as 46,443. Table 2.2-10 lists the maximum operations at the SWRA for the years 2019 through 2045. As shown in Table 2.2-14, the addition of 400 operations at the SWRA to support a future air show is bounded by the maximum number of operations between 2019 and 2045.

Therefore, the addition of a future air show at the SWRA is bounded by the current analysis.

2.2.2.5.4 Results of Evaluation of Airways and Airports

NUREG-1537, Part 1, does not provide acceptance criteria to be used to evaluate the aircraft accident probability posed by nearby airports and airways (USNRC, 1996). DOE-STD-3014-96 (DOE, 2006) provides a screening value of 1E-6 per year, where the risk of an aircraft accident is considered acceptable if the frequency of occurrence is less than 1E-6 per year. The calculated crash probability for small non-military aircraft does not meet this criterion (3.92E-4); therefore, the safety-related structures of the facility credited to prevent release in excess of regulatory limits are designed to withstand the impact of a small non-military aircraft (see Section 3.4). The combined probability of all other aircraft crashes does meet this criterion (3.09E-7).

2.2.3 ANALYSIS OF POTENTIAL ACCIDENTS AT FACILITIES

On the basis of the information provided in Subsection 2.2.1 and Subsection 2.2.2, the potential accidents to be considered as design-basis events and the potential effects of those accidents on the facility, in terms of design parameters (e.g., overpressure, missile energies) or physical phenomena (e.g., impact, flammable or toxic clouds) were identified in accordance with NUREG-1537, Part 1 (USNRC, 1996). The events are discussed in the following subsections.

2.2.3.1 Determination of Design Basis Events

Design basis events, internal and external to the facility, are defined as those accidents that have a probability of radiological release to the public on the order of magnitude of 1E-6 per year, or greater. The following accident categories were considered in selecting design-basis events: explosions, flammable vapor clouds (delayed ignition), toxic chemicals, and fires. The postulated accidents that would result in a chemical release were analyzed at the following locations:

- Nearby transportation routes such as US 51 and I-90/39, the Union Pacific Railway, and nearby natural gas pipelines.
- Nearby chemical and fuel storage facilities (industry in the towns of Janesville and Beloit, Wisconsin).
- Chemicals stored or used at the facility.

2.2.3.1.1 Explosions

Accidents involving detonations of high explosives, munitions, chemicals, or liquid and gaseous fuels were considered for facilities and activities in the vicinity of the plant or on-site where such materials are processed, stored, used, or transported in quantity. The effects of explosions are a concern in analyzing structural response to blast pressures. The effects of blast pressure from explosions from nearby railways, highways, or facilities to critical plant structures were evaluated to determine if the explosion would have an adverse effect on plant operation or would prevent a safe shutdown.

The allowable (i.e., standoff) and actual distances of hazardous chemicals transported or stored were determined in accordance with Regulatory Guide 1.91, Revision 1, Evaluations of Explosions Postulated to Occur on Transportation Routes Near Nuclear Power Plants (USNRC, 1978). Regulatory Guide 1.91 cites 1 pound per square inch differential pressure (psid) (6.9 kilopascal [kPa]) as a conservative value of peak positive incident overpressure, below which no significant damage would be expected. Regulatory Guide 1.91 defines this standoff distance by the relationship $R \geq kW^{1/3}$ where R is the distance in feet from an exploding charge of W pounds of trinitrotoluene (TNT); and the value k is a constant. The TNT mass equivalent, W, was determined by comparing the heat of combustion of the chemical to the heat of combustion of TNT.

For those chemicals where the standoff distance using the NUREG-1805, Fire Dynamics Tools (FDTs) (USNRC, 2004), methods are greater than the actual distance from the chemical to the nearest safety-related building, a probabilistic analysis is used. The probabilistic analysis must show that “the rate of exposure to a peak positive incident overpressure in excess of 1 psid (6.9 kPa) is less than 1E-6 per year, when based on conservative assumptions, or 1E-7 per year when based on realistic assumptions.”

Conservative assumptions were used to determine a standoff distance, or minimum separation distance, required for an explosion to have less than 1 psid (6.9 kPa) peak incident pressure. In each of the explosion scenario analyses, conservative yield factors were chosen. The yield factor is an estimation of the available combustion energy released during the explosion as well as a measure of the explosion confinement. For confined explosions, a yield factor of 100 percent was applied to account for an in-vessel confined explosion. This is a conservative assumption because a 100 percent yield factor is not achievable:

- For some atmospheric liquids (e.g., diesel) the storage vessel was assumed to contain fuel vapors at the upper explosive limit. This is conservative because the upper explosive limit produces the maximum explosive mass, given that it is the fuel vapor, not the liquid fuel that explodes. These assumptions are consistent with those used in Chapter 15 of NUREG-1805, Fire Dynamics Tools (FDTs) (USNRC, 2004).
- For compressed or liquefied gases (i.e., propane, hydrogen), it was conservatively assumed that the entire content of the storage vessel is between the upper and lower explosive limits, given that the instantaneous depressurization of the vessel would result in vapor concentrations throughout the explosive range at varying pressures and temperatures that could not be assumed. Therefore, the entire content of the storage vessel was considered as the explosive mass.

For unconfined explosions of propane, methane, or hydrogen, the yield factor is 3 percent from the Handbook of Chemical Hazard Analysis Procedures (FEMA, 1989).

In addition, the site has a liquid nitrogen storage tank located outside the facility buildings. The tank and its associated process piping are designed in accordance with applicable codes, including overpressure protection.

In some cases, chemicals are screened as being bounded by other chemicals. Three properties of the chemical hazard are used to determine if one of the hazards is bounded by another. First, chemicals that are gases at standard conditions will be more volatile and have a larger explosive mass per storage mass than chemicals that are liquids at standard conditions. Second, chemicals with a smaller lower explosive limit (LEL) and a greater upper explosive limit (UEL) will be more explosive. A larger flammable or explosive range will make an explosion more likely and increase the explosive mass per storage mass. Third, chemicals with a greater heat of combustion will have a larger amount of energy released in an explosion. In addition, the mass of the chemical and the distance from the chemical to the facility are screening factors. Where chemicals exhibit similar properties, those chemicals that are closer to the site and in larger tanks are chosen as bounding over chemicals that are farther or smaller.

The on-site and off-site chemicals in Table 2.2-15 are evaluated to ascertain which hazardous materials have the potential to explode, thereby requiring further analysis. The effects of selected explosion events are summarized in Table 2.2-16 and in the following subsections relative to the release source.

2.2.3.1.1.1 Pipelines

A stationary explosion of a pipeline is bounded by the delayed ignition explosion of a pipeline. This is because the constant mass release rate from the pipe results in a much larger total explosive mass, and because the wind is assumed to blow the release towards the site. The distance from the point of the explosion to the facility is therefore much smaller for flammable vapor clouds than for pipeline explosions at the release point.

2.2.3.1.1.2 Waterway Traffic

There is no navigable waterway within 5 mi. (8 km) of the facility.

2.2.3.1.1.3 Highways

Table 2.2-15 includes the hazardous materials potentially transported on US 51 and I-90/39. The materials that were identified as the bounding chemicals for explosive potential were diesel, ethylene oxide, gasoline, and propane on US 51, and hydrogen on I-90/39. The remaining chemicals are either non-explosive or are bounded based on the comparison method discussed in Subsection 2.2.3.1.1 (ammonia, propylene oxide, and styrene).The maximum quantity of the identified chemicals assumed to be transported on the roadway was 50,000 pounds (lb.) (22,679 kilograms [kg]) per Regulatory Guide 1.91, except for the hydrogen, where at most 3300 lb. (1,496 kg) is on a single truck per 49 CFR 173.318.

An analysis of the identified chemicals was conducted using TNT equivalency methodologies, as described in Subsection 2.2.3.1.1. The results indicate that the minimum separation distances (i.e., safe standoff distances) are less than the shortest distance to a safety-related SHINE structure from any point on US 51 or I-90/39. A tank of diesel that contains 1,258,091 lb. (570,660 kg) of diesel is acceptable at 0.22 mi. (0.35 km). A tank of ethylene oxide that contains 440,000 lb. (199,580 kg) of ethylene oxide is acceptable at 0.22 mi. (0.35 km). A tank of gasoline

that contains 133,946 lb. (60,756 kg) is acceptable at 0.22 mi. (0.35 km). A tank of jet fuel containing 500,000 lb. (226,796 kg) is acceptable at 0.22 mi. (0.35 km). A tank of propane that contains 55,724 lb. (25,275 kg) is acceptable at 0.22 mi. (0.35 km). The closest safety-related SHINE area is located approximately 0.22 mi. (0.35 km) from US 51.

The propane truck was also analyzed for a boiling liquid expansion vapor explosion (BLEVE) overpressure. The standoff distance to a 1 psid (6.9 kPa) overpressure is 332 ft. (101 meters [m]). This is much less than the actual distance from US 51 to the facility (0.22 mi. [0.35 km]).

A tank containing 18,196 lb. (8253 kg) of hydrogen is acceptable at a distance of 0.22 mi. (0.35 km). The closest safety-related SHINE area is 2.1 mi. (3.4 km) from I-90/39.

The limiting stationary explosions are shown in Table 2.2-16.

Based on the above, an explosion involving potentially transported hazardous materials on US 51 or I-90/39, would not adversely affect operation of SHINE.

2.2.3.1.1.4 On-Site Chemicals

On-site stationary chemicals were analyzed using the TNT equivalency methodologies, as described in Subsection 2.2.3.1.1. One chemical was identified as being a potential explosive hazard on-site: deuterium/tritium.

The deuterium and tritium are used in the production facility and are treated for this analysis as hydrogen gas. The maximum expected mass in one container is 0.39 lbs (0.18 kg) of deuterium and 0.25 lbs (0.10 kg) of tritium. These maximum expected masses are very low; however, because these chemicals are used in production, there is no separation between the hazard and the SHINE safety-related area. The deuterium and tritium gas systems and processes are designed to minimize the probability of an explosion. With safety features, and the very small mass of each chemical, the probability of an explosion causing enough damage to the facility to cause a radiological release to the public is low.

Therefore, an explosion of any of these chemicals would not adversely affect operation of SHINE.

2.2.3.1.1.5 Nearby Facilities and Railways

There are three additional off-site facilities and railways that have explosive chemicals that are identified as the bounding instances of explosion analysis. The hazardous materials stored at nearby facilities that were identified for further analysis with regard to explosive potential are ethylene oxide stored at Abitec and gasoline at Janesville Jet Center. The ethylene oxide is analyzed as a bounding instance between the stationary tank at the facility and the tank transported by rail. In addition, bounding instances of diesel fuel and jet fuel (kerosene) are analyzed. All other nearby chemicals or chemicals transported by railway were dispositioned as being bounded by one of these four bounding instances using the methodology discussed in Subsection 2.2.3.1.1.

A conservative analysis using TNT equivalency methods as described in Subsection 2.2.3.1 was used to determine standoff distances for the storage of the identified hazardous materials.

The largest diesel tank, containing 1,258,091 lb. (570,660 kg) of liquid, corresponding to 668 lb. (303 kg) of vapor, would be acceptable at a distance of 0.22 mi. (0.35 km). The nearest tank of diesel is greater than 0.5 mi. (0.8 km) from the facility.

The largest ethylene oxide tank, containing 440,000 lb. (199,580 kg) of liquid, corresponding to 896 lb. (406 kg) of vapor, would be acceptable at a distance of 0.22 mi. (0.35 km). The nearest instance (transportation via the railroad) of ethylene oxide is 1.6 mi. (2.6 km) from the facility.

The largest gasoline tank, containing 133,946 lb. (60,756 kg) of liquid, corresponding to 69 lb. (31 kg) of vapor, would be acceptable at a distance of 0.22 mi. (0.35 km). The nearest tank of gasoline is 0.9 mi. (1.45 km) from the facility.

A 500,000 lb. jet fuel tank was analyzed at 0.22 mi. (0.35 km) and found to be acceptable. The largest jet fuel (kerosene) tank contains 79,968 lb. (36,272 kg) of liquid, corresponding to 27 lb. (12 kg) of vapor, and is therefore acceptable with margin. The nearest instance of jet fuel (truck on US 51) is 0.22 mi. (0.35 km) from SHINE.

The results using this methodology indicate that the minimum separation distances (i.e., safe standoff distances) are less than the shortest distance from a SHINE safety-related area to the storage location of the identified chemicals. Therefore, an explosion of any of these chemicals would not adversely affect operation of SHINE.

2.2.3.1.1.6 Explosion-Related Impacts Affecting the Design

A facility is acceptable when the calculated rate of occurrence of severe consequences from any external accident is less than 1E-6 occurrences per year and reasonable qualitative arguments can demonstrate that the realistic probability is lower. Regulatory Guide 1.91 (USNRC, 1978) cites 1 psid (6.9 kPa) as a conservative value of peak positive incident overpressure, below which no significant damage would be expected. SHINE safety-related areas are designed to withstand a peak positive overpressure of at least 1 psid (6.9 kPa) without loss of function/significant damage.

The analyses presented in this subsection demonstrate that a 1 psid (6.9 kPa) peak positive overpressure will not be exceeded at a safety-related structure for any of the postulated explosion event scenarios. As a result, postulated explosion event scenarios will not result in severe consequences.

2.2.3.1.2 Flammable Vapor Clouds (Delayed Ignition)

Flammable gases in the liquid or gaseous state can form an unconfined vapor cloud that could drift toward the plant before ignition occurs. When a flammable chemical is released into the atmosphere and forms a vapor cloud, it disperses as it travels downwind. The parts of the cloud where the concentration is within the flammable range, between the lower and upper flammability limits, may burn if the cloud encounters an ignition source. The speed at which the flame front moves through the cloud determines whether it is a deflagration or a detonation. If the cloud burns fast enough to create a detonation, an explosive force is generated.

On-site and off-site chemicals are shown in Table 2.2-15. These chemicals were evaluated to ascertain which hazardous materials had the potential to form a flammable vapor cloud or vapor cloud explosion. For those chemicals with an identified flammability range, the Areal Locations of

Hazardous Atmospheres (ALOHA) air dispersion model was used to determine the distances where the vapor cloud may exist between the UEL and the LEL, presenting the possibility of ignition and potential thermal radiation effects (ALOHA, 2008).

The identified chemicals were also evaluated to determine the possible effects of a flammable vapor cloud explosion. ALOHA was used to model the worst case accidental vapor cloud explosion, including the standoff distances and overpressure effects at the nearest SHINE safety-related area. To model the worst case in ALOHA, ignition by detonation was chosen for the ignition source. The standoff distance was measured as the distance from the spill site to the location where the pressure wave is at 1 psid (6.9 kPa) overpressure.

Conservative assumptions were used in both ALOHA analyses with regard to meteorological inputs and identified scenarios. The following meteorological assumptions were used as inputs to the computer model, ALOHA: Pasquill Stability Class F (stable), with a wind speed of 1 meter per second (m/s) (3.3 feet per second [fps]); ambient temperature of 81°F (27°C); relative humidity 50 percent; cloud cover 50 percent; and an atmospheric pressure of 1 atmosphere. Pasquill Stability Class F was selected based on local weather data. Class F represents the 5 percent worst case weather conditions at the facility. For each of the identified liquid chemicals, it was conservatively assumed that the entire contents of the vessel leaked forming a 1 cm (0.4 in.) thick puddle. For gaseous chemicals the entire contents were released instantaneously as a gas. This provides a significant surface area to maximize evaporation and the formation of a vapor cloud in the case of liquid releases and maximizes the peak concentration in the case of gas releases.

The analyzed effects of flammable vapor clouds and vapor cloud explosions from internal and external sources are summarized in Table 2.2-17 and are described in the following subsections relative to the release source.

2.2.3.1.2.1 Pipelines

There are three bounding pipelines within 5 mi. (8 km) of the facility. The nearest feeder line runs north-south along the west side of US 51. The nearest approach of the feeder line is 0.28 mi. (0.45 km). The nearest transmission line is roughly a half mile east of I-90/39. The nearest approach of the transmission line is 2.5 mi. (4.0 km). The third pipeline feeds the facility. The pipeline is pressurized upstream of a pressure reducing station that is roughly 100 yards (yd.) (91.4 m) from the nearest safety-related building. Downstream of the pressure reducing facility, the line supplies many site buildings. These bounding three pipelines are depicted in Figure 2.2-1. More information is shown about these bounding pipelines in Table 2.2-2. The two limiting off-site pipelines were analyzed using the methods detailed above. The distance from the transmission pipeline to where the concentration drops below the LEL is 2.2 mi. (3.5 km). Therefore, the concentration of natural gas will always be below the LEL at SHINE. The distance from the feeder pipeline to where the concentration drops below the LEL is 427 yd. (390 m), or 0.24 mi. (0.39 km). Therefore, the concentration of natural gas will always be below the LEL at SHINE. Because the concentrations are below the LEL, a delayed flammable vapor cloud ignition cannot occur at SHINE, and therefore there will be no explosive overpressure. The results of flammable vapor cloud ignition analyses are summarized in Table 2.2-17.

The on-site natural gas pipeline was analyzed probabilistically. Accident data was taken from NUREG/CR-6624, Recommendations for Revision of Regulatory Guide 1.78 (USNRC, 1999) and the Handbook of Chemical Hazard Analysis Procedures (FEMA, 1989). The accident rate for

pipelines is 1.5E-3 accidents per year. Only 20 percent of these accidents involve a complete pipeline rupture, the other 80 percent of releases are modeled as released from a 1-in. (2.54 cm) hole. An additional probability factor was applied to account for the fact that few pipeline releases, especially releases of low mass, result in an explosion. Available data show a connection between the hydrocarbon release rate and the probability of ignition.

The probabilistic analysis involved four cases:

- Case 1 determined that small releases from 1-in. (2.54 cm) diameter holes in the pipe are potentially damaging within the pressure reducing station distance. A 1-in. (2.54 cm) pipeline break would release only 26 lb. (12 kg) of natural gas in 5 minutes. The probability of ignition of this small amount of natural gas is less than 0.1 percent. All explosions within the pressure reducing station distance are assumed to damage a SHINE safety-related structure.
- Case 2 is for releases outside the pressure reducing station that occur when the Pasquill stability class is Class G. A complete break in the 3-in. (7.62 cm) diameter pipe releases 500 lb. (227 kg) of natural gas in 5 minutes. The probability of ignition of this amount of natural gas is 0.2 percent; however, 0.5 percent was conservatively used to model this pipeline.
- Case 3 is similar to Case 2 except that the release occurs when the Pasquill stability class is Class F. It was determined that when the stability class is Class E to Class A, a release upstream of the pressure regulating station is not a hazard to SHINE.
- Case 4 is for a complete release downstream of the pressure regulating station. Any ignition downstream of the pressure regulating station is conservatively assumed to damage a SHINE safety-related structure.

The results of the probability analysis are in Table 2.2-18. The probability of a hazard to the site is 7.7E-7 hazards per year. This analysis is very conservative for four reasons. First, all ignitions downstream of the pressure regulating station are considered hazards. Second, prevailing wind direction is not accounted for. For each release, at least half of the wind directions would blow the release away from the facility. Third, plume rise is not modeled. Natural gas is lighter than air and would rise. Fourth, the pipeline accident rate is higher by an order of magnitude than some of those found in other sources. Therefore, the site natural gas pipeline is not a threat to the facility.

2.2.3.1.2.2 Waterway Traffic

There is no navigable waterway within 5 mi. (8 km) of the facility.

2.2.3.1.2.3 Highways

The closest SHINE safety-related area is located approximately 0.22 mi. (0.35 km) from US 51. The hazardous materials potentially transported on US 51 that were identified for further analysis are diesel, ethylene oxide, gasoline, and propane. The closest SHINE safety-related area is located approximately 2.1 mi. (3.4 km) from I-90/39. The hazardous chemical potentially transported on I-90/39 that was identified for further analysis was hydrogen.

The methodology presented previously in Subsection 2.2.3.1.2 was used for determining the standoff distance for vapor cloud ignition and delayed vapor cloud explosion. Consistent with Regulatory Guide 1.91 (USNRC, 1978), it was conservatively estimated that at most, tanker

trucks carry and release 50,000 lb. (22,679 kg) of the identified chemical. The largest amount of hydrogen on a truck that was analyzed was 3300 lb. (1496 kg).

The distance to the LEL for a gasoline release from a truck on US 51 is 376 yd. (344 m), or 0.214 mi. (0.344 km). This is less than the distance from US 51 to SHINE, 0.22 mi. (0.35 km).

The distance to the LEL for the hydrogen release from a truck on I-90/39 is 1351 yd. (1235 m), or 0.77 mi. (1.24 km). This is less than the distance from I-90/39 to SHINE, 2.1 mi. (3.4 km).

The ethylene oxide trucks were analyzed using a probabilistic analysis. Accident data was taken from NUREG/CR-6624 and the Handbook of Chemical Hazard Analysis Procedures (USNRC, 1999; FEMA, 1989). The accident frequency used was 2E-6 accidents per truck mile, where 20 percent of accidents result in a spill. When a spill occurs, 20 percent of spills are of between 10 percent and 30 percent of the contents, and 20 percent of spills are complete releases. The analysis showed that a release is acceptable at 0.5 mi. (0.8 km) for all stability classes, and that a spill of only 10 percent of the contents is acceptable at 0.22 mi. (0.35 km). There are a total of 99 allowable shipments per year of ethylene oxide on US 51 past SHINE.

Both of the ethylene oxide users within 5 mi. (8 km) of the facility were contacted with regard to ethylene oxide shipments. Both facilities stated that they get ethylene oxide by rail. Therefore, the number of shipments of ethylene oxide past the site will be much less than 99 shipments per year.

The propane trucks were analyzed using a probabilistic analysis. Again, the accident frequency used was 2E-6 accidents per truck mile, where 20 percent of accidents result in a spill. When a spill occurs, 20 percent of spills are greater than 30 percent of the contents. The analysis showed that a release is acceptable for Class F and lower at 0.3 mi. (0.5 km), is acceptable for Class G at 0.5 mi. (0.8 km), and is always acceptable for releases of 30 percent or less of the contents. There are a total of 404 allowable shipments per year of propane on US 51 past SHINE.

Though the annual number of shipments is unknown, this expected shipment frequency is acceptable for several reasons. First, there are no instances of propane listed in the Tier II reports for any facility within 5 mi. (8 km) of the facility. This implies that nearby industrial businesses are not receiving shipments of propane, and that trucks are supplying propane to residences or farms, which are less likely to require a 50,000 lb. (22,679 kg) truck delivery. Second, there are large propane facilities that service the surrounding area facility in Janesville, Milton, and Beloit, Wisconsin. These facilities are likely to distribute to locations nearer to them, which limits the expected number of trucks that travel between Janesville and Beloit, Wisconsin. These facilities are also expected to get their deliveries from I-90/39, as opposed to US 51. Propane trucks on I-90/39 (distance of 2.1 mi. [3.4 km]) are acceptable based on the results presented above. Therefore, it is expected that the number of shipments of 50,000 lb. (22,679 kg) of propane down US 51 is less than 404 per year.

The results of flammable vapor cloud ignition and explosion analyses are summarized in Table 2.2-17.

2.2.3.1.2.4 On-Site Chemicals

On-site chemicals are also analyzed for flammable vapor cloud explosions. The only on-site chemicals analyzed for a flammable vapor cloud are the deuterium and tritium used in the facility.

The bounding volume of deuterium at risk in one IU cell is roughly 1000 standard liters, which contains 0.39 lbs (0.18 kg) of deuterium. At the LEL for hydrogen, 4 percent, this corresponds to a volume of 883 ft3 (25 cubic meters [m^3]). The IU cells containing these gases are larger than these volumes; therefore, a deuterium detonation explosion is not expected. The tritium purification system (TPS) contains the largest inventory of tritium gases in a single location in the facility. The volume of the tritium purification system is larger than the volume required for to stay below the 4 percent LEL for hydrogen. Therefore, a tritium detonation explosion is not expected.

The results of flammable vapor cloud ignition and explosion analyses are summarized in Table 2.2-17.

2.2.3.1.2.5 Nearby Facilities and Railways

There are three additional off-site facilities and railways that store explosive chemicals that are identified for further analysis. The hazardous materials stored at nearby facilities that were identified for further analysis with regard to explosive potential are gasoline stored at Janesville Jet Center, ethylene oxide at Abitec, and methyl chloride and n-butyl alcohol at Evonik Goldschmidt. In addition, the methyl chloride and ethylene oxide are transported on the Union Pacific Railway. The methodology presented previously in Subsection 2.2.3.1.2 was used for determining the standoff distance for vapor cloud ignition and delayed vapor cloud explosion.

The 133,946 lb. (60,756 kg) tank of gasoline at Janesville Jet Center has a standoff distance to where the concentration falls below the LEL of 628 yd. (574 m), 0.36 mi. (0.57 km). The Janesville Jet Center is 0.9 mi. (1.45 km) from the facility.

A 440,000 lb. (199,580 kg) tank of ethylene oxide has a standoff distance to where the concentration falls below the LEL of 947 yd. (866 m), 0.54 mi. (0.87 km). The nearest instance of a large tank of ethylene oxide is the potential travel of such a tank via the Union Pacific Railway, 1.6 mi. (2.6 km) from the facility.

A 320,000 lb. (145,149 kg) tank of methyl chloride has a standoff distance to where the concentration falls below the LEL of 425 yd. (388 m), 0.24 mi. (0.39 km). The nearest instance of a large tank of methyl chloride is the Union Pacific Railway, 1.6 mi. (2.6 km) from the facility.

The ALOHA model shows that the vapor pressure of n-butyl alcohol at the analysis temperature of 81°F (27°C) is less than the LEL. Therefore, n-butyl alcohol cannot support a vapor cloud explosion at a distance of 3 mi. from the facility and a quantity of 25,160 lb.

The results of flammable vapor cloud ignition and explosion analyses are summarized in Table 2.2-17.

2.2.3.1.2.6 Flammable Vapor Cloud (Delayed Ignition) Related Impacts Affecting the Design

A facility is acceptable when the calculated rate of occurrence of severe consequences from any external accident is less than 1E-6 occurrences per year and reasonable qualitative arguments can demonstrate that the realistic probability is lower. Regulatory Guide 1.91 (USNRC, 1978) cites 1 psid (6.9 kPa) as a conservative value of peak positive incident overpressure, below which no significant damage would be expected. The facility's safety-related areas are designed to withstand a peak positive overpressure of at least 1 psid (6.9 kPa) without loss of function.

The analyses presented in this subsection demonstrate that a 1 psid (6.9 kPa) peak positive overpressure is not exceeded at a safety-related structure for any of the postulated flammable vapor cloud, delayed ignition event scenarios.

2.2.3.1.3 Toxic Chemicals

Accidents involving the release of chemicals in the vicinity of the plant or on-site were considered for their potential toxicity and ability to affect personnel in the facility control room.

On-site chemical releases are evaluated using the methodology described in Section 13b.3. Off-site chemical releases are evaluated in this subsection.

The potential for an off-site toxic gas release was evaluated within 5 mi. (8 km) of the site.

SHINE considered stationary sources and mobile sources expected to be transported on US 51, I-90/39, or on local railroads. The effects of a chemical release from a pipeline were considered bounded by the delayed ignition explosion of a pipeline.

Chemicals are screened in several ways. Only chemicals with vapor pressures greater than 10 Torr at 100°F were considered for further evaluation. Mobile sources were not considered if their shipment was not frequent (i.e., less than 10 shipments per year for truck traffic or 30 shipments per year for rail traffic).

In some cases, chemicals are screened as being bounded by other chemicals. A chemical determined to not present a toxic hazard to the site can be considered bounding to other chemicals that meet these four criteria: (1) have similar or lower vapor pressure; (2) have similar or lower toxicity; (3) are located similar or a farther distance away; and (4) are present in a similar or lower quantity. Additionally, to bound some chemicals, it was assumed that given identical meteorological conditions, initial chemical inventories, and travel distances:

a. A chemical that exists as a gas or vapor will result in higher downwind concentrations than one that exists as a liquid.
b. Volatile liquids, liquids with higher vapor pressures, or liquids with low boiling points near ambient temperatures will result in higher downwind concentrations than non-volatile liquids, liquids with lower vapor pressures, and liquids with high boiling points.
c. A spill or leak of a solid chemical will not result in significant atmospheric concentrations capable of incapacitating an operator at the site, regardless of the chemical. This is because solids typically have very low vapor pressures, and solid particulates are heavier than vapor or gas molecules, and are therefore much less widely dispersed in air.

Only those chemicals exceeding the above screening criteria are included in the list of bounding toxic chemicals provided in Table 2.2-19.

For these chemicals, airborne dispersion was evaluated deterministically, using worst-case wind directions, and a temperature and wind speed with an annual exceedance probability of 5 percent. Only maximum concentration accidents were evaluated based on releases of the maximum expected amounts of chemicals. These deterministic evaluations were performed using ALOHA, Version 5.4.4 (ALOHA, 2013) or through comparative analysis for chemicals that could not be directly modeled.

The facility control room in this evaluation was assumed to have an air-exchange rate of 1.2 exchanges per hour.

A two-minute exposure to National Institute for Occupational Safety and Health (NIOSH) Immediately Dangerous to Life and Health (IDLH) concentrations is considered the threshold for uninhabitability. For chemicals with no defined IDLH limit, Protective Action Criteria (PAC) Level 2 limits were used, or the chemical was screened against qualitative toxicity information if no quantitative limits were available. An on-site toxic gas release will not cause an accident or incapacitate operators. An off-site toxic gas release impacting the plant during normal operations does not initiate a design basis accident. This is because the target solution and related process products are contained within robust systems or within confinement barriers that would be unaffected by a toxic gas release. Therefore, an off-site toxic gas release will not adversely impact safety-related systems, structures, and components.

Although the automatic safety systems are designed to protect the public and maintain the plant in safe shutdown without operator intervention, and these safety systems would operate even if the operators are incapacitated, such operation would not be required in the event of a toxic gas release because an accident would not be initiated as a result of the release.

2.2.3.1.3.1 Pipelines

As discussed in Subsection 2.2.3.1.2.1, there are three bounding natural gas pipelines within 5 mi. (8 km) of the facility. Natural gas is predominantly methane. The toxicity hazard from methane is that of a simple asphyxiant, and there are no defined IDLH or Emergency Response Planning Guideline (ERPG) levels for methane. A cloud of methane would reach potentially explosive concentrations before displacing enough oxygen to cause asphyxiation. Therefore, the bounding hazard from natural gas is a potential explosion or fire, which was addressed in Subsection 2.2.3.1.2.1 and determined to not be a threat to the facility.

2.2.3.1.3.2 Waterway Traffic

There is no navigable waterway within 5 mi. (8 km) of the facility.

2.2.3.1.3.3 Highways

Table 2.2-19 provides a bounding list of toxic materials that may be transported on US 51 and I-90/39.

The closest SHINE safety-related area is located approximately 0.22 mi. (0.35 km) from US 51, and approximately 2.1 mi. (3.4 km) from I-90/39. For this analysis, these distances were also used as the distance from US 51 and I-90/39, respectively, to the facility control room.

The hazardous chemicals evaluated were primarily based on those chemicals identified in 2010 Tier II reports in Rock County, Wisconsin (Wisconsin Emergency Management, 2011). The selection of mobile sources for an analysis of potential impact to the facility control room was based on: (1) the mobile sources of hazardous chemicals described in Table 2.2-5; (2) stationary sources within 5 mi. (8 km) where deliveries or shipments could be transported on local roads; (3) large quantities of stationary sources elsewhere in the county where deliveries or shipments could be transported on major roads or rail lines; and (4) direct communication with facilities regarding their types, quantities, and frequencies of shipments.

If a chemical is known to be in a tank (i.e., chemicals transported by rail or on US 51 or I-90/39), the dispersion is modeled in ALOHA as a tank source, with the tank volume set to accommodate the entire mass of the chemical. A hole in the bottom of the tank is sized so that the entire tank inventory is released in one minute (minimum release time for ALOHA), and if the chemical is a liquid, forms a puddle that spreads to a maximum area that can be modeled, as determined by ALOHA. Ground type is the ALOHA default soil and ground temperatures are set to ambient conditions.

Chemicals transported by truck were modeled as release of 50,000 lbs of the chemical except for chlorine and sodium bisulfite.

Chlorine is shipped in 150-lb cylinders, one-ton containers, cargo tankers (15 to 22 tons), and up to 90-ton rail cars. The only users of chlorine within 5 mi. (8 km) of the site are the City of Janesville and the City of Beloit water utilities. The chlorine used is obtained in standard 150-lb cylinders (City of Beloit, 2015 and City of Janesville, 2015a). The maximum amount of chlorine at any one site is 900 lb. Therefore, a release of chlorine on US 51 is considered only for the case of the failure of one 150-lb cylinder. Chlorine releases on I-90/39 were considered for standard-size shipment containers (one ton containers (2,000 lbs) and 22 ton cargo tankers (44,000 lbs)).

Sodium bisulfite (which could generate sulfur dioxide) was modeled as a 15,000 lb release from US 51, since 15,000 lbs is the maximum inventory size of any current stationary location of sodium bisulfite (City of Janesville, 2015b).

Of the releases analyzed deterministically, only the following were found to be a potential hazard to the facility control room:

- Ammonia (50,000 lbs) from US 51
- Chlorine (44,000 lbs) from I-90/39
- Propylene oxide (50,000 lbs) from I-90/39
- Sodium bisulfite (15,000 lbs) from US 51

These mobile sources of chemicals were evaluated using a simple probabilistic model, based on shipment or inventory information from local users of those chemicals. The acceptance criteria for releases evaluated in this manner is 1E-6 releases per year because the resultant low levels of radiological risk are considered acceptable.

The following equation was used to determine the maximum number of shipments past the facility before the probability of a release exceeded 1E-6 per year.

$$R_{haz} = P_{spill} \times R_{accident} \times P_{weather} \times D_{trip} \qquad \text{(Equation 2.2-6)}$$

Where:

- R_{haz} is the rate of hazards per vehicle trip near the site (hazardous spills/trip)
- P_{spill} is the probability of the spill size (spills/accident)
- $R_{accident}$ is the rate of accidents (accidents/vehicle mile)
- $P_{weather}$ is the adverse wind direction probability (hazardous weather conditions at the site)
- D_{trip} is the hazardous trip length, the total number of miles that a vehicle travels past the site each trip where an accident could result in a hazardous condition (vehicle miles/trip)

Chlorine, propylene oxide and sodium bisulfite were eliminated as a hazard to the facility control room using this probabilistic method.

For chlorine, 53 cargo tanker shipments per year on I-90/39 past the site are required to exceed a release frequency of 1E-6. Without large producers or users of chlorine in the county, there are expected to be fewer than 53 cargo tanker shipments per year, and this release scenario therefore is not considered a hazard to the facility control room.

For propylene oxide, 58 truck shipments per year on US 51 are required to exceed a release frequency of 1E-6. Since the only user of propylene oxide within 5 mi. (Abitec Corporation) that receives shipments via truck has 6 shipments per year (Abitec Corporation, 2015), propylene oxide is not considered a hazard to the facility control room.

For sodium bisulfite, 553 truck shipments per year on US 51 are required to exceed a release frequency of 1E-6. Since the only current user of sodium bisulfite within 5 mi. has a reported storage quantity of 15,000 lbs, it is very unlikely they send or receive 553 shipments per year. Sodium bisulfite is therefore not considered a hazard to the facility control room.

A simple probabilistic analysis is not sufficient to eliminate ammonia from consideration as a hazard to the site. However, in the most limiting case of the closest, maximum inventory release, worst case wind directions, and 5 percent annual exceedance maximum wind speeds and atmospheric stability classes, the indoor toxicity limit is approached approximately one minute after the release, and outdoor concentrations begin to rise about 20 seconds after the release. Although there are only approximately 40 seconds between potential detection on-site and reaching the IDLH limit in the facility control room, the IDLH limit can be tolerated for 2 minutes without physical incapacitation. Therefore, the operators will be able to place the facility in a safe condition prior to the need to use personal protective equipment.

2.2.3.1.3.4 On-Site Chemicals

On-site chemical hazards are evaluated in Section 13b.3. This evaluation included exposure concentrations for workers located 328 ft. (100 m) downwind of a potential spill. The worker exposure calculations are considered representative of exposure to control room personnel. The results of this evaluation are presented in Table 13b.3-2.

These concentrations are calculated for a release of the largest container of each chemical on-site. The chemical dose or concentration for the nearest residence is below the PAC-1 level. For the workers postulated to be located within the boundary 328 ft. (100 m) downwind, the concentrations are below the PAC-1 values. Since the worker concentrations are below the PAC-1 levels for all chemicals considered, on-site chemical releases are not a hazard to the facility control room.

2.2.3.1.3.5 Nearby Facilities and Railways

Table 2.2-19 provides stationary sources of bounding toxic chemicals located within 5 mi. (8 km) of the site and bounding toxic chemicals potentially transported by rail near the facility.

The hazardous chemicals evaluated were primarily based on those chemicals identified in Tier II reports in Rock County, Wisconsin. Direct communication with individual facilities was used to augment the stationary source information identified in the Tier II reports.

Releases from rail lines are set at 1.6 mi. (2.6 km), which is the distance of the nearest approach of the Union Pacific Railway to the facility. Chemicals stored or situated at distances greater than 5 mi. (8 km) from the plant need not be considered because, if a release occurs at such a distance, atmospheric dispersion will dilute and disperse the incoming plume to such a degree that either toxic limits will never be reached or there would be sufficient time for the control room operators to take appropriate action.

The Tier II Report was reviewed for other chemicals used within in the region, not necessarily within 5 mi. (8 km) of the site, in a significant quantity (i.e., over 50,000 lbs), such that they may be frequently shipped by rail near the site. Chemicals already determined to not be hazardous based on vapor pressure or toxicity were not included.

Based on this review, acrylonitrile, which is used by a chemical manufacturer located greater than 5 mi. (8 km) from the site, was also considered for analysis based on the large amounts used by this manufacturer.

Assumptions for a rail line tank release were the same as used for highway tank release, as described in Subsection 2.2.3.1.3.3. The tank size for a rail line release was set to 30,000 gallons, and converted to an equivalent mass based on the estimated density of each material.

No release from a stationary source was determined to be a hazard to the facility control room, as shown in Table 2.2-19. For rail line releases, only ammonia had the potential to exceed toxicity levels in the facility control room under 5 percent annual exceedance probability worst case meteorological conditions. A probabilistic evaluation was not undertaken for rail shipments of ammonia, since this release was bounded by a postulated tanker truck release, as discussed in Subsection 2.2.3.1.3.3.

2.2.3.1.3.6 Toxic Chemical Related Impacts Affecting the Design

Of the chemicals evaluated, only an ammonia release could have a greater than 1E-6 per year potential to result in an uninhabitable control room, based on a simple probabilistic analysis. For the closest ammonia release, the evaluation shows that the control room operators would be able to shut down the facility (i.e., have at least two minutes) by manually tripping the target solution vessels (TSVs) prior to needing to use personal protective equipment. This single action ensures:

- Target solution is drained to the criticality-safe TSV dump tank(s);
- Decay heat from the target solution is removed via conduction through the dump tank(s) walls to the light water pool; and
- Hydrogen buildup in the primary system boundary is controlled via the target solution vessel off-gas system.

These actions will maintain the target solution in a safe shutdown condition. There are no radiological consequences to the workers or the public due to an off-site toxic gas release that affects the facility.

2.2.3.1.4 Fires

Accidents leading to high heat fluxes in the vicinity of the plant were considered. Fires in adjacent industrial plants and storage facilities, oil and gas pipelines, and fires from transportation accidents were evaluated as events that could lead to high heat fluxes.

Three types of fires are analyzed for high heat flux: BLEVE fireballs, pool fires, and jet fires. A BLEVE fireball occurs when a tank containing a flammable liquefied gas bursts. Similar to a BLEVE overpressure, the liquefied gas flashes. The energy released causes the flammable gas to ignite causing a large fireball. A BLEVE fireball typically has a high heat flux, but a short duration. Pool fires occur when a chemical that is liquid at standard conditions spills and catches fire. A jet fire occurs when a pipeline ruptures or pressurized tank has a hole causing the continuous release of flammable gas. Pool fires and jet fires can have much longer durations.

The limiting BLEVE fireball for the facility is the rupture of the propane truck. The truck contains 50,000 lb. (22,679 kg) of liquefied propane and is 0.22 mi. (0.35 km) from the facility. The computer program ALOHA was used to calculate the heat flux and duration of the fireball. The results show that the heat flux on the facility is 3424 British thermal units per hour per square foot (Btu/hr-ft^2) (10.8 kilowatts per square meter [kW/m^2])and that the duration of the fireball is 11 seconds (sec.). This would cause a temperature rise on a concrete wall surface of 32.4°F (18°C). This is not a significant temperature rise when compared to ACI 349-13, Code Requirements for Nuclear Safety-Related Concrete Structures and Commentary (ACI, 2014) standards for short- and long-term maximum concrete temperatures.

The limiting pool fire would come from a gasoline truck on US 51. The truck contains 50,000 lb. (22,679 kg) of gasoline and is 0.22 mi. (0.35 km) from the facility. The computer program ALOHA was used to calculate the heat flux for the pool fire. The results show that the maximum heat flux is 926 Btu/hr-ft^2 (2.92 kW/m^2) and that the fire lasts for 53 s. This would cause a temperature rise on a concrete wall surface of 43.2°F (24°C). This is not a significant temperature rise when compared to ACI 349-13 (ACI, 2014) standards for short- and long-term maximum concrete temperatures.

The limiting off-site jet fire is from the feeder pipeline 0.28 mi. (0.45 km) from the facility. The computer program ALOHA was used to calculate the heat flux for the jet fire. The results show that the maximum heat flux is 3.5 Btu/hr-ft^2 (0.011 kW/m^2). This heat flux is negligible compared with the solar heat flux (approximately 317 Btu/hr-ft^2 [1 kW/m^2]). Therefore, the pipeline jet fire is not considered a threat to the facility.

The limiting on-site jet fire is from the 3-in. pipeline that feeds the facility. The pressure is 115 pounds per square inch gauge (psig) (793 kilopascal [kPa] gauge) upstream of a pressure reducing station, and 54 psig (372 kPag) downstream of the pressure reducing station. The pressure reducing station is roughly 100 yd. (91.4 m) from the nearest safety-related area. The computer program ALOHA was used to calculate the heat flux for the jet fire. The results show that the maximum heat flux from a fire upstream of the pressure reducing station is 17.9 Btu/hr-ft^2 (0.0565 kW/m^2). This heat flux is negligible compared with the solar heat flux (approximately 317 Btu/hr-ft^2 [1 kW/m^2]).

Downstream of the pressure reducing station, the safe standoff distance to a 317 Btu/hr-ft^2 (1 kW/m^2) is 20 yd. (18 m). The accident rate, release rate and ignition rate apply here as they do in the vapor cloud explosion analysis. Because the standoff distance for a jet fire is substantially

less than the standoff distance for a vapor cloud explosion for the on-site pipeline, the jet fire analysis is bounded by the vapor cloud explosion analysis. A single ignition of gas from this pipeline is modeled as a failure for both explosion and fire analysis and would not be counted twice in the total probability.

The limiting heat fluxes due to chemical hazards are shown in Table 2.2-20.

Table 2.2-1 – Significant Industrial Facilities within 8 km (5 mi.) of the Site

Facility	Primary Function	Major Products Produced or Stored
Abitec Corporation	Chemical manufacturing	Personal care, pharmaceutical, and chemical manufacturing products
Crop Production Services	Agricultural retail supplier	Agricultural products, including fertilizers
Evonik Goldschmidt Corporation	Chemical manufacturing	Manufactures surfactants, specialty cleaning compounds, industrial organic chemicals and shampoo additives, alkyl sulfates, betaines, ether sulfates, quaternaries, sultaines, anti-foaming agents
Janesville Jet Center	Jet fuel supplier	Jet fuel
School District of Beloit Turner	Facilities for school	Diesel oil storage
United Parcel Service	Distribution	Parcel distribution
Dollar General Distribution Center	Distribution	Household products and consumables

References:
Abitec Corporation, 2012.
Crop Production Services, 2012.
Evonik Industries, 2012.
Manta, 2012(a-c)

Table 2.2-2 – Pipelines within 8 km (5 mi.) of the Site

Pipeline Owner	Fluid Carried	Closest Approach (mi.)	Nominal Size (inches)	Operating Pressure (psig)	Line Type
Alliant	Natural Gas	0.3	[ ]SRI	[ ]SRI	Feeder
Alliant	Natural Gas	2.6	[ ]SRI	[ ]SRI	Main Line
Alliant	Natural Gas	2.8	[ ]SRI	[ ]SRI	Main Line
Alliant	Natural Gas	3.8	[ ]SRI	[ ]SRI	Feeder
Alliant	Natural Gas	3.9	[ ]SRI	[ ]SRI	Feeder
Alliant	Natural Gas	4.0	[ ]SRI	[ ]SRI	Feeder
Alliant	Natural Gas	4.4	[ ]SRI	[ ]SRI	Feeder
ANR	Natural Gas	3.6	[ ]SRI	[ ]SRI	Main Line

References:
Alliant Energy, 2012
NPMS, 2019

Table 2.2-3 – Airports and Heliport Operations Located within 10 mi. (16 km) of the Site

Airport	Distance from SHINE Facility Center Point in Statute (km)	Number of Operations in 2018	Projected Number of Operations in 2045	$200d^2$ Screening Criterion[(a)] Screen Out (Yes/No)
Southern Wisconsin Regional Airport	0.63	37,674	46,443	N/A[(b)] (No)
Omniflight Heliport	0.63	Sporadic[(c)]	Sporadic[(c)]	N/A[(d)] (Yes)
St. Mary's Hospital Heliport	6.44	N/A[(e)]	Sporadic[(c)]	N/A[(d)] (Yes)
Mercy Hospital Heliport	7.24	Sporadic[(c)]	Sporadic[(c)]	N/A[(d)] (Yes)
Beloit Hospital Heliport	8.53	Sporadic[(c)]	Sporadic[(c)]	14,550 (Yes)
Hacklander Airport	12.55	Sporadic[(c)]	Sporadic[(c)]	31,515 (Yes)
Melin Farms Airport	14.00	Sporadic[(c)]	Sporadic[(c)]	39,207 (Yes)
Archie's Seaplane Base[(f)]	13.16	Sporadic[(c)]	Sporadic[(c)]	34,660 (Yes)
Beloit Airport	14.81	19,710[(g)]	19,710[(g)]	43,843 (Yes)
Miller Airport	14.97	Sporadic[(c)]	Sporadic[(c)]	44,801 (Yes)

(a) Airports considered in analysis if the airport is within 5 mi. (8 km) of the SHINE site, or if, for airports located a distance between 5 mi. (8 km) and 10 mi. (16 km) from the SHINE site, an airport has annual operations of more than $200d^2$ (where d is the distance to the SHINE facility in kilometers).
(b) Probabilistic hazard analysis needed because the distance is less than 5 mi. (8 km).
(c) Operations of private airports or those with no aircraft stationed at the airport are considered sporadic.
(d) Within 5 mi. (8 km), however, screens out. The subject heliports do not require separate analysis as they would be bounded by the analysis performed for the SWRA which utilizes larger aircraft, has significantly greater number of operations and is closer in distance to the facility.
(e) Heliport was established in 2014.
(f) This private airport does not appear to be in operation since operational data for the airport dates from 1991. It is, however, listed for completeness.
(g) Based on 54 operations per day.

Table 2.2-4 – Federal Airways within 10 mi. (16 km) of the Site

Airway	Distance from Airway Centerline to SHINE Site (mi.)[(a)]	Airway Width (mi.)[(a)]	Distance from Airway Edge to Center of SHINE Facility (mi.)[(a)]
V177	5.8	9.2	1.2
V24-97	10.5	9.2	5.9
V216	6.9	9.2	2.3
V63	5.3	9.2	0.7
V9-177	4.8	9.2	0.2
V97	12.4	9.2	7.8
V24	11.6	9.2	7
V9-63-128	10.9	9.2	6.3
V228	9.8	9.2	5.2
V246	11.6	9.2	7
J90	5.5	11.5	(b)

(a) Statute miles.
(b) The site is within the airway width.

Table 2.2-5 – Hazardous Chemicals Potentially Transported on Highways within 8 km (5 mi.) of the Site

Chemical	Quantity (lbs.)	Highway	DIstance to Site (mi.)
Ammonia	50,000	US 51	0.22
Asphyxiant Model (Carbon Monoxide)	50,000	US 51	0.22
Bounding Amide (Formamide)	50,000	US 51	0.22
Chlorine	150	US 51	0.22
Diesel	50,000	US 51	0.22
Ethylene Oxide	50,000	US 51	0.22
Gasoline	50,000	US 51	0.22
Jet Fuel (Kerosene)	50,000	US 51	0.22
Hydrogen Peroxide	50,000	US 51	0.22
Isopropanol	50,000	US 51	0.22
n-Butyl Alcohol	50,000	US 51	0.22
Propane	50,000	US 51	0.22
Propylene Oxide	50,000	US 51	0.22
Sodium Bisulfite (Sulfur Dioxide)	15,000	US 51	0.22
Styrene	50,000	US 51	0.22
Acetone	50,000	I-90/39	2.1
Chlorine	44,000	I-90/39	2.1
Hydrogen	3,300	I-90/39	2.1
Methyl Acetate	50,000	I-90/39	2.1
n-Heptane	50,000	I-90/39	2.1
Nitric Acid	50,000	I-90/39	2.1
Sodium Bisulfate (Sulfur Dioxide)	50,000	I-90/39	2.1
Sodium Hypochlorite (Chlorine)	50,000	I-90/39	2.1

Table 2.2-6 – Holding Patterns near the SHINE Facility

Airport	Holding Pattern	Runway	Distance from Holding Pattern to SHINE Facility Center Point (mi.)
Southern Wisconsin Regional Airport	CULMO	4	15.0
	TAYOR	14	14.4
	OTLEE	22	12.6
	TIRRO	32	12.4
Beloit Airport	Unnamed	7	6.7
Poplar Grove Airport	Unnamed	17	23.0

Table 2.2-7 – Maximum CONUS Values for Crashers per Year for Commercial and Military Aviation Nonairport Operations

	$N_j P_j f(x,y)$ Value[(a)] ($1/mi^2$)
Air Carrier	2E-06
Air Taxi	8E-06
General Aviation	3E-03
Small Military	6E-06
Military Helicopter	3.3E-07

Effective Area

	Wingspan[(b)] (ft.)	cot(φ)[(c)]	Skid Distance[(d)] (ft.)
Air Carrier	98	10.2	1440
Air Taxi	59	10.2	1440
General Aviation	50	8.2	60
Small Military	110	10.4	447
Military Helicopter	57.25[(e)]	0.58	0

(a) Reference (DOE, 2006), Tables B-14, B-15, and B-43
(b) Reference (DOE, 2006), Table B-16
(c) Reference (DOE, 2006), Table B-17
(d) Reference (DOE, 2006), Table B-18
(e) Wingspan noted is the helicopter length for the Bell UH-1 helicopter. The Bell UH-1 length is greater than its wingspan.

Table 2.2-8 – Calculated Effective Areas of Safety-Related Structure

Aircraft Type	Effective Area (mi^2)
Air Carrier	2.8E-02
Air Taxi	2.5 E-02
General Aviation	7.5 E-02[3]
Small Military	1.6 E-02
Military Helicopter	2.1 E-03

Table 2.2-9 – Total Crash Probability

	Large Non-Military Aircraft	Small Non-Military Aircraft	Military Aircraft
Total Probability	1.10E-7	3.92E-4	1.99E-7
Total Probability Considering Air Shows	1.90E-7	N/A[(a)]	5.37E-7[(b)]

(a) Small non-military aircraft increased air traffic is within 1 percent of total operations assumed in the total crash probability and is therefore excluded from evaluation.
(b) All military aircraft are assumed to be large military aircraft for a bounding evaluation.

Table 2.2-10 – Maximum Number of Operations per Year at Southern Wisconsin Regional Airport

Aircraft Type	Number of Operations
Air Carrier (itinerant)	17
Air Taxi (itinerant)	11,245
General Aviation (itinerant)	17,407
Military (itinerant)	343
Civil (local)	23,500
Military (local)	553

References:
USDOT, 2019a
USDOT, 2019b

Table 2.2-11 – Aircraft Operations[(a)] by Aircraft Type on Each Runway

Runway	Air Carrier	Air Taxi	General Aviation	Small Military	Military Helicopter
14	2	1574	5727	1	124
32	4	2361	8590	2	186
4	5	3374	12272	3	266
22	3	2249	8181	2	177
18	1	843	3068	1	67
36	1	843	3068	1	67

(a) Number (per year) of movements by each aircraft

Table 2.2-12 – Distance from Southern Wisconsin Regional Airport to SHINE Facility

Runway Number	Distance (mi.)[(a)]
14	1.57
32	0.87
4	1.54
22	0.44
18	0.64
36	0.89

(a) Distance from each runway end to the facility center point

Table 2.2-13 – Crash Probability[(a)] (x 10^{-8}) by Aircraft and Distance from the Site

Distance from site (mi.)	Runway	Air Carrier	Air Taxi	General Aviation	USN/ USMC[(b)]	USAF[(c)]
1.57	14	4	26	15	1	2
0.87	32	17	109	84	8	5
1.54	4	4	26	15	1	2
0.44	22	17	109	84	8	5
0.64	18	17	109	84	8	5
0.89	36	17	109	84	8	5

(a) Probability per square mile of a crash per aircraft movement
(b) U.S. Navy/U.S. Marine Corps
(c) U.S. Air Force

Table 2.2-14 – Maximum Operations at the Southern Wisconsin Regional Airport for the Years 2019 through 2045 and Projected Operations from a Future Air Show

Aircraft Type	Maximum Operations 2019 through 2045	Projected Operations from Future Air Show
Air Carrier	17	15
Air Taxi	11,245	77
General Aviation	17,407	77
Civil	23,500	77
Military (itinerant)	343	77
Military (local)	503	77

Table 2.2-15 – Bounding Explosive Chemical Hazards within 5 mi. (8 km) of the Site

Chemical	Location	DIstance	Quantity	Explosion Type
Diesel Fuel	Bounding Instance	0.5 mi.	1,258,091 lbs.	Stationary
Ethylene Oxide	Abitec / Rail	1.6 mi.	440,000 lbs.	Stationary, Vapor Cloud
Gasoline	Janesville Jet Center	0.9 mi.	133,946 lbs.	Stationary, Vapor Cloud
Jet Fuel (Kerosene)	Bounding Instance	0.22 mi.	79,968 lbs.	Stationary
Methylchloride	Evonik / Rail	1.6 mi.	320,000 lbs.	Vapor Cloud
n-Butyl Alcohol	Evonik Goldschmidt	3 mi.	25,160 lbs.	Vapor Cloud
Deuterium/Tritium	On-site	N/A	280 g	Stationary, Vapor Cloud
Diesel Fuel	Truck (Highway 51)	0.22 mi.	50,000 lbs.	Stationary
Ethylene Oxide	Truck (Highway 51)	0.22 mi.	50.000 lbs.	Stationary, Vapor Cloud
Gasoline	Truck (Highway 51)	0.22 mi.	50,000 lbs.	Stationary, Vapor Cloud
Propane	Truck (Highway 51)	0.22 mi.	50,000 lbs.	Stationary, Vapor Cloud, BLEVE
Hydrogen	Truck (I-90/39)	2.1 mi.	3,300 lbs.	Stationary, Vapor Cloud
Natural Gas (Methane)	Pipeline (West of Hwy 51)	0.28 mi.	NA	Vapor Cloud
Natural Gas (Methane)	Pipeline (East of I-90/39)	2.5 mi.	NA	Vapor Cloud
Natural Gas (Methane)	On-site service	NA	NA	Vapor Cloud

References:
Abitec Corporation, 2012.
Crop Production Services, 2012.
Evonik Industries, 2012.
Manta, 2012(a-c).
Rock County, 2012.

Table 2.2-16 – Stationary Explosion Analysis

Chemical	Location	Distance	Quantity	Acceptable Instance[(a)]
Diesel Fuel	Bounding Instance	0.5 mi.	1,258,091 lbs.	1,258,091 lbs. at 0.22 mi.
Ethylene Oxide	Abitec / Rail	1.6 mi.	440,000 lbs.	440,000 lbs. at 0.22 mi.
Gasoline	Janesville Jet Center	0.9 mi.	133,946 lbs.	133,946 lbs. at 0.22 mi.
Jet Fuel (Kerosene)	Bounding Instance	0.22 mi.	79,968 lbs.	500,000 lbs. at 0.22 mi.
Deuterium/Tritium	On-site	N/A	280 grams	Low probability; Safety features designed into systems
Diesel Fuel	Truck (Highway 51)	0.22 mi.	50,000 lbs.	1,258,091 lbs. at 0.22 mi.
Ethylene Oxide	Truck (Highway 51)	0.22 mi.	50.000 lbs.	440,000 lbs. at 2 mi.
Gasoline	Truck (Highway 51) bounding	0.22 mi.	50,000 lbs.	133,946 lbs. at 0.22 mi.
Propane	Truck (Highway 51)	0.22 mi.	50,000 lbs.	55,724 lbs. at 0.22 mi.
Propane BLEVE	Truck (Highway 51)	0.22 mi.	50,000 lbs.	50,000 lbs. at 0.22 mi.
Hydrogen	Truck (I-90/39)	2.1 mi.	3300 lbs.	18,196 lbs. at 0.22 mi.

(a) The Acceptable Instance shows the analyzed condition that bounds the hazard in both distance and mass.

Table 2.2-17 – Flammable Vapor Cloud Explosion Analysis

Chemical	Location	Distance	Mass/ Volume	Acceptable (Standoff Distance)
Ethylene Oxide	Abitec / Rail	1.6 mi.	440,000 lbs.	0.54 mi.
Gasoline	Janesville Jet Center	0.9 mi.	133,946 lbs.	0.36 mi.
Methylchloride	Evonik / Rail	1.6 mi.	320,000 lbs.	0.24 mi.
N-Butyl Alcohol	Evonik Goldschmidt	3 mi.	25,160 lbs.	Vapor Pressure < LEL, no flammable vapor cloud
Deuterium/Tritium	On-site	N/A	280 grams	Vapor Volume at LEL < volume of room, not confined
Ethylene Oxide	Truck (Highway 51)	0.22 mi.	50,000 lbs.	99 allowable shipments, few expected
Gasoline	Truck (Highway 51)	0.22 mi.	50,000 lbs.	0.214 mi.
Propane	Truck (Highway 51)	0.22 mi.	50,000 lbs.	404 allowable shipments
Hydrogen	Truck (I-90/39)	2.1 mi.	3300 lbs.	0.77 mi.
Natural Gas (Methane)	Pipeline (West of Hwy 51)	0.28 mi.	NA	0.24 mi.
Natural Gas (Methane)	Pipeline (East of I-90/39)	2.5 mi.	NA	2.2 mi.
Natural Gas (Methane)	On-site service	NA	NA	Probability < 1.1E-6/yr

Table 2.2-18 – On-Site Pipeline Analysis

Parameter	Case 1: Small Break	Case 2: Upstream of Regulator Class G Big Break	Case 3: Upstream of Regulator Class F Big Break	Case 4: On-site Big Break
Accident Rate (breaks per pipeline-mi. per year)	1.5E-3	1.5E-3	1.5E-3	1.5E-3
Break Size Probability	0.8	0.2	0.2	0.2
Explosion Probability Given Release (explosions per break)	1E-3	5E-3	5E-3	5E-3
Probability of Adverse Weather	1	0.11349	0.10080	1
Exposure Distance (pipeline-mi.)	0.27	0.17	0.08	0.27
Explosions (/yr)	3.2E-7	2.9E-8	1.2E-8	4.1E-7
Total for four cases (/yr)	7.7E-7			

Table 2.2-19 – Bounding Toxic Chemical Hazards within 8 km (5 mi.) of the Site (Sheet 1 of 3)

Chemical	Location	Distance (mi.)	Mass (lbs.)	Disposition
Polymer dispersion (1,3-butadiene)	Humane Manufacturing	1	58,800	No Hazard
Polymer dispersion (benzene)	Humane Manufacturing	1	58,800	No Hazard
Asphyxiant Model (carbon monoxide)	Linde Merchant Production	2	5,000,000	No Hazard
Bounding Amide (Formamide)	Abitec Corporation and Evonik Goldschmidt (Bounding Case)	2	640,000	No Hazard
Bounding Amine (diethylamine)	Abitec Corporation and Evonik Goldschmidt (Bounding Case)	2	640,000	No Hazard
Bounding Amine (n-Butylamine)	Abitec Corporation and Evonik Goldschmidt (Bounding Case)	2	640,000	No Hazard
Ethylene Oxide	Abitec Corporation	2	440,000	No Hazard
Isopropanol	Abitec Corporation	2	185,800	No Hazard
Oxygen	Linde Merchant Production	2	2,150,000	No Hazard
Volatile Amine (cyclohexylamine)	WI School for the Visually Handicapped	2	300	No Hazard
Benzyl acetate	Evonik Goldschmidt	3	12,321	No Hazard
Chlorine	Janesville Pump Station #12	3	900	No Hazard
Ethyl Alcohol	Evonik Goldschmidt	3	168,000	No Hazard
Hydrogen Peroxide	Evonik Goldschmidt	3	60,000	No Hazard
Methyl Chloride	Evonik Goldschmidt	3	320,000	No Hazard
n-Heptane	Evonik Goldschmidt	3	125,000	No Hazard
Sodium Bisulfite (as sulfur dioxide)	Evonik Goldschmidt	3	15,000	No Hazard
Sodium Chlorite (as chlorine dioxide)	Evonik Goldschmidt	3	14,000	No Hazard
Styrene	Monterey Mills	3	225,280	No Hazard
Volatile Amine (DMAPA)	Evonik Goldschmidt	3	12,045	No Hazard

Table 2.2-19 – Bounding Toxic Chemical Hazards within 8 km (5 mi.) of the Site (Sheet 2 of 3)

Chemical	Location	Distance (mi.)	Mass (lbs.)	Disposition
Propylene Oxide	Evonik Goldschmidt and Rail (Bounding Case)	1.6	360,000	No Hazard
Acrylonitrile	Rail	1.6	199,852	No Hazard
Ammonia	Rail	1.6	150,054	Additional Evaluation
Bounding Amide (Formamide)	Rail	1.6	282,214	No Hazard
Bounding Amine (diethylamine)	Rail	1.6	175,391	No Hazard
Bounding Amine (n-Butylamine)	Rail	1.6	183,538	No Hazard
Ethylene Oxide	Rail	1.6	216,317	No Hazard
Methyl Chloride	Rail	1.6	227,428	No Hazard
Vinylidene Chloride	Rail	1.6	300,966	No Hazard
Ammonia	Truck (US 51)	0.22	50,000	Additional Evaluation
Asphyxiant Model (Carbon Monoxide)	Truck (US 51)	0.22	50,000	No Hazard
Bounding Amide (Formamide)	Truck (US 51)	0.22	50,000	No Hazard
Chlorine	Truck (US 51)	0.22	150	No Hazard
Ethyl Alcohol	Truck (US 51)	0.22	50,000	No Hazard
Gasoline (as butane)	Truck (US 51)	0.22	50,000	No Hazard
Gasoline (as toluene)	Truck (US 51)	0.22	50,000	No Hazard
Hydrogen Peroxide	Truck (US 51)	0.22	50,000	No Hazard
Isopropanol	Truck (US 51)	0.22	50,000	No Hazard
n-Butyl Alcohol	Truck (US 51)	0.22	50,000	No Hazard
Propane	Truck (US 51)	0.22	50,000	No Hazard
Propylene Oxide	Truck (US 51)	0.22	50,000	Additional Evaluation
Sodium Bisulfite (as sulfur dioxide)	Truck (US 51)	0.22	15,000	Additional Evaluation
Styrene	Truck (US 51)	0.22	50,000	No Hazard
Acetone	Truck (I-90/39)	2.1	50,000	No Hazard

Table 2.2-19 – Bounding Toxic Chemical Hazards within 8 km (5 mi.) of the Site (Sheet 3 of 3)

Chemical	Location	Distance (mi.)	Mass (lbs.)	Disposition
Chlorine	Truck (I-90/39)	2.1	2,000	No Hazard
Chlorine	Truck (I-90/39)	2.1	44,000	Additional Evaluation
Hydrogen	Truck (I-90/39)	2.1	50,000	No Hazard
Methyl Acetate	Truck (I-90/39)	2.1	50,000	No Hazard
n-Heptane	Truck (I-90/39)	2.1	50,000	No Hazard
Nitric Acid	Truck (I-90/39)	2.1	50,000	No Hazard
Sodium Bisulfite (as sulfur dioxide)	Truck (I-90/39)	2.1	50,000	No Hazard
Sodium Hypochlorite (as chlorine)	Truck (I-90/39)	2.1	50,000	No Hazard

Table 2.2-20 – Heat Flux Analysis

Chemical	Location	Distance (mi.)	Mass/Volume	Heat Flux	Duration	Concrete Wall Heat Up[(a)]
Gasoline	Truck (Highway 51)	0.22	50,000 lbs	2.92 kW/m^2	53 sec.	43°F
Propane	Truck (Highway 51)	0.22	50,000 lbs	10.8 kW/m^2	11 sec.	32°F
Natural Gas (Methane)	Pipeline (West of Highway 51)	0.28	N/A	0.011 kW/m^2	Indefinite	Indefinite
Natural Gas (Methane)	On-site service	N/A	N/A	Bounded by VCE analysis (Table 2.2-18)	Indefinite	Indefinite

(a) From ACI standard 349-13, temporary concrete temperatures of up to 350°F and long-term concrete temperatures of 150°F are acceptable. The 43°F temperature increase above ambient temperature does not exceed the ACI limits.

Figure 2.2-1 – Facilities and Transportation within 8 km (5 mi.) of the Site

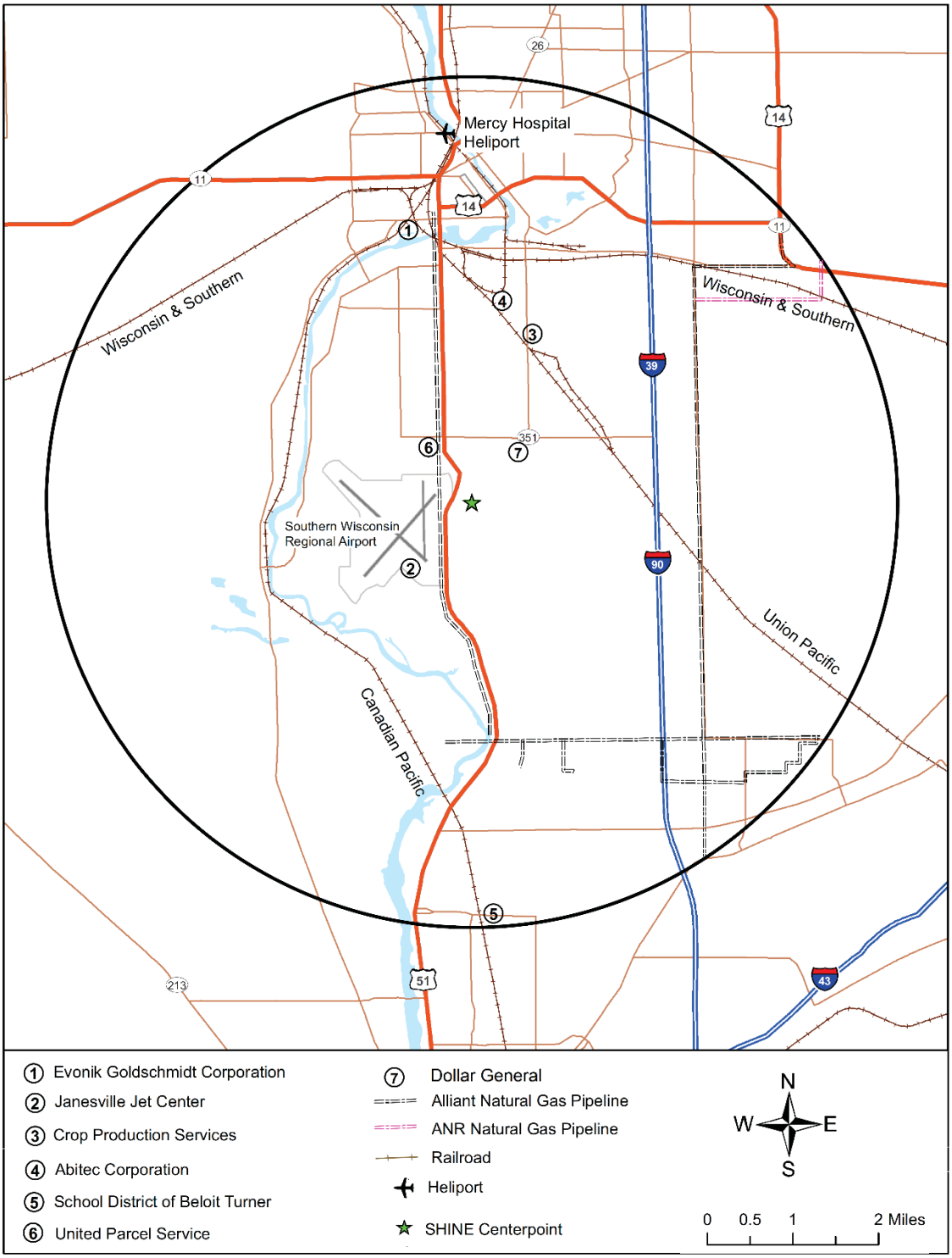

Figure 2.2-2 – Airports/Heliports and Airway Centerlines within 10 mi. (16 km) of the Facility

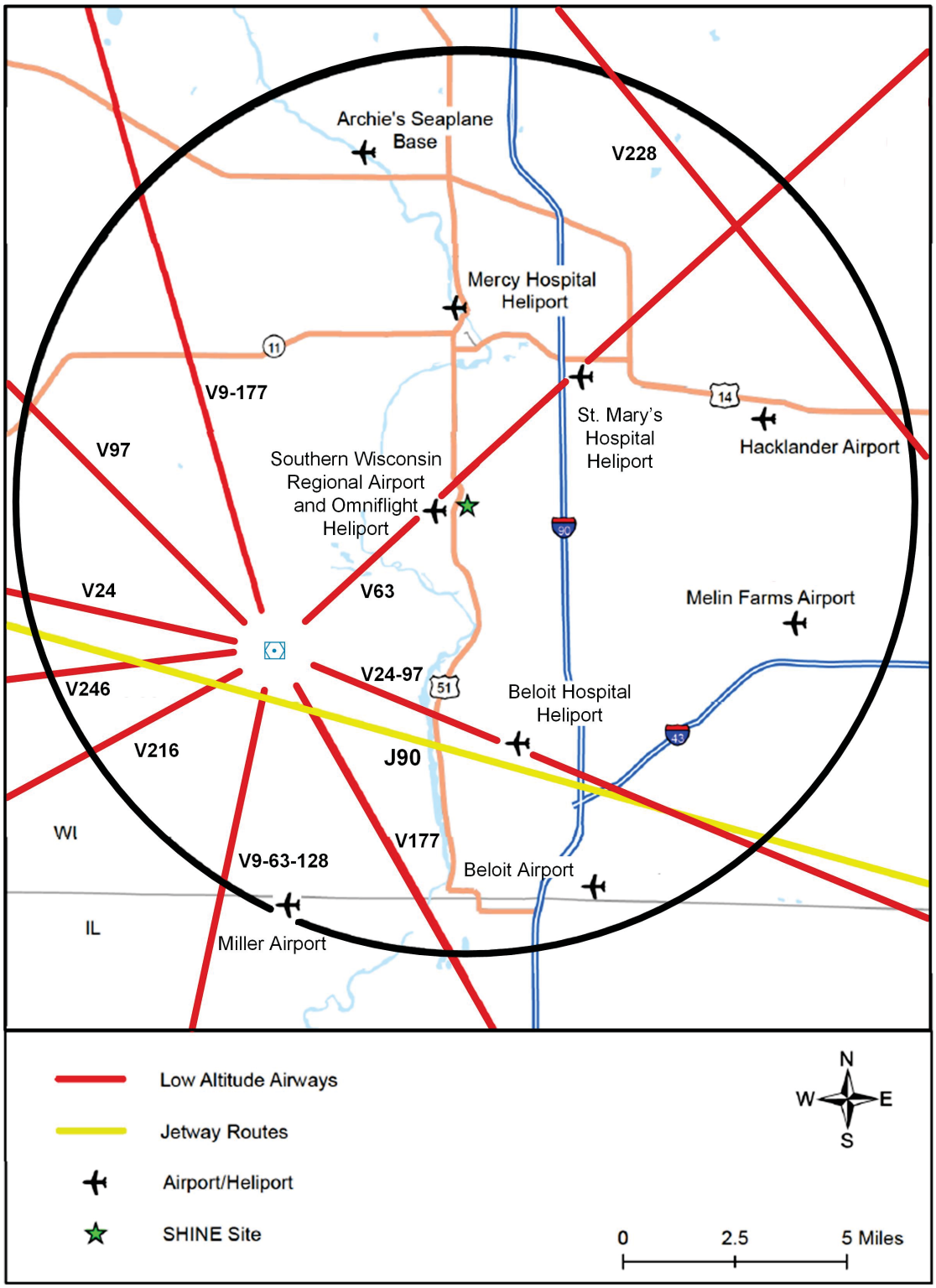

2.3 METEOROLOGY

2.3.1 GENERAL AND LOCAL CLIMATE

2.3.1.1 Introduction

Climate is a statistical description of the weather conditions that occur during a long period of time, usually several decades. Weather refers to short term variations (minutes to months) in the atmosphere.

Sources of data typically used to analyze the climate at a site include weather maps (depictions of areal weather phenomena at one instant of time), atlas maps summarizing long term climate, records of weather at specific monitoring stations at single instants of time, and long term climatic statistics at specific monitoring stations.

The purpose of analysis of regional climate is to understand the local climate at the SHINE site in the context of the climate of the surrounding area. Climate phenomena are then analyzed at progressively smaller scales and within progressively smaller areas. As the area being analyzed decreases, some monitoring stations that are considered initially in the broad analysis are excluded because these stations are found to be unrepresentative of the site climate. The end result is a documented, systematic approach that defines local climate within a context that includes a broad surrounding region.

2.3.1.2 Regional Climate

The SHINE site is located in south-central Wisconsin. The following discussion summarizes a variety of information that describes the general region in which the site is located. Because the information is derived from a variety of sources, the geographic area implied by the term "region" is somewhat variable in this introductory discussion. Subsection 2.3.1.2.1 defines a more specific region considered to have a climate representative of the site, and the subsequent subsections present detailed climatological data for that specific region.

The SHINE site is located in a region with the Köeppen classification "Daf", which is a humid continental climate with warm summers, snowy winters, and humid conditions (Trewartha, 1954). The climate features a large annual temperature range and frequent short duration temperature changes (NCDC, 2019a). Although there are no pronounced dry seasons, most of the annual precipitation falls during the summer. During the autumn, winter, and spring, strong synoptic scale surface cyclones and anticyclones frequently move across the site region. During the summer, synoptic scale cyclones are usually weaker and pass north of the site region. Most air masses that affect the site region are generally of polar origin. However, air masses occasionally originate from arctic regions, or the Gulf of Mexico. Air masses originating from the Gulf of Mexico generally do not reach the site region during winter months. There are occasional episodes of extreme heat or high humidity in the summer. The windiest months generally occur during the spring and autumn. The annual average number of days with thunderstorms varies from approximately 45 at the southwest corner of the state of Wisconsin, to approximately 35 at the northeast corner of the state (Moran, J. M. and E. J. Hopkins, 2002). Hail is most frequent in the southwestern and west central portions of the state, and is most common during summer months, peaking in late July. Tornadoes are relatively infrequent. Winter storms that affect the region generally follow one of three tracks shown in Figure 2.3-1: Alberta, Panhandle, and Gulf

Coast tracks. During an average winter, the ground is covered with 1 inch (in.) (2.54 centimeters [cm]) or more of snow about 60 percent of the time (NCDC, 2019b).

Regional land use is primarily cropland (corn and beans) and dairying (Rand McNally, 1982 and 2005). The natural vegetation includes broadleaf deciduous trees (oak and hickory), evergreen trees, and medium height prairie grass. There are also several urban areas. The soil at the site is well-drained silt loam.

The landforms of Wisconsin are described by the five physiographic provinces plotted on the map in Figure 2.3-2. Details of vegetation, topography, and elevations for those provinces are described in Table 2.3-1 (Moran, J. M. and E. J. Hopkins, 2002). Most of the surface water impoundments in Wisconsin are located in the Northern Highland and Eastern Ridges and Lowlands physiographic provinces. Water also flows through extensive wetlands in the form of marshes and swamps. The Northern Highland province has the highest elevations, from which water drains northward to Lake Superior; eastward to Lake Michigan via the Menominee and Wolf Rivers; and westward to the Mississippi River via the St. Croix, Chippewa, Black, and Wisconsin Rivers. The Western Uplands province, which comprises most of the western border of the state with Minnesota, escaped recent glaciation. This allowed streams and rivers to form deeply incised valleys over geologic time. Portions of the uplands are referred to as the "driftless area" due to the lack of glacial debris, or "drift".

Lake breeze phenomena occur near the shorelines of large bodies of water, such as Lake Michigan, which borders Wisconsin on the east (Moran, J. M. and E. J. Hopkins, 2002). These phenomena feature a circulation system in which air rises over the land and descends over the water, flows from the water toward the land near the ground surface, and flows from land toward the lake aloft. At the surface, the lake breeze appears as a relatively cool and humid wind that sweeps inland. The leading edge of a lake breeze is a miniature cold front and is referred to as the lake breeze front. As the lake breeze front moves inland, it lifts warmer air upward, sometimes causing clouds or showers. The inland penetration of the lake breeze front varies from a few hundred yards to as much as 25 miles (mi.) (40.2 kilometers [km]) (Moran, J. M. and E. J. Hopkins, 2002). Since the site is located approximately 60 mi. (96.6 km) west of Lake Michigan, it is located too far from the lake be affected by lake breezes. Inland lakes that are located in the SHINE site region are too small to be associated with lake breeze circulations. Therefore, lake breeze circulations are not expected to affect the project site.

The local radiation balance and winds determine temperatures across the state. Movement of air masses, synoptic scale fronts, and synoptic scale cyclones and anticyclones strongly influence local temperature and precipitation. Seasonal changes in the intensity and movements of air masses and synoptic-scale weather systems, plus changes in radiation exposure at the ground bring about seasonal changes in temperature and precipitation. North and northwest winds generally bring cold, dry air. South and southeast winds typically bring warm, humid air. Calm wind conditions allow pooling of colder, denser air at locations with lower elevations such as valleys. Unequal rates of diurnal heating of the ground cause some local valley and hillside airflows.

Maps of monthly mean dry bulb temperatures in Wisconsin are presented in Figure 2.3-3 through Figure 2.3-6 (Moran, J. M. and E. J. Hopkins, 2002). Mean monthly temperatures for winter (Figure 2.3-3) show cooler temperatures at the northern end of the state, warmer temperatures near Lake Michigan, and slightly warmer temperatures near Lake Superior. Figure 2.3-4 presents mean monthly temperatures in the spring. The springtime monthly temperature pattern

in Figure 2.3-4 is similar to the wintertime temperature pattern in Figure 2.3-3, with colder temperatures in the north interior. The counties that border the Great Lakes have cooler temperatures during spring, since the water warms at a slower rate than the land and thereby cools the air near the shorelines.

Mean monthly temperatures for summer (Figure 2.3-5) show a pattern similar to springtime monthly mean temperatures in Figure 2.3-4, with warmer interior temperatures in the south. Counties adjacent to Lakes Michigan and Superior are slightly cooler because the lake surfaces are relatively cooler than the land during the summer.

Mean monthly temperatures for autumn (Figure 2.3-6) show warmer conditions in the southern interior. The temperatures show a pattern similar to those in the winter, with warmer temperatures at counties near the lake, since the land cools more quickly than the water.

Wisconsin counties that border Lakes Michigan and Superior experience somewhat cooler summers, milder winters, and longer agricultural growing seasons than those counties at greater distances from the lakes. The lakes also occasionally produce lake effect snow during late autumn through winter.

Maps of monthly mean liquid-equivalent precipitation in Wisconsin are presented in Figure 2.3-7 through Figure 2.3-10 (Moran, J. M. and E. J. Hopkins, 2002). Generally, the average annual precipitation is higher in southern portions of the Midwest due to the proximity of the Gulf of Mexico, which is a major source of moisture (EDS, 1968). That same general pattern is observed over the state of Wisconsin. Superimposed over that general pattern is a local pattern of periodic lake effect precipitation. During lake effect precipitation events, Lakes Superior and Michigan are local sources of moisture that can cause precipitation adjacent to and downwind of the lake shorelines. Those periods of precipitation enhancement tend to occur when the lake water is warmer than the air, which is generally in winter. For example, the winter month precipitation in Figure 2.3-7 shows higher monthly water equivalent precipitation totals (approximately 1.2 to 2.2 in. [3.0 to 5.6 cm]) near the north and east boundary counties, caused by lake effect snow from Lakes Michigan and Superior.

The Madison, Wisconsin and Rockford, Illinois National Oceanic and Atmospheric Administration (NOAA) weather observing stations from Madison, WI and Rockford, IL were used (NCDC, 2019b, NCDC, 2019c). "First-order" stations are defined as those on a 24-hour per day, year-round observing schedule with trained, certified observers. The weather stations are located approximately 40 mi. (64.4 km) north-northwest and 30 mi. (48.3 km) south-southwest of the site, respectively.

Climatic statistics for Madison presented in Table 2.3-2 (NCDC, 2019b) show that monthly mean wind speeds range from 6.4 miles per hour (mph) (2.9 meters per second [m/s]) during the month of August to 9.9 mph (4.4 m/s) during the month of April. The annual mean wind speed is 8.2 mph (3.7 m/s). Monthly prevailing wind directions are from the south-southwest during all months except the winter months of January and February, when the monthly prevailing winds are all from the northwest. The annual prevailing wind is from the south-southwest.

Climatic statistics for Rockford presented in Table 2.3-3 (NCDC, 2019c) show that monthly mean wind speeds are similar to those for Madison and range from 6.8 mph (3.0 m/s) during the month of August, to 11.1 mph (5.0 m/s) during the month of April. The annual mean wind speed is 9.2 mph (4.1 m/s). Monthly prevailing wind directions are similar to Madison and blow from the

south-southwest direction during all months except the period January through April, when the monthly prevailing winds have northerly components. The annual prevailing wind is from the south-southwest.

Monthly mean relative humidities for Madison range from 66 percent during April and May, to 78 percent during December (Table 2.3-2). Rockford monthly mean relative humidities presented are similar to those from Madison, ranging from 66 percent during April and May, to 80 percent during December (Table 2.3-3).

Mean monthly water equivalent precipitation and snowfall for Madison and Rockford (Table 2.3-2 and Table 2.3-3) are similar. Water equivalent precipitation ranges from minima of 1.23 in. (3.12 cm) during January in Madison and 1.37 in. (3.48 cm) during January in Rockford, to maxima during June of 4.54 in. (11.53 cm) at Madison, and during June of 4.65 in. (11.81 cm) in Rockford.

Mean monthly snowfall is limited to the months October through April at Rockford and October through May at Madison. Snowfall ranges from a minimum of 0.1 in. (0.25 cm) during October at Rockford to a maximum of 13.5 in. (34.29 cm) during December at Madison. Annual snowfall is 50.9 in. (129.29 cm) at Madison and 36.7 in. (93.22 cm) at Rockford.

Table 2.3-4 presents the mean numbers of days per month and per year of rain or drizzle, freezing rain or drizzle, snow, and hail or sleet at Madison and Rockford. Those parameters have very similar values for the two stations. Snow typically occurs during 75 days per year at Madison, and 68 days per year at Rockford. Hail or sleet typically occurs during 2 days per year at both Madison and Rockford. Freezing rain or drizzle typically occurs during 2 days per year at both Madison and Rockford.

2.3.1.2.1 Identification of Region with Climate Representative of the Site

The process of comparison of local (site) and regional climates requires a determination of which region is considered "representative" of climate at the SHINE site. That determination is described in this subsection.

The SHINE site is located in central Rock County, Wisconsin which is at the south-central edge of the state. It is located near the boundary of two Wisconsin physiographic provinces as presented in Figure 2.3-2; the Western Uplands and the Eastern Ridges and Lowlands. It is located in NOAA Cooperative Observer Network (COOP) Climate Division 8 South Central (Figure 2.3-11). The finished site grade elevation is approximately 825 ft. (252 m) NAVD 88. The land use in the site area is rural.

Summarizing, the site location is defined by the following characteristics:

- Located in south-central Wisconsin, on rural prairie silt-loam soil.
- Located within till plains glacial deposits on the Central Lowland Province of the Interior Plains Division of the United States. It is on the border between the state of Wisconsin Eastern Ridge/Lowland and Western Upland Terrain, and most like the ridge/lowland to the east because the local topography is relatively gently rolling.
- Located outside the zone of influence of Lake Michigan lake breeze circulation systems.
- Located within the zone of influence of Lake Michigan effects on temperature and precipitation, including the following: added local warmth during winter and autumn,

cooling during summer and spring, and additional local precipitation during winter, spring, and autumn.

Based on the above summary characteristics, the perimeter of a surrounding geographic region, which is characterized as having the same climate as the site, is plotted on the regional map in Figure 2.3-12. That perimeter is bounded as follows:

- Bounded on the east by the 25-mi. (40.2 km) distance of maximum inland penetration of lake breeze circulations from Lake Michigan.
- Bounded on the south by the approximate southward limit of Lake Michigan's effects on the local climate of north-central Illinois, as presented in the mean precipitation and snowfall patterns in Figure 2.3-13 and as described by local climatological data summaries for major Illinois monitoring stations. Annual isohyets and lines of equal snowfall are oriented northwest to southeast at the northeast corner of Illinois as shown in Figure 2.3-13 and Figure 2.3-14, illustrating the effects of Lake Michigan on northern Illinois precipitation. Increased clouds and cooling effects due to Lake Michigan (Figure 2.3-15) are described in the climatological summary for Rockford, Illinois (NCDC, 2019c), but are not described in the climatological summaries for Springfield, Illinois farther to the south (NCDC, 2019d), or Moline, Illinois farther to the southwest (NCDC, 2019e).
- Bounded on the west by the approximate westward limit of Lake Michigan’s effects on the local climate of southern Wisconsin, as presented in the mean monthly temperature and precipitation, maps in Figure 2.3-3 through Figure 2.3-10.
- Bounded on the north by the approximate northward limit of Lake Michigan’s effects on the local climate of central Wisconsin, as presented in the mean temperature and precipitation maps in Figure 2.3-3 through Figure 2.3-10.
- Bounded on the north by the approximate mean southern boundary of the Wisconsin Central Plain, as presented in Figure 2.3-2.

This site climate region is then used to identify regional weather monitoring stations and Wisconsin and Illinois counties that can be used for comparisons in the analysis of local and regional climate.

2.3.1.2.2 Regional Data Sources

The site climate region is identified in Identification of Region with Climate Representative of the Site. Meteorological parameters from weather stations in the site climate region are available from a number of published data sources. Those data sources are described below.

- Climatography of the United States No. 20 (Clim-20) statistical summaries from the National Climatic Data Center (NCDC).

  Clim-20 publications are typically available for cooperative (COOP) daily weather monitoring stations located within the site climate region. Those publications are of particular interest to agriculture, industry, and engineering applications. The publications include a variety of climate statistics useful for regional climate analysis. Those parameters include dry bulb temperature, daily precipitation, and snow fall. Descriptive statistics of those parameters include: mean, extremes, and mean number of days exceeding threshold values. After 2000, the Clim-20 publications were replaced with summaries in digital format (NCDC, 2019f-aa).

COOP stations do not generally record humidity related parameters, such as relative humidity, dew point or wet bulb temperatures. Therefore, wet bulb temperatures that are coincident with extreme dry bulb temperatures, which are of interest in regional climate analysis, are generally not available for COOP stations. Therefore, for COOP stations, it is often necessary to estimate coincident wet bulb temperatures using wet bulb temperatures recorded at other stations.

- Climatological statistics available from Local Climatological Data (LCD) summaries published by NCDC.

  LCD annual summaries are typically available for meteorological stations located at major airports. Those summaries include climatic normals, averages and extremes. Thirty-year monthly histories are provided for the following parameters: mean temperature, total precipitation, total snowfall, and heating/cooling degree days. The summaries also include a narrative description of the local climate.

- Statistical summaries available from the International Station Meteorological Climate Summary (ISMCS) (NCDC, 1996a).

  Those summaries are available for many domestic and international airports and military installations. The summaries include tabulations of statistics for several parameters of interest in regional climate analysis. The summaries also include a narrative description of local climate. Particularly useful and unique statistics available in the ISMCS are joint-frequency tables of dry bulb and wet bulb (MCWB) temperature depression, and single-parameter frequency distributions of dry bulb and wet bulb temperatures.

- Statistical summaries published by the American Society of Heating, Refrigerating and Air-Conditioning Engineers, Inc. (ASHRAE) (ASHRAE, 2017).

  ASHRAE climatic percentile information is available for worldwide locations including many U.S. airports with hourly surface weather observing stations. Parameters include dry bulb, wet bulb and dew point temperatures. Also included are: statistical design values of dry bulb with mean coincident wet bulb temperature, design wet bulb temperature with mean coincident dry bulb temperature, and design dew point with mean coincident dry bulb temperature.

- Statistical summaries published by the U.S. Air Force Combat Climatology Center (AFCCC) (AFCCC, 1999). The AFCCC statistical summaries include values for dry and wet bulb temperatures and wind speed parameters.

- American Society of Civil Engineers (ASCE) structural design standards for the site climate region (ASCE, 2006).

- The ASCE standards provide minimum load requirements for the design of buildings and other structures that are subject to building code requirements. Particularly useful and unique statistics of interest for climate analysis are values of basic wind speed on a map of the U.S. The basic speed is required by standards for determination of design wind loads. Also included are various adjustments and supplementary information dependent on site and structure characteristics. ASCE also provides maps of 50-year return interval

snow pack and a methodology for converting 50-year values extracted from the maps to other return intervals (ASCE, 2006).

- 48-hour probable maximum precipitation (PMP).

  The 48-hour probable maximum precipitation (PMP) is available from a study published by the U.S. Department of Commerce (USDOC) (USDOC, 1978). The study contains maps of estimated maximum probable precipitation amounts for a number of time periods (USDOC, 1978).

- Tornado, waterspout, and other weather event statistics for counties in the site climate region from the NCDC online Storm Events Database (NCDC, 2011a and NCDC, 2018a) and "Storm Data" publications.

  The Storm Events Database contains a chronological listing, by state, of climate statistics of interest for climate analysis. Those statistics include: tornadoes, thunderstorms, hail, lightning, high winds, snow, temperature extremes, and other weather phenomena. Also included are statistics on personal injuries and property damage estimates.

  The "Storm Data" publications are monthly summaries of severe weather events published by NCDC. These publications provide supplemental information about specific severe weather events.

- Maps of climatological parameters from the Climate Atlas of the United States (NCDC, 2002a).

  This digital atlas provides color maps of climatic elements for the U.S., such as: temperature, precipitation, snow, wind, and pressure. The period of record for most maps is 1961-1990. The user extracts data from the atlas by selecting a parameter (e.g., dry bulb temperature), a statistical measure (e.g., mean), and a state.

- Hourly meteorological data files in digital TD3505 (NCDC, 2006a; NCDC, 2011b and NCDC, 2011c) and TD3280 (NCDC, 2005a; NCDC, 2011d and NCDC, 2011e) formats. The data were used to develop a meteorological data to support relative atmospheric concentration (χ/Q) and radiological dose assessments. The surface meteorological data set covered the 2005-2010 period.

  TD3280 is an older data file format that has been replaced by the TD3505 format. Hourly meteorological data files are available in TD3280 format through December, 2009. Digital data files are available for worldwide locations from NCDC. These data sets contain hourly values of dry bulb temperature, humidity, wind speed/direction and cloud cover. These data sets allow analysis of coincident meteorological conditions. TD3505 data sets are available from NCDC, 2018b.

2.3.1.2.3 Identification and Selection for Analysis of Weather Monitoring Stations Located within the Site Climate Region

Figure 2.3-16 and Figure 2.3-17 present maps of the site climate region (identified in Figure 2.3-12), with additional annotations of locations within that region of NOAA Automated Surface Observing Stations (ASOS stations) (Figure 2.3-16), and NOAA COOP stations

(Figure 2.3-17) for which NOAA "Clim-20" publications and digital updates have been published by NCDC.

Table 2.3-5 and Table 2.3-6 present lists of the ASOS and COOP stations that are identified in Figure 2.3-16 and Figure 2.3-17. It should be noted that the ground elevations shown in Table 2.3-5 and Table 2.3-6 are given in ft. MSL (above Mean Sea Level) because that is the terminology used by NOAA in describing the ASOS and COOP stations (NCDC, 2001a-x; and NCDC, 2019ab). However, the MSL elevations are functionally equivalent to the NAVD 88 elevations used elsewhere in this section.

A subset of the ASOS stations presented in Figure 2.3-16 is selected for analysis. The following criteria were used to select that subset of stations. The two first-order stations Rockford and Madison are selected because of the extra statistical summaries in the form of NOAA annual summary LCD publications available for them. They also represent the geographical center of the site climate region. Four additional stations located approximately near the four corners of the site climate region are also selected to geographically bracket that region and avoid duplicate representation of similar areas. Those four additional stations are: Baraboo (at the northwest corner of the region), Fond du Lac (at the northeast corner of the region), Freeport (at the southwest corner of the region), and DuPage County (at the southeast corner of the region).

All of the COOP stations presented in Figure 2.3-17 and Table 2.3-6 are analyzed. Input information for that analysis includes statistics in the NOAA Clim-20 documents and updates for each station, that summarize climatic conditions during the 30-year period 1971 through 2000 (NCDC, 2001a-x) and subsequent updates through 2018 (NCDC, 2019f-aa).

2.3.1.2.4 Extreme Wind

A statistic known as the "basic" wind speed is used for design and operating bases. Basic wind speeds are 50 year recurrence interval nominal design 3-second gust wind speeds (mph) at 33 ft. (10.1 m) above ground for Exposure C category in Chapter 6 of ASCE, 2006.

Several sources are considered to determine the wind speeds for the SHINE site. The basic wind speed for the SHINE site is 90 mph (40.2 m/s), based on the plot of basic wind speeds in Figure 6-1 of ASCE, 2006. Basic wind speeds reported in AFCCC, 1999 for hourly weather stations in the site climate region are as follows: 90 mph (40.2 m/s) for Madison, Wisconsin, and 90 mph (40.2 m/s) for DuPage County Airport, West Chicago, Illinois. Consistency of the three values confirms the basis for selecting a value of 90 mph (40.2 m/s) for the project site. That value applies to a recurrence interval of 50 years.

Section C6.5.5 of ASCE, 2006 provides a method to calculate wind speeds for other recurrence intervals. Based on that method, a 100 year return period value is calculated by multiplying the 50 year return-period value (90 mph [40.2 m/s]) by a factor of 1.07. That approach produces a 100 year return period three second gust wind speed for the project site area of 96.3 mph (43.0 m/s) (96.3 mph = 90 mph x 1.07).

Design of the facility structure (FSTR) against extreme wind is discussed in Subsection 3.2.1.

2.3.1.2.5 Tornadoes and Waterspouts

The NCDC Storm Events Database (NCDC, 2018a) provides information on historic storm events on a county basis. To use that database, 30 regional counties that are at least partially included within the site climate region are selected and presented on the map in Figure 2.3-18. Those counties approximate the representative climate region defined above in Identification of Region with Climate Representative of the Site, and have a combined area of 21,056 square miles (sq. mi.) (54,534 square kilometers [sq. km]). The 30 counties are listed in Table 2.3-7 (U.S. Census Bureau, 2007).

The NCDC Storm Events Database (NCDC, 2018a) was accessed to extract statistics on regional tornadoes and waterspouts. Information is extracted for the 30 counties that are either wholly or partially included within the site climate region. Those tornado and waterspout statistics, for the 68-year period May, 1950 through November, 2018, are presented in Table 2.3-7. As presented in Table 2.3-7, total tornadoes and waterspouts reported in the 30-county area during the 68-year period are 794 and 3, respectively.

Strongest tornadoes in the database for Rock County (in which the site is located) are reviewed and are found to be of intensity F2. Table 2.3-8 (NCDC, 2018a) provides additional details on the most intense Rock County tornadoes.

The strongest tornadoes found in the database for the seven counties adjacent to Rock County: Dane, Jefferson, Walworth, Boone, Winnebago, Stephenson, and Green counties, were reviewed and found to be F3 and F4 storms in Boone County, Illinois, and F3 storms in Dane County, Green County, and Jefferson County, Wisconsin. Table 2.3-9 (NCDC, 2018a) presents additional details on the strongest tornadoes in counties adjacent to Rock County.

IAEA guidance for siting research reactors (IAEA, 1987) was reviewed. This guidance requires design tornado information to be based on the maximum historical intensity within a radius of about 100 km (62 mi.) from the site. For the SHINE site, a 100 km (62 mi.) radius partially extends outside of the representative site climate region included within the 30-county region described above. An F5 intensity tornado was recorded on 8 June 1984 in Iowa County, Wisconsin, at the town of Barneveld, which is located approximately 50 mi. (80 km) west northwest of the SHINE site (NCDC, 1984a).

2.3.1.2.6 Water Equivalent Precipitation Extremes

This subsection examines and compares water equivalent precipitation extremes within the site climate region, and locally near the site. Daily total water equivalent precipitation is measured at the local NOAA COOP monitoring station at Beloit, Wisconsin, and several regional COOP stations within the site climate region.

A PMP value for the site is presented in Snowpack and Probable Maximum Precipitation (PMP).

Table 2.3-10 presents maximum recorded 24-hour and monthly water equivalent precipitation values for the local COOP station at Beloit, and the COOP stations located within the site climate region defined on the map in Figure 2.3-17.

The regional historic maximum recorded 24-hour liquid-equivalent precipitation from the local Beloit station or for regional stations is 9.62 in. (24.43 cm) at Charmany Farm, Wisconsin. The

event occurred August 20-21, 2018. An organized and slow-moving low-pressure system within a very moist airmass caused the event. The weather system produced rainfalls ranging from 9 in. (22.86 cm) to 15 in. (38.10 cm) and flash flooding from the west side of Madison to Mazomanie, and south to Belleville (NCDC, 2018a).

The regional historic maximum monthly liquid-equivalent precipitation from records for either the local Beloit station or for regional stations is 18.27 in. (46.41 cm) at Portage, Wisconsin in June 2008. The regional recorded maximum 24-hour snowfall is (21.0 in.) (53.34 cm) at Dalton, Wisconsin and the regional recorded maximum monthly snowfall is (50.4 in.) (128.0 cm) at Watertown, Wisconsin in January 1979.

2.3.1.2.7 Hail, Snowstorms and Ice Storms

Mean hail or sleet frequencies during winter, spring, summer, autumn, and annual periods for Rockford and Madison are listed in Table 2.3-11. Mean hail frequencies are less than one day per season at both stations. Statistics are very similar at Rockford and Madison, verifying some consistency across the site climate region.

Hail events that are either severe (with hail size exceeding 0.75 in. [1.91 cm] in diameter) or large (with hail exceeding 1.00 in. [2.54 cm] in diameter) are reported to have occurred in Rock County, Wisconsin on 11 occasions during the period 1961 - 1990, or with a frequency of approximately 0.37 occurrences per year (NCDC, 2002a).

The Storm Events Database through December 31, 2018 lists the largest hailstones that Rock County has experienced as follows: of diameter 3.00 in. (7.62 cm) on one occasion during June 1975; of diameter 2.50 in. (6.35 cm) on one occasion during August 2006; of diameter 2.25 in. (5.72 cm) in August 2011; of diameter 2.00 in. (5.08 cm) on one occasion during June 1975 and one occasion during June 1998 and one occasion in July 2012. The largest hailstone observed in Rock County remains at 3.00 in. (7.62 cm) in diameter observed in June 1975.

Daily total snowfall amounts are measured at the local NOAA COOP monitoring station at Beloit, Wisconsin, as well as at several regional COOP stations within the site climate region.

Maximum recorded 24-hour snowfall for either the local Beloit station or for regional stations is 21.0 in. (53.34 cm) at Dalton, Wisconsin (Table 2.3-10). That event occurred on 2 January 1999. It was due to a major winter synoptic cyclone (the "Blizzard of 1999") that developed in Colorado, curved northeast through the Great Lakes, then entered Canada (NCDC, 1999a and NCDC, 2000a). On 2 January 1999 the synoptic surface low was centered at the southern tip of Illinois. A warm maritime tropical air mass with temperatures in the 80s°F was present to the south, and a continental arctic air mass with temperatures primarily in the teens °F was present to the north. An area of heavy snow covered the site climate region. This blizzard paralyzed south central and southeast Wisconsin. Ten to 21 in. (25.40 to 53.34 cm) of snow were deposited and wind gusts of 45 to 63 mph (20.1 to 28.2 m/s) occurred. Nearly all cities and villages declared snow emergencies, and airports were closed. Visibility in blowing snow was typically 0.5 mi. (0.8 km). Structural damage to buildings and power lines was reported.

Overall historic maximum monthly snowfall from records for either the local Beloit station or for regional stations is 50.4 in. (128.0 cm) at Watertown, Wisconsin. That month was January 1979.

Overall, extreme snowfall conditions recorded at the local station at Beloit, Wisconsin are bracketed by conditions recorded at stations within the site climate region, supporting conclusions regarding climate region representativeness.

A snow pack value for the site is presented in Snowpack and Probable Maximum Precipitation (PMP).

The mean number of days with freezing rain or drizzle is 2 days per year at both Madison, Wisconsin and Rockford, Illinois (Table 2.3-4). A summary of 14 ice storms that affected Rock County, Wisconsin during the period 1995-2011 is presented in Table 2.3-12 (NCDC, 2011a). That summary indicates the following.

a. Several ice storms, as many as two or three, can occur per year.
b. Ice can accumulate periodically or during a consecutive period of anywhere from approximately 2 hours to 11 hours.
c. Ice accumulations typically range from one-tenth to one-quarter inch, but can reach one-half inch.
d. Hazardous driving conditions are a typical result of the storms.

Updates to the NCDC Storm Events Database through December 31, 2018 (NCDC, 2018a) did not show additional records of heavy snow and ice storms in Rock County since 2011 through December 31, 2018.

A 50-year return-interval atmospheric ice load due to freezing rain is estimated to be 0.75 in. (1.91 cm) for the site (ASCE, 2006). The estimated concurrent three-second wind gust is 40 mph (17.9 m/s). A 500-year return-interval atmospheric ice load due to freezing rain is estimated to be 1.5 in. (3.81 cm) for the site (ASCE, 2006). The estimated concurrent three-second wind gust from ASCE, 2006 is 40 mph (17.9 m/s).

2.3.1.2.8 Thunderstorms and Lightning

Thunderstorm statistics for the regional NOAA first order weather stations at Rockford, Illinois and Madison, Wisconsin are published and available for the site climate region (NCDC, 2019b; and NCDC, 2019c). Thunderstorms occur during an average of 43.1 days per year at Rockford, and 39.5 days per year at Madison. Mean seasonal thunderstorm frequencies for Rockford and Madison are listed in Table 2.3-13 (NCDC, 2019c and NCDC, 2019b). Thunderstorms are most frequent in summer and least frequent in winter at both stations.

The mean frequency of lightning strikes to earth is calculated via a method from the Electric Power Research Institute (EPRI), per the U. S. Department of Agriculture Rural Utilities Service (USDA, 1998). The method assumes a relationship between the average number of thunderstorm days per year (T), and the number of lightning strikes to earth per square mile per year (N). The mathematical relationship is as follows:

$$N = [0.31][T] \qquad \text{(Equation 2.3-1)}$$

Based on the average number of thunderstorm days per year at Rockford during the 63-year period 1955-2018 (43.1, which is slightly higher than the value of 39.5 days for Madison and is therefore used here), the frequency of lightning strikes to earth per square mile per year is 13.4 (5.2 strikes per square km per year) for the site and surrounding area. For comparison, based on

a 10-year period of record (NLSI, 2014), indicates 6 to 12 flashes per square mile per year for the site region, which corresponds to 2.3 to 4.6 flashes per square kilometer per year. The EPRI value therefore is shown to be a reasonable indicator.

2.3.1.2.9 Snowpack and Probable Maximum Precipitation (PMP)

ASCE 7-05 (ASCE, 2006) provides site-specific estimates of the 50-year snow load. Based on the location of the SHINE facility, the 50-year ground snow load is 30 pounds per square foot (lb/ft^2). A factor of 1.22 is used to account for the 100-year recurrence interval. The resulting 100-year ground snow load as 36.6 lb/ft^2 (178.7 kilograms per square meter [kg/m^2]).

The weight of the 48-hour PMP for the site vicinity was derived by multiplying the 48-hour PMP (in inches) from Figure 21 of USDOC, 1978 by the weight of one inch of water (one inch of water covering one square foot weighs 5.2 lb [2.4 kg]).The estimated 48-hour PMP for the site from Figure 21 of USDOC, 1978 is 34 in. (86.4 cm). The resulting estimated weight of the 48-hour PMP for the site is 176.8 lb/ft^2 (863.2 kg/m^2).

2.3.1.2.10 Design Dry Bulb and Wet Bulb Temperatures

Site design basis dry bulb temperatures (DBTs) and wet bulb temperatures (WBTs) are defined for the site and its climate area. Those include the following statistics:

a. Maximum DBT with annual exceedance probability of 0.4 percent
b. Mean coincident WBT (MCWB) at the 0.4 percent DBT
c. Maximum DBT with annual exceedance probability of 2.0 percent
d. MCWB at the 2.0 percent DBT
e. Minimum DBT with annual exceedance probability of 0.4 percent
f. Minimum DBT with annual exceedance probability of 1.0 percent
g. Maximum WBT with annual exceedance probability of 0.4 percent
h. Maximum DBT with annual exceedance probability of 5 percent
i. Minimum DBT with annual exceedance probability of 5 percent
j. 100-year return maximum annual DBT
k. MCWB at the 100-year return maximum annual DBT
l. 100-year return maximum annual WBT
m. 100-year return minimum annual DBT

Statistics for (a)-(g) are readily available from ASHRAE, 2017. Since those statistics are available from a well-known reference, no additional data analysis is required. ASHRAE, 2017 includes values for the following stations in the site climate region: Fond du Lac, Wisconsin; Madison, Wisconsin; Rockford, Illinois; and DuPage County Airport, Illinois. These stations represent climatic conditions in the northern, central and southern portions of the climate region, respectively (Figure 2.3-16). Worst-case (bounding) values for (a)-(g) are selected from those four stations. To maintain thermodynamic consistency between DBT and coincident WBTs, DBT/ MCWB pairs are retained for a single station. The resulting statistics are listed in Table 2.3-14.

Statistics for the maximum and minimum DBT with an annual exceedance probability of 5 percent (items [h] and [i] above) are not available from ASHRAE, 2017. In lieu of values from other sources, values are extracted from published DBT and wet-bulb depression joint-frequency

tables in NCDC, 1996a. Joint-frequency tables are available only for Madison and Rockford. The extracted statistics for Madison and Rockford are listed in Table 2.3-14.

The 100-year return interval maximum annual DBTs and WBTs (items [j], [l] and [m] above) were estimated using a technique described in ASHRAE, 2017. The technique estimates the n-year return-interval extreme temperature from a series of annual maximum and minimum temperatures. The ASHRAE technique uses the following equation:

$$T_n = M + I F_s \qquad \text{(Equation 2.3-2)}$$

Where:

- T_n is the n-year return period value of the extreme temperature computed, in years
- M is the mean annual extreme maximum or minimum temperature
- I is +1 if the maximum temperature is computed; -1 if the minimum temperature is computed
- s is the standard deviation of the annual extreme maximum or minimum temperatures
- n is the return period in years (n =100 for a 100-year return interval).

$$F = -\frac{\sqrt{6}}{\pi}\left\{0.5772 + \ln\left[\ln\left(\frac{n}{n-1}\right)\right]\right\} \qquad \text{(Equation 2.3-3)}$$

Where:

- F is a function that converts the standard deviation of annual extreme temperature parameter s (such as the annual extreme temperature in °F) to a new variable that is linearly related to the n-year return-interval extreme temperature T_n.

Since the MCWB coincident with the 100-year return interval maximum DBT is required (item [k] above), this technique is only applied at meteorological stations in the climate region which had: (1) digital records of hourly DBT and coincident WBT and (2) published annual extreme DBTs (i.e., NOAA annual summary LCD publications, such as NCDC 2011f). The published annual extreme DBTs are required to check annual extreme DBTs extracted from the digital records. There were only two stations in the climate region which meet these requirements: Rockford, Illinois and Madison, Wisconsin.

The ASHRAE technique is applied to hourly TD3280 and TD3505 digital datasets (NCDC, 2011b-e; NCDC, 2011g) for each of these stations. The extreme DBT and WBT are first identified for each year which has at least 90 percent of possible hourly coverage of DBT and WBT. This produces a time-series of annual maximum and minimum DBTs and WBTs for 53 years for Madison and 30 years for Rockford through 2010. Each time-series is then input into the ASHRAE technique. The resulting estimated 100-year return period annual DBTs and WBTs (items [j], [l] and [m] above) are listed in Table 2.3-15.

The estimated 100-year return maximum annual DBT at Rockford (104.8°F [40.4ºC]; Table 2.3-15) is only 0.8°F (0.44ºC) above the record maximum DBT at Rockford (104°F [40.0ºC]) (NCDC, 2011h). Instead of attempting to derive a statistical relationship between the DBT and WBT useful over the short DBT interval of 104°F (40.0ºC) to 104.8°F (40.4ºC), the MCWB coincident with the estimated 100-year return maximum annual DBT at Rockford (104.8°F [40.4ºC]) are taken to be the WBT coincident with the record maximum DBT at

Rockford (104°F [40.0ºC]). The WBT coincident with the record maximum DBT at Rockford is 80°F (26.7ºC) (NCDC, 2011e and NCDC, 2011c). Therefore, the estimated MCWB coincident with the 100-year return maximum annual DBT at Rockford is 80°F (26.7ºC).

A similar approach is taken for the 100-year return maximum annual DBT for Madison. The 100-year return maximum annual DBT for Madison (104.3°F [40.2ºC]; Table 2.3-15) is only 0.3°F (0.17ºC) above the record maximum DBT for Madison (104°F [40.0ºC]) (NCDC, 2011f). Therefore, the MCWB coincident with the estimated 100-year return maximum annual DBT is taken to be the WBT coincident with the record maximum DBT for Madison. The WBT coincident with the record maximum DBT at Madison is 75°F (23.9ºC) (NCDC, 2011d and NCDC, 2011b). Therefore, the estimated MCWB coincident with the 100-year return maximum annual DBT for Madison is 75°F (23.9ºC). The 100 year maximum annual DBT and MCWB pairs (items [j] and [k] above) for Rockford and Madison are listed in Table 2.3-15.

The estimated 100-year return maximum and minimum annual DBTs described above were derived from 53 years of data from Madison and 30 years from Rockford using data through 2010. Subsequent updates to the climatological data show that the record maximum DBT at Rockford has increased by 1°F (0.55 ºC) from 104°F (40.0ºC) to 105°F (40.6ºC) in July 2012 (NCDC, 2011h and NCDC, 2019c). The record maximum DBT for Madison (104°F [40.0ºC]) set in 1976 tied in July 2012, and thus is unchanged (NCDC, 2011f and NCDC, 2019b). The record minimum temperatures at Rockford (-27°F [-32.8ºC] set in 1982 [NCDC, 2019c]) and Madison (-37°F [-38.3ºC] set in 1951 [NCDC, 2019b]) are also both unchanged. The subsequent minor changes in temperature extremes represent no significant changes to the estimated 100-year return maximum and minimum annual DBTs and extreme WBTs derived from data through 2010

2.3.1.2.11 Extreme Dry Bulb Temperatures

An additional review of regional extreme DBTs is done using NOAA COOP climate monitoring stations in the site climate region. The locations of those stations are shown in Figure 2.3-17. The COOP climate monitoring stations do not measure WBT and do not record hourly DBTs. Those stations only record maximum and minimum daily DBTs and daily precipitation totals. Therefore, it is not possible to identify WBTs coincident with the extreme DBTs recorded at those stations.

Table 2.3-16 presents extreme DBTs recorded at the climate monitoring stations (NCDC, 2001a-x; NCDC, 2019f-aa). For completeness, Table 2.3-16 also includes the extreme DBTs recorded at the two first-order stations in the site climate region (Madison, Wisconsin and Rockford, Illinois) from NCDC, 2019b and NCDC, 2019c.

Regarding the climate region, the overall extreme DBTs for the climate region are: a maximum of 109°F (42.8ºC) recorded on 14 July 1936 at Marengo in Boone County, Illinois, and a minimum of -45°F (-42.8ºC) recorded on 30 January 1951 at Baraboo in Sauk County, Wisconsin.

Since Marengo is a COOP station, the WBT coincident with the extreme DBT at Marengo (109°F [42.8ºC]) is not available. Further, DBT and coincident WBT data in digital format that are available for stations in the climate region do not extend as far back as 1936 (Table 2.3-5). Therefore, it is necessary to estimate a WBT coincident with the overall extreme DBT.

A graphical extrapolation method is used to estimate the WBT coincident with the overall extreme DBT of 109°F (42.8ºC). A simple graphical approach is appropriate for several reasons:

a. A simple graphical approach is appropriate because at the extreme high end of the DBT range there are only a small number of observations. Use of an objective numerical technique to project larger DBT values using a small population as input is unjustified because it is effectively no less subjective than a graphical approach.
b. The requirement is only for a mean coincident WBT value. A mean WBT value is simply identified for any DBT value on the graph, therefore a set of such means is easily plotted, and form the basis of an extrapolation line.
c. Published DBT/WBT depression joint frequency distribution (JFD) tables are available for Madison and Rockford (NCDC, 1996a). The tables are suitable for use in sketching the graphical relationship between regional DBT and WBT during conditions of the peak DBT.

The closest first-order station to Marengo is Rockford, Illinois which is located approximately 25 mi. (40.2 km) west of Marengo (Figure 2.3-17). Therefore, the DBT/WBT depression JFD table from Rockford is used to estimate the WBT coincident with an overall extreme DBT of 109°F (42.8ºC) recorded at Marengo. The upper DBT limit of the DBT/WBT depression JFD table from Rockford is 103°F (39.4ºC). Therefore, it is necessary to extrapolate the upper end of the JFD table to the observed DBT of 109°F (42.8ºC). Graphical extrapolation of the DBT/WBT depression relationship to a DBT of 109°F (42.8ºC) results in an estimated WBT depression of 30°F (16.7ºC), which corresponds to a MCWB of 79°F (26.1ºC) (109°F - 30°F = 79°F). Therefore, the estimated MCWB coincident with the overall extreme DBT of 109°F (42.8ºC) at Marengo is 79°F (26.1ºC).

2.3.1.2.12 Restrictive Dispersion Conditions

Major air pollution episodes are typically a result of persistent surface high pressure weather systems that cause light and variable surface winds and stagnant meteorological conditions for four or more consecutive days. Estimates of the stagnation frequency are provided in (NOAA, 1999; Figures 1 and 2). Those estimates indicate that, on average, the site location experiences less than 10 days with stagnation per year. When stagnation occurs, stagnation lasts, on average, less than two days.

2.3.1.2.13 Air Quality

The site is located in Rock County, Wisconsin which is part of the Rockford-Janesville-Beloit Interstate Air Quality Control Region (WDNR, 2013). This air quality control region combines agricultural activities with the Beloit-Janesville, Wisconsin and Rockford, Illinois urban-industrial areas. The Wisconsin portion of the air quality control region, Rock County, is mostly flat to gently rolling farmland. Industry in the region consists of manufacturing, foundry operations and electrical power plants (WDNR, 2013). Rock County is currently in attainment for criteria pollutants (ozone, particulate matter, carbon monoxide, nitrogen oxides, sulfur dioxide, and lead (USEPA, 2019).

Maintenance areas are those geographic areas with a history of non-attainment but are currently meeting the National Ambient Air Quality Standards. In April 2004, the EPA designated the following 10 counties in eastern Wisconsin as being in non-attainment with the 8-hour ozone air quality standard: Door, Kewaunee, Manitowoc, Sheyboygan, Washington, Ozaukee, Waukesha,

Milwaukee, Racine, and Kenosha. However, by July 31, 2012 those counties, with exception of Sheboygan, had been re-designated as being in attainment with the 8-hour ozone standard (USEPA, 2019). Sheboygan county is situated to the east of the Rockford Janesville Beloit Interstate Air Quality Control Region, along the western shore of Lake Michigan.

In October 2015, the USEPA strengthened the 8-hour National Ambient Air Quality Standard (NAAQS) for ground-level ozone by decreasing the standard from 75 parts per billion (ppb) to 70 ppb. The new standard became effective on December 28, 2015 (USEPA, 2015).

On May 1, 2018 the USEPA published the list of counties that are not in attainment with the 70 ppb standard based on ozone monitoring data. This was in advance of the Final Rule that the USEPA issued on June 4, 2018 (USEPA, 2018). A number of counties in the vicinity of the SHINE facility are out of compliance with the 2015 revised ozone standard: Door, Kenosha, Manitowoc, Milwaukee, Ozaukee and Sheboygan. Rock County, Wisconsin is in compliance with the strengthened ozone standard.

USEPA guidance (USEPA, 1990) states that a Class I visibility impact analysis is necessary for a major source locating within 100 km (62 mi.) of a Federal Class I area. Class I areas are national parks and wilderness areas that are potentially sensitive to visibility impairment. Table 2.3-17 lists the nearest Class I areas to the SHINE site (NPS, 2011). The table shows that the closest Federal Class I area is the Rainbow Lake Wilderness Area, Wisconsin which is located approximately 455 km (approximately 283 mi.) northwest of the site in far northern Wisconsin.

2.3.1.2.14 Climate Change

Trends in global climatic conditions are currently the subject of considerable discussion in the scientific community and in the media. There are differences of opinion regarding the nature and causes of such trends. There is also controversy regarding the reliability of projections. Generally, projections of climatic changes have been done at global scales. Attempts to predict changes at regional scales, for example for the Midwestern U.S., have been problematic. And, certainly, predictions of changes at a single station or at a relatively small area, such as the site climate region, are not reliable.

It is not appropriate to attempt to predict climate changes in the site climate region because of the above uncertainties. It is also not appropriate to try to use such predictions to enhance, or replace, the standard approach of identifying historical extreme climatic conditions in the site climate region. Plant design is most reliably based on a standard approach of projecting via scientifically defensible statistical methods, using historic statistics as input.

It is nevertheless valid to examine historic records for indications of long-term trends for informational purposes. Trends of interest are those of climate elements such as temperature, pressure, or winds that are sustained over periods of several decades or longer (AMS, 2012).

Trends of the following parameters are examined, for the climate region within which the SHINE site is located:

a. Values, for six separate 30-year division normal periods, of mean annual dry bulb temperature and mean annual precipitation. Division normals are climate normals for 30-year periods within a climate division. Climate divisions are segments of individual states that the NOAA has identified as being climatologically homogeneous. By definition,

the division normal periods: (1) are 30 years long, (2) overlap, and (3) are updated every 10 years. Division normals for the site that are reviewed include the section of Wisconsin labeled “WI-08 South Central Wisconsin” (NCDC, 2002b and NCDC, 2002c). The normals for the most recent period (1981-2010) were taken from the NOAA dataset (Arguez et al., 2012). Variation of mean annual dry bulb temperature and mean annual precipitation from division normal data are identified in the top half of Table 2.3-18.

b. During six separate single-decade periods of record, extremes at Madison, Wisconsin of hourly dry bulb temperature, one-day liquid-equivalent precipitation, one-day snowfall, and strongest tornadoes. Variations of those historic meteorological parameters are identified in the bottom half of Table 2.3-18. The ending years of the time periods are selected to match those of the normal periods in the top half of Table 2.3-18, but without overlaps of the beginning years of the time periods, and with time period lengths of 10 years instead of the 30-year length of the normal periods.

The statistics in Table 2.3-18 show the following:

a. State climate division temperature

   State division normal temperature fell by 1.7 percent (0.8ºF) (0.4ºC) from 46.7 to 45.9ºF (8.2 to 7.7ºC) during the first three division normal periods combined, then fell and rose by 0.4 percent (0.2ºF) (0.1ºC) during the fourth and fifth periods respectively. The normal temperature rose by 1.1 percent (0.5ºF) (0.3ºC) in the most recent sixth period. The maximum value (46.7ºF) (8.2ºC) occurred during the first period (1931 to 1960).

b. Division normal precipitation

   State climate division precipitation fell by 0.35 percent (0.11 in.) (0.28 cm) from 31.24 to 31.13 in. (79.35 to 79.07 cm) during the first two division normal periods, then rose by 9.5 percent (2.98 in.) (7.57 cm) from 31.13 to 34.11 in. (79.07 to 86.64 cm) during the third through fifth division normal periods. The normal precipitation rose by 1.1 percent (0.37 in.) (0.94 cm) from 34.11 in. to 34.48 in. (86.64 cm to 87.58 cm) during the most recent sixth period. The maximum value (34.48 in.) (87.58 cm) occurred during the sixth and most recent period (1981 to 2010).

c. Maximum daily precipitation

   Maximum daily precipitation at Madison fell during the second (30 percent) and fourth (5 percent) periods, and rose during the third (6 percent), fifth (23 percent), and sixth (17 percent) periods. The historical period maximum (5.28 in.) (13.41 cm) occurred during the most recent (sixth) period (2001 to 2010).

d. Extreme high daily snowfall

   Maximum 24-hour snowfall at Madison fell during periods three (15 percent), five (18 percent), and six (16 percent), and rose during periods two (48 percent) and four (27 percent). Maximum occurred during the fourth period (17.3 in.) (43.94 cm).

e. Extreme high dry bulb temperature

The historical period extreme high dry bulb temperature (104ºF) (40.0ºC) occurred during the third climate period (1971 to 1980). The lowest extreme high (97ºF) (36.1ºC) occurred during the second climate period (1961 to 1970). Otherwise, this parameter value was relatively constant at 101 or 102ºF (38.3 or 38.9ºC), with exception of the second and most recent periods, during which the parameter was 97ºF (36.1ºC) and 98ºF (36.7ºC), respectively.

f. Extreme low dry bulb temperature

The historical period extreme low dry bulb temperature (-37ºF) (-38.3ºC) occurred in 1951 during the first climate period (1951 to 1960). Warmest extreme low (-19ºF) (-28.3ºC) occurred during the most recent period (2001 to 2010). Otherwise, this parameter value was relatively constant at around -29ºF (-33.9ºC).

g. Strongest tornadoes

The strongest tornado recorded within the site climate region was an F4 tornado (Table 2.3-9) observed in 1967 during the second climate period (1961 to 1970). Otherwise, strongest tornado intensity values within the site climate region were relatively constant at F2 or F3 (Table 2.3-8 and Table 2.3-9). In order to satisfy IAEA guidance (IAEA, 1987) tornado intensity within approximately 100 km (62 mi.) of the site also was considered. An F5 tornado occurred during the fourth climate period (1981 to 1990) at the town of Barneveld, Wisconsin (NCDC, 1984a), which is outside of the site climate region but within 100 km (62 mi.) of the site.

Overall, changes in state division normal (30-year period) mean precipitation and temperature during the 79-year historical period 1931 to 2010 do not indicate consistent trends of rate of increase, or decrease, with time. Between-decade changes of short-term extremes of daily precipitation and extreme high and low temperatures during the 79-year historical period 1931 to 2010 do not indicate consistent trends, or increase in severity, with time. The highest 30-year mean annual precipitation (34.48 in.) (87.58 cm) and daily (5.28 in.) (13.41 cm) extreme liquid-equivalent precipitation occurred during the most recent available periods, but those values are not part of consistent long-term trends.

The year 2010 marks the end of the most recent 30-year climate period. Recent climatological data for Madison through the end of 2018 (NCDC, 2019b) show that the values for the extreme high DBT (104ºF) (40.0ºC); extreme low DBT (-37ºF) (-38.3ºC); extreme high daily precipitation (5.28 in.) (13.41 cm) and the extreme high daily snowfall (17.3 in.) (43.94 cm) in Table 2.3-18 have not changed.

2.3.2 SITE METEOROLOGY

The purpose of this local climate analysis is to understand dispersion conditions in the vicinity of the site. That characterization is input to, and provides a context for, assessment of atmospheric impact of the facility on the environment.

Local dispersion climatology includes consideration of airflow and atmospheric turbulence. The following subsections address local topography, the source of local meteorological data, wind roses, and atmospheric stability distribution.

2.3.2.1 Topography

The site is located approximately at the center of Rock County, Wisconsin, about 13 mi. (20.9 km) north of the Illinois/Wisconsin border, and 2.5 mi. (4.0 km) east of the Rock River. The site is located within till plains glacial deposits on the Central Lowland Province of the Interior Plains Division of the United States. Within a radial distance from the site of approximately 10 mi. (16.1 km), additional ground surface features include the following:

a. There is terminal kettle-moraine topography in the central, north, and east sections, which represent effects of the last advance of the continental glacier, including uneven hills and ridges, varying drainage patterns, and gently rolling terrain (WISDOT, 2017).
b. There is dissected upland with isolated bluffs in the west and southwest sections, part of the “driftless area” (Regional Climate) which was not overrun by ice during the last continental glaciation (Moran and Hopkins, 2002).
c. The Rock River watershed, the main waterway, bisects the county from north to south (Rock County, 2012). The Rock River valley is typically less than 1 mi. (1.6 km) wide, with minor slopes at the edges of the river floodplain with heights of approximately 50 ft (15.2 m).
d. Most land is used for agriculture, including corn and soybean farming (Rand McNally, 1982 and 2005).
e. The main urban centers of Janesville and Beloit are located along the Rock River.
f. The finished site grade elevation is approximately 825 ft. (251 m) NAVD 88. The project site and adjacent ground within a radius of approximately 1 mi. (1.6 km) is flat farmland. Within a 10 mi. (16.1 km) radius from the site, topographic elevations range from approximately 750 ft. (230 m) NAVD 88 along the Rock River, to approximately 1033 ft. (315 m) NAVD 88 at the highest bluffs (USGS, 1980). Therefore, the topography within a 10 mi. (16.1 km) radius ranges from approximately 72 ft. (21.9 m) below the site elevation, to 206 ft. (62.8 m) NAVD 88 above the site elevation.

2.3.2.2 Local Data Sources

To support relative atmospheric concentration (χ/Q) and radiological dose assessments, a surface meteorological data set covering the period of 2005-2010 was developed as described below.

Surface meteorological data were available from the Southern Wisconsin Regional Airport (SWRA) in Janesville, Wisconsin (NOAA station identifier KJVL). That airport is located approximately 0.25 mi. (0.40 km) west of the site. The SWRA meteorological monitoring station is an automated weather observation station (AWOS) with precipitation sensors installed (AWOS IIIP). The FAA describes the specifications of an AWOS system in an Advisory Circular (FAA, 2017). Specifications from this Advisory Circular are listed in Table 2.3-19. The AWOS anemometer height at SWRA for the period of interest in this study (2005 to 2010) is 26 ft. (7.9 m) above ground level (NCDC, 2012).

The FAA Advisory Circular (FAA, 2017) describes the FAA standard for procurement, construction, installation, activation, and maintenance of non-Federal AWOS systems. That

standard is provided in an FAA Order (FAA, 1992), which requires inspections that meet specified technical standards and tolerances. On-site instrument calibration is required annually unless more frequent calibration is specified by the FAA region. Calibrations are required to be done by a qualified technician with FAA verification authority and witnessed by a qualified FAA non-Federal inspector. Facilities Maintenance Log and Technical Performance Record forms are maintained. In addition, NCDC subjects surface meteorological data collected at AWOS stations such as SWRA to documented quality assurance and analysis procedures (Del Greco et al., 2006).

Raw meteorological data from SWRA are obtained from NCDC (NCDC, 2011g). Hourly dry bulb temperature, humidity, wind speed, and wind direction data are extracted from the raw data. Table 2.3-20 shows the annual data recovery rates for dry bulb temperature, humidity, wind speed, and wind direction. The table shows that the annual data recovery rate for each variable exceeded 90 percent for 2005, 2006, 2008 to 2010, and that the recovery rate was approximately 87 percent for each variable in 2007. Data from 2005 through 2010 are chosen for analysis in order to produce a data set with the most recent contiguous 5 years of data, and with 5 years of data having recovery rates better than 90 percent. Table 2.3-21 presents a summary of meteorological parameter statistics from the SWRA during the 2005 to 2010 period.

2.3.2.3 Plans to Access Local Meteorological Data during License Period

Meteorological measurements will be available for use in responding to accidental radiological releases or other emergencies, and other routine purposes that require access to meteorological information during the licensing period. That meteorological information will be obtained for local government weather monitoring stations that observe wind and other surface meteorological parameters on an hourly basis.

When needed during an emergency, real-time hourly surface meteorological measurements of wind direction, wind speed, air temperature, and weather type will be accessed by SHINE through government data sources. Access will be attempted during the emergency in the following sequence, until reliable data are obtained, as follows:

a. Internet access to hourly surface weather observations recorded at the SWRA AWOS, at URL: http://www.weather.gov/data/obhistory/KJVL.html.
b. Telephone access to an automated synthesized voice recording of the most recent hourly surface observations recorded at the SWRA AWOS, at number: (608) 758-1723.
c. If weather observations are not available from the SWRA AWOS, then weather information from another station with hourly meteorological data in the Site Climate Region will be used. The following stations will be used, in the order listed below. The stations are listed in order of increasing distance from Janesville, Wisconsin:
    1. Rockford, Illinois: http://www.weather.gov/data/obhistory/KRFD.html
    2. Monroe, Wisconsin: http://www.weather.gov/data/obhistory/KEFT.html
    3. Burlington, Wisconsin: http://www.weather.gov/data/obhistory/KBUU.html
    4. Madison, Wisconsin: http://www.weather.gov/data/obhistory/KMSN.html

During normal operations, hourly data will be obtained by internet access to hourly surface weather observations recorded at the SWRA AWOS, at URL: https://w1.weather.gov/data/obhistory/KJVL.html.

2.3.2.4 Comparison of Local and Regional Wind Roses

Local Data Sources describes the meteorological monitoring system at the SWRA in Janesville, Wisconsin. As described in that subsection, wind speed and direction measurements are collected at the 26 ft. (7.9 m) level. Wind speed and direction from the 26 ft. (7.9 m) level are used to determine JFDs that are input to relative atmospheric concentration (χ/Q) and radiological dose assessments in this report.

Figure 2.3-19 through Figure 2.3-35 show the annual, monthly, and seasonal wind roses from SWRA. The period of record on which those plots are based is the six years from January 1, 2005 through December 31, 2010 (Local Data Sources). That period of record is also used for JFD input to χ/Q and radiological dose assessments in this report.

An annual wind rose (Figure 2.3-19) shows dominant wind frequencies from the west (approximately 8 percent of the period) and from the south (approximately 7.5 percent of the period). The remaining directions include a group (N, E, SSW, SW, WNW, and NW) with frequencies of occurrence that range from approximately 5 to 7 percent of the period, and another group (NNE, NE, ENE, ESE, SE, SSE, WSW, and NNW) with frequencies of occurrence that range from approximately 3.5 to 5 percent of the period. The multi-modal nature of the annual wind rose reflects airflows associated with seasonal shifts of mean North American surface pressure belts and centers, seasonal changes in paths and frequencies of synoptic-scale surface cyclones and anticyclones that move across the area, and seasonal changes in frequency of development of synoptic surface fronts (Trewartha, 1954; Trewartha, 1961; Rand McNally, 2005; and EDS, 1968). The corresponding monthly wind roses are provided for reference in Figure 2.3-20 - Figure 2.3-31).

The winter season wind rose (Figure 2.3-32) shows most frequent wind directions during that season from the west, northwest and north. This is a reflection of polar and arctic air masses that flow from Canada that are dominant during the winter. The large Icelandic low pressure center that intensifies during Northern Hemisphere winter causes a pressure gradient pattern that is oriented in a northwest to southeast direction over Canada and the U.S. that guides surface high pressure systems that contain the polar and arctic air masses in a southeast direction from Canada to the Midwest and eastern U.S. Upper air meridional flow (relatively parallel to lines of longitude) is more prevalent than zonal flow (relatively parallel to lines of latitude), and surface cyclonic storms more frequently occupy the Alberta storm track that extends from southwest Canada into the central U.S.

The spring season wind rose (Figure 2.3-33) shows dominant wind direction frequencies from the east, south, and west. During spring, the Icelandic low weakens, the southwest U.S. surface thermal low intensifies, and the north Atlantic Azores high pressure cell intensifies. Because of the northward shift of the subtropical high pressure belt (including the Azores high), storm systems and Canadian air masses are not always pushed towards the southeast, but rather stay farther north during their movement over the Midwest and eastern U.S. Intensification of the southwest U.S. thermal low increases winds from the south over the central U.S. Warm and stationary fronts form more frequently over the Midwest U.S. at the boundaries between northern and southern air masses. Surface pressure troughs at those fronts draw moist modified maritime tropical air from the south that results in surface convergence, lifting, and formation of precipitation at the fronts. The combined results of these changes are increased frequencies of west, south, and east winds as air masses converge on the area from more locations in the southwest, south, and southeast U.S. than during winter.

During the summer season, the subtropical high-pressure belt reaches its maximum intensity. It reinforces development of individual surface anticyclones, which follow in a general easterly direction behind weak cold fronts as they move eastward. Surface lows and precipitation are largely suppressed. The summer season wind rose (Figure 2.3-34) shows dominant wind direction frequencies from the south and southwest, reflecting flow out of the relatively slow-moving surface high pressure centers.

The autumn wind rose (Figure 2.3-35) reverts back to some cool season circulation patterns, which are also characteristic of the spring season. It shows dominant wind direction frequencies from the south and west, but east winds occur less frequently than during the spring season. East winds are less frequent because the subtropical surface pressure ridge extends westward from the north Atlantic to the central U.S. during autumn, whereas it is strongest off the Atlantic coastline during Spring. Airflow therefore moves north out of surface anticyclones that are reinforced by the mean autumn subtropical ridge position across the east central U.S., and airflow relatively infrequently moves towards the west.

Wind roses were generated for regional climate stations from TD-3505 hourly surface dataset files through 2010 (NCDC, 2018b). The climate stations (Baraboo, Wisconsin; Madison, Wisconsin; Fond du Lac, Wisconsin; Freeport, Illinois; Rockford, Illinois; and Du Page County Airport, Illinois) were identified in Subsection 2.3.1.2.3. Rockford and Madison represent the geographical center of the site climate region. Baraboo, Fond du Lac, Freeport and Du Page County represent the northwest, northeast, southwest and southeast corners of the climate region, respectively.

Figure 2.3-36 shows a comparison of annual wind roses for the SWRA in Janesville and the six regional stations. The wind roses are arranged in the figure to match the approximate physical locations of the stations relative to Janesville, Wisconsin. The annual wind rose from Fond du Lac shows a bimodal southwest and northeast wind direction distribution. The northeast winds appear to be local effects of nearby Lake Winnebago, which is located approximately three miles northeast of the Fond du Lac airport (Figure 2.3-16). However, the annual wind roses at the other five regional stations (Baraboo, Madison, Freeport, Rockford, and Du Page County Airport) show overall multi-modal patterns similar to the annual wind rose from Janesville. This consistency verifies the representativeness of wind measurements from the SWRA in Janesville for purposes of dispersion modeling.

2.3.2.5 Atmospheric Stability

Pasquill stability class is derived from hourly wind speed, ceiling height, and sky cover measurements from the AWOS at the SWRA in Janesville, Wisconsin (Local Data Sources). The Pasquill stability class is derived using computer code from USEPA, 1999 which implements the method described by Turner, 1964. Table 2.3-22 shows the joint data recovery of wind speed, wind direction, and the computed Pasquill stability class. Joint data recovery exceeds 90 percent for 2005, 2006, and 2008 to 2010 and is 86 percent for 2007.

Table 2.3-23 presents the annual Pasquill class frequency distributions for the combined local data period 2005 to 2010, and each individual year in the combined period. This table shows that the Pasquill class "D" stability class is the most frequently occurring stability class for each year and for the combined period. The Pasquill "A" class is the least frequently occurring class. Both of these results are consistent with generally observed stability class climatologies. A similar distribution is also presented, for example, in Stern et al. (1984).

The results in Table 2.3-23 are presented in the form of JFDs of wind direction and wind speed stratified by Pasquill stability class in Table 2.3-24 through Table 2.3-30. These JFDs are used for χ/Q and radiological dose calculations presented later in this report.

A study of historical wind data from SWRA was conducted in 2018 to assess historical changes in wind speed/direction. The study compared data from SWRA from January 2000 through December 2010 with data from January 2007 through December 2017. The datasets jointly represent an 18-year (inclusive) period with some overlap that includes the data from SWRA described in Table 2.3-20 through Table 2.3-30 and Figure 2.3-19 through Figure 2.3-35. The study documented small and insignificant differences between the distributions of wind speeds/directions and Pasquill stability classes between the two data sets. Therefore, the JFDs presented in Table 2.3-24 through Table 2.3-30 based on 2005-2010 data represent atmospheric transport and dispersion characteristics at the SHINE site.

Table 2.3-1 – Selected Characteristics of Wisconsin Physiographic Provinces

Characteristics are based on Moran and Hopkins (2002) and Rand McNally (2005).

	Lake Superior Lowlands	Northern Highlands	Central Plain	Eastern Ridges and Lowlands	Western Uplands
Vegetation	Broadleaf deciduous and needleleaf evergreen trees	Agriculture is limited by lakes, swamps, and short growing season	Marginally suited for agriculture. Irrigation required. Tamarack bogs occur above impervious lake clays.	Broadleaf deciduous and needleleaf evergreen trees	Broadleaf deciduous trees
Topography	Gently sloping plains with steep escarpments at the southern shore of Lake Superior.	The southernmost portion of the Canadian Shield of crystalline bedrock. Weathering and erosion have reduced terrain to nearly a plain. Scattered hills of resistant bedrock remain. Lake and swamp terrain.	Relatively flat or gently rolling topography with occasional sandstone mesas, buttes, pinnacles.	Numerous glacial landforms, lowest elevations of Wisconsin. Lake Winnebago is remnant of a larger glacial lake. Niagara cuesta is a rock ridge in the northeast in Door and Waukesha Counties.	Escaped recent glaciation, allowing streams and rivers to form steep valleys. Portion of the uplands are referred to as the “driftless area” due to the lack of glacial debris or “drift”.
Elevations	Several hundred feet above elevation of the Great Lakes	1,400 to 1.650 feet NAVD 88	750 to 850 feet NAVD 88	Topographic relief of 100 to 200 feet above the elevation of Lake Michigan (mean lake elevation is approximately 600 ft. NAVD 88).	Approximately 1,000 to 1,200 feet NAVD 88, including some topographic relief approaching 500 feet. Rock bluffs, mounds (highest approximately 1,716 ft. NAVD 88).

Table 2.3-2 – Madison, Wisconsin Climatic Means and Extremes
(Sheet 1 of 2)

NORMALS, MEANS, AND EXTREMES
MADISON (KMSN)

LATITUDE: 43° 8'N LONGITUDE: 89° 20'W ELEVATION (FT): GRND: 866 BARO: 860 TIME ZONE: CENTRAL (UTC -6) WBAN: 14837

	ELEMENT	POR	JAN	FEB	MAR	APR	MAY	JUN	JUL	AUG	SEP	OCT	NOV	DEC	YEAR
TEMPERATURE °F	NORMAL DAILY MAXIMUM	30	26.4	31.1	43.1	57.3	68.4	77.9	81.6	79.4	71.8	58.9	44.1	30.2	55.9
	MEAN DAILY MAXIMUM	72	26.3	30.8	42.4	57.5	69.6	78.9	83.0	80.9	72.7	60.8	44.5	31.2	56.6
	HIGHEST DAILY MAXIMUM	80	56	68	83	94	95	101	104	102	99	90	76	65	104
	YEAR OF OCCURRENCE		1989	2017	2012	1980	2018	1988	2012	1988	1953	1976	1964	2012	JUL 2012
	MEAN OF EXTREME MAXS.	76	44.8	49.0	66.6	79.5	86.1	91.3	93.3	91.8	87.9	79.3	64.8	50.7	73.8
	NORMAL DAILY MINIMUM	30	11.1	15.1	24.8	35.8	46.1	56.1	61.0	59.0	50.2	38.8	28.2	15.9	36.8
	MEAN DAILY MINIMUM	72	9.5	13.0	23.4	35.0	45.6	55.4	60.1	58.2	49.5	39.0	27.4	15.7	36.0
	LOWEST DAILY MINIMUM	80	-37	-29	-29	0	19	31	36	35	25	13	-11	-25	-37
	YEAR OF OCCURRENCE		1951	1996	1962	1982	1978	1972	1965	1968	1974	1988	1947	1983	JAN 1951
	MEAN OF EXTREME MINS.	76	-13.1	-9.0	2.9	20.0	30.4	40.7	47.3	44.7	33.4	23.7	9.9	-5.9	18.8
	NORMAL DRY BULB	30	18.8	23.1	34.0	46.6	57.3	67.0	71.3	69.2	61.0	48.9	36.2	23.0	46.4
	MEAN DRY BULB	72	18.0	21.9	32.9	46.3	57.6	67.2	71.6	69.6	61.1	49.9	35.9	23.4	46.3
	MEAN WET BULB	35	16.5	19.3	28.6	38.5	49.9	59.8	64.1	62.9	55.3	43.4	31.6	21.5	41.0
	MEAN DEW POINT	35	15.2	18.1	27.0	36.7	48.5	58.6	63.2	62.1	54.3	42.0	30.5	20.1	39.7
	NORMAL NO. DAYS WITH:														
	MAXIMUM >= 90	30	0.0	0.0	0.0	0.0	0.1	1.3	2.8	1.5	0.1	0.0	0.0	0.0	5.8
	MAXIMUM <= 32	30	20.4	14.4	4.9	0.3	0.0	0.0	0.0	0.0	0.0	0.0	4.4	16.9	61.3
	MINIMUM <= 32	30	29.9	26.3	24.0	10.3	1.4	0.0	0.0	0.0	0.5	7.9	19.6	28.6	148.5
	MINIMUM <= 0	30	7.1	4.1	0.4	0.0	0.0	0.0	0.0	0.0	0.0	0.0	0.1	3.6	15.3
H/C	NORMAL HEATING DEG. DAYS	30	1434	1173	963	558	266	60	10	27	171	505	866	1300	7333
	NORMAL COOLING DEG. DAYS	30	0	0	0	4	26	120	206	157	51	4	0	0	568
RH	NORMAL (PERCENT)		76	74	71	66	66	68	72	76	76	73	76	78	73
	HOUR 00 LST	30	79	79	78	76	77	80	83	87	87	81	81	81	81
	HOUR 06 LST	30	80	82	82	81	81	82	85	91	91	86	84	83	84
	HOUR 12 LST	30	70	67	61	54	53	55	57	61	60	59	67	72	61
	HOUR 18 LST	30	75	71	64	56	54	56	59	64	68	68	74	77	66
S	PERCENT POSSIBLE SUNSHINE	50	47	51	52	52	58	64	67	64	60	54	39	40	54
W/O	MEAN NO. DAYS WITH:														
	HEAVY FOG(VISBY <= 1/4 MI)	55	2.0	1.9	2.7	1.0	1.3	1.2	1.3	2.2	1.9	1.3	1.6	2.8	21.2
	THUNDERSTORMS	71	0.2	0.3	1.8	3.7	5.3	7.2	7.4	6.4	4.2	1.9	0.8	0.3	39.5
CLOUDINESS	MEAN:														
	SUNRISE-SUNSET (OKTAS)														
	MIDNIGHT-MIDNIGHT (OKTAS)														
	MEAN NO. DAYS WITH:														
	CLEAR														
	PARTLY CLOUDY														
	CLOUDY														

Table 2.3-2 – Madison, Wisconsin Climatic Means and Extremes
(Sheet 2 of 2)

PR	MEAN STATION PRESSURE(IN)	35	29.10	29.12	29.09	29.02	29.02	29.01	29.06	29.09	29.11	29.09	29.08	29.11	29.08
	MEAN SEA-LEVEL PRES. (IN)	35	30.08	30.09	30.05	29.96	29.95	29.93	29.97	30.00	30.03	30.02	30.04	30.08	30.02
WINDS	MEAN SPEED (MPH)	35	8.7	8.8	9.3	9.9	8.4	7.4	6.7	6.4	7.0	8.0	8.9	8.5	8.2
	PREVAIL.DIR(TENS OF DEGS)	47	31	31	19	19	19	19	19	19	19	19	19	19	19
	MAXIMUM 2-MINUTE:														
	SPEED (MPH)	23	34	40	37	41	39	41	48	44	43	32	38	35	48
	DIR. (TENS OF DEGS)		06	01	17	06	17	36	01	04	15	33	18	05	01
	YEAR OF OCCURRENCE		1999	2011	2014	2013	2012	1998	2016	2014	2000	2018	1998	2015	JUL 2016
	MAXIMUM 3-SECOND														
	SPEED (MPH)	23	48	47	48	53	56	59	66	52	74	53	52	49	74
	DIR. (TENS OF DEGS)		29	16	19	26	13	02	02	03	15	34	21	25	15
	YEAR OF OCCURRENCE		2013	2016	2017	1997	2010	2013	2004	2014	2000	2018	1998	2017	SEP 2000
PRECIPITATION	NORMAL (IN)	30	1.23	1.45	2.20	3.40	3.55	4.54	4.18	4.27	3.13	2.40	2.39	1.74	34.48
	MAXIMUM MONTHLY (IN)	80	2.87	3.30	6.19	7.11	10.84	10.93	10.93	15.18	9.51	5.63	7.49	4.09	15.18
	YEAR OF OCCURRENCE		2013	2008	2009	1973	2004	2008	1950	2007	1941	1984	2003	1987	AUG 2007
	MINIMUM MONTHLY (IN)	80	0.14	0.06	0.28	0.96	0.64	0.31	1.08	0.70	0.11	0.06	0.11	0.25	0.06
	YEAR OF OCCURRENCE		1981	1995	1978	1946	1981	2012	2014	1948	1979	1952	1976	1960	FEB 1995
	MAXIMUM IN 24 HOURS (IN)	80	1.84	1.59	3.01	2.83	4.37	5.28	5.25	5.00	3.67	2.78	3.43	2.19	5.28
	YEAR OF OCCURRENCE		2013	2001	1998	1975	2004	2008	1950	2007	2009	1984	2003	1990	JUN 2008
	NORMAL NO. DAYS WITH:														
	PRECIPITATION >= 0.01	30	10.2	9.2	10.5	12.1	11.9	11.1	10.6	9.4	9.3	9.8	10.6	10.1	124.8
	PRECIPITATION >= 1.00	30	0.1	0.2	0.3	0.7	0.7	1.2	1.3	1.2	0.7	0.3	0.5	0.2	7.4
SNOWFALL	NORMAL (IN)	30	12.9	10.6	7.0	2.6	0.2	0.0	0.0	0.0	0.0	0.5	3.6	13.5	50.9
	MAXIMUM MONTHLY (IN)	71	27.5	37.0	25.4	17.4	3.0	T	T	T	T	3.9	18.3	40.4	40.4
	YEAR OF OCCURRENCE		1995	1994	1959	1973	1990	2011	2009	2014	2012	1997	1985	2008	DEC 2008
	MAXIMUM IN 24 HOURS (IN)	71	13.0	14.2	13.6	12.9	3.0	T	T	T	T	3.8	9.0	17.3	17.3
	YEAR OF OCCURRENCE'		1996	1994	1971	1973	1990	2011	2009	2014	2012	1997	1985	1990	DEC 1990
	MAXIMUM SNOW DEPTH (IN)	71	32	28	16	14	4	0	0	0	0	4	9	17	32
	YEAR OF OCCURRENCE		1979	1979	1986	1973	1994					1997	1985	1990	JAN 1979
	NORMAL NO. DAYS WITH:														
	SNOWFALL >= 1.0	30	3.6	3.2	2.0	0.7	0.1	0.0	0.0	0.0	0.0	0.1	1.2	3.8	14.7

published by: NCEI Asheville, NC 3 30 year Normals (1981-2010)

References:
NCDC, 2019b

Table 2.3-3 – Rockford, Illinois Climatic Means and Extremes
(Sheet 1 of 2)

NORMALS, MEANS, AND EXTREMES
ROCKFORD (KRFD)

LATITUDE: 42° 11'N LONGITUDE: 89° 5'W ELEVATION (FT): GRND: 730 BARO: 731 TIME ZONE: CENTRAL (UTC -6) WBAN: 94822

	ELEMENT	POR	JAN	FEB	MAR	APR	MAY	JUN	JUL	AUG	SEP	OCT	NOV	DEC	YEAR
TEMPERATURE °F	NORMAL DAILY MAXIMUM	30	29.5	34.2	46.9	60.7	71.8	81.1	84.5	82.4	75.4	62.7	47.6	33.2	59.2
	MEAN DAILY MAXIMUM	68	28.0	32.5	44.6	59.1	71.1	80.2	83.9	81.9	74.8	62.6	46.6	33.0	58.2
	HIGHEST DAILY MAXIMUM	68	63	70	85	91	99	101	105	104	102	90	77	69	105
	YEAR OF OCCURRENCE		2008	2017	1986	2002	2012	1988	2012	1988	1953	2010	2016	2012	JUL 2012
	MEAN OF EXTREME MAXS.	68	48.0	51.5	69.4	80.8	87.5	92.6	93.8	92.4	89.5	81.6	66.9	53.0	75.6
	NORMAL DAILY MINIMUM	30	13.5	17.7	27.5	38.1	48.4	58.5	63.0	61.3	52.4	40.7	30.3	17.7	39.1
	MEAN DAILY MINIMUM	68	11.9	16.0	26.4	37.4	48.2	57.9	62.7	60.9	52.2	40.9	29.3	17.8	38.5
	LOWEST DAILY MINIMUM	68	-27	-24	-11	5	24	37	43	41	27	15	-10	-24	-27
	YEAR OF OCCURRENCE		1982	1996	2014	1982	1966	2003	1967	1986	1984	1952	1977	1983	JAN 1982
	MEAN OF EXTREME MINS.	68	-10.9	-5.6	7.4	22.0	33.4	45.2	51.3	49.5	36.7	25.7	12.4	-4.4	21.9
	NORMAL DRY BULB	30	21.5	25.9	37.2	49.4	60.1	69.8	73.8	71.9	63.9	51.7	38.9	25.4	49.1
	MEAN DRY BULB	68	20.0	24.3	35.5	48.3	59.7	69.2	73.3	71.4	63.5	51.8	38.0	25.4	48.4
	MEAN WET BULB	35	18.3	21.2	30.7	40.1	51.3	60.9	65.1	64.0	56.2	44.5	33.2	23.0	42.4
	MEAN DEW POINT	35	17.6	20.5	29.5	38.6	49.9	59.7	64.2	63.2	55.3	43.4	32.4	22.2	41.4
	NORMAL NO. DAYS WITH:														
	MAXIMUM >= 90	30	0.0	0.0	0.0	0.0	0.6	3.4	5.7	4.0	1.1	0.1	0.0	0.0	14.9
	MAXIMUM <= 32	30	17.3	10.7	3.0	0.1	0.0	0.0	0.0	0.0	0.0	0.0	2.3	12.6	46.0
	MINIMUM <= 32	30	29.0	25.0	21.8	7.5	0.5	0.0	0.0	0.0	0.3	5.1	16.8	27.4	133.4
	MINIMUM <= 0	30	5.5	2.9	0.2	0.0	0.0	0.0	0.0	0.0	0.0	0.0	0.0	2.9	11.5
H/C	NORMAL HEATING DEG. DAYS	30	1348	1093	862	476	198	31	3	11	117	422	782	1226	6569
	NORMAL COOLING DEG. DAYS	30	0	0	0	8	47	175	274	223	84	9	0	0	820
RH	NORMAL (PERCENT)		78	76	71	66	66	68	72	76	74	72	77	80	73
	HOUR 00 LST	30	81	81	78	74	76	79	84	88	86	82	81	82	81
	HOUR 06 LST	30	82	83	83	80	81	82	87	91	91	87	84	84	85
	HOUR 12 LST	30	72	68	62	55	54	55	58	60	57	57	67	73	62
	HOUR 18 LST	30	77	73	65	55	55	56	60	64	65	65	73	78	66
S	PERCENT POSSIBLE SUNSHINE														
W/O	MEAN NO. DAYS WITH:														
	HEAVY FOG(VISBY <= 1/4 MI)	55	2.3	2.2	2.4	0.8	0.9	0.6	1.0	1.6	1.5	1.5	1.9	3.0	19.7
	THUNDERSTORMS	63	0.2	0.5	2.0	4.1	6.0	8.1	7.5	6.5	4.5	2.3	1.1	0.3	43.1
CLOUDINESS	MEAN:														
	SUNRISE-SUNSET (OKTAS)														
	MIDNIGHT-MIDNIGHT (OKTAS)														
	MEAN NO. DAYS WITH:														
	CLEAR														
	PARTLY CLOUDY														
	CLOUDY														

Table 2.3-3 – Rockford, Illinois Climatic Means and Extremes
(Sheet 2 of 2)

PR	MEAN STATION PRESSURE(IN)	35	29.27	29.28	29.20	29.17	29.17	29.17	29.21	29.21	29.26	29.24	29.26	29.28	29.23
	MEAN SEA-LEVEL PRES. (IN)	35	30.12	30.11	30.07	29.97	29.97	29.95	29.99	30.02	30.05	30.05	30.07	30.10	30.04
WINDS	MEAN SPEED (MPH)	35	10.0	10.0	10.8	11.1	9.7	8.2	7.3	6.8	7.5	9.0	10.0	9.7	9.2
	PREVAIL.DIR(TENS OF DEGS)	44	31	31	31	07	19	19	19	19	19	19	19	19	19
	MAXIMUM 2-MINUTE:														
	SPEED (MPH)	23	40	49	44	47	45	55	52	57	46	44	45	39	57
	DIR. (TENS OF DEGS)		29	22	30	23	27	31	02	29	30	23	24	29	29
	YEAR OF OCCURRENCE		2014	1999	2004	1997	2011	2011	2015	1998	2011	2010	1998	2004	AUG 1998
	MAXIMUM 3-SECOND														
	SPEED (MPH)	23	52	68	67	64	63	69	66	74	58	61	56	56	74
	DIR. (TENS OF DEGS)		28	22	19	26	19	31	33	28	30	34	22	26	28
	YEAR OF OCCURRENCE		2017	1999	2009	1997	2008	2011	2015	1998	2011	2018	1998	2017	AUG 1998
PRECIPITATION	NORMAL (IN)	30	1.37	1.41	2.32	3.35	4.02	4.65	3.95	4.59	3.35	2.67	2.58	1.98	36.24
	MAXIMUM MONTHLY (IN)	68	4.66	3.61	5.82	9.92	11.75	14.23	11.81	13.98	10.68	8.32	5.55	5.04	14.23
	YEAR OF OCCURRENCE		1960	2018	2009	1973	1996	2018	1952	2007	1961	1969	2015	1971	JUN 2018
	MINIMUM MONTHLY (IN)	68	0.18	0.04	.43	0.99	0.48	0.46	0.75	0.48	0.05	0.01	0.38	0.37	0.01
	YEAR OF OCCURRENCE		1961	1969	2005	1989	1992	1988	2001	2003	1979	1952	1976	1976	OCT 1952
	MAXIMUM IN 24 HOURS (IN)	68	2.89	1.73	2.50	5.55	4.77	6.07	5.32	6.42	5.56	5.22	3.20	2.50	6.42
	YEAR OF OCCURRENCE		1960	1966	1976	1973	1996	2002	2010	1987	1961	1954	1961	2003	AUG 1987
	NORMAL NO. DAYS WITH:														
	PRECIPITATION >= 0.01	30	9.4	8.2	10.5	11.3	12.2	10.4	9.4	9.7	8.3	9.4	10.2	10.2	119.2
	PRECIPITATION >= 1.00	30	0.1	0.2	0.5	0.8	1.2	1.3	0.9	1.2	0.8	0.5	0.5	0.2	8.2
SNOWFALL	NORMAL (IN)	30	10.2	7.7	4.8	0.9	0.0	0.0	0.0	0.0	0.0	0.1	1.7	11.3	36.7
	MAXIMUM MONTHLY (IN)	66	26.1	30.2	22.7	7.7	1.0	T	T	T	T	2.2	15.8	30.1	30.2
	YEAR OF OCCURRENCE		1979	1994	1964	1982	1966	1996	2008	2014	2016	1967	2018	2000	FEB 1994
	MAXIMUM IN 24 HOURS (IN)	66	9.9	10.9	10.4	6.7	0.2	T	T	T	T	2.2	11.7	11.4	11.7
	YEAR OF OCCURRENCE'		1979	2011	1972	1970	1990	1996	1994	2014	2016	1967	2018	1987	NOV 2018
	MAXIMUM SNOW DEPTH (IN)	56	13	19	15	2	0	0	0	0	0	2	11	13	19
	YEAR OF OCCURRENCE		2014	2011	2013	2018						1993	2018	2008	FEB 2011
	NORMAL NO. DAYS WITH: SNOWFALL >= 1.0	30	3.3	2.3	1.5	0.3	0.0	0.0	0.0	0.0	0.0	0.0	0.5	3.1	11.0

published by: NCEI Asheville, NC 3 30 year Normals (1981-2010)

References:
NCDC, 2019c

Table 2.3-4 – Madison, Wisconsin and Rockford, Illinois Additional Climatic Means and Extremes
(Sheet 1 of 2)

Parameter	Period	Madison	Rockford
Mean number of days with rain or drizzle (NCDC, 1996a)	January	5	6
	February	5	5
	March	10	11
	April	15	15
	May	16	16
	June	15	14
	July	15	14
	August	14	13
	September	13	13
	October	13	13
	November	10	11
	December	7	8
	Annual	138	139
Mean number of days with freezing rain or drizzle (NCDC, 1996a)	January	1	1
	February	< 0.5	< 0.5
	March	< 0.5	< 0.5
	April	< 0.5	< 0.5
	May	0	0
	June	0	0
	July	0	0
	August	0	0
	September	0	0
	October	< 0.5	0
	November	< 0.5	< 0.5
	December	1	1
	Annual	2	2

Table 2.3-4 – Madison, Wisconsin and Rockford, Illinois Additional Climatic Means and Extremes
(Sheet 2 of 2)

Parameter	Period	Madison	Rockford
Mean number of days with snow (NCDC, 1996a)	January	18	17
	February	14	13
	March	13	11
	April	4	3
	May	< 0.5	<0.5
	June	0	0
	July	0	0
	August	0	0
	September	< 0.5	0
	October	1	1
	November	9	8
	December	16	15
	Annual	75	68
Mean number of days with hail or sleet (NCDC, 1996a)	January	0	< 0.5
	February	0	< 0.5
	March	< 0.5	< 0.5
	April	< 0.5	< 0.5
	May	< 0.5	< 0.5
	June	< 0.5	< 0.5
	July	< 0.5	< 0.5
	August	< 0.5	< 0.5
	September	< 0.5	< 0.5
	October	< 0.5	< 0.5
	November	< 0.5	< 0.5
	December	< 0.5	0
	Annual	2	2

Table 2.3-5 – List of NOAA ASOS Stations Located within the Site Climate Region[a][b][c]

Name	USAF ID No.	WBAN ID No.	St.	County	North Latitude (deg min sec)	West Longitude (deg min sec)	Ground Elev. (ft. MSL)	Approximate Available DS 3505 Period of Record (years)
Baraboo	726503	54833	WI	Sauk	43 31 19	89 46 26	976	1997-2018 (22)
Burlington	722059	04866	WI	Racine	42 41 24	88 18 14	779	1945-2018 (74)
De Kalb Taylor Municipal Airport	722075	04871	WI	De Kalb	41 55 55	88 42 29	915	1973-2018 (46)
Juneau Dodge County	726509	04898	WI	Dodge	43 25 34	88 42 11	936	1997-2018 (22)
Du Page County	725305	94892	IL	Du Page	41 54 50	88 14 46	754	1973-2018 (46)
Fond du Lac County Airport	726506	04840	WI	Fond du Lac	43 46 8	88 29 28	807	1997-2018 (22)
Freeport Albertus Airport	722082	04876	IL	Stephenson	42 14 46	89 34 55	859	2004-2018 (15)
Janesville Southern Wisconsin Regional	726415	94854	WI	Rock	42 37 1	89 1 59	808	1973-2018 (46)
Madison Dane County Truax Field	726410	14837	WI	Dane	43 8 28	89 20 42	866	1948-2018 (71)
Middleton Municipal Morey Field	720656	n/a	WI	Dane	43 6 50	89 31 55	928	2009-2013 (5)
Monroe Municipal	726414	04873	WI	Green	42 36 54	89 35 28	1085	2001-2018 (18)
Rochelle Municipal Airport Koritz Field	722182	04890	IL	Ogle	41 53 35	89 4 41	781	2004-2018 (15)
Chicago Rockford Intl Airport	725430	94822	IL	Winnebago	42 11 35	89 5 35	730	1973-2018 (46)
Watertown Municipal Airport	726464	54834	WI	Jefferson	43 10 1	88 43 1	820	1995-2018 (24)

a. The site climate region and station locations are defined via the map in Figure 2.3-16.
b. Extracted from NCDC 2019ab.
c. MSL elevations are functionally equivalent to the NAVD 88 elevations in this table.

Table 2.3-6 – List of NOAA COOP Stations in the Site Climate Region for which Clim-20 Summaries and Updates are Available

Name	St.	County	North Latitude (deg min)	West Longitude (deg min)	Ground Elev. (ft. MSL)	Approx. Period of Available Digital Record
Arboretum Univ of WI	WI	Dane	43 3	89 24	865	1971-2018
Arlington Univ Farm	WI	Columbia	43 18	89 21	1080	1962-2018
Baraboo	WI	Sauk	43 27	89 44	823	1948-2018
Beaver Dam	WI	Dodge	43 27	88 51	840	1948-2018
Beloit	WI	Rock	42 30	89 2	780	1948-2018
Brodhead	WI	Green	42 37	89 23	790	1948-2018
Charmany Farm	WI	Dane	43 4	89 29	910	1959-2018
Dalton	WI	Green Lake	43 39	89 12	860	1948-2007
De Kalb	IL	De Kalb	41 56	88 47	873	1966-2018
Fond du Lac	WI	Fond du Lac	43 48	88 27	760	1948-2018
Ft Atkinson	WI	Jefferson	42 54	88 51	800	1948-2018
Hartford 2 W	WI	Washington	43 20	88 25	980	1948-2018
Horicon	WI	Dodge	43 26	88 38	880	1970-2018
Lake Geneva	WI	Walworth	42 36	88 26	880	1948-2018
Lake Mills	WI	Jefferson	43 5	88 55	852	1948-2018
Madison Dane Co AP	WI	Dane	43 8	89 21	858	1948-2018
Marengo	IL	McHenry	42 15	88 36	810	1901-2018
Oconomowoc	WI	Waukesha	43 6	88 30	856	1948-2018
Portage	WI	Columbia	43 32	89 26	775	1948-2018
Prairie du Sac 2 N	WI	Sauk	43 19	89 44	780	1947-2008
Rockford AP	IL	Winnebago	42 12	89 6	733	1951-2018
Stoughton	WI	Dane	42 37	89 45	840	1948-2018
Watertown	WI	Jefferson	43 11	88 44	825	1924-2018
Wisconsin Dells	WI	Columbia	43 37	89 46	835	1948-2018

Table 2.3-7 – Regional Tornadoes and Waterspouts[a][b][c]

State	County	Area (mi.^{2})	Number of Tornadoes	Number of Waterspouts
IL	Boone	282	14	0
IL	Carroll	466	18	0
IL	Cook	1635	53	0
IL	De Kalb	635	14	0
IL	Du Page	337	26	0
IL	Kane	524	20	0
IL	Lake	1368	17	1
IL	Lee	729	29	0
IL	McHenry	611	19	0
IL	Ogle	763	22	0
IL	Stephenson	565	15	0
IL	Whiteside	697	30	0
IL	Winnebago County	519	16	1
WI	Adams	689	17	0
WI	Columbia	796	36	0
WI	Dane	1238	64	0
WI	Dodge	907	58	0
WI	Fond du Lac	766	44	0
WI	Green	585	25	0
WI	Green Lake	380	30	0
WI	Jefferson	583	33	0
WI	Juneau	804	23	0
WI	Kenosha	754	9	0
WI	Marquette	464	20	0
WI	Racine	792	20	1
WI	Rock	726	25	0
WI	Sauk	848	23	0
WI	Walworth	577	26	0
WI	Washington	436	18	0
WI	Waukesha	580	30	0
	Totals	21,056	794	3

a. Period of record is May, 1950 through November, 2018.
b. NCDC, 2018a.
c. Additionally, an F5 tornado occurred on 8 June 1984 at Barneveld in Iowa County, Wisconsin, which is located approximately 50 miles (80 km) west-northwest of the site (NCDC, 1984a).

Table 2.3-8 – Details of Strongest Tornadoes in Rock County, Wisconsin[a][b]

Tornado Intensity	Date	Path Length (mi.)	Path Width (yd.)	Property Damage ($)	Additional Description
F2	15 Nov 1960	2	Narrow	500 – 5,000	Occurred 1.5 mi (2.4 km) north of Union, Wisconsin. Damage occurred to farm buildings, an abandoned restaurant, and a school roof.
F2	22 Sep 1961	5	Narrow	50,000 – 500,000	Occurred 1 mi. (1.6 km) south of Whitewater, Wisconsin. Damage occurred to at least 15 farms. There was 1 injury.
F2	9 Oct 1970	15	50	50,000 – 500,000	The tornado moved NNW from the banks of the Rock River just north of Riverside Park (NW of Janesville) and 5 mi. (8.0 km) west of Edgerton toward Stoughton. An outbuilding was damaged. There was 1 injury.
F2	1 Nov 1971	3	100	50,000 – 500,000	A small tornado moved northeast in a mostly residential area along a line from 2.5 mi. (4.0 km) NNW to about 4 mi NNE of downtown Beloit. Several homes and garages were severely damaged. There was 1 injury.
F2	8 May 1988	27	175	50,000 – 500,000	Tornado affected Rock, Dane, and Jefferson counties. Many farm buildings and two homes were damaged.
F2	27 Mar 1991	35	440	5 million – 50 million	Tornado affected Green, Rock, Dane, and Jefferson counties. There were 5 injuries and 1 fatality.
F2	25 Jun 1998	2.5	100	845,000	Tornado moved from 2.3 mi. (3.7 km) WNW of Leyden to 1 mi. (1.6 km) NNE of Leyden.

a. Period of record is May, 1950 through November, 2018.
b. Based on NCDC, 1960a; NCDC, 1961a; NCDC, 1970a; NCDC, 1971a; NCDC, 1988a; NCDC, 1991a; NCDC, 1998a; and NCDC, 2018a.

Table 2.3-9 – Details of Strongest Tornadoes in Surrounding Counties Adjacent to Rock County, Wisconsin[a][b][c][d][e][f] (Sheet 1 of 2)

Tornado Intensity	Date	County	Path Length (mi.)	Path Width (yd.)	Property Damage ($)	Additional Description
F4	21 Apr 1967	Boone	28	600-1200	5 million – 50 million	Tornado moved near 50 mph (22.4 m/s) towards ENE to E, from 2 mi. (3.2 km) SE of Cherry Valley to 2 mi. (3.2 km) north of Woodstock. Numerous reports of multiple funnel sightings were substantiated by damage. Almost complete destruction directly in path with major wind damage on either side. Many farm homes completely destroyed. Woods were stripped with large trees uprooted or snapped off. About 5% of the path was through an urban area, which was the SE corner of Belvidere, where a high school was hit. There were 450 injuries and 24 fatalities.
F3	7 Jan 2008	Boone	6.9	100	2.0 million	Tornado traveled from about 1.2 mi. (1.9 km) N of Poplar Grove in Boone County, to about 3.2 mi (5.1 km) NE of Harvard in McHenry County. A large barn and farmhouse were destroyed, and other buildings severely damaged. Damage also occurred to power lines. Large trees were snapped, uprooted, and stripped of branches. There were 4 injuries.
F3	2 Aug 1967	Dane	1	100	5,000 – 50,000	Tornado moved SE on the N shore of Lake Mendota in the town of Westport, about 100 yards (0.1 km) inland. Three cottages were destroyed and several homes slightly damaged. There were 5 injuries and 2 fatalities.
F3	4 Jun 1975	Dane	4	33	5,000 – 50,000	Tornado touched down 3 mil. (4.8 km) north of Sun Prairie and moved towards the east. Two farms had extensive damage and one home was destroyed.
F3	17 Jun 1992	Dane	16	400	5 million – 50 million	Tornado skipped along a path from 2 mi. (3.2 km) north of Belleville to 1 mi. (1.6 km) east of McFarland, injuring 30 people.

Table 2.3-9 – Details of Strongest Tornadoes in Surrounding Counties Adjacent to Rock County, Wisconsin[a][b][c][d][e][f] (Sheet 2 of 2)

Tornado Intensity	Date	County	Path Length (mi.)	Path Width (yd.)	Property Damage ($)	Additional Description
F3	18 Aug 2005	Dane	17	600	34.3 million	Strong and destructive tornado started about 2.8 mi. (4.5 km) SE of Fitchburg and moved slowly ESE to the southern edge of Lake Kegonsa through residential neighborhoods including Dunn, Pleasant Springs, and Stoughton. There was extensive damage to homes, businesses, farm buildings, vehicles, power lines, and trees. There were 23 injuries and 1 fatality.
F3	16 Jun 2014	Dane	0.96	100	14.0 million	2 mi. (3.2 km) NW of Verona. A tornado severely damaged the Country View Elementary school, which will have to be rebuilt. At least 30 homes sustained major damage, 19 of which were rendered uninhabitable. Estimated winds up to 140 mph. No injuries or fatalities.
F3	24 Jan 1967	Green	25	25	50,000 – 500,000	Severe thunderstorms caused widespread wind damage across Green, Rock, Jefferson, Waukesha, Washington, and Ozaukee counties. One tornado destroyed several farm buildings from near Brodhead in Green County to northwest of Janesville. Janesville Country Club was extensively damaged. No injuries or fatalities.
F3	5 Jun 1980	Jefferson	4	n/a	5,000 – 50,000	Tornado formed near Rock River at 0.25 mi. (0.4 km) E of Watertown, lifted and moved SE where it touched down a second time 1 mi. (1.6 km) SE of Pipersville. No injuries or fatalities.

a. The project site is in Rock County, WI.
b. Counties adjacent to Rock County include: Green (WI), Dane (WI), Jefferson (WI), Walworth (WI), Boone (IL), Winnebago (IL), and Stephenson (IL).
c. Period of record is May, 1950 through November, 2018.
d. Based on NCDC, 1967a-c; NCDC, 1975a; NCDC, 1980a; NCDC, 1992a; NCDC, 2005b; NCDC, 2008a; NCDC, 2014; and NCDC, 2018a.
e. "n/a" means information not available in the respective Storm Report.
f. An F5 tornado occurred on 8 June 1984 at Barneveld in Iowa County, Wisconsin, approximately 50 mi. (80 km) west-northwest of the SHINE site (NCDC, 1984a).

Table 2.3-10 – Precipitation Extremes at Local and Regional NOAA COOP Meteorological Monitoring Stations within the Site Climate Region[a][b][c]

Station Name	State	County	Maximum Recorded 24-Hour Rainfall (in.)	Maximum Recorded Monthly Rainfall (in.)	Maximum Recorded 24-Hour Snowfall (in.)	Maximum Recorded Monthly Snowfall (in.)
Arboretum Univ of WI	WI	Dane	6.01	13.49	13.5	31.7
Arlington Univ Farm	WI	Columbia	5.10	13.66	14.0	31.0
Baraboo	WI	Sauk	7.78	17.17	12.0	45.9
Beaver Dam	WI	Dodge	4.41	15.73	14.4	45.6
Beloit	WI	Rock	5.77	14.39	15.0	37.6
Brodhead	WI	Green	6.62	15.57	14.0	35.4
Charmany Farm	WI	Dane	**9.62**	14.62	14.0	31.1
Dalton	WI	Green Lake	5.90	13.77	**21.0**	37.1
DeKalb	IL	De Kalb	8.09	14.23	15.7	34.5
Fond du Lac	WI	Fond du Lac	6.83	13.47	14.0	45.2
Ft Atkinson	WI	Jefferson	4.47	11.26	15.2	39.0
Hartford 2 W	WI	Washington	5.20	14.09	13.0	44.0
Horicon	WI	Dodge	5.94	14.72	16.0	40.0
Lake Geneva	WI	Walworth	3.88	11.30	13.2	38.5
Lake Mills	WI	Jefferson	5.59	17.75	12.0	37.5
Madison Dane Co AP	WI	Dane	5.28	15.18	17.3	40.4
Marengo	IL	McHenry	8.20	14.19	18.0	28.0
Oconomowoc	WI	Waukesha	5.38	11.56	11.5	42.4
Portage	WI	Columbia	6.29	**18.27**	12.5	41.9
Prairie du Sac 2 N	WI	Sauk	5.73	11.41	11.6	23.5
Rockford AP	IL	Winnebago	6.42	14.23	11.7	30.2
Stoughton	WI	Dane	6.03	16.40	14.0	42.6
Watertown	WI	Jefferson	6.65	14.82	13.0	**50.4**
Wisconsin Dells	WI	Columbia	7.67	14.13	14.0	38.6

a. The site climate region and station locations are defined in Figure 2.3-17.
b. Based on 1971 - 2000 data in NCDC, 2001a-x with updates through 2018 from NCDC, 2019a-c and NCDC, 2019f-aa.
c. Maximum regional values of the respective parameter are in bold font.

Table 2.3-11 – Mean Seasonal and Annual Hail or Sleet Frequencies at Rockford, Illinois and Madison, Wisconsin

Station	Winter	Spring	Summer	Autumn	Annual
Rockford	<0.3	<0.5	<0.5	<0.5	2
Madison	<0.2	<0.5	<0.5	<0.5	2

Reference:
NCDC, 1996a

Table 2.3-12 – Ice Storms that have Affected Rock County, Wisconsin[a]

Date of Storm	Description of Ice Storm
26 Feb 1995	Freezing rain and freezing drizzle. Coating of ice up to one-quarter inch.
26 Nov 1995	Two to six-hour period of sleet and/or freezing rain glazed road surfaces.
13 Dec 1995	Ice accumulations of one-quarter to one-half inch on top of one to five inches of snow. A glazing of less than one-quarter inch of freezing rain or freezing drizzle.
4 Feb 1997	Several hours of freezing rain, accumulated to one-quarter inch. Sheets of ice on roads and sidewalks, especially rural
3 Feb 2003	Periodic light freezing drizzle of light freezing rain glazed roads and sidewalks.
7 Apr 2003	Freezing drizzle left crusty layers.
16 Jan 2004	Freezing rain caused road surfaces to become very slippery due to initial ice glazing of one-sixteenth to one-eighth inch.
7 Mar 2004	Freezing drizzle/rain generated a thin layer of ice on road surfaces.
18 Dec 2004	Light freezing drizzle coated roads and bridges during morning hours.
1 Jan 2005	Pockets of freezing rain or drizzle resulted in a light glaze of ice on many road surfaces and sidewalks.
17 Feb 2008	Ice storm affected a 25 to 30 mile-wide area stretching from Janesville to Ft. Atkinson to Delafield to West Bend to Port Washington, with about 11 hours of freezing rain. Ice accumulations ranged from one-quarter to one-half inch. Roads were icy.
8 Dec 2008	Freezing rain produced ice accumulations of one-tenth to two-tenths inch near the Illinois border.
28 Mar 2009	Mixture of sleet, rain, freezing rain, and snow caused very hazardous driving conditions. Ice accumulations were one-tenth inch.
23 Dec 2009	Freezing rain during afternoon hours resulted in a low-end ice storm with ice accumulations of one-quarter to one-half inch. Trees and power lines were coated, causing them to break.

a. Based on 1995 – 2011 data in NCDC, 2011a.

Table 2.3-13 – Mean Seasonal Thunderstorm Frequencies at Rockford, Illinois and Madison, Wisconsin[a]

Station	Winter	Spring	Summer	Autumn
Rockford	0.3	4.0	7.4	2.6
Madison	0.3	3.6	7.0	2.3

a. From NCDC, 2019b and NCDC, 2019c.

Table 2.3-14 – Design Wet and Dry Bulb Temperatures

Statistic	Bounding Value
Maximum DBT with annual exceedance probability of 0.4 percent	90.9°F (Rockford)
Mean coincident WBT (MCWB) at the 0.4 percent DBT	74.4°F (Rockford)
Maximum DBT with annual exceedance probability of 2.0 percent	85.4°F (Rockford)
Mean coincident WBT (MCWB) at the 2.0 percent DBT	71.6°F (Rockford)
Minimum DBT with annual exceedance probability of 0.4 percent	-6.3°F (Madison and Fond du Lac)
Minimum DBT with annual exceedance probability of 1.0 percent	-1.2°F (Madison)
Maximum WBT with annual exceedance probability of 0.4 percent	77.9°F (Du Page County Airport)
Maximum DBT with annual exceedance probability of 5 percent	81°F (Rockford)
Minimum DBT with annual exceedance probability of 5 percent	9°F (Madison)

Reference:
ASHRAE, 2017

Table 2.3-15 – Estimated 100-Year Return Maximum and Minimum DBT, MCWB Coincident with the 100-Year Return Maximum DBT, Historic Maximum WBT and Estimated 100-Year Annual Maximum Return WBT

Station	Estimated 100-yr maximum DBT (^{o}F)	MCWB coincident with 100-yr maximum DBT (^{o}F)	Historic maximum WBT (^{o}F)	Estimated 100-yr maximum WBT (^{o}F)	Estimated 100-yr minimum DBT (^{o}F)
Rockford	104.8	80	83.6	85.9	-35.1
Madison	104.3	75	85.0	86.0	-33.4
Bounding Value	104.8	80	85.0	86.0	-35.1

Table 2.3-16 – Dry Bulb Temperature Extremes at Local and Regional NOAA COOP Meteorological Monitoring Stations within the Site Climate Region[a][b][c]

Station Name	State	County	Maximum Dry Bulb Temperature (°F)	Minimum Dry Bulb Temperature (°F)
Arboretum Univ of WI	WI	Dane	108	-38
Arlington Univ Farm	WI	Columbia	103	-36
Baraboo	WI	Sauk	103	**-45**
Beaver Dam	WI	Dodge	102	-36
Beloit	WI	Rock	102	-26
Brodhead	WI	Green	103	-36
Charmany Farm	WI	Dane	103	-34
Dalton	WI	Green Lake	104	-39
DeKalb	IL	De Kalb	103	-27
Fond du Lac	WI	Fond du Lac	103	-41
Ft Atkinson	WI	Jefferson	103	-39
Hartford 2 W	WI	Washington	105	-35
Horicon	WI	Dodge	102	-36
Lake Geneva	WI	Walworth	106	-27
Lake Mills	WI	Jefferson	104	-33
Madison Dane Co AP	WI	Dane	104	-37
Marengo	IL	McHenry	**109**	-29
Oconomowoc	WI	Waukesha	103	-33
Portage	WI	Columbia	103	-35
Prairie du Sac 2N	WI	Sauk	103	-42
Rockford AP	IL	Winnebago	105	-27
Stoughton	WI	Dane	103	-35
Watertown	WI	Jefferson	103	-33
Wisconsin Dells	WI	Columbia	102	-43

a. The site climate region and station locations are defined in Figure 2.3-17.
b. Based on 1971 - 2000 data in NCDC, 2001a-x with updates through 2018 from NCDC, 2019b-c and NCDC, 2019f-aa.
c. The highest and lowest dry bulb temperatures in the region are in bold font.

Table 2.3-17 – Nearest Class I Areas to the Project Site[a]

Class I Area	Distance from Project Site (km)	Distance from Project Site (mi.)	Direction from Project Site
Rainbow Lake Wilderness Area, WI	455	283	Northwest
Seney Wilderness Area, MI	475	295	North-northwest
Isle Royale National Park, MI	610	379	North
Mammoth Cave National Park, KY	630	391	South-southeast
Boundary Waters Canoe Area, MN	640	398	North-northwest
Mingo Wilderness Area, MO	645	401	South
Voyageurs National Park, MN	730	454	North

a. Based on NSPS, 2011.

Table 2.3-18 – Mean Temperature and Precipitation Climate Parameters for Available Normal (30-year) Periods and Extreme Precipitation, Temperature, and Tornado Occurrence Climate Parameters for Historic (10-year) Periods[(a)]

Normal Period

Period	1	2	3	4	5	6
	1931 - 1960	**1941 - 1970**	**1951 - 1980**	**1961 - 1990**	**1971 - 2000**	**1981 - 2010**
Wisconsin South Central Climate Division Temperature (°F)	46.7	46.3	45.9	45.7	45.9	46.4
Wisconsin South Central Climate Division Precipitation (in.)	31.24	31.13	31.75	32.27	34.11	34.48

Historic Period

Period	1	2	3	4	5	6
	1951 - 1960	**1961 - 1970**	**1971 - 1980**	**1981 - 1990**	**1991 - 2000**	**2001 - 2010**
Madison Wisconsin extreme high daily precipitation (in.)	5.25	3.67	3.89	3.68	4.51	5.28
Madison Wisconsin extreme high daily snow (in.)	10.8	16.0	13.6	17.3	14.2	11.9
Madison Wisconsin extreme high temperature (°F)	102	97	104	102	101	98
Madison Wisconsin extreme low temperature (°F)	-37	-30	-28	-28	-29	-19
Rock County and adjacent counties WI strongest tornado	F2	F4	F3	F2	F3	F3

a. Data extracted from NCDC, 1952; NCDC, 1953; NCDC, 1954; NCDC, 1955; NCDC, 1956; NCDC, 1957; NCDC,1958; NCDC, 1959; NCDC, 1960b; NCDC, 1961b; NCDC, 1962; NCDC, 1963; NCDC, 1964; NCDC, 1965; NCDC, 1966; NCDC, 1967d; NCDC, 1968; NCDC, 1969; NCDC, 1970b; NCDC, 1971b; NCDC, 1972; NCDC, 1973; NCDC,1974; NCDC, 1975b; NCDC, 1976; NCDC, 1977; NCDC, 1978; NCDC, 1979; NCDC, 1980b; NCDC, 1981; NCDC, 1982; NCDC, 1983; NCDC, 1984b; NCDC, 1985; NCDC, 1986; NCDC, 1987; NCDC, 1988b; NCDC, 1989; NCDC,1990; NCDC, 1991b; NCDC, 1992b; NCDC, 1993; NCDC, 1994; NCDC, 1995; NCDC, 1996b; NCDC, 1997; NCDC, 1998b; NCDC, 1999b; NCDC, 2000b; NCDC, 2001y; NCDC, 2002b; NCDC, 2002c; NCDC, 2002d; NCDC, 2003; NCDC, 2004; NCDC, 2005c; NCDC, 2006b; NCDC, 2007; NCDC, 2008b; NCDC, 2009; NCDC, 2010; NCDC, 2011f; and NCDC, 2019b

Table 2.3-19 – FAA Specifications for Automated Weather Observing Stations[a]

Parameter	Range	Accuracy	Resolution	Other
Dry bulb temperature	-30° – +130°F (-35° – +55°C)	1°F RMSE over entire range with maximum error of 2°F	≤ 1°F	time constant ≤ 2 min
Relative humidity	5 – 100%	≤ 5%	≤ 1°%	time constant < 2 min
Wind speed	2 – 85 knots	a) ± 2 knots up to 40 knots b) RMSE ± 5% above 40 knots	1 knot	a) distance constant < 10 m b) 2 knot threshold
Wind direction	1°– 360° azimuth	± 5% RMSE	1°	a) time constant < 2 seconds b) 2 knot threshold
Pressure	17.58 – 31.53 in. Hg	a) ± 0.02 in. Hg RMSE; b) maximum error 0.02 in. Hg	0.001 in. Hg	drift ± 0.02 in. RMSE Hg for period not less than 6 months
Visibility	< 1/4 – 10 mi.	a) 1/4 – 1-1/4 mi.: ± 1/4 mi. b) 1-1/2 – 1-3/4 mi.: + 1/4, -1/2 mi. c) 2 – 2-1/2 mi.: ± 1/2 mi. d) 3 – 3-1/2 mi.: +1/2, -1 mi. e)≥ 4 mi.: ± 1 mi.	< 1/4, 1/4, 1/2, 3/4, 1, 1-1/4, 1-1/2, 2, 2-1/2, 3, 4, 5, 7, 10, and > 10 mi.	time constant ≤ 3 min
Precipitation	0.01 – 5 in./hr	0.002 in./hr RMSE or 4%, whichever is greater	in.	
Cloud height	0 to ≥ 12,500 ft	100 ft. or 5%, whichever is greater	a) 0 – 5,500 ft.: 50 ft. b) 5,501 – 10,000 ft.: 250 ft. c) > 10,000 ft.: 500 ft.	a) sampling rate at least once every 30 seconds b) at least three cloud layers when visibility ≥ 1/4 mi.
Time	0000 – 2359 UTC	within 15 seconds each month	1 second	

a. from FAA, 2017.

Table 2.3-20 – Table Annual Data Recovery Rates (in Percent) of Dry Bulb Temperatures, Relative Humidity, Wind Speed, and Wind Direction from the Southern Wisconsin Regional Airport for 2005-2010

Year	Dry Bulb Temperature	Relative Humidity	Wind Speed	Wind Direction
2005	95.9	95.8	94.0	94.0
2006	93.0	92.9	91.1	91.1
2007	87.7	87.6	87.3	87.3
2008	92.6	92.6	91.2	91.2
2009	93.9	93.6	92.7	92.6
2010	93.8	93.7	92.4	92.4

Table 2.3-21 – Historical Dry Bulb Temperatures, Relative Humidity, and Wind Speed from the Southern Wisconsin Regional Airport for 2005-2010

	Dry Bulb Temperature (^{o}F)			Relative Humidity (%)	Wind Speed (mph)	
Month	Maximum	Minimum	Average	Average	Maximum	Average
January	61	-20	22.6	79.2	35	9.2
February	59	-17	24.2	76.0	49	8.7
March	77	7	36.8	72.7	33	8.9
April	84	19	49.7	63.2	40	10.4
May	93	30	59.2	65.5	31	8.8
June	93	43	69.0	71.3	48	7.0
July	97	46	71.9	74.7	31	6.1
August	93	45	71.9	73.3	38	5.8
September	95	34	64.0	72.8	30	6.5
October	90	23	51.5	72.4	38	8.0
November	77	12	40.1	73.1	33	9.2
December	55	-8	24.0	82.4	44	8.6
Average	81	18	48.7	73.1	38	8.1

Table 2.3-22 – Annual Joint Data Recovery Rates of Wind Speed, Wind Direction, and Computed Pasquill Stability Class from the Southern Wisconsin Regional Airport for 2005-2010

Year	Joint Data Recovery (%)
2005	93.6
2006	90.5
2007	86.0
2008	90.6
2009	91.7
2010	91.7

Table 2.3-23 – Pasquill Stability Class Frequency Distributions from the Southern Wisconsin Regional Airport (Percent) 2005-2010

	Frequency of Occurrence (Percent)						
Pasquill Class	**2005**	**2006**	**2007**	**2008**	**2009**	**2010**	**2005-2010**
A	0.78	0.67	0.86	0.68	1.18	1.16	0.89
B	5.00	3.43	3.61	3.64	5.24	5.39	4.40
C	11.88	11.31	10.15	11.18	10.67	11.98	11.21
D	52.90	56.45	56.67	55.44	54.00	50.19	54.24
E	8.83	8.24	8.15	7.41	7.31	7.08	7.83
F	10.10	10.28	10.35	9.69	9.59	10.48	10.08
G	10.51	9.62	10.21	11.96	12.01	13.72	11.35
Total	100.00	100.00	100.00	100.00	100.00	100.00	100.00

Table 2.3-24 – Joint Frequency Distribution of Wind Speed and Wind Direction from the Southern Wisconsin Regional Airport 2005-2010 (Pasquill Stability Class A)

Speed (m/s)	N	NNE	NE	ENE	E	ESE	SE	SSE	S	SSW	SW	WSW	W	WNW	NW	NNW	Total
Calm																	323
0.00 < WS < 1.00	0	0	0	0	0	0	1	0	0	0	0	0	0	0	0	0	1
1.00 < WS < 2.00	0	0	1	1	2	1	0	2	0	0	0	0	2	0	0	0	9
2.00 < WS < 3.00	6	2	3	9	5	7	9	6	9	5	5	3	9	5	5	4	92
3.00 < WS < 4.00	0	0	0	0	0	0	0	0	0	0	0	0	0	0	0	0	0
4.00 < WS < 5.00	0	0	0	0	0	0	0	0	0	0	0	0	0	0	0	0	0
5.00 < WS < 6.00	0	0	0	0	0	0	0	0	0	0	0	0	0	0	0	0	0
6.00 < WS < 8.00	0	0	0	0	0	0	0	0	0	0	0	0	0	0	0	0	0
8.00 < WS < 10.00	0	0	0	0	0	0	0	0	0	0	0	0	0	0	0	0	0
> 10.00	0	0	0	0	0	0	0	0	0	0	0	0	0	0	0	0	0
Totals	6	2	4	10	7	8	10	8	9	5	5	3	11	5	5	4	425
Speed (m/s)																	
Calm																	0.68
0.00 < WS < 1.00	0.00	0.00	0.00	0.00	0.00	0.00	0.00	0.00	0.00	0.00	0.00	0.00	0.00	0.00	0.00	0.00	0.00
1.00 < WS < 2.00	0.00	0.00	0.00	0.00	0.00	0.00	0.00	0.00	0.00	0.00	0.00	0.00	0.00	0.00	0.00	0.00	0.02
2.00 < WS < 3.00	0.01	0.00	0.01	0.02	0.01	0.01	0.02	0.01	0.02	0.01	0.01	0.01	0.02	0.01	0.01	0.01	0.19
3.00 < WS < 4.00	0.00	0.00	0.00	0.00	0.00	0.00	0.00	0.00	0.00	0.00	0.00	0.00	0.00	0.00	0.00	0.00	0.00
4.00 < WS < 5.00	0.00	0.00	0.00	0.00	0.00	0.00	0.00	0.00	0.00	0.00	0.00	0.00	0.00	0.00	0.00	0.00	0.00
5.00 < WS < 6.00	0.00	0.00	0.00	0.00	0.00	0.00	0.00	0.00	0.00	0.00	0.00	0.00	0.00	0.00	0.00	0.00	0.00
6.00 < WS < 8.00	0.00	0.00	0.00	0.00	0.00	0.00	0.00	0.00	0.00	0.00	0.00	0.00	0.00	0.00	0.00	0.00	0.00
8.00 < WS < 10.00	0.00	0.00	0.00	0.00	0.00	0.00	0.00	0.00	0.00	0.00	0.00	0.00	0.00	0.00	0.00	0.00	0.00
> 10.00	0.00	0.00	0.00	0.00	0.00	0.00	0.00	0.00	0.00	0.00	0.00	0.00	0.00	0.00	0.00	0.00	0.00
Totals	0.01	0.00	0.01	0.02	0.01	0.02	0.02	0.02	0.02	0.01	0.01	0.01	0.02	0.01	0.01	0.01	0.89

Table 2.3-25 – Joint Frequency Distribution of Wind Speed and Wind Direction from the Southern Wisconsin Regional Airport 2005-2010 (Pasquill Stability Class B)

Speed (m/s)	N	NNE	NE	ENE	E	ESE	SE	SSE	S	SSW	SW	WSW	W	WNW	NW	NNW	Total
Calm																	697
0.00 < WS < 1.00	0	0	0	0	0	0	0	0	0	0	0	0	0	0	0	0	0
1.00 < WS < 2.00	5	10	12	8	11	11	5	4	8	13	8	7	12	5	13	4	136
2.00 < WS < 3.00	31	25	27	23	29	23	21	22	21	28	40	27	35	33	23	19	427
3.00 < WS < 4.00	47	39	34	29	38	31	37	47	45	56	61	43	62	61	31	37	698
4.00 < WS < 5.00	3	5	9	10	6	2	5	3	13	21	8	5	19	12	8	9	138
5.00 < WS < 6.00	0	0	0	0	0	0	0	0	0	0	0	0	0	0	0	0	0
6.00 < WS < 8.00	0	0	0	0	0	0	0	0	0	0	0	0	0	0	0	0	0
8.00 < WS < 10.00	0	0	0	0	0	0	0	0	0	0	0	0	0	0	0	0	0
> 10.00	0	0	0	0	0	0	0	0	0	0	0	0	0	0	0	0	0
Totals	86	79	82	70	84	67	68	76	87	118	117	82	128	111	75	69	2096
Speed (m/s)																	
Calm																	1.46
0.00 < WS < 1.00	0.00	0.00	0.00	0.00	0.00	0.00	0.00	0.00	0.00	0.00	0.00	0.00	0.00	0.00	0.00	0.00	0.00
1.00 < WS < 2.00	0.01	0.02	0.03	0.02	0.02	0.02	0.01	0.01	0.02	0.03	0.02	0.01	0.03	0.01	0.03	0.01	0.29
2.00 < WS < 3.00	0.07	0.05	0.06	0.05	0.06	0.05	0.04	0.05	0.04	0.06	0.08	0.06	0.07	0.07	0.05	0.04	0.90
3.00 < WS < 4.00	0.10	0.08	0.07	0.06	0.08	0.07	0.08	0.10	0.09	0.12	0.13	0.09	0.13	0.13	0.07	0.08	1.46
4.00 < WS < 5.00	0.01	0.01	0.02	0.02	0.01	0.00	0.01	0.01	0.03	0.04	0.02	0.01	0.04	0.03	0.02	0.02	0.29
5.00 < WS < 6.00	0.00	0.00	0.00	0.00	0.00	0.00	0.00	0.00	0.00	0.00	0.00	0.00	0.00	0.00	0.00	0.00	0.00
6.00 < WS < 8.00	0.00	0.00	0.00	0.00	0.00	0.00	0.00	0.00	0.00	0.00	0.00	0.00	0.00	0.00	0.00	0.00	0.00
8.00 < WS < 10.00	0.00	0.00	0.00	0.00	0.00	0.00	0.00	0.00	0.00	0.00	0.00	0.00	0.00	0.00	0.00	0.00	0.00
> 10.00	0.00	0.00	0.00	0.00	0.00	0.00	0.00	0.00	0.00	0.00	0.00	0.00	0.00	0.00	0.00	0.00	0.00
Totals	0.18	0.17	0.17	0.15	0.18	0.14	0.14	0.16	0.18	0.25	0.25	0.17	0.27	0.23	0.16	0.14	4.40

Table 2.3-26 – Joint Frequency Distribution of Wind Speed and Wind Direction from the Southern Wisconsin Regional Airport 2005-2010 (Pasquill Stability Class C)

Speed (m/s)	N	NNE	NE	ENE	E	ESE	SE	SSE	S	SSW	SW	WSW	W	WNW	NW	NNW	Total
Calm																	1118
0.00 < WS < 1.00	0	0	0	0	0	0	0	0	0	0	0	0	0	0	0	0	0
1.00 < WS < 2.00	15	2	5	7	15	6	7	3	15	15	16	6	18	14	14	9	167
2.00 < WS < 3.00	34	24	27	34	25	19	25	28	37	38	57	35	59	53	58	30	583
3.00 < WS < 4.00	52	39	39	39	24	39	24	56	65	83	72	72	105	94	60	59	922
4.00 < WS < 5.00	71	72	49	57	54	45	45	81	111	136	148	114	159	150	120	101	1513
5.00 < WS < 6.00	42	29	31	27	36	26	17	45	81	105	87	65	61	91	53	56	852
6.00 < WS < 8.00	0	5	5	6	4	5	6	5	12	12	21	18	23	8	10	2	142
8.00 < WS < 10.00	0	0	0	1	3	0	0	0	4	3	6	3	11	1	0	0	32
> 10.00	0	0	0	0	1	1	0	2	2	0	3	0	5	0	1	0	15
Totals	214	171	156	171	162	141	124	220	327	392	410	313	441	411	316	257	5344
Speed (m/s)																	
Calm																	2.35
0.00 < WS < 1.00	0.00	0.00	0.00	0.00	0.00	0.00	0.00	0.00	0.00	0.00	0.00	0.00	0.00	0.00	0.00	0.00	0.00
1.00 < WS < 2.00	0.03	0.00	0.01	0.01	0.03	0.01	0.01	0.01	0.03	0.03	0.03	0.01	0.04	0.03	0.03	0.02	0.35
2.00 < WS < 3.00	0.07	0.05	0.06	0.07	0.05	0.04	0.05	0.06	0.08	0.08	0.12	0.07	0.12	0.11	0.12	0.06	1.22
3.00 < WS < 4.00	0.11	0.08	0.08	0.08	0.05	0.08	0.05	0.12	0.14	0.17	0.15	0.15	0.22	0.20	0.13	0.12	1.93
4.00 < WS < 5.00	0.15	0.15	0.10	0.12	0.11	0.09	0.09	0.17	0.23	0.29	0.31	0.24	0.33	0.31	0.25	0.21	3.17
5.00 < WS < 6.00	0.09	0.06	0.07	0.06	0.08	0.05	0.04	0.09	0.17	0.22	0.18	0.14	0.13	0.19	0.11	0.12	1.79
6.00 < WS < 8.00	0.00	0.01	0.01	0.01	0.01	0.01	0.01	0.01	0.03	0.03	0.04	0.04	0.05	0.02	0.02	0.00	0.30
8.00 < WS < 10.00	0.00	0.00	0.00	0.00	0.01	0.00	0.00	0.00	0.01	0.01	0.01	0.01	0.02	0.00	0.00	0.00	0.07
> 10.00	0.00	0.00	0.00	0.00	0.00	0.00	0.00	0.00	0.00	0.00	0.01	0.00	0.01	0.00	0.00	0.00	0.03
Totals	0.45	0.36	0.33	0.36	0.34	0.30	0.26	0.46	0.69	0.82	0.86	0.66	0.93	0.86	0.66	0.54	11.21

Table 2.3-27 – Joint Frequency Distribution of Wind Speed and Wind Direction from the Southern Wisconsin Regional Airport 2005-2010 (Pasquill Stability Class D)

Speed (m/s)	N	NNE	NE	ENE	E	ESE	SE	SSE	S	SSW	SW	WSW	W	WNW	NW	NNW	Total
Calm																	1353
0.00 < WS < 1.00	0	0	0	0	0	0	0	0	0	0	0	0	0	0	0	0	0
1.00 < WS < 2.00	39	31	40	36	45	32	25	18	31	27	24	30	47	35	28	40	528
2.00 < WS < 3.00	241	168	165	158	204	164	154	137	183	185	180	140	254	201	212	150	2896
3.00 < WS < 4.00	323	205	205	224	271	220	203	213	342	282	237	240	331	239	260	236	4031
4.00 < WS < 5.00	326	189	186	200	274	190	161	202	382	250	182	203	319	235	267	241	3807
5.00 < WS < 6.00	374	229	248	263	297	205	194	256	468	476	321	253	486	344	381	326	5121
6.00 < WS < 8.00	259	151	201	291	346	218	174	227	617	488	381	334	605	448	471	379	5590
8.00 < WS < 10.00	63	28	61	90	148	59	31	53	139	170	112	112	239	144	166	115	1730
> 10.00	27	6	8	27	68	25	14	21	72	67	81	96	120	74	55	39	800
Totals	1652	1007	1114	1289	1653	1113	956	1127	2234	1945	1518	1408	2401	1720	1840	1526	25856
Speed (m/s)																	
Calm																	2.84
0.00 < WS < 1.00	0.00	0.00	0.00	0.00	0.00	0.00	0.00	0.00	0.00	0.00	0.00	0.00	0.00	0.00	0.00	0.00	0.00
1.00 < WS < 2.00	0.08	0.07	0.08	0.08	0.09	0.07	0.05	0.04	0.07	0.06	0.05	0.06	0.10	0.07	0.06	0.08	1.11
2.00 < WS < 3.00	0.51	0.35	0.35	0.33	0.43	0.34	0.32	0.29	0.38	0.39	0.38	0.29	0.53	0.42	0.44	0.31	6.07
3.00 < WS < 4.00	0.68	0.43	0.43	0.47	0.57	0.46	0.43	0.45	0.72	0.59	0.50	0.50	0.69	0.50	0.55	0.50	8.46
4.00 < WS < 5.00	0.68	0.40	0.39	0.42	0.57	0.40	0.34	0.42	0.80	0.52	0.38	0.43	0.67	0.49	0.56	0.51	7.99
5.00 < WS < 6.00	0.78	0.48	0.52	0.55	0.62	0.43	0.41	0.54	0.98	1.00	0.67	0.53	1.02	0.72	0.80	0.68	10.74
6.00 < WS < 8.00	0.54	0.32	0.42	0.61	0.73	0.46	0.37	0.48	1.29	1.02	0.80	0.70	1.27	0.94	0.99	0.80	11.73
8.00 < WS < 10.00	0.13	0.06	0.13	0.19	0.31	0.12	0.07	0.11	0.29	0.36	0.23	0.23	0.50	0.30	0.35	0.24	3.63
> 10.00	0.06	0.01	0.02	0.06	0.14	0.05	0.03	0.04	0.15	0.14	0.17	0.20	0.25	0.16	0.12	0.08	1.68
Totals	3.47	2.11	2.34	2.70	3.47	2.33	2.01	2.36	4.69	4.08	3.18	2.95	5.04	3.61	3.86	3.20	54.24

Table 2.3-28 – Joint Frequency Distribution of Wind Speed and Wind Direction from the Southern Wisconsin Regional Airport 2005-2010 (Pasquill Stability Class E)

Speed (m/s)	N	NNE	NE	ENE	E	ESE	SE	SSE	S	SSW	SW	WSW	W	WNW	NW	NNW	Total
Calm																	0
0.00 < WS < 1.00	0	0	0	0	0	0	0	0	0	0	0	0	0	0	0	0	0
1.00 < WS < 2.00	0	0	0	0	0	0	0	0	0	0	0	0	0	0	0	0	0
2.00 < WS < 3.00	59	35	48	49	77	82	76	70	91	85	75	44	75	50	53	38	1007
3.00 < WS < 4.00	51	35	54	52	90	84	82	94	167	115	68	61	136	81	73	36	1279
4.00 < WS < 5.00	42	21	37	32	64	31	18	58	150	127	73	54	126	76	76	54	1039
5.00 < WS < 6.00	23	9	11	16	17	16	6	30	65	44	16	26	62	23	27	19	410
6.00 < WS < 8.00	0	0	0	0	0	0	0	0	0	0	0	0	0	0	0	0	0
8.00 < WS < 10.00	0	0	0	0	0	0	0	0	0	0	0	0	0	0	0	0	0
> 10.00	0	0	0	0	0	0	0	0	0	0	0	0	0	0	0	0	0
Totals	175	100	150	149	248	213	182	252	473	371	232	185	399	230	229	147	3735
Speed (m/s)																	
Calm																	0.00
0.00 < WS < 1.00	0.00	0.00	0.00	0.00	0.00	0.00	0.00	0.00	0.00	0.00	0.00	0.00	0.00	0.00	0.00	0.00	0.00
1.00 < WS < 2.00	0.00	0.00	0.00	0.00	0.00	0.00	0.00	0.00	0.00	0.00	0.00	0.00	0.00	0.00	0.00	0.00	0.00
2.00 < WS < 3.00	0.12	0.07	0.10	0.10	0.16	0.17	0.16	0.15	0.19	0.18	0.16	0.09	0.16	0.10	0.11	0.08	2.11
3.00 < WS < 4.00	0.11	0.07	0.11	0.11	0.19	0.18	0.17	0.20	0.35	0.24	0.14	0.13	0.29	0.17	0.15	0.08	2.68
4.00 < WS < 5.00	0.09	0.04	0.08	0.07	0.13	0.07	0.04	0.12	0.31	0.27	0.15	0.11	0.26	0.16	0.16	0.11	2.18
5.00 < WS < 6.00	0.05	0.02	0.02	0.03	0.04	0.03	0.01	0.06	0.14	0.09	0.03	0.05	0.13	0.05	0.06	0.04	0.86
6.00 < WS < 8.00	0.00	0.00	0.00	0.00	0.00	0.00	0.00	0.00	0.00	0.00	0.00	0.00	0.00	0.00	0.00	0.00	0.00
8.00 < WS < 10.00	0.00	0.00	0.00	0.00	0.00	0.00	0.00	0.00	0.00	0.00	0.00	0.00	0.00	0.00	0.00	0.00	0.00
> 10.00	0.00	0.00	0.00	0.00	0.00	0.00	0.00	0.00	0.00	0.00	0.00	0.00	0.00	0.00	0.00	0.00	0.00
Totals	0.37	0.21	0.31	0.31	0.52	0.45	0.38	0.53	0.99	0.78	0.49	0.39	0.84	0.48	0.48	0.31	7.83

Table 2.3-29 – Joint Frequency Distribution of Wind Speed and Wind Direction from the Southern Wisconsin Regional Airport 2005-2010 (Pasquill Stability Class F)

Speed (m/s)	N	NNE	NE	ENE	E	ESE	SE	SSE	S	SSW	SW	WSW	W	WNW	NW	NNW	Total
Calm																	975
0.00 < WS < 1.00	0	0	0	0	0	0	0	0	0	0	0	0	0	0	0	0	0
1.00 < WS < 2.00	26	14	21	18	41	31	21	19	28	32	18	26	36	15	23	19	388
2.00 < WS < 3.00	117	74	90	111	158	153	148	164	196	176	164	131	265	192	204	101	2444
3.00 < WS < 4.00	37	26	53	32	51	49	50	82	100	85	84	60	109	71	71	38	998
4.00 < WS < 5.00	0	0	0	0	0	0	0	0	0	0	0	0	0	0	0	0	0
5.00 < WS < 6.00	0	0	0	0	0	0	0	0	0	0	0	0	0	0	0	0	0
6.00 < WS < 8.00	0	0	0	0	0	0	0	0	0	0	0	0	0	0	0	0	0
8.00 < WS < 10.00	0	0	0	0	0	0	0	0	0	0	0	0	0	0	0	0	0
> 10.00	0	0	0	0	0	0	0	0	0	0	0	0	0	0	0	0	0
Totals	180	114	164	161	250	233	219	265	324	293	266	217	410	278	298	158	4805
Speed (m/s)																	
Calm																	2.05
0.00 < WS < 1.00	0.00	0.00	0.00	0.00	0.00	0.00	0.00	0.00	0.00	0.00	0.00	0.00	0.00	0.00	0.00	0.00	0.00
1.00 < WS < 2.00	0.05	0.03	0.04	0.04	0.09	0.07	0.04	0.04	0.06	0.07	0.04	0.05	0.08	0.03	0.05	0.04	0.81
2.00 < WS < 3.00	0.25	0.16	0.19	0.23	0.33	0.32	0.31	0.34	0.41	0.37	0.34	0.27	0.56	0.40	0.43	0.21	5.13
3.00 < WS < 4.00	0.08	0.05	0.11	0.07	0.11	0.10	0.10	0.17	0.21	0.18	0.18	0.13	0.23	0.15	0.15	0.08	2.09
4.00 < WS < 5.00	0.00	0.00	0.00	0.00	0.00	0.00	0.00	0.00	0.00	0.00	0.00	0.00	0.00	0.00	0.00	0.00	0.00
5.00 < WS < 6.00	0.00	0.00	0.00	0.00	0.00	0.00	0.00	0.00	0.00	0.00	0.00	0.00	0.00	0.00	0.00	0.00	0.00
6.00 < WS < 8.00	0.00	0.00	0.00	0.00	0.00	0.00	0.00	0.00	0.00	0.00	0.00	0.00	0.00	0.00	0.00	0.00	0.00
8.00 < WS < 10.00	0.00	0.00	0.00	0.00	0.00	0.00	0.00	0.00	0.00	0.00	0.00	0.00	0.00	0.00	0.00	0.00	0.00
> 10.00	0.00	0.00	0.00	0.00	0.00	0.00	0.00	0.00	0.00	0.00	0.00	0.00	0.00	0.00	0.00	0.00	0.00
Totals	0.38	0.24	0.34	0.34	0.52	0.49	0.46	0.56	0.68	0.61	0.56	0.46	0.86	0.58	0.63	0.33	10.08

Table 2.3-30 – Joint Frequency Distribution of Wind Speed and Wind Direction from the Southern Wisconsin Regional Airport 2005-2010 (Pasquill Stability Class G)

Speed (m/s)	N	NNE	NE	ENE	E	ESE	SE	SSE	S	SSW	SW	WSW	W	WNW	NW	NNW	Total
Calm																	4053
0.00 < WS < 1.00	0	0	0	0	0	0	0	0	0	0	0	0	0	0	0	0	0
1.00 < WS < 2.00	77	35	38	62	113	106	95	61	101	74	55	72	183	126	92	67	1357
2.00 < WS < 3.00	0	0	0	0	0	0	0	0	0	0	0	0	0	0	0	0	0
3.00 < WS < 4.00	0	0	0	0	0	0	0	0	0	0	0	0	0	0	0	0	0
4.00 < WS < 5.00	0	0	0	0	0	0	0	0	0	0	0	0	0	0	0	0	0
5.00 < WS < 6.00	0	0	0	0	0	0	0	0	0	0	0	0	0	0	0	0	0
6.00 < WS < 8.00	0	0	0	0	0	0	0	0	0	0	0	0	0	0	0	0	0
8.00 < WS < 10.00	0	0	0	0	0	0	0	0	0	0	0	0	0	0	0	0	0
> 10.00	0	0	0	0	0	0	0	0	0	0	0	0	0	0	0	0	0
Totals	77	35	38	62	113	106	95	61	101	74	55	72	183	126	92	67	5410
Speed (m/s)																	
Calm																	8.50
0.00 < WS < 1.00	0.00	0.00	0.00	0.00	0.00	0.00	0.00	0.00	0.00	0.00	0.00	0.00	0.00	0.00	0.00	0.00	0.00
1.00 < WS < 2.00	0.16	0.07	0.08	0.13	0.24	0.22	0.20	0.13	0.21	0.16	0.12	0.15	0.38	0.26	0.19	0.14	2.85
2.00 < WS < 3.00	0.00	0.00	0.00	0.00	0.00	0.00	0.00	0.00	0.00	0.00	0.00	0.00	0.00	0.00	0.00	0.00	0.00
3.00 < WS < 4.00	0.00	0.00	0.00	0.00	0.00	0.00	0.00	0.00	0.00	0.00	0.00	0.00	0.00	0.00	0.00	0.00	0.00
4.00 < WS < 5.00	0.00	0.00	0.00	0.00	0.00	0.00	0.00	0.00	0.00	0.00	0.00	0.00	0.00	0.00	0.00	0.00	0.00
5.00 < WS < 6.00	0.00	0.00	0.00	0.00	0.00	0.00	0.00	0.00	0.00	0.00	0.00	0.00	0.00	0.00	0.00	0.00	0.00
6.00 < WS < 8.00	0.00	0.00	0.00	0.00	0.00	0.00	0.00	0.00	0.00	0.00	0.00	0.00	0.00	0.00	0.00	0.00	0.00
8.00 < WS < 10.00	0.00	0.00	0.00	0.00	0.00	0.00	0.00	0.00	0.00	0.00	0.00	0.00	0.00	0.00	0.00	0.00	0.00
> 10.00	0.00	0.00	0.00	0.00	0.00	0.00	0.00	0.00	0.00	0.00	0.00	0.00	0.00	0.00	0.00	0.00	0.00
Totals	0.16	0.07	0.08	0.13	0.24	0.22	0.20	0.13	0.21	0.16	0.12	0.15	0.38	0.26	0.19	0.14	11.35

Figure 2.3-1 – Principal Tracks of Winter Synoptic Cyclones that Potentially Affect Wisconsin Weather[a]

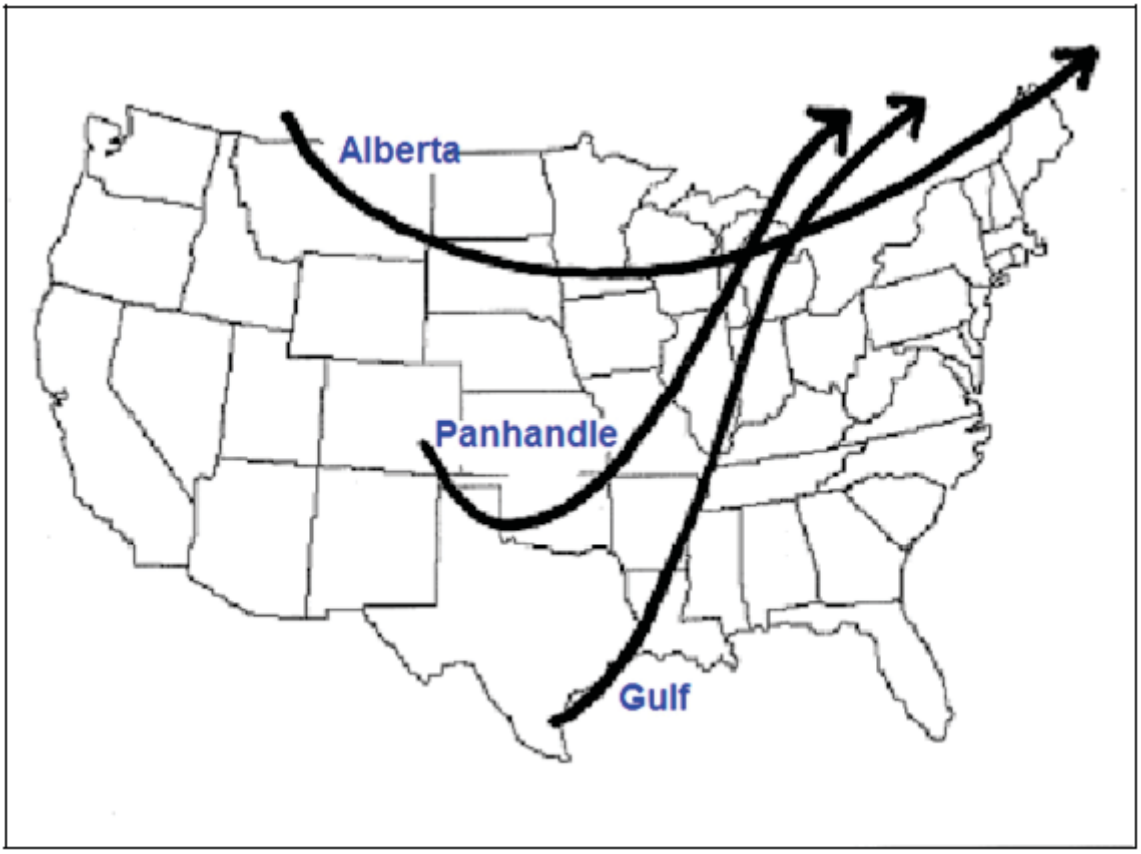

a. Based on Moran, J. M. and E. J. Hopkins, 2002.

Figure 2.3-2 – Physiographic Provinces in Wisconsin[a]

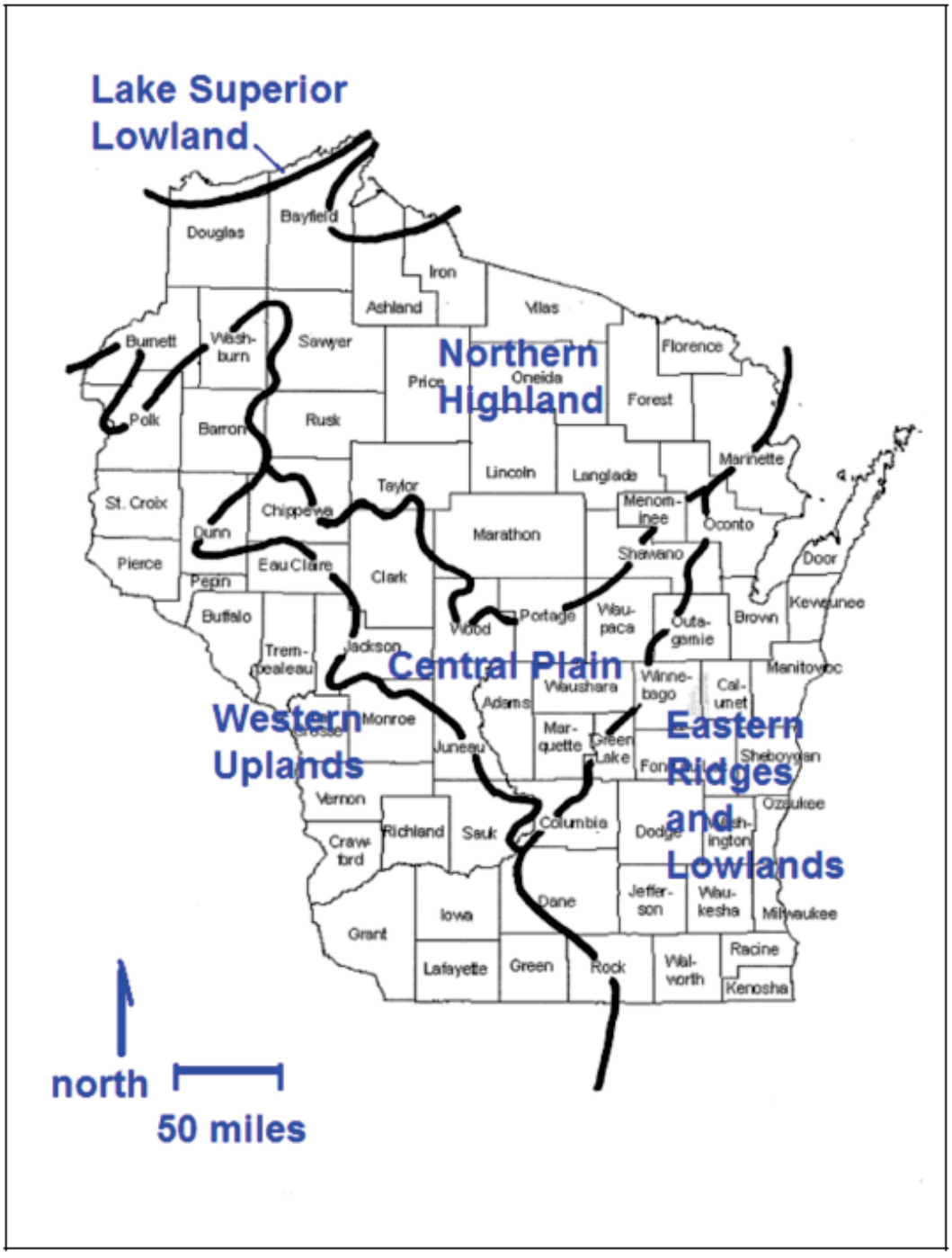

a. Based on Moran, J. M. and E. J. Hopkins, 2002.

Figure 2.3-3 – Mean Wisconsin Winter Month Temperature[a]

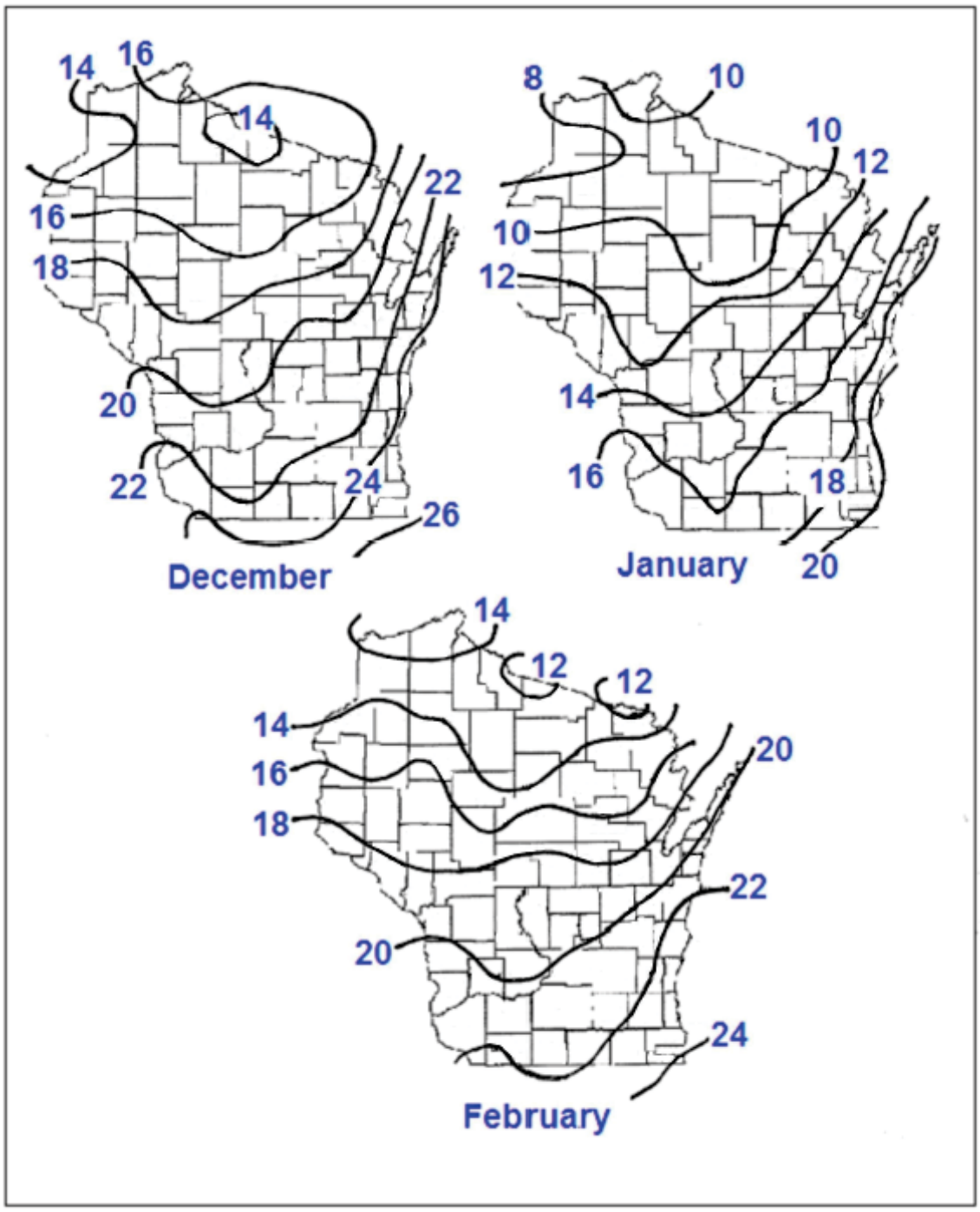

a. Dry bulb temperatures in ^{o}F. Based on Moran, J. M. and E. J. Hopkins, 2002.

Figure 2.3-4 – Mean Wisconsin Spring Month Temperature[a]

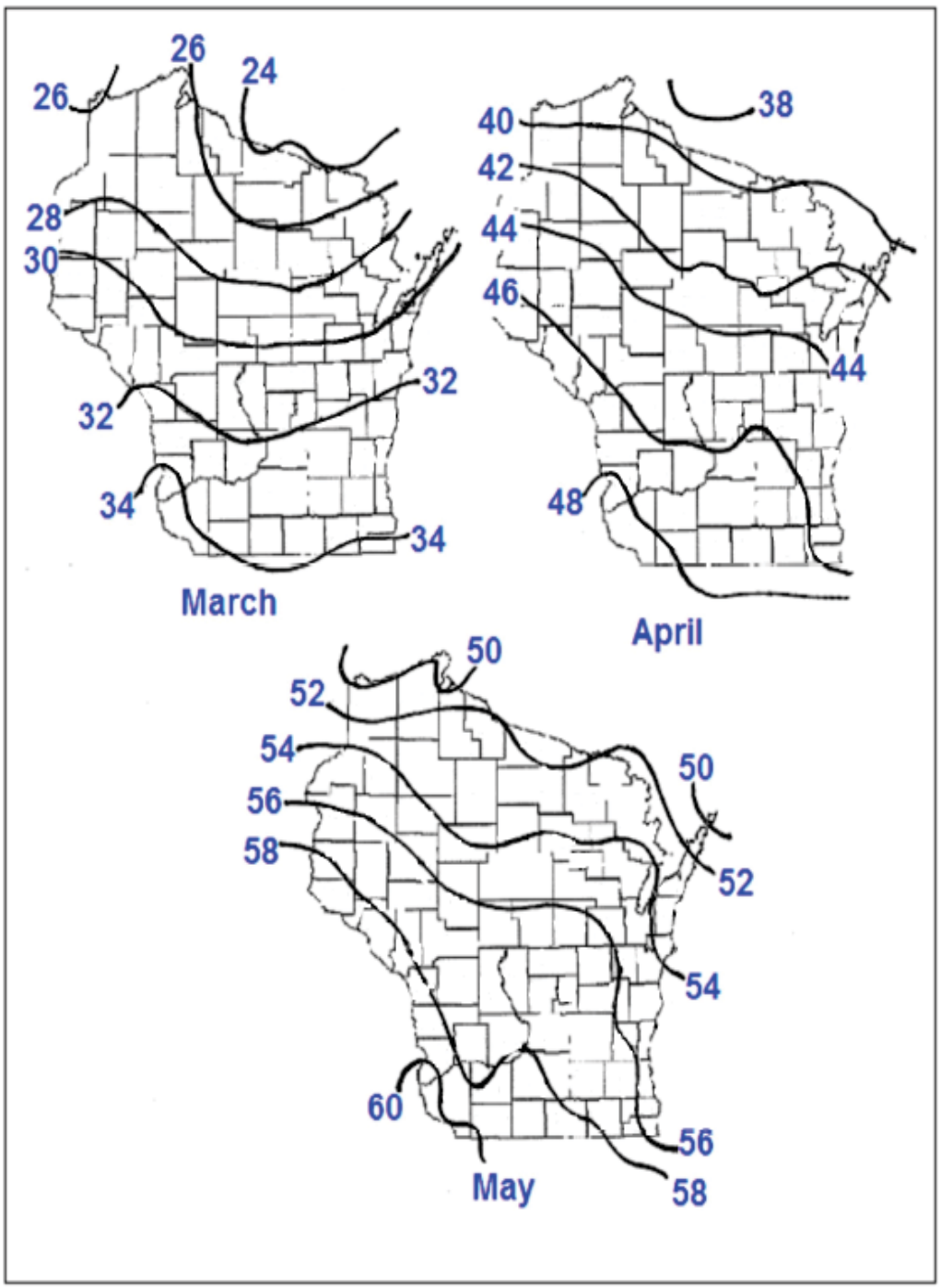

a. Dry bulb temperatures in ^{o}F. Based on Moran, J. M. and E. J. Hopkins, 2002.

Figure 2.3-5 – Mean Wisconsin Summer Month Temperature[(a)]

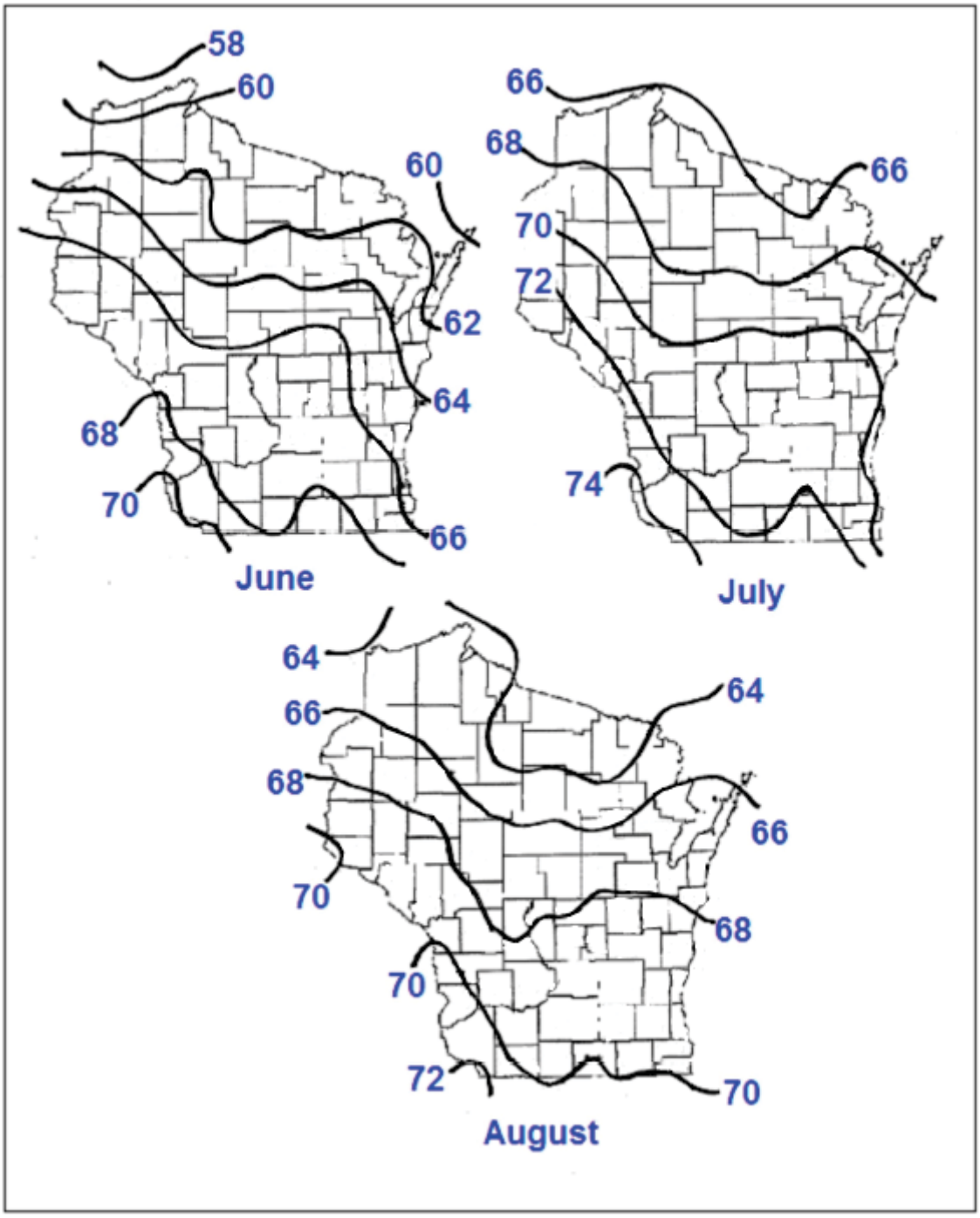

a. Dry bulb temperatures in ^{o}F. Based on Moran, J. M. and E. J. Hopkins, 2002.

Figure 2.3-6 – Mean Wisconsin Autumn Month Temperature[a]

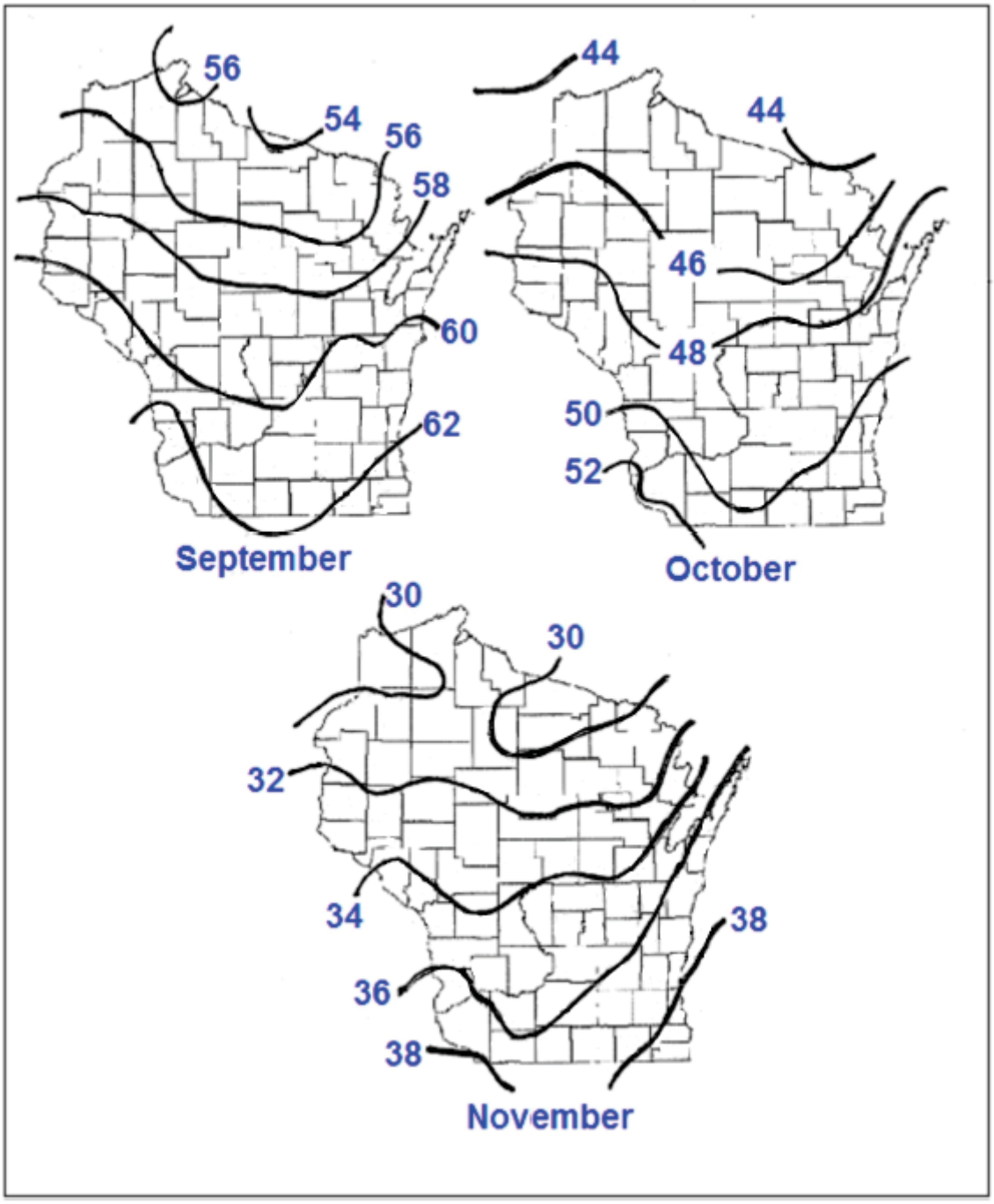

a. Dry bulb temperatures in ^{O}F. Based on Moran, J. M. and E. J. Hopkins, 2002.

Figure 2.3-7 – Mean Wisconsin Winter Month Precipitation(1)

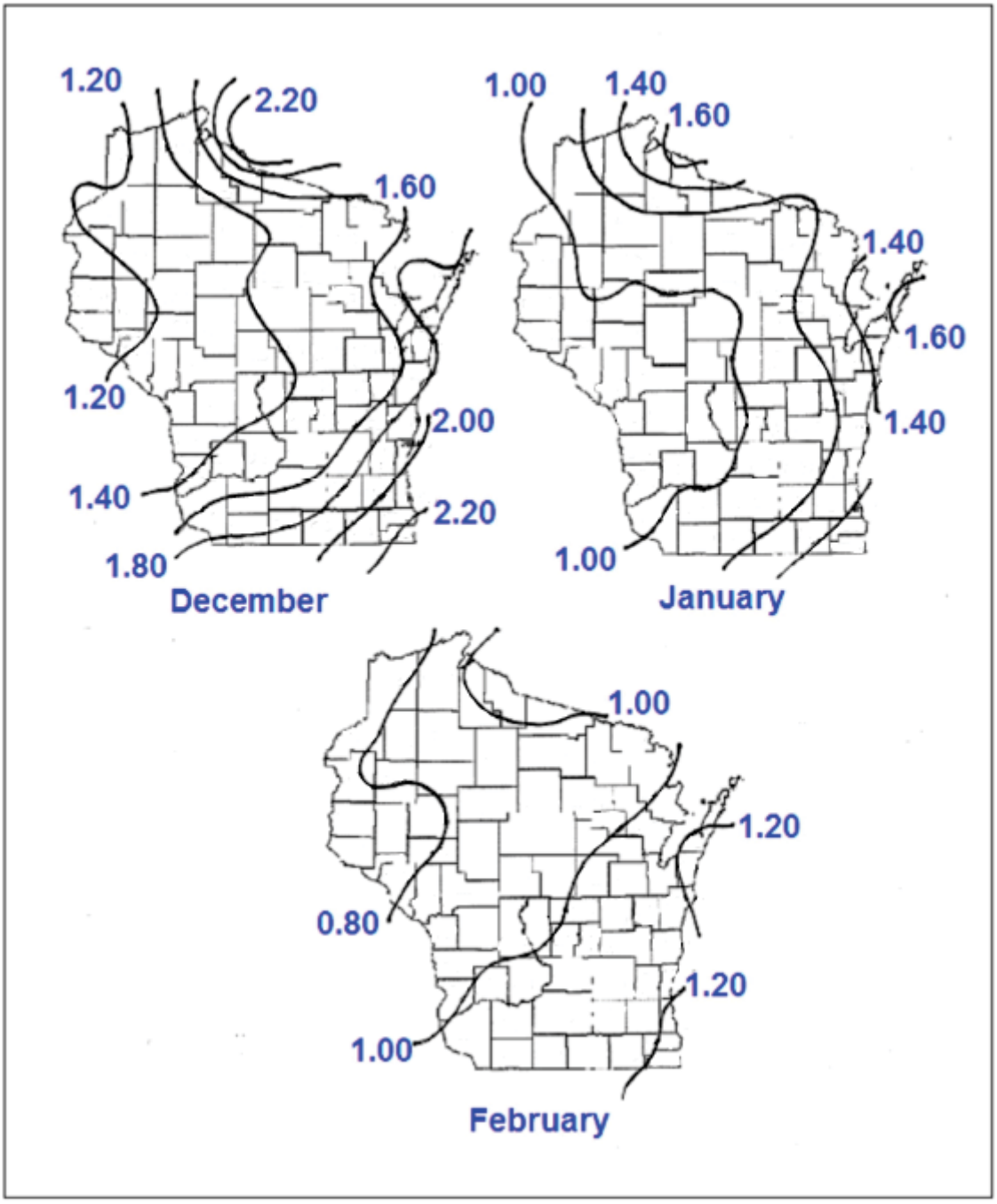

1. Water equivalent precipitation in inches. Based on Moran, J. M. and E. J. Hopkins, 2002.

Figure 2.3-8 – Mean Wisconsin Spring Month Precipitation[a]

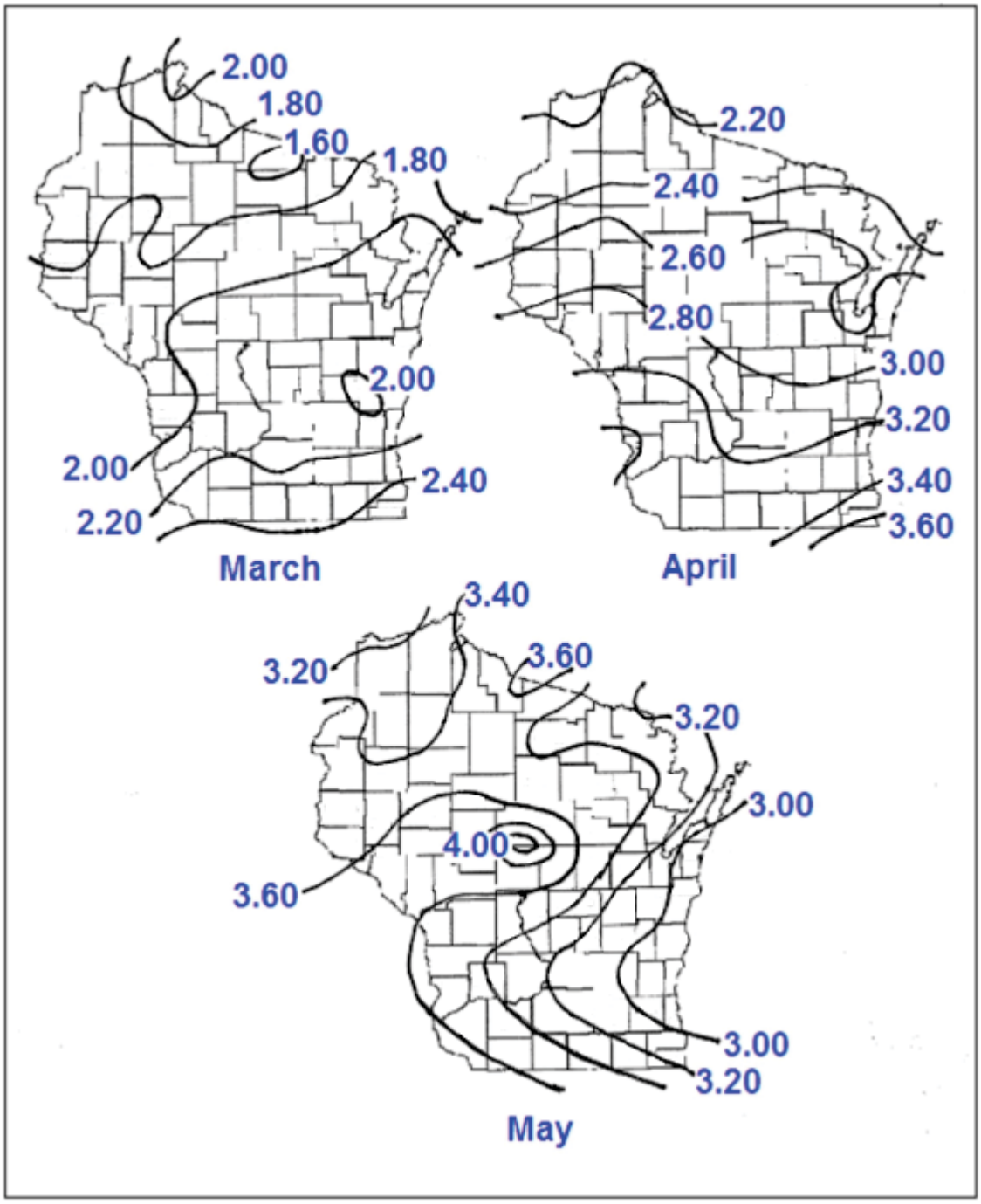

a. Water equivalent precipitation in inches. Based on Moran, J. M. and E. J. Hopkins, 2002.

Figure 2.3-9 – Mean Wisconsin Summer Month Precipitation[(a)]

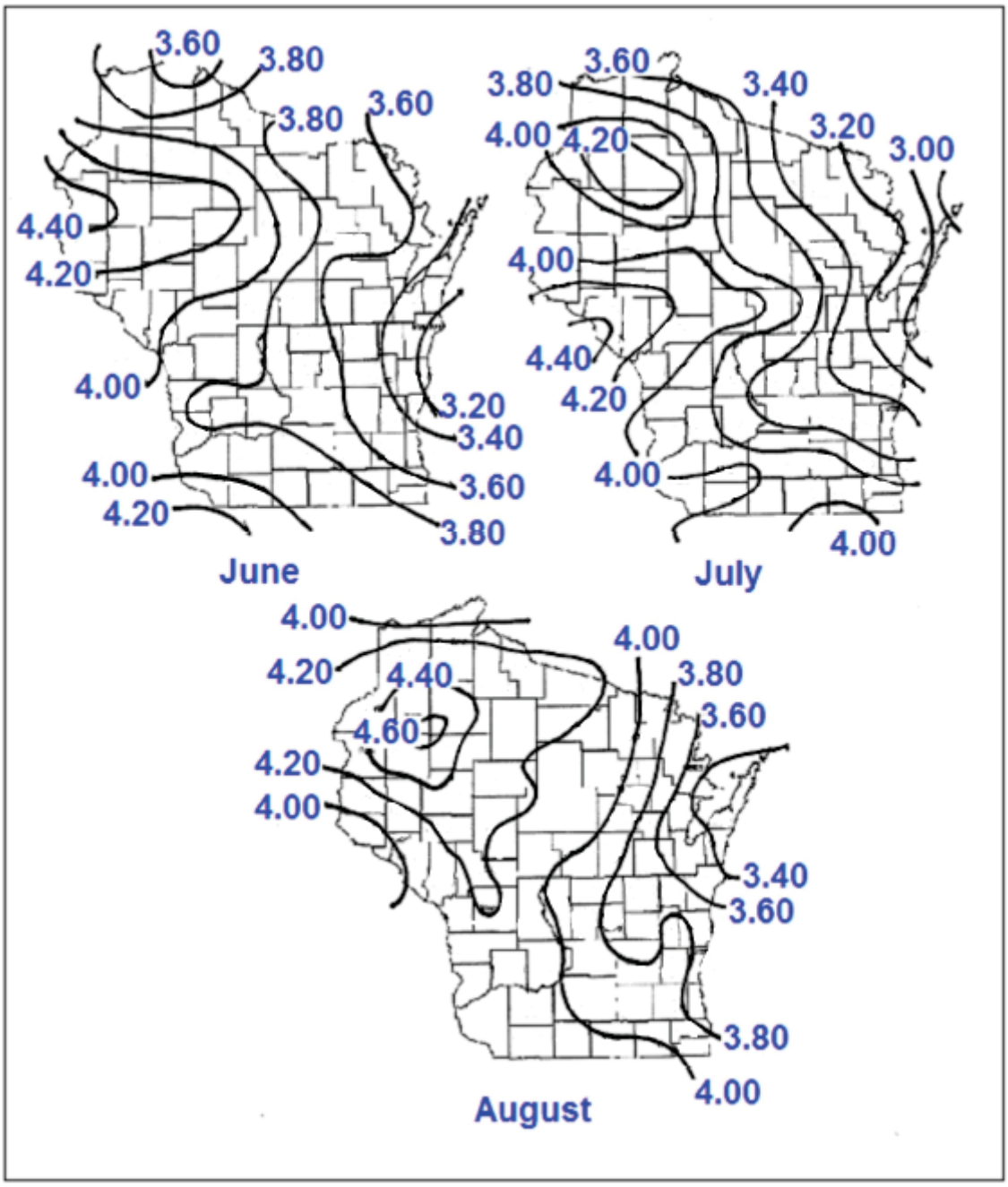

a. Water equivalent precipitation in inches. Based on Moran, J. M. and E. J. Hopkins, 2002.

Figure 2.3-10 – Mean Wisconsin Autumn Month Precipitation[a]

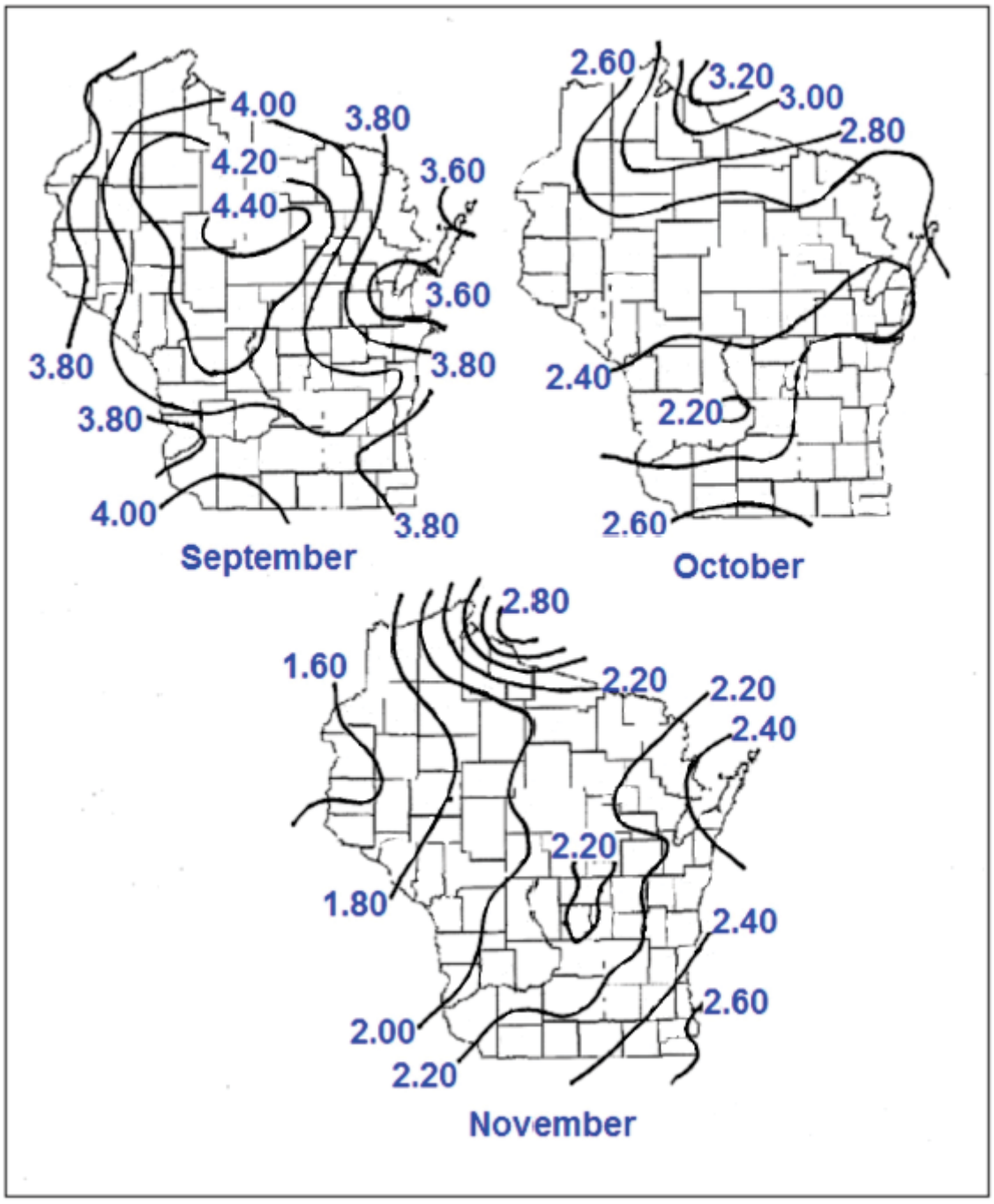

a. Water equivalent precipitation in inches. Based on Moran, J. M. and E. J. Hopkins, 2002.

Figure 2.3-11 – NOAA COOP Network Climate Divisions of Wisconsin[a]

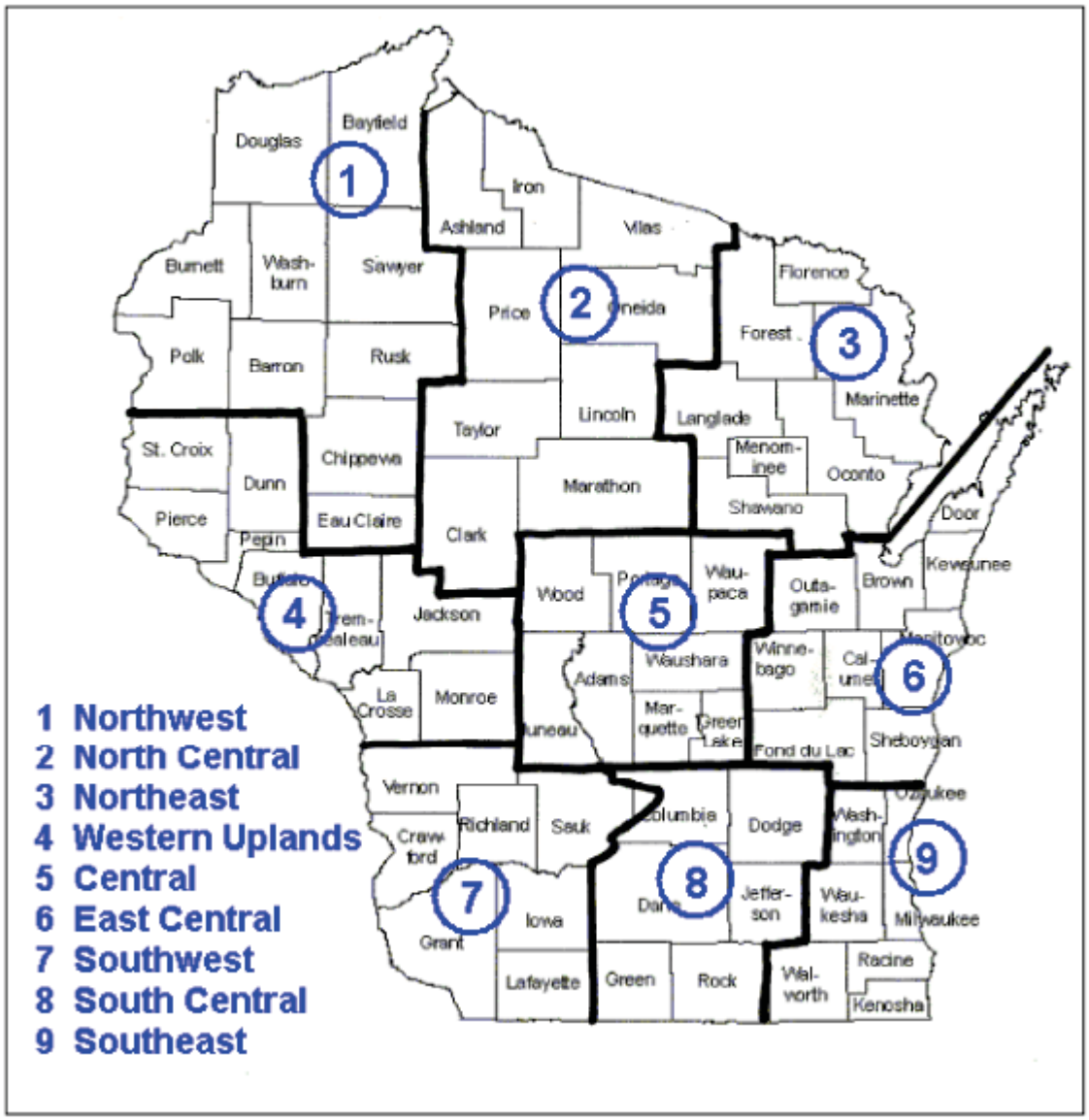

a. Based on NCDC, 2011j.

Figure 2.3-12 – Outline of Climate Region Representative of the Site

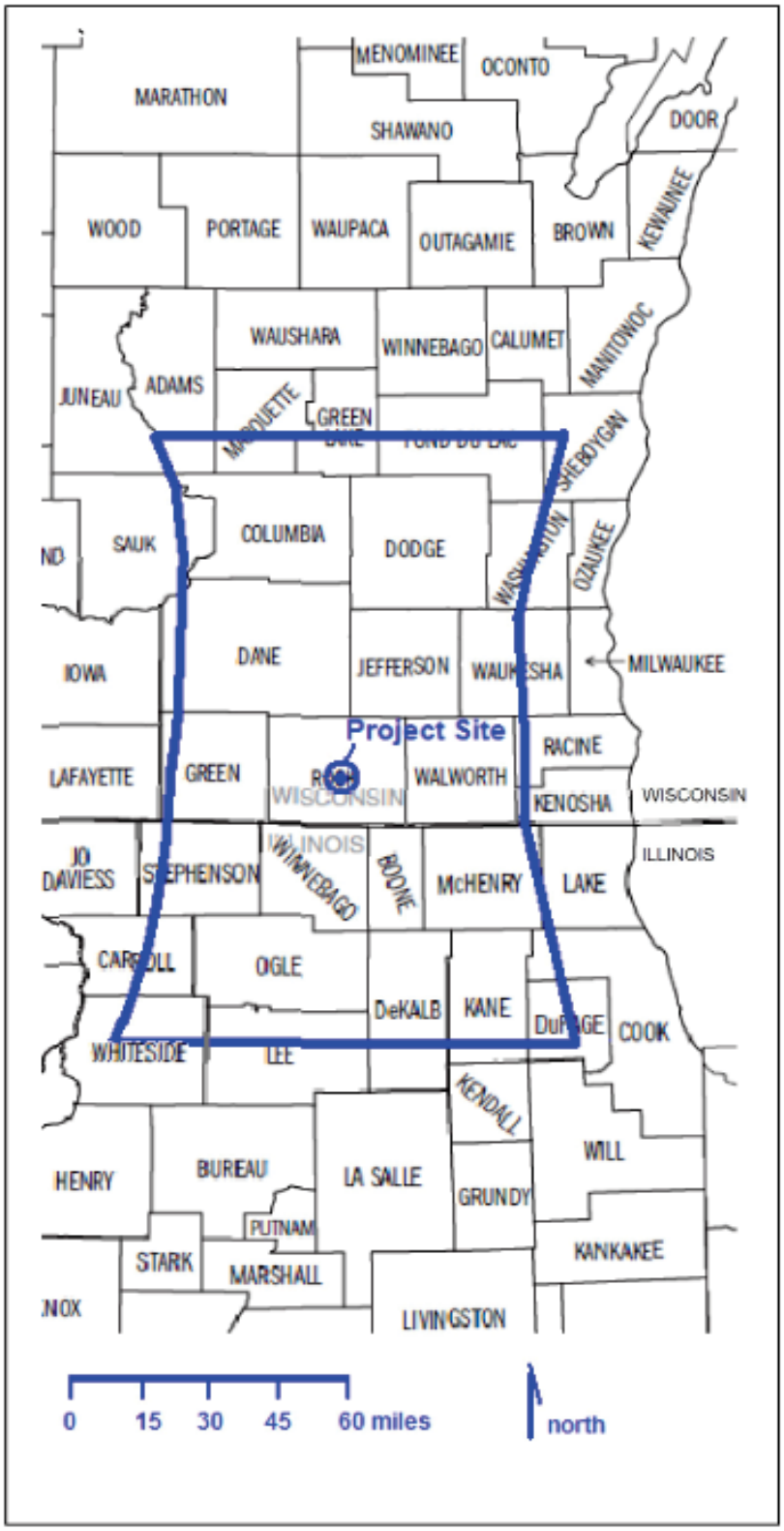

Figure 2.3-13 – Illinois Annual Mean Water Equivalent Precipitation[(a)]

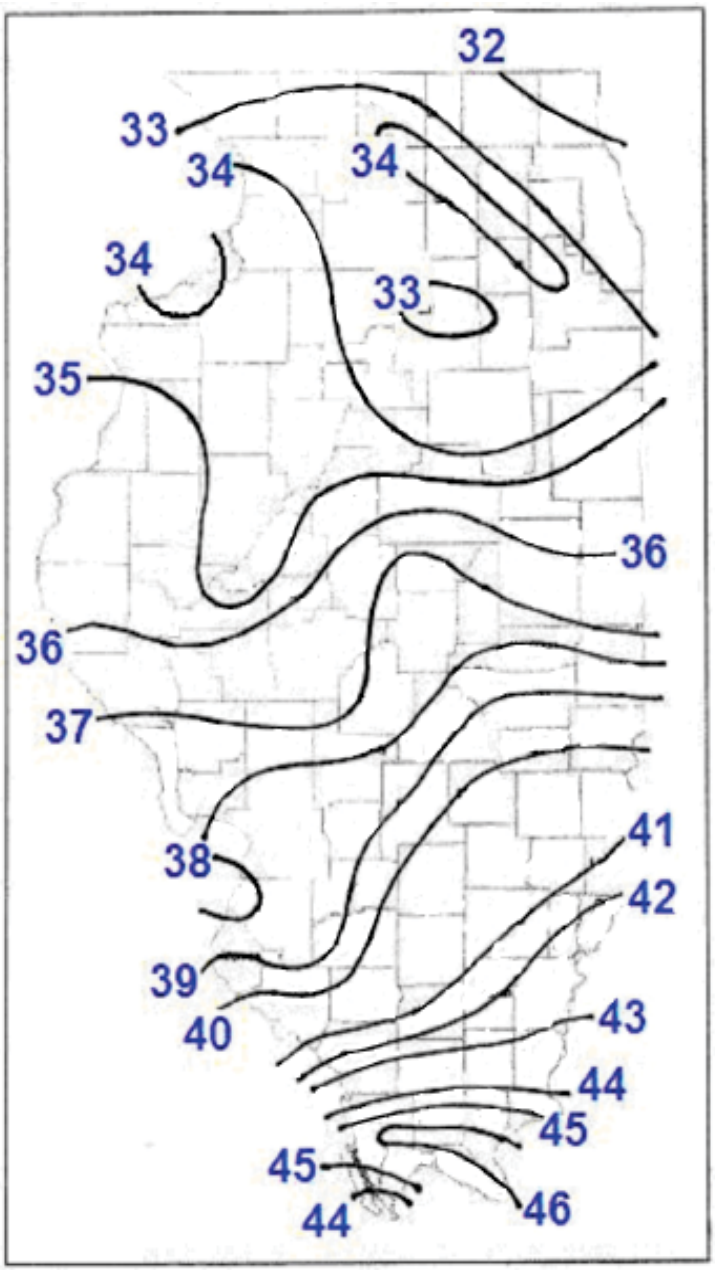

a. Precipitation in inches. Based on Changnon et al., 2004; NCDC, 2011i; and NCDC, 2011j.

Figure 2.3-14 – Illinois Annual Mean Snowfall[a]

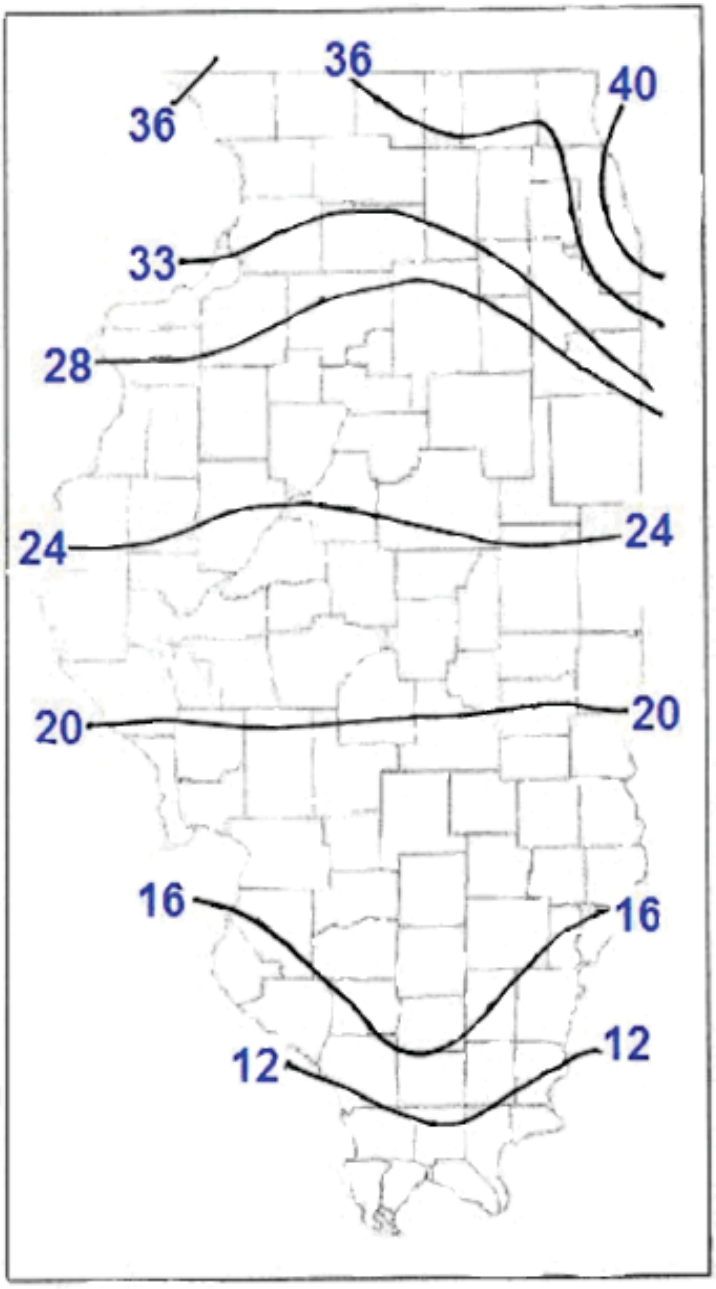

a. Snowfall in inches. Based on Changnon et al., 2004; NCDC, 2011i; and NCDC, 2011j.

Figure 2.3-15 – Illinois Annual Mean Dry Bulb Temperatures[a]

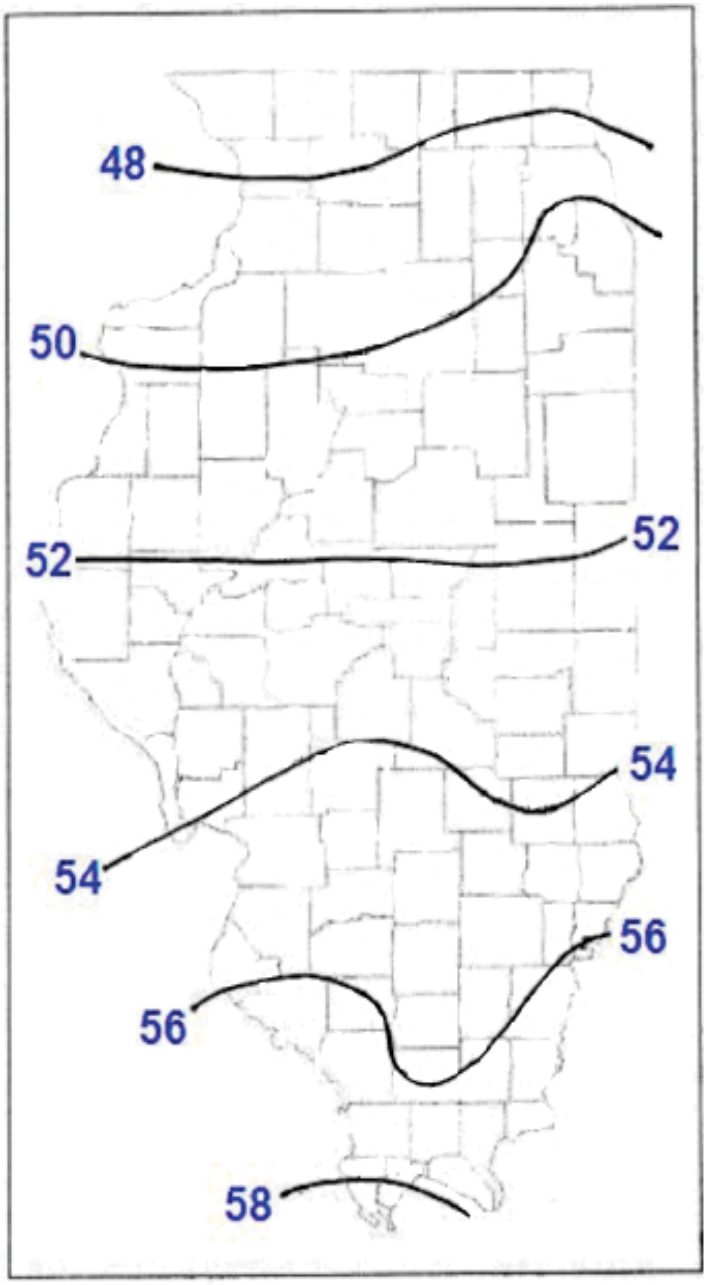

a. Dry bulb temperature in ºF. Based on Changnon et al., 2004; NCDC, 2011i; and NCDC, 2011j.

Figure 2.3-16 – NOAA ASOS Stations Located within the Site Climate Region

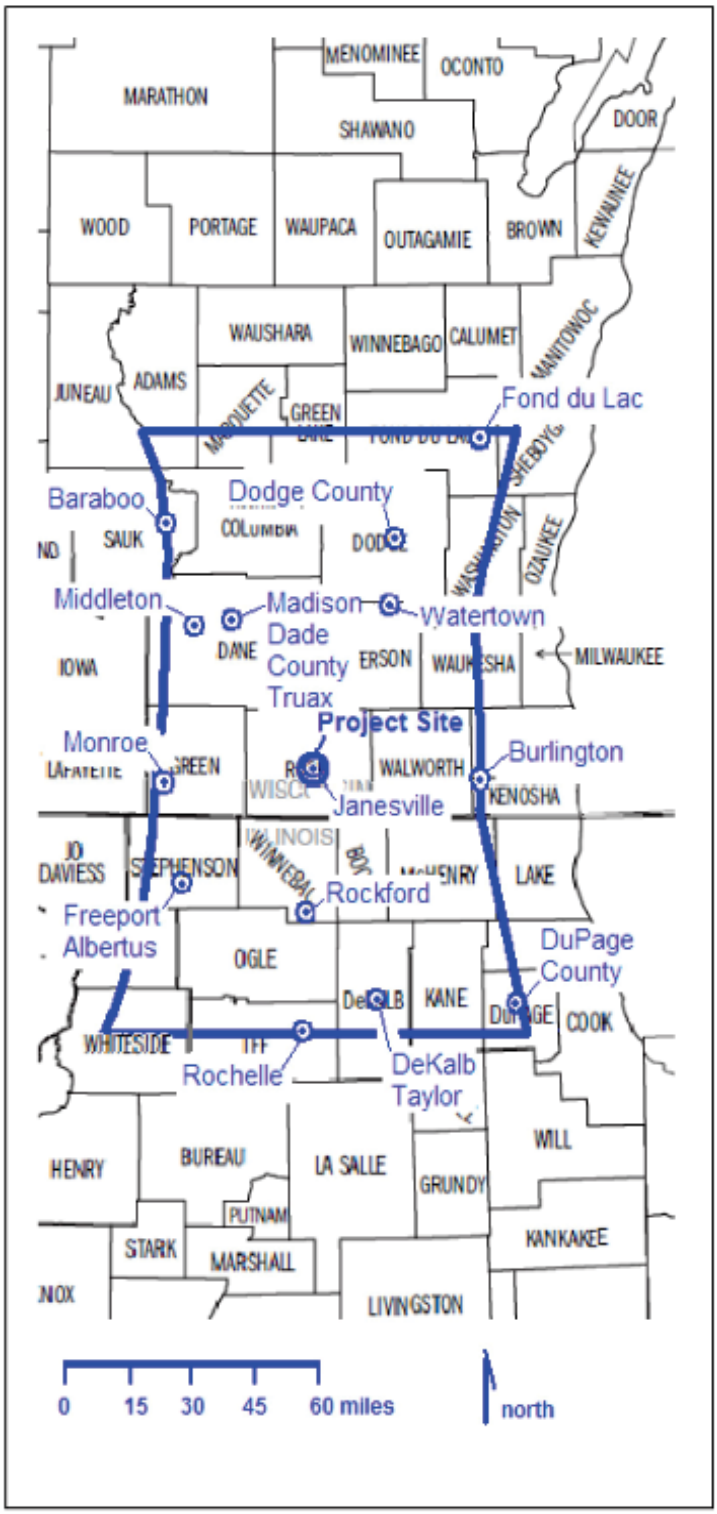

Figure 2.3-17 – NOAA COOP Stations Located within the Site Climate Region

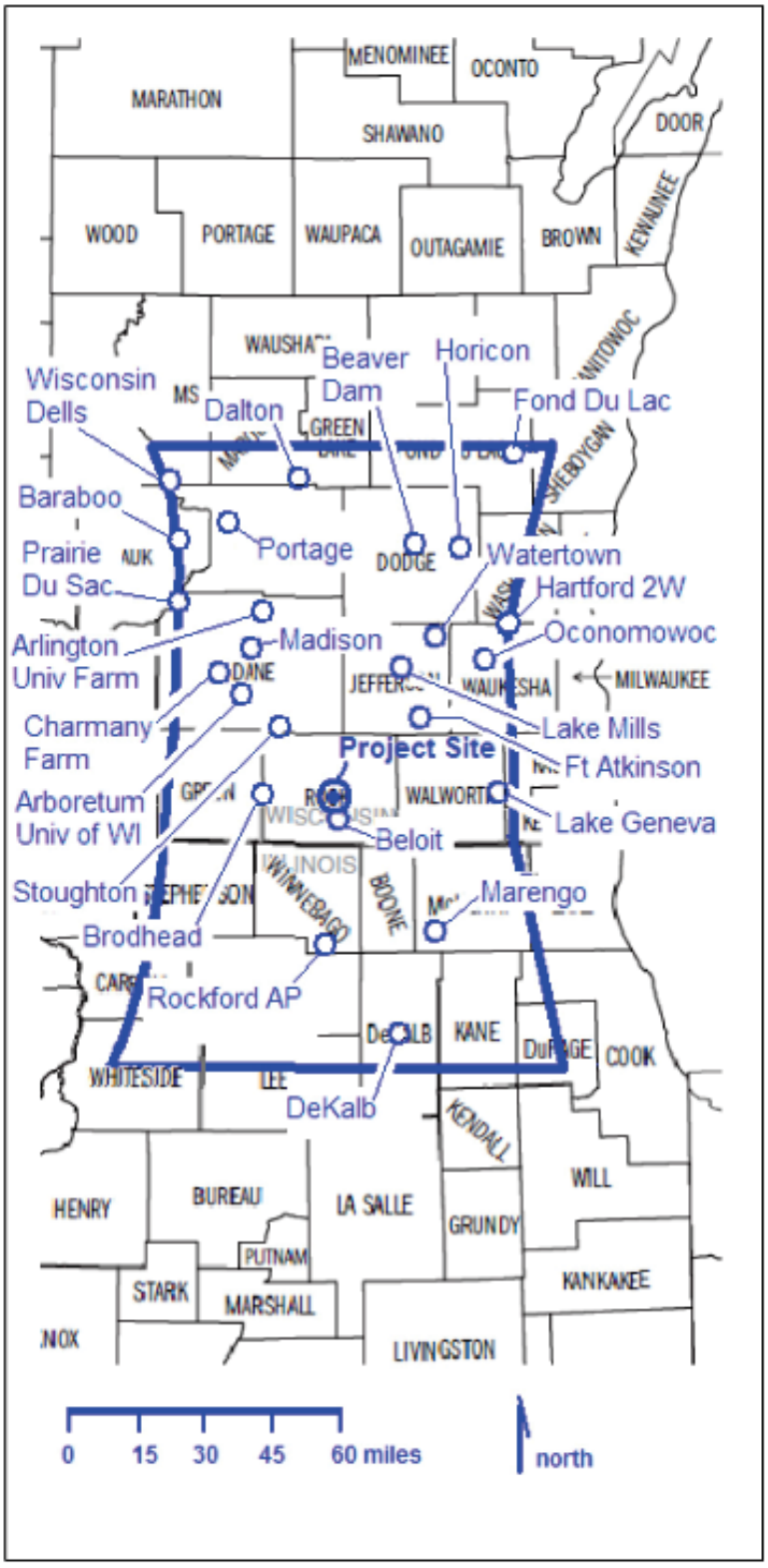

Figure 2.3-18 – Wisconsin and Illinois Counties within Site Climate Region Selected for Investigation of Severe Weather Phenomena

Figure 2.3-19 – Annual Wind Rose Southern Wisconsin Regional Airport (2005-2010)

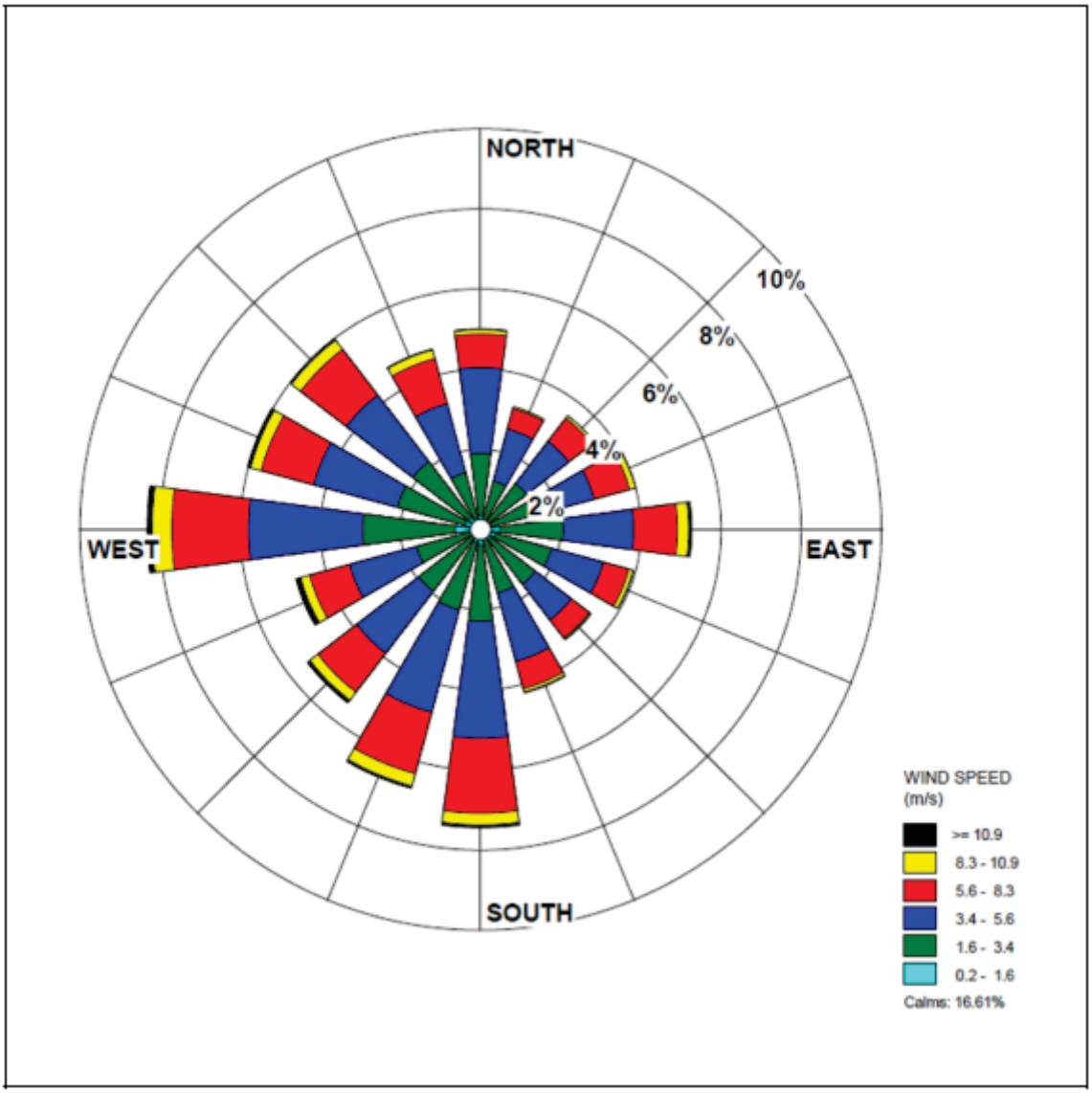

Figure 2.3-20 – January Wind Rose Southern Wisconsin Regional Airport (2005-2010)

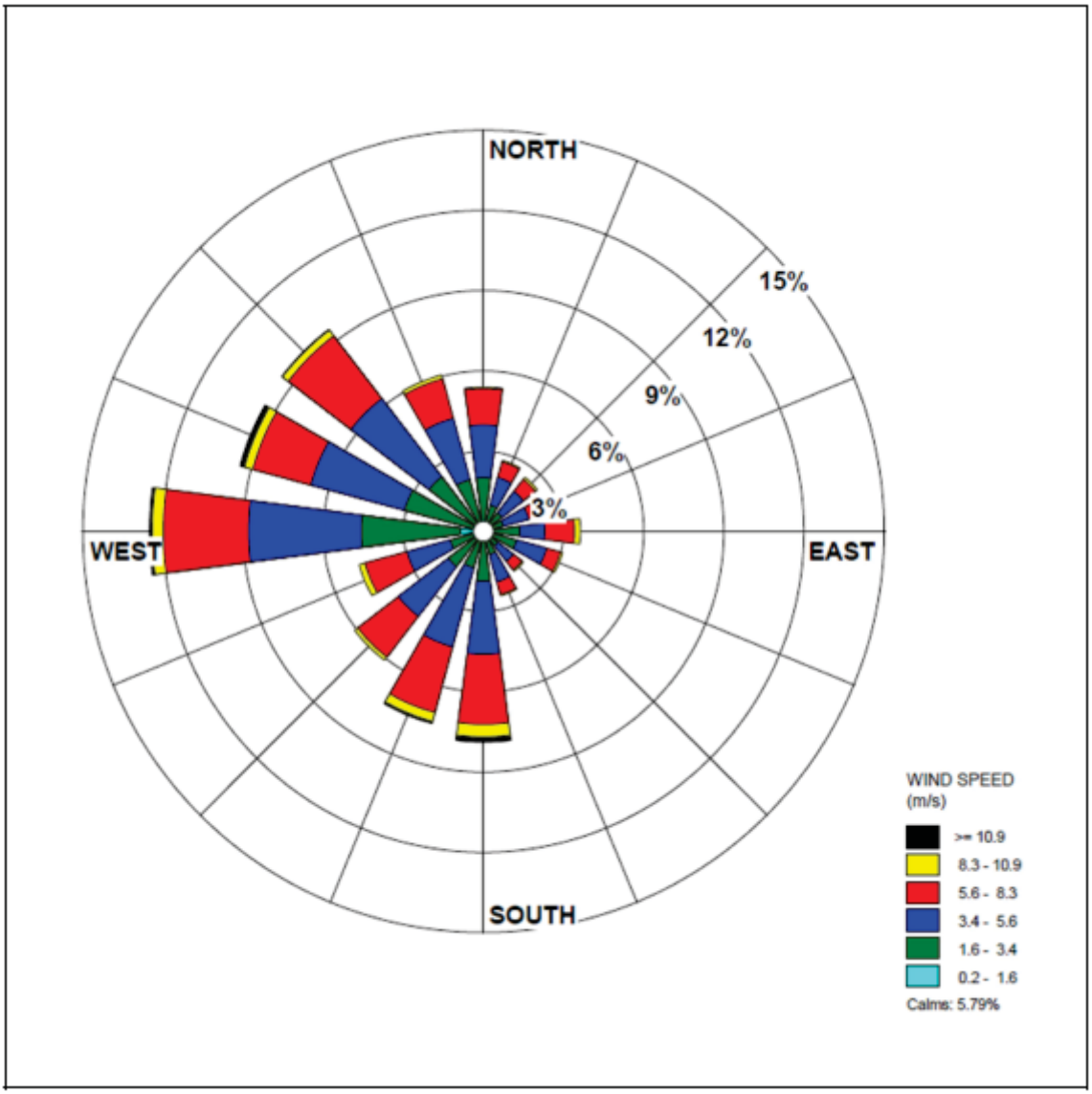

Figure 2.3-21 – February Wind Rose Southern Wisconsin Regional Airport (2005-2010)

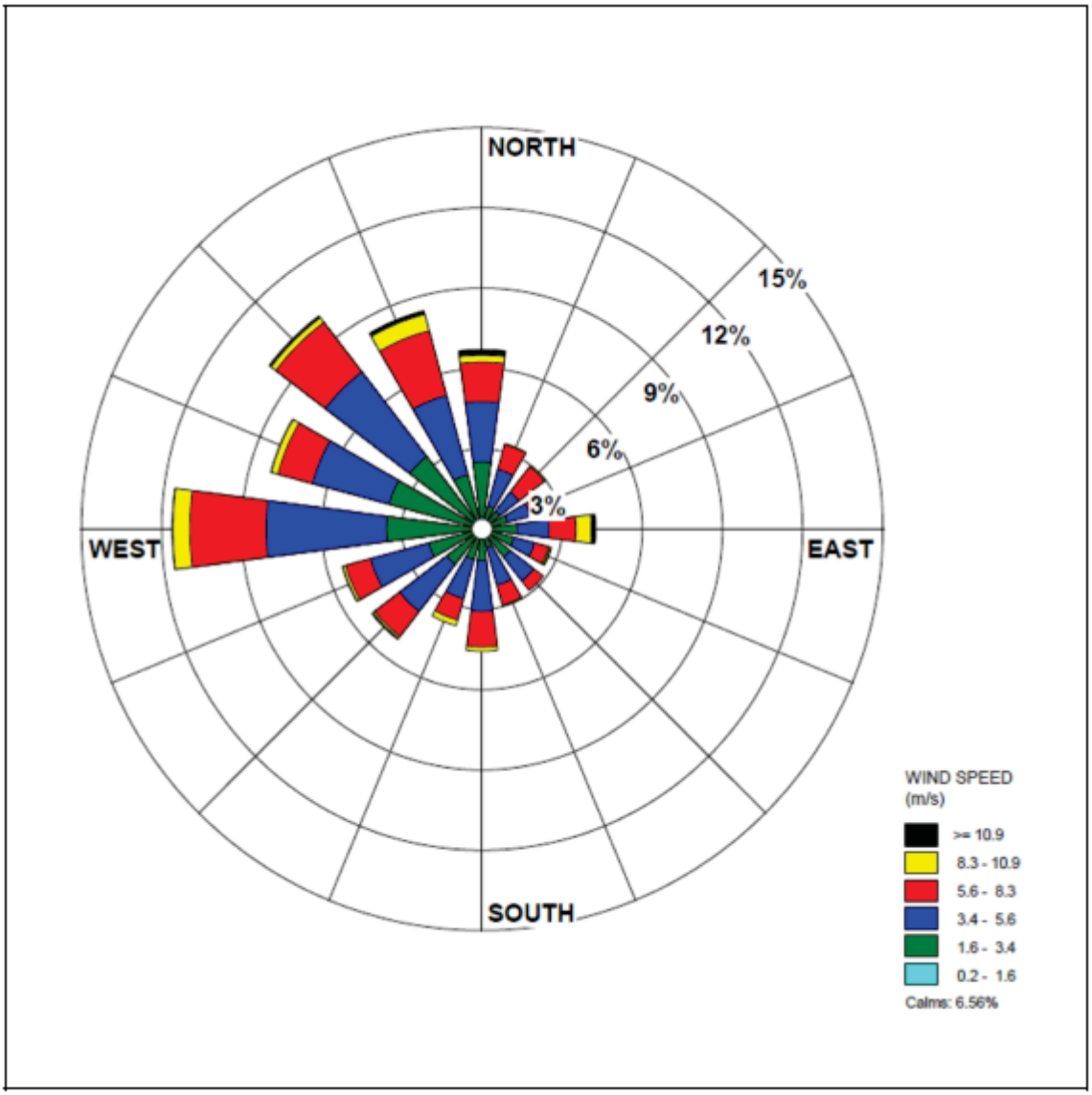

Figure 2.3-22 – March Wind Rose Southern Wisconsin Regional Airport (2005-2010)

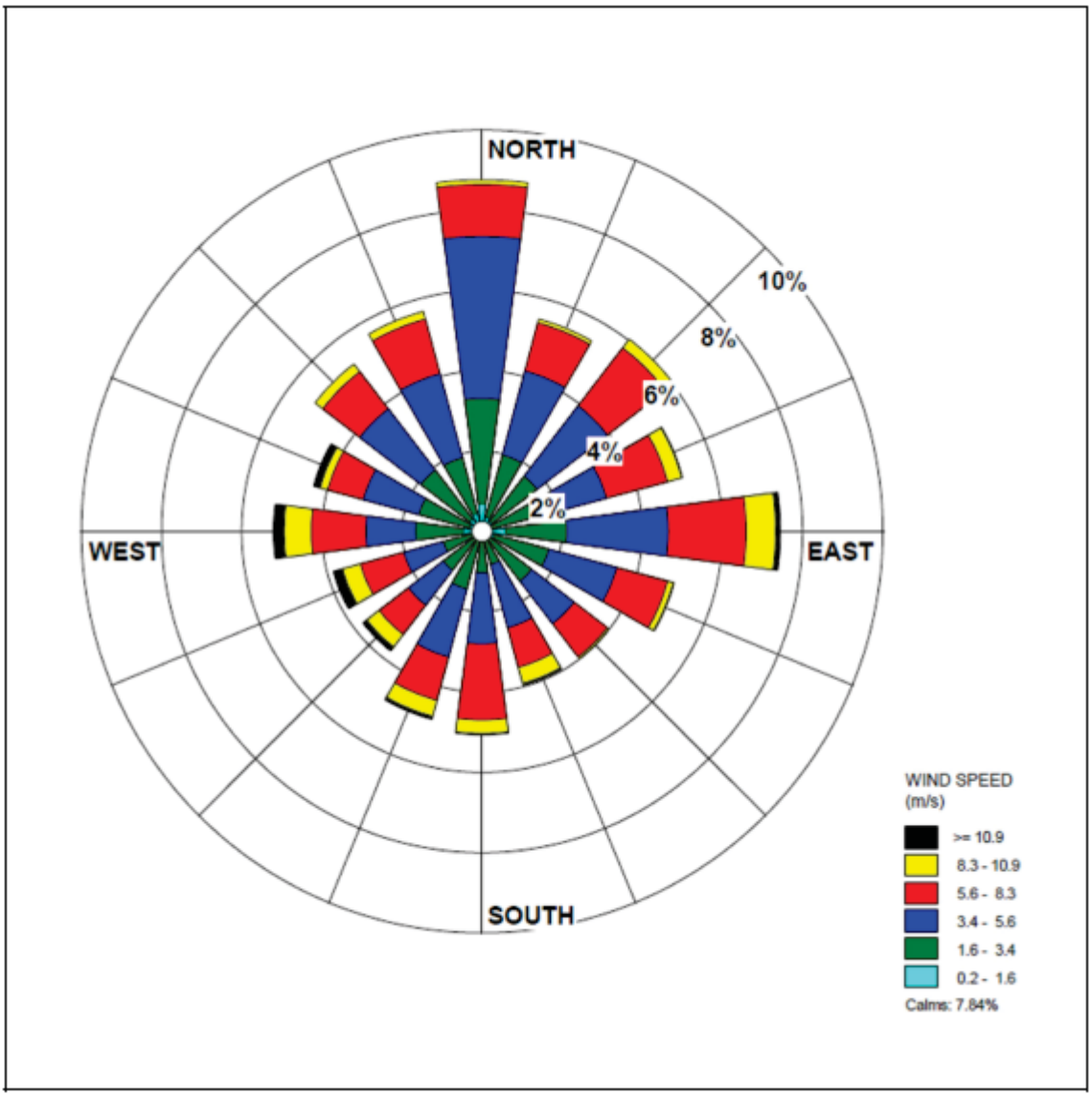

Figure 2.3-23 – April Wind Rose Southern Wisconsin Regional Airport (2005-2010)

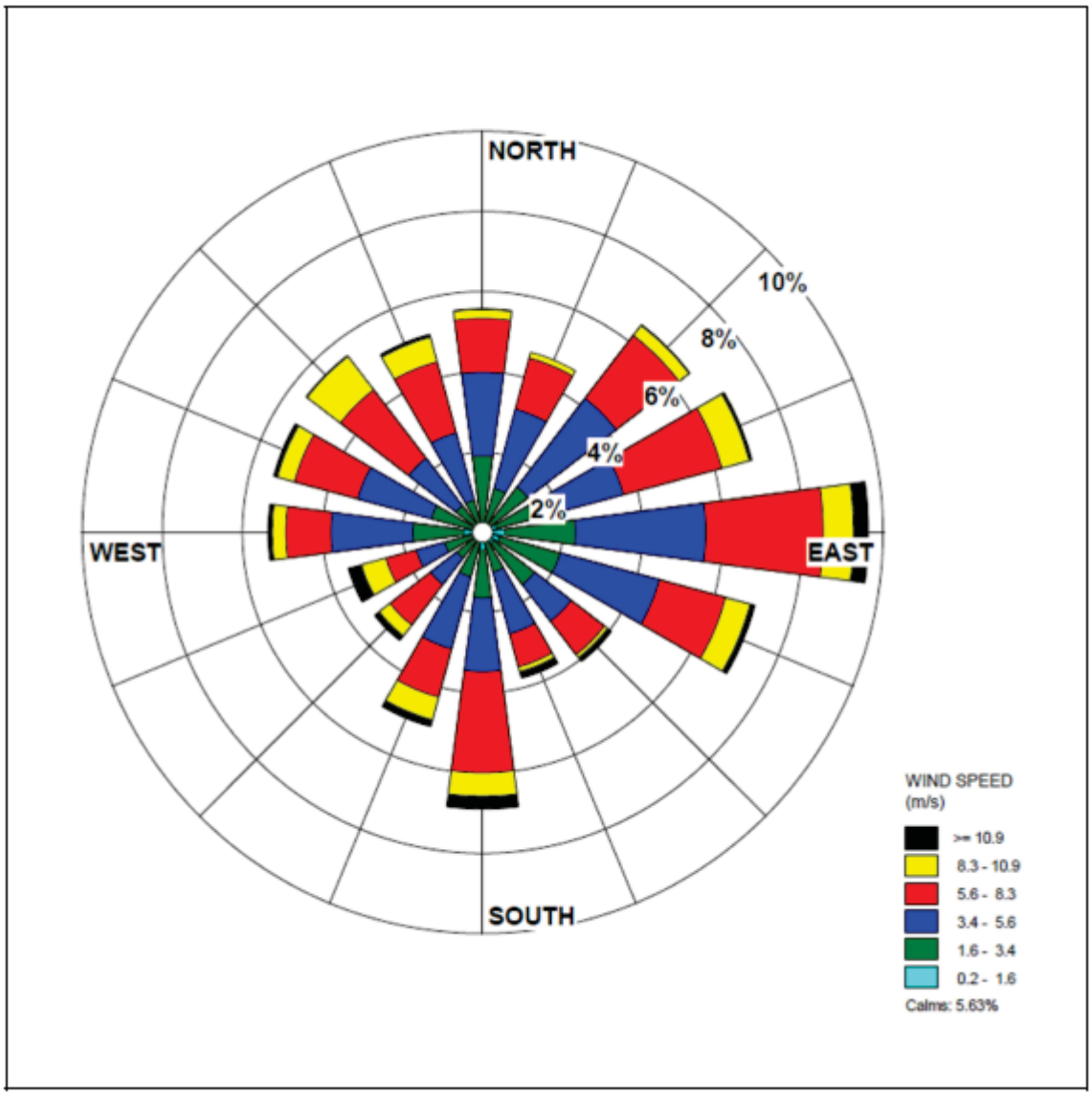

Figure 2.3-24 – May Wind Rose Southern Wisconsin Regional Airport (2005-2010)

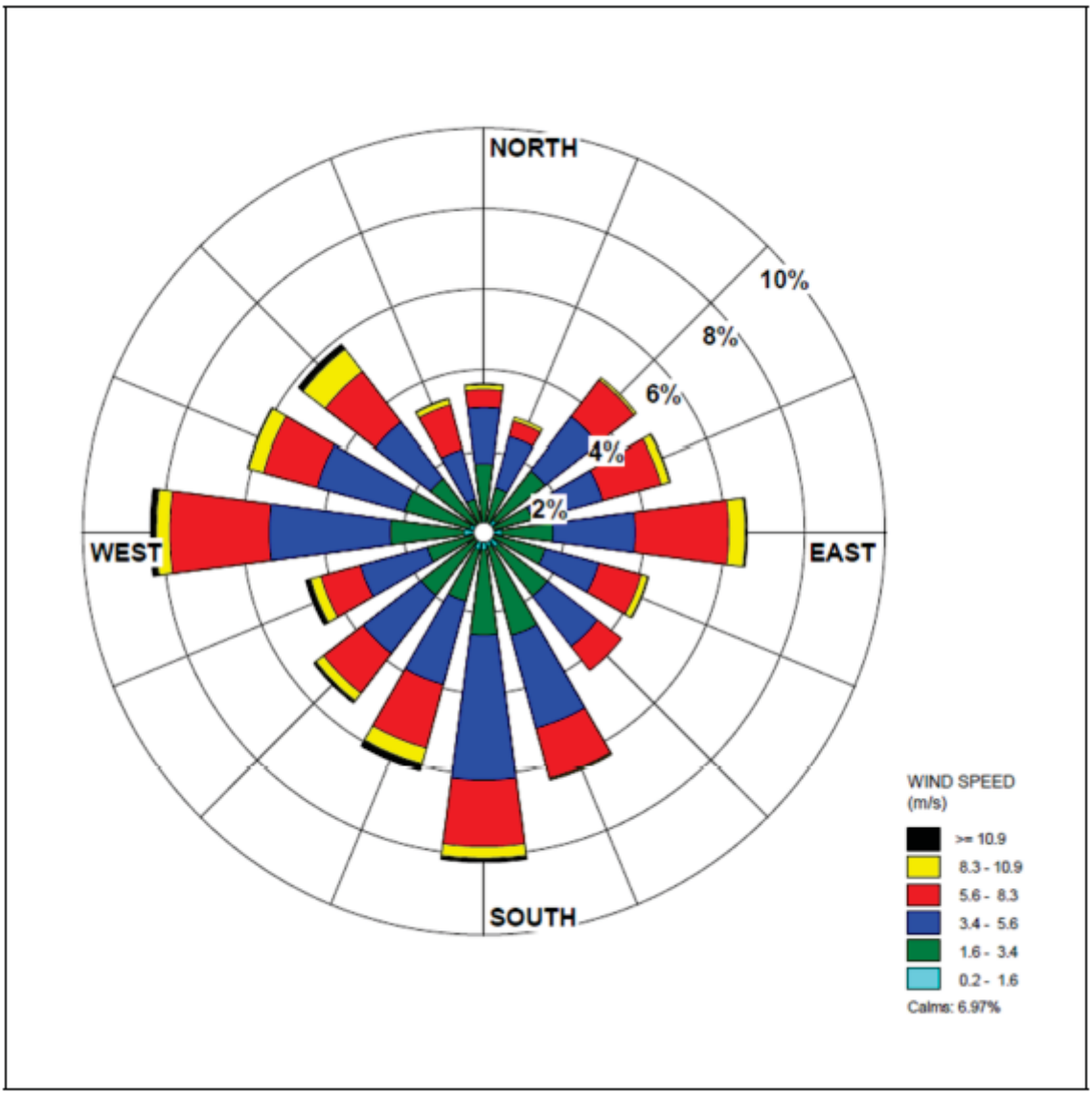

Figure 2.3-25 – June Wind Rose Southern Wisconsin Regional Airport (2005-2010)

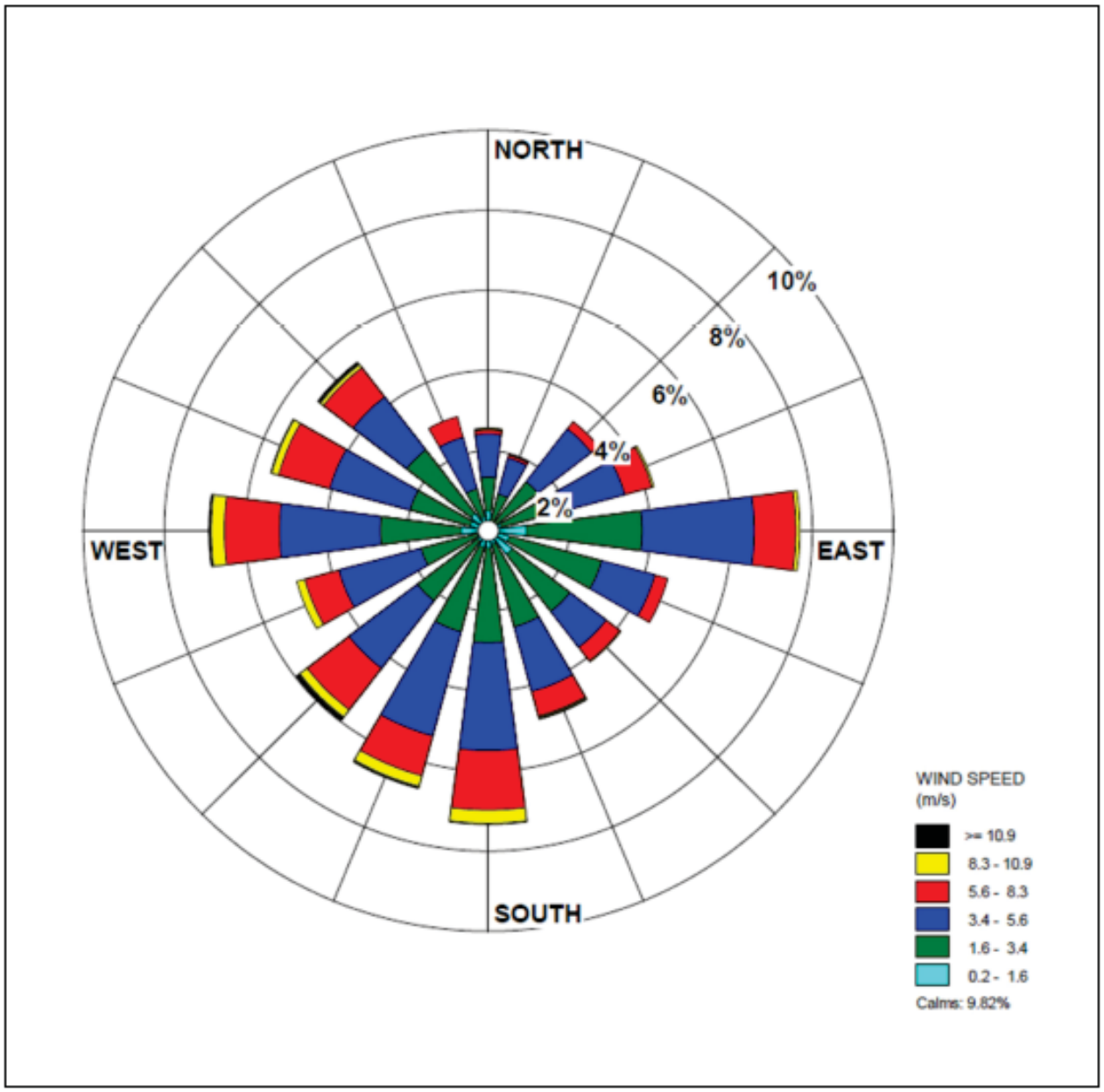

Figure 2.3-26 – July Wind Rose Southern Wisconsin Regional Airport (2005-2010)

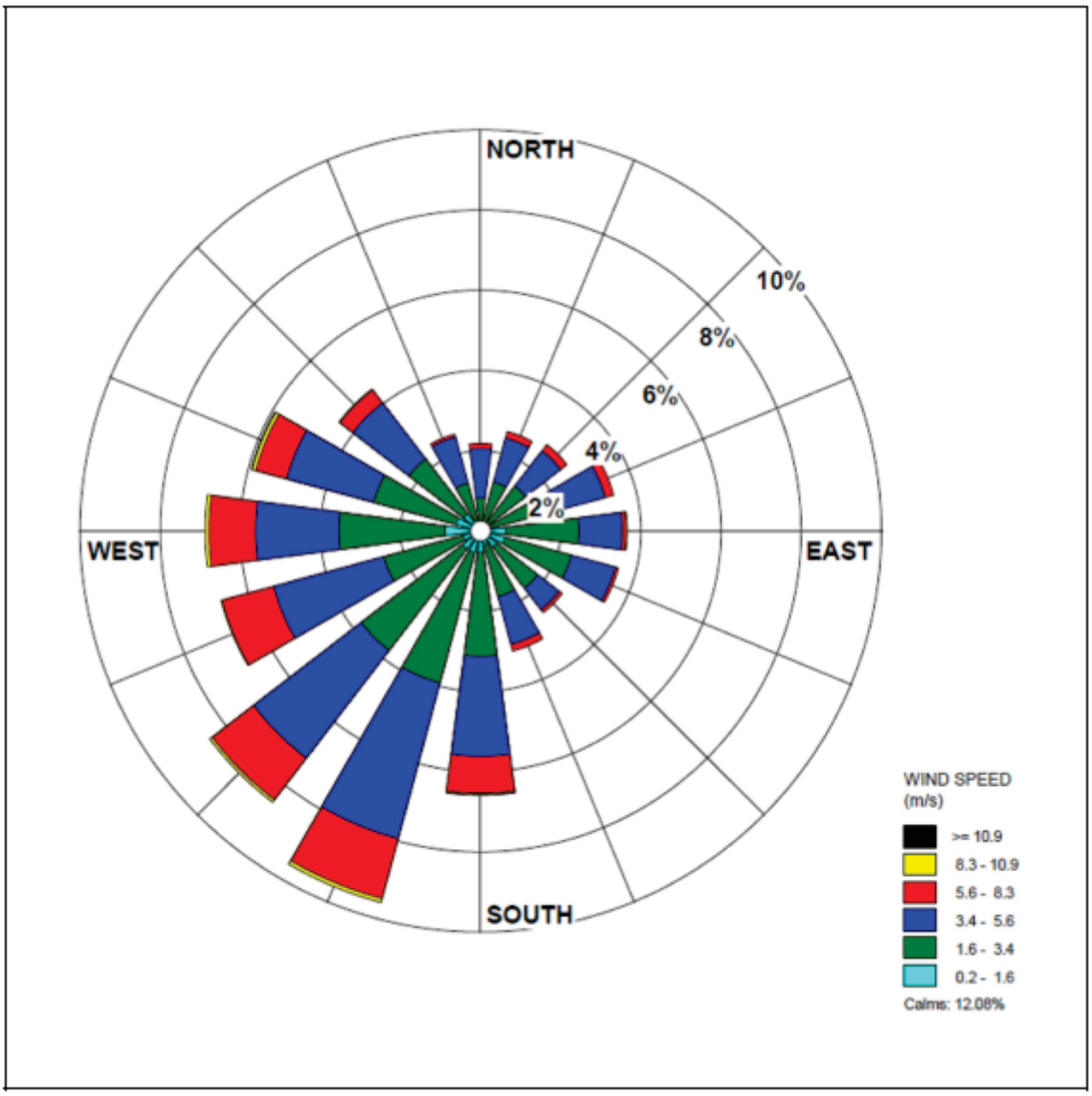

Figure 2.3-27 – August Wind Rose Southern Wisconsin Regional Airport (2005-2010)

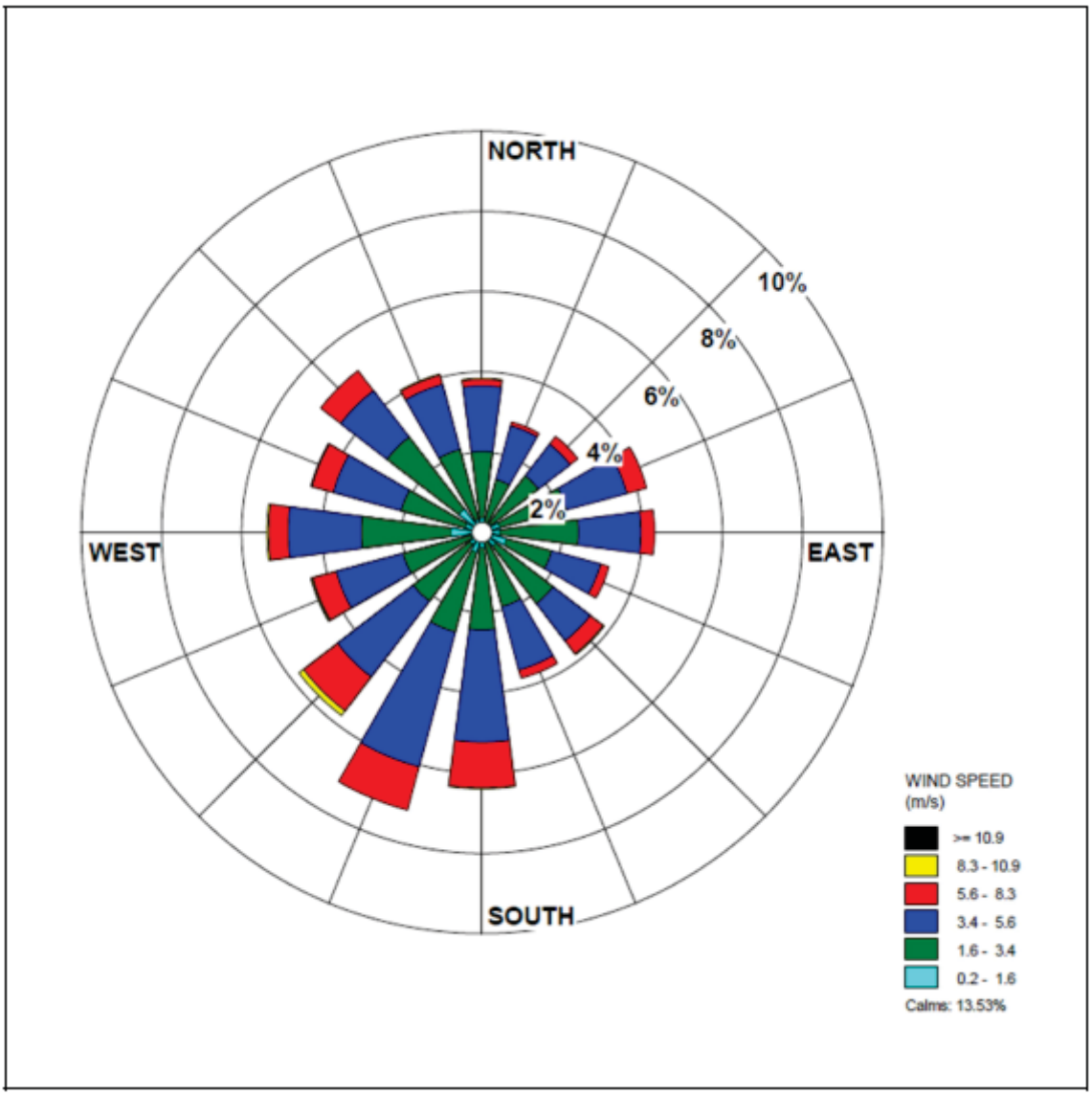

Figure 2.3-28 – September Wind Rose Southern Wisconsin Regional Airport (2005-2010)

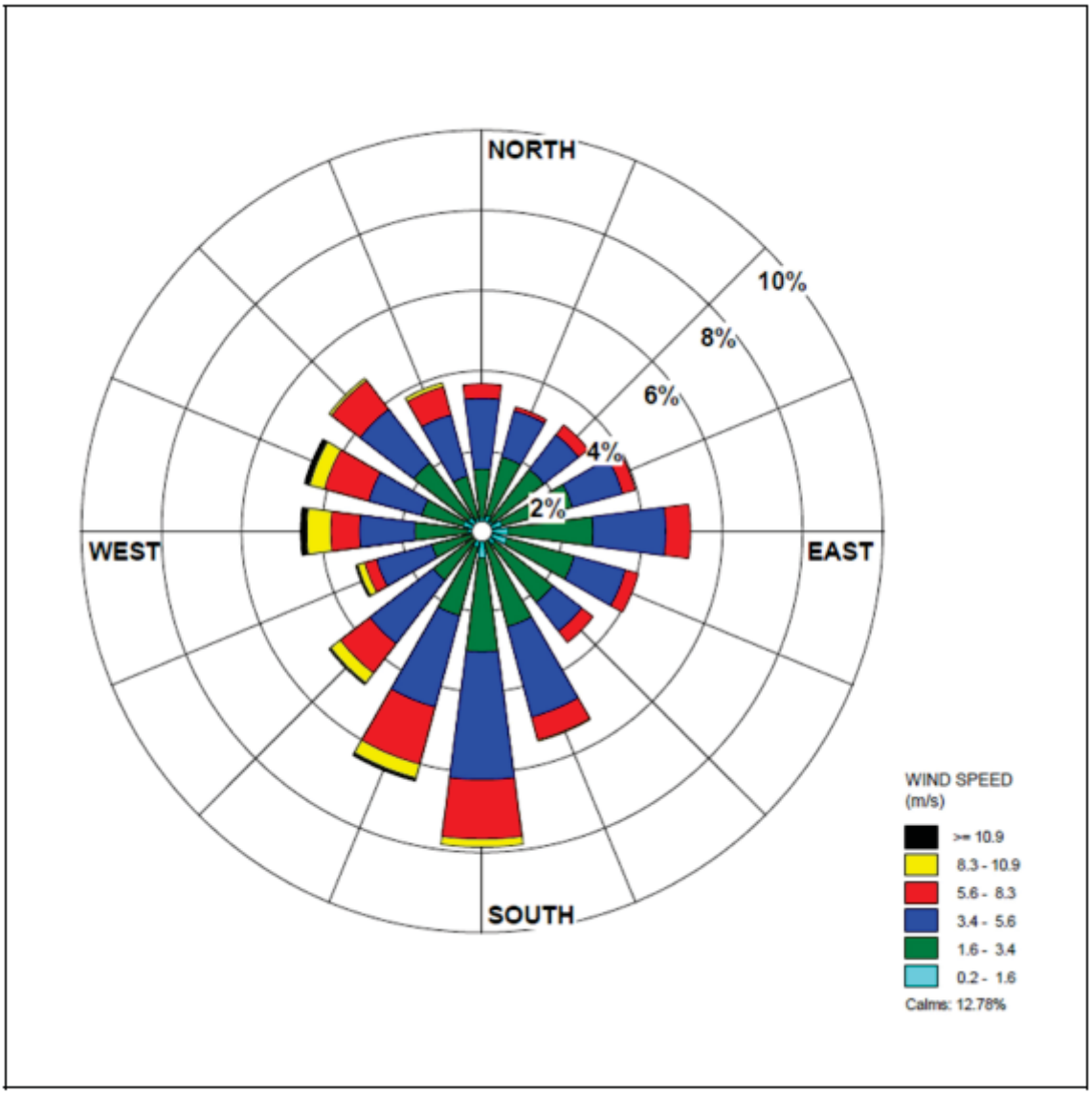

Figure 2.3-29 – October Wind Rose Southern Wisconsin Regional Airport (2005-2010)

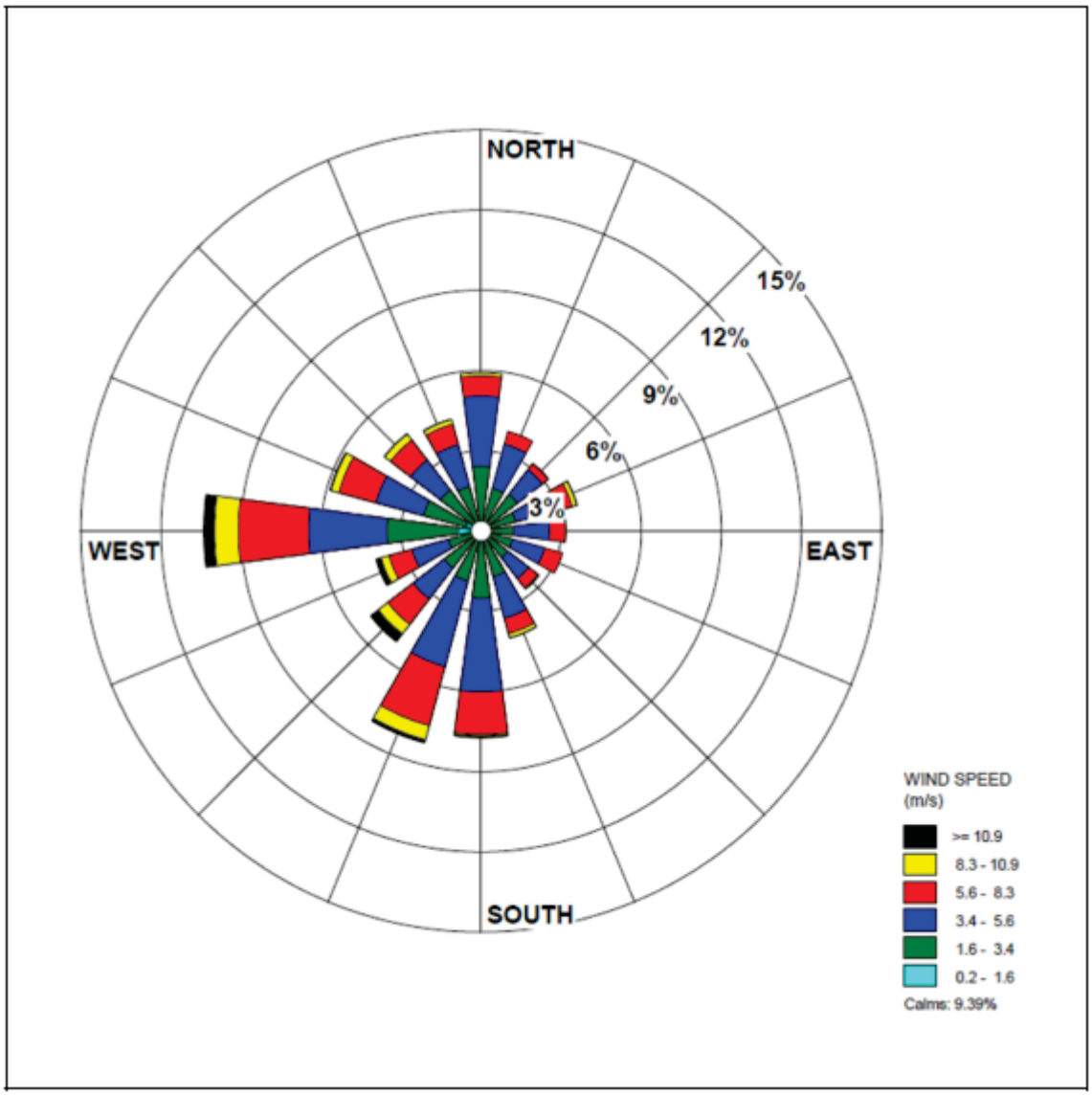

Figure 2.3-30 – November Wind Rose Southern Wisconsin Regional Airport (2005-2010)

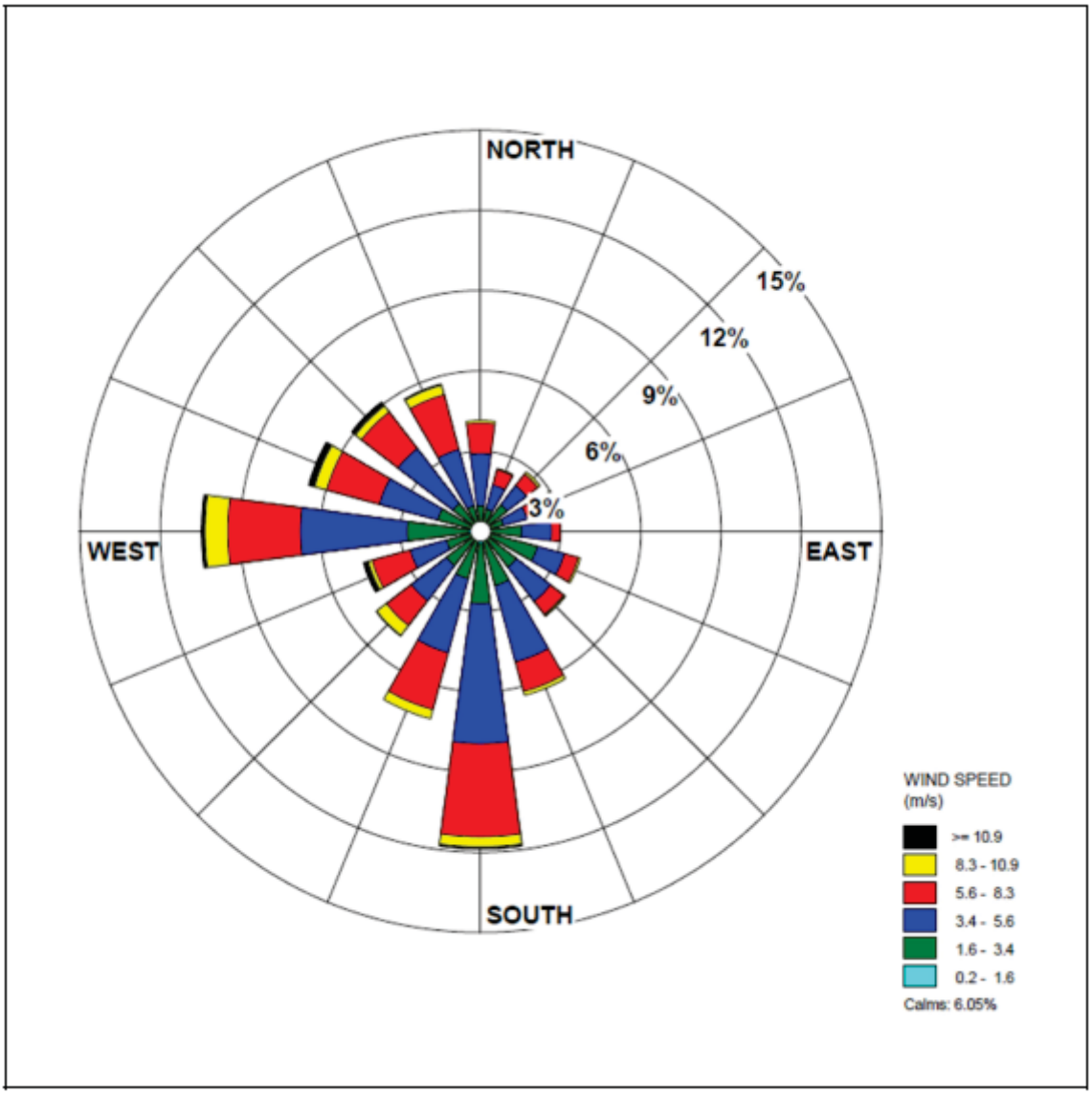

Figure 2.3-31 – December Wind Rose Southern Wisconsin Regional Airport (2005-2010)

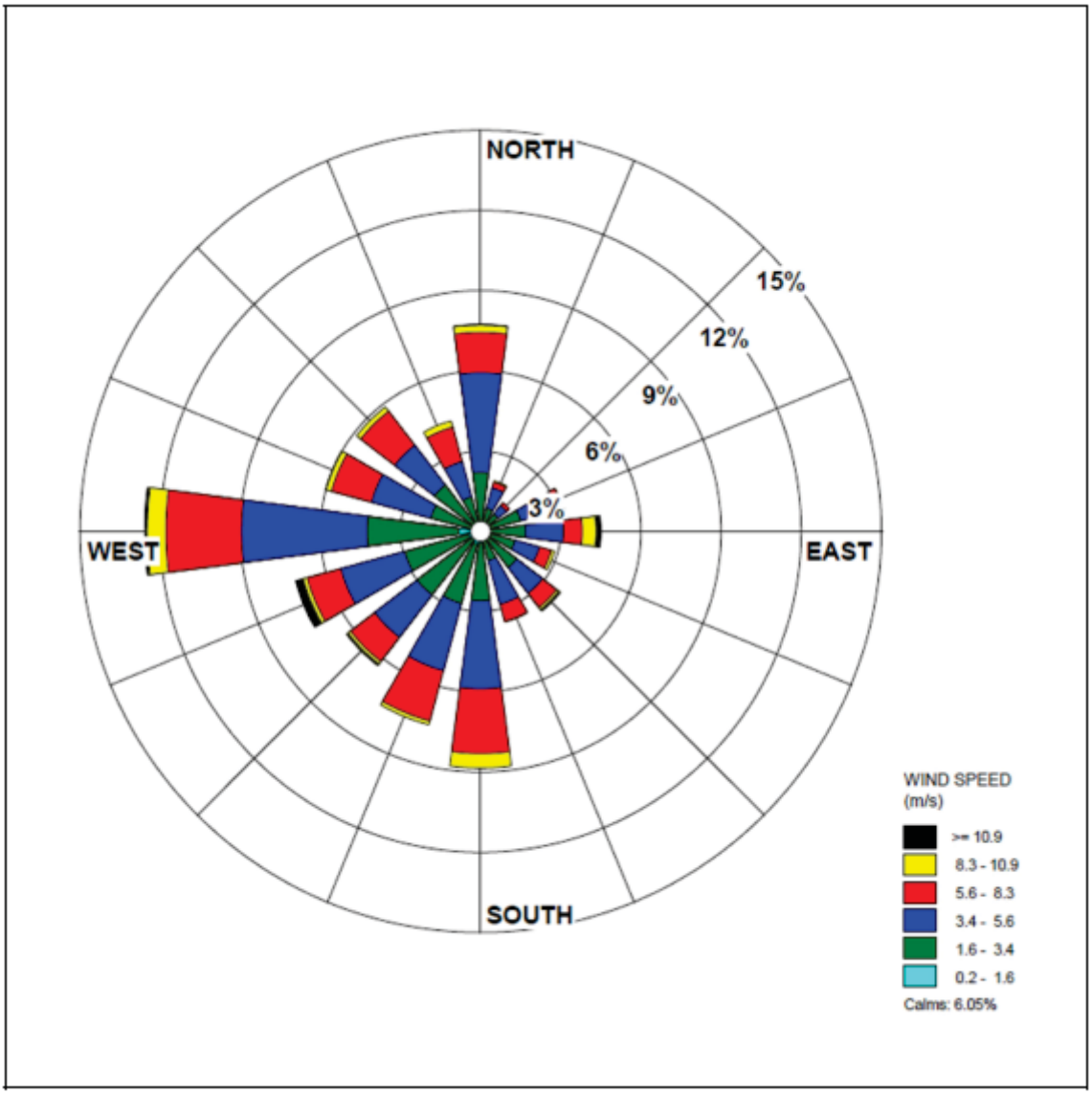

Figure 2.3-32 – Winter Wind Rose Southern Wisconsin Regional Airport (2005-2010)

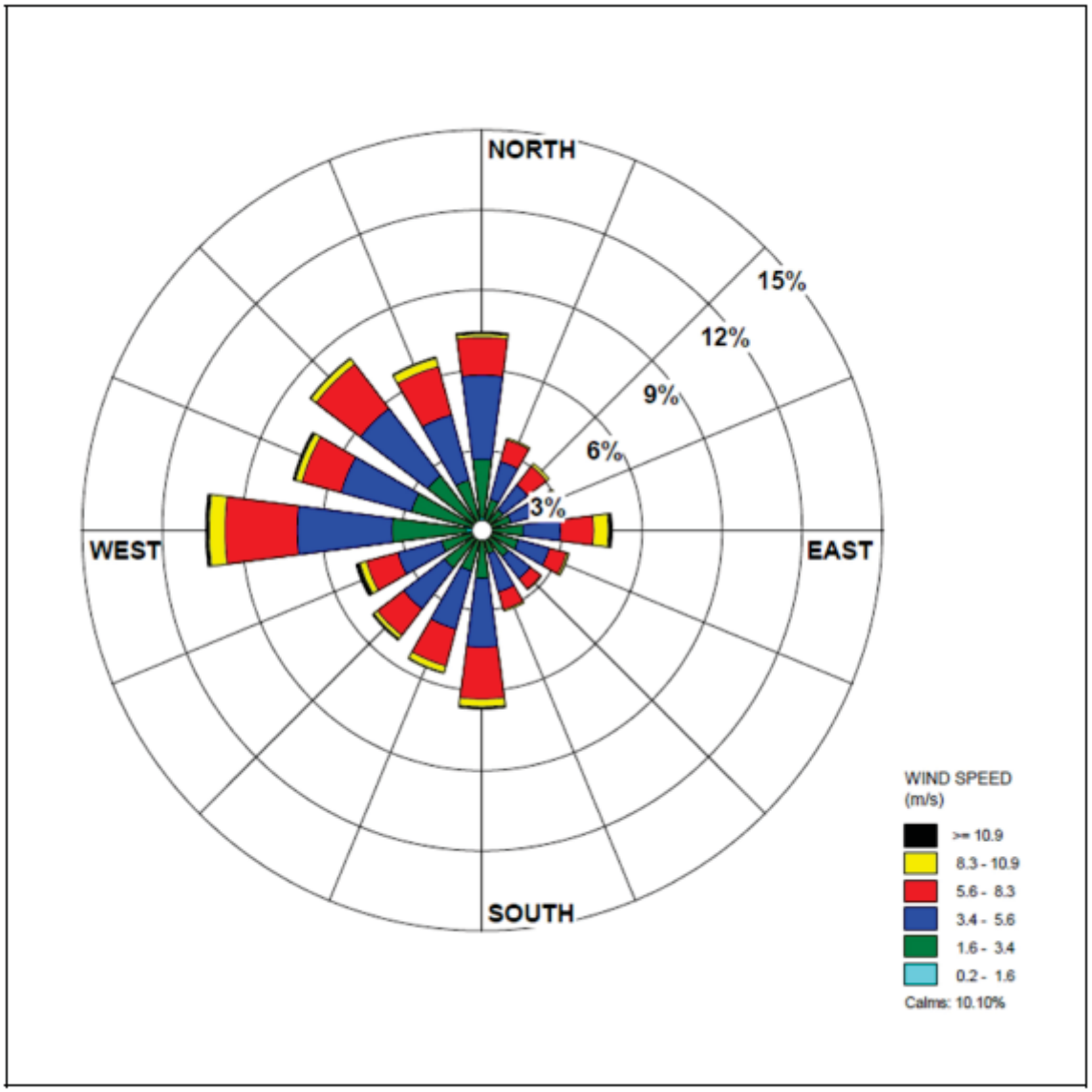

Figure 2.3-33 – Spring Wind Rose Southern Wisconsin Regional Airport (2005-2010)

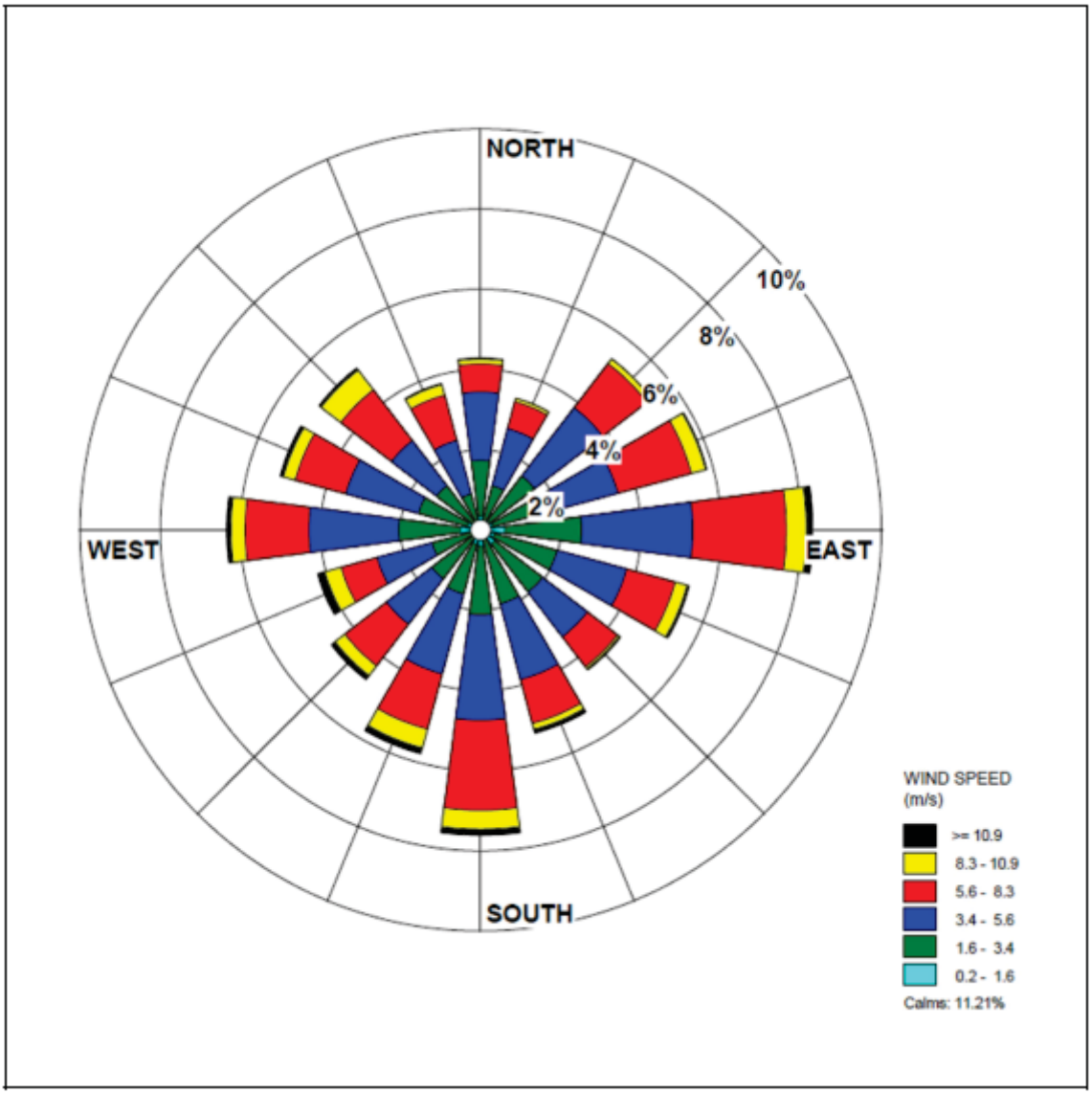

Figure 2.3-34 – Summer Wind Rose Southern Wisconsin Regional Airport (2005-2010)

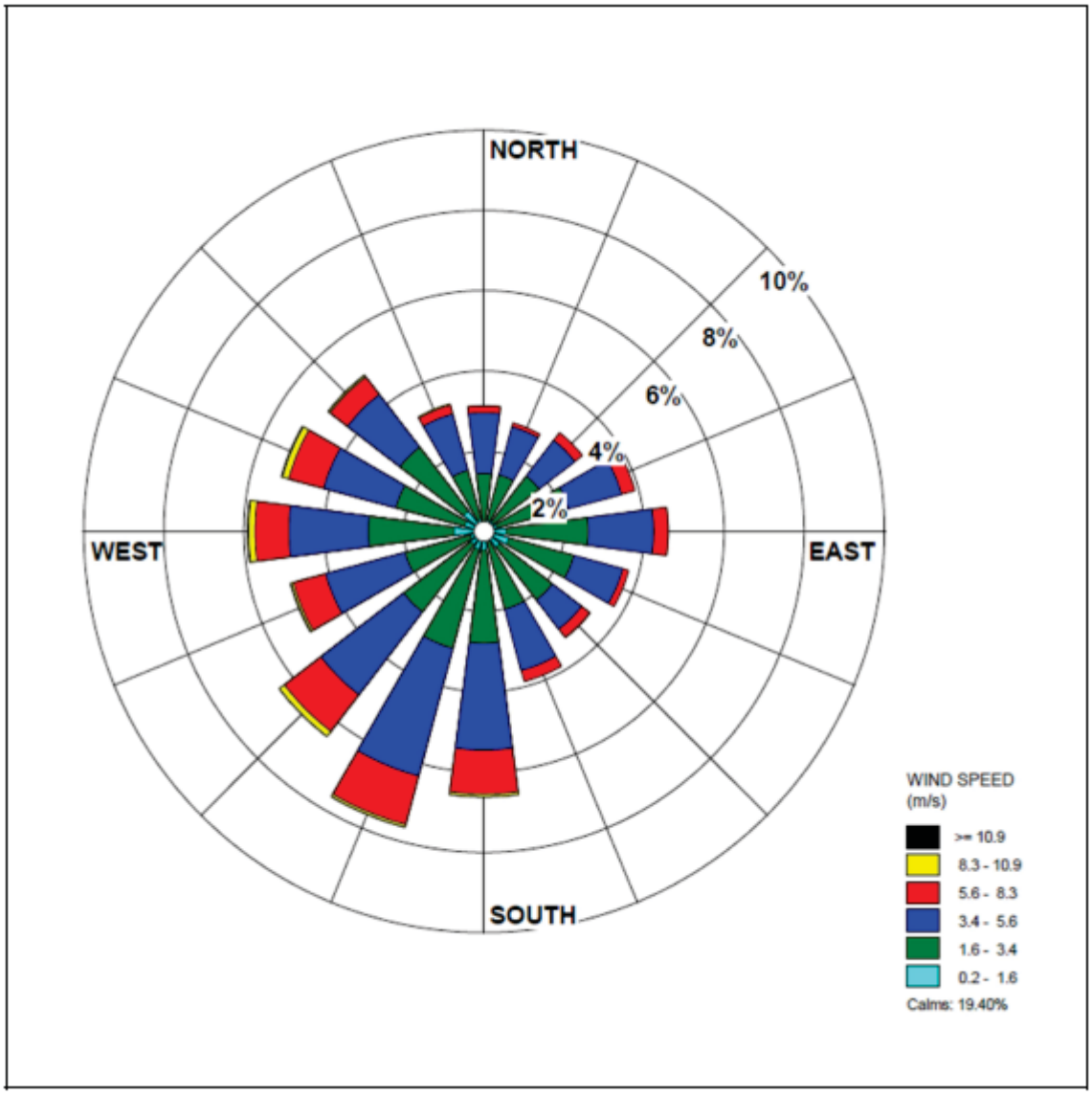

Figure 2.3-35 – Autumn Wind Rose Southern Wisconsin Regional Airport (2005-2010)

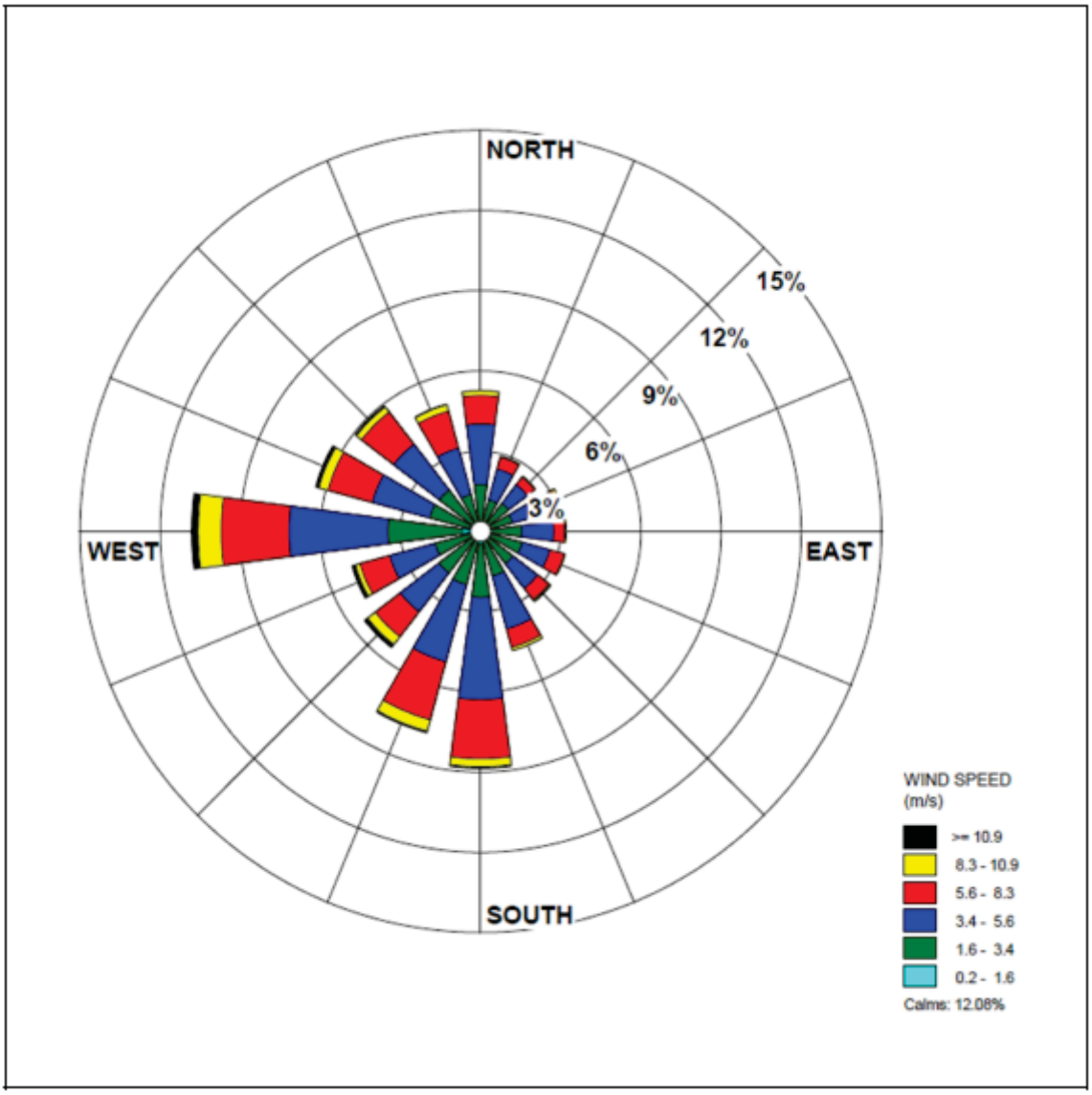

Figure 2.3-36 – Annual Wind Rose Southern Wisconsin Regional Airport (Janesville, WI) and Regional Stations

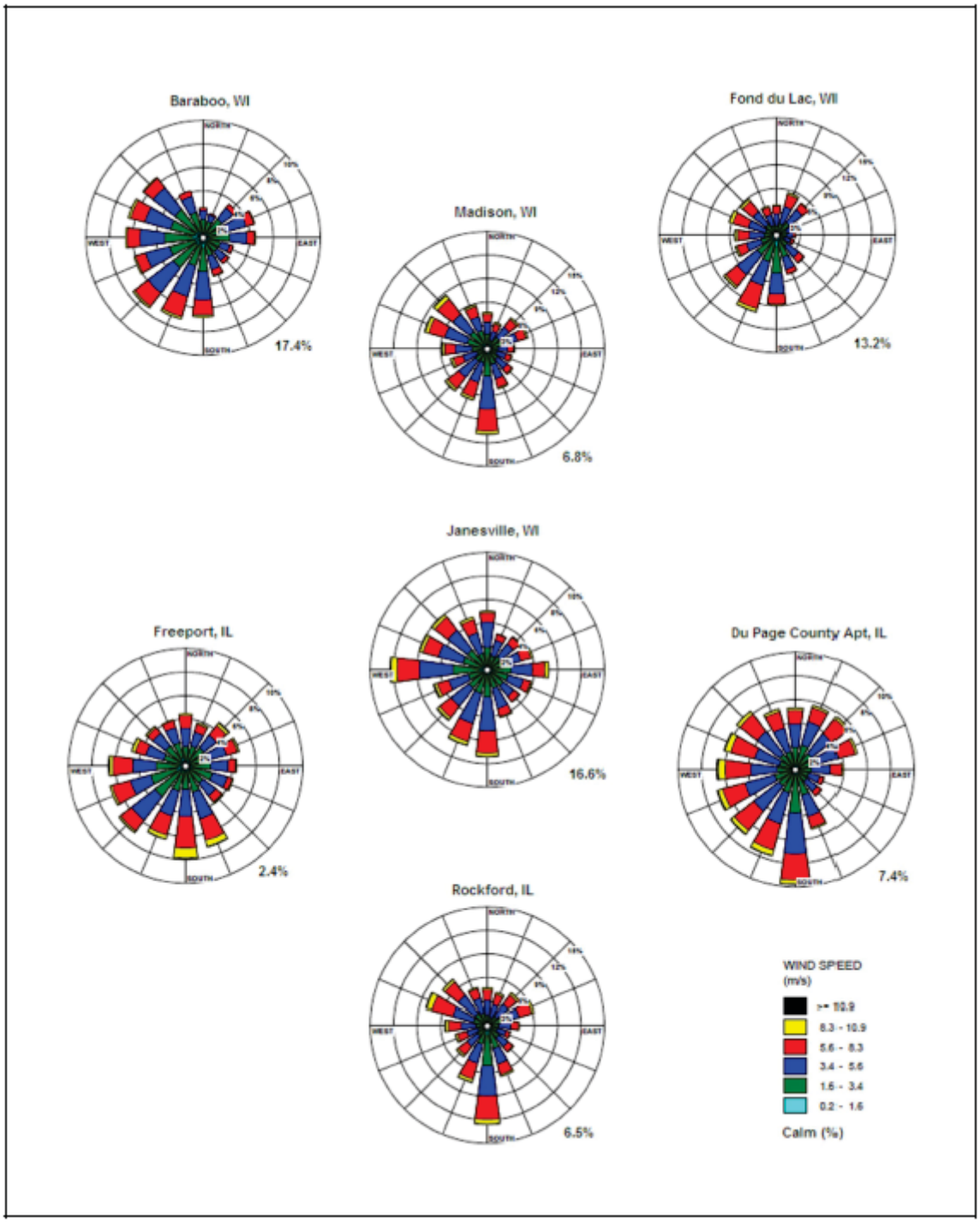

2.4 HYDROLOGY

NUREG-1537 requires an assessment of applicable hydrologic, hydrogeologic, and solute transport risks to nuclear facilities, both during operation and post-closure. Surface water (i.e., hydrologic flows) related to rivers and streams that may impact the site are addressed herein. Stormwater runoff at the site scale is addressed under separate studies. The purpose of this chapter is to identify hydrological processes that could contribute to radioactive releases, and to characterize the parameters that describe those processes.

This section was prepared using available information including 12 months of groundwater elevation data. The elevations in this section are reported according to the North American Vertical Datum of 1988 (NAVD 88).

NUREG-1537 states that the facility design must consider leakage or loss of primary coolant to groundwater. The light water pool provides decay heat removal from the target solution within the target solution vessel (TSV) dump tank during normal operations and extended periods of shutdown. A primary coolant spill is not a credible scenario, as described in Section 3.3; however, small leakage is credible. The light water pool is designed with a leak chase to collect to enable the detection and collection of small leaks of the pool to prevent releases to groundwater. The light water pool leak chase system directs the collected leakage to a central point for monitoring.

Additionally, leakage of primary cooling water is credible from the primary closed loop cooling system (PCLS). Instrumentation identifies and quantifies leakage rates, including very small leaks, from the PCLS. The facility structure (FSTR) provides barriers at ground level exits, steel liners and drip pans in vaults and trenches, and water stops in construction joints below grade to prevent the release of potentially contaminated water to the environment and groundwater. Therefore, leaks in the PCLS do not result a release of primary cooling water outside of the radiologically controlled area.

The facility design provides for confinement of radioactive materials, as described in Chapter 6, and Chapter 13 describes the mitigation of loss of system integrity events. Additionally, the facility has a sanitary drains water management system that confines the postulated maximum discharge of water in the radiologically controlled area (RCA), such as from a fire system discharge, which prevents potentially contaminated water from reaching the groundwater. A radioactive drain system (RDS) also provides capture and confinement of radioactive liquids from postulated leakage or overflow events. Therefore, the required spill scenario would consider the effects of accidental releases of unspecified liquid effluents in groundwater.

2.4.1 HYDROLOGICAL DESCRIPTION

This subsection identifies the site surface water, groundwater aquifers, types of on-site groundwater use, sources of recharge, present known withdrawals and likely future withdrawals, flow rates, travel time, gradients, and other properties that affect movement of accidental contaminants in groundwater, groundwater levels beneath the site, seasonal and climatic fluctuations, monitoring and protection requirements, and man-made changes that have the potential to cause long-term changes in local groundwater regime.

2.4.1.1 General Setting – Surface Water

Rock County is drained entirely by the Rock River and its tributaries (see Figure 2.4-1). The site is located approximately 172 river miles (mi.) (272 kilometers [km]) (FEMA, 2008) upstream from the mouth of the Rock River where it joins with the Mississippi River. The Rock River is located approximately 2 mi. (3.2 km) west of the site and flows generally north to south from Janesville (located just to the north), around the site. The Rock River has a contributing drainage area of approximately 3340 square miles (sq. mi.) (8650 square kilometers [sq. km]) at the Afton U.S. Geological Survey (USGS) Gauge located just southwest of the site (FEMA, 2008) (Figure 2.4-1). Water surface elevations along the Rock River channel during normal flow conditions range from approximately 760 feet (ft.) (232 meters [m]) at Janesville, directly north of the site, to approximately 750 ft. (229 m) to the west and south of the site.

Major tributaries to the Rock River include the Yahara River, the Sugar River, Raccoon Creek, and Turtle Creek. Turtle Creek drains the southeastern portion of Rock County, to its confluence with the Rock River near South Beloit, located approximately 8 mi. (13 km) south of the site. An unnamed creek is located approximately 1 mi. (1.6 km) southeast of the site and is referred to as the unnamed tributary in this section. This tributary stream flows east-to-west to where it meets the Rock River approximately 2 mi. (3.2 km) south of the site. The stream has a tributary area of approximately 18.4 sq. mi. (47.7 sq. km) (FEMA, 2008).

The central and southeastern portions of Rock County are characterized as flat glacial outwash plains. The majority of the County's rivers and stream valleys are filled with thick deposits of alluvial sand and gravel. The alluvial sediments and upland plains are the result of glacial activity. Surface soils include silt loam which are underlain by glacial till or stratified sand and gravel outwash units, which then serve as the source sediments to rivers and streams (FEMA, 2008).

The site was originally an agricultural field with a center-pivot irrigation system. The fields were cultivated with corn and soybeans. Generalized surface topography of the area sloped gently to the southwest. In 2012, the ground surface across the proposed site area sloped gently to the northwest with grades dropping about 7 ft. (2 m) from the southeast to the northwest (i.e., from corner-to-corner). In 2012, the ground elevation at the site ranged from approximately 819 ft. to 826 ft. (250 m to 252 m) NAVD 88.

Site climatology is discussed in Section 2.3.

2.4.1.2 General Setting – Groundwater

The site is located in a glacial deposition subjected to post-glacial erosional and depositional processes. The topsoil is under-drained by a relatively clean, fine to coarse grained sand extending to depths of 180 to 185 ft. (55 to 56 m). Occasional gravel layers may occur. Below this is a layer of sandy silt that is 10 to 18 ft. (3 to 5.5 m) deep, which is underlain by silty sand to the borehole termination depth of 221 ft. (64 m). Bedrock was not encountered during drilling, although soil sampling equipment hit firm surfaces in the three deep boreholes at depths between 170 and 180 ft. (52 to 55 m). Depth to bedrock at the site may be as deep as 300 ft. (91 m) (Subsection 2.5.2.1) and it consists of Cambrian and Ordovician sedimentary bedrock (conglomerate, dolomite, limestone, sandstone, shale). The carbonate bedrock is susceptible to dissolution (WGNHS, 2009). The Rock County Hazard Mitigation Plan (Vierbicher, 2010) indicates a potential for karst features to form in the county, particularly in the eastern third of the county, which is east of the site.

Based on this simplified stratigraphy, the top sand layers are considered as the primary aquifer. Deeper silty sand and Paleozoic aquifers are considered to be isolated by the sandy silt layer encountered in the deeper boreholes.

The monitoring well and remaining geotechnical boreholes were terminated at depths between 60 and 71 ft. (18 and 22 m). Groundwater was encountered in the boreholes during drilling at elevations ranging from about 754 to 766 ft. (230 to 233 m), which is about 60 to 65 ft. (18 to 20 m) below grade. Groundwater levels are expected to fluctuate seasonally and annually with changes in precipitation patterns. Apart from the exploration holes, there is no man-made activity at the site which affects natural groundwater conditions. However, there are irrigation wells operated on properties in the vicinity that have the potential to influence groundwater levels.

The groundwater is expected to be recharged through precipitation (infiltration) and underground flow from the background domains. Underground water flow is assumed to occur within the unsaturated zone (the thickness of this zone is about 50 to 60 ft. [15 to 18 m]) and the saturated zone. The ultimate discharge of the flow system is represented by the Rock River and its tributaries.

Well data was obtained from the Wisconsin Department of Natural Resources (WDNR) database that provided information on wells established since 1988. While historic well construction reports could be obtained from the Wisconsin Geological and Natural History Survey (WGNHS, 2009), the WDNR database was determined to provide a better basis for evaluation of current flow rates and flow directions for site characterization as the well data was more recent and more accurate. Publicly available information from the WDNR included well locations, pumping rates, and screened intervals. The well coordinates were estimated using the street address reported from the WDNR database. From this data set, potentiometric surfaces within four square miles of the site were generated for analysis. Figure 2.4-7 and Figure 2.4-8 provide four mile by four mile scale potentiometric surfaces based on these wells using non-pumped (static) and pumped conditions, respectively. These surfaces were created by using the Kriging process on the wells. The groundwater flow direction on the site is towards the Rock River for both the pumped and non-pumped conditions. Consequently, withdrawals from wells within a five mile radius of the site are not expected to change the flow direction of groundwater on the site. During a review of the well listing, well UJ792, which is located about 2,000 ft. from the site, was determined to have the lowest pumping head of the wells closest to the site. Using Darcy's Law, the advective travel times for well UJ792 was calculated to be 0.1 years, using expected permeability and porosity assumptions, and 0.01 years, using conservative permeability and porosity assumptions (Table 2.4-12).

2.4.1.3 Present Withdrawals and Known and Likely Future Withdrawals

The facility design does not include groundwater withdrawal or injection, and no planned future injection or withdrawal is expected to have a significant impact on facility operation or safety.

2.4.1.4 Groundwater Flow

The following paragraphs describe the local and regional groundwater flow conditions. The flow system contains the following steps as shown in Figure 2.4-2 (Gaffield et al., 2002):

- Recharge
  - Precipitation, infiltration
  - Underground recharge
- Underground flow
  - Unsaturated flow
  - Saturated flow
- Discharge

This order of steps follows the evolution of the flow system and can be used to track potential contaminant pathways. NUREG-1537 requires the consideration and assessment of risks related to hydrologic, hydrogeologic and solute transport processes. To meet this requirement at each step, potential hazards and safety factors are discussed in detail.

At the regional scale, there is a large body of literature on the groundwater system (LeRoux, 1963 and Gaffield et al., 2002); however, at the scale of the site, the available information is based primarily on drilling, testing and geotechnical analyses at the site.

As depicted in Figure 2.4-2, recharge of the flow system may occur in two ways:

- Precipitation and infiltration through the ground surface
- Underground flow from background domains

No site-specific information is available to estimate infiltration rates. Gaffield et al. used a calibration procedure for their model to get the best fit between measured and simulated groundwater levels and streamflows in Rock County (Gaffield et al., 2002). This study considered that 457 feet per day (ft./day) (139 meters per day [m/day]) hydraulic conductivity for sand and gravel layers close to the surface (Figure 2.4-2) and determined that the corresponding recharge rate for these layers would be 12.7 inches per year (in./yr) (32.3 centimeters per year [cm/yr]).

Another groundwater recharge mechanism at the site is flow from the surrounding upland areas with higher groundwater levels. Evidence for this process is provided by the site monitoring system (Figure 2.4-3), which reveals that flow direction is NNE-SSW year-round (Figure 2.4-4). A permanent recharge from upland areas is expected under the site because groundwater moves from higher to lower potentials.

As part of the precipitation infiltrates into the soil layers, water moves first through the unsaturated zone, then reaches the water table and travels through the saturated zone to the potential discharge regions. The highest conductivity values can be measured in the saturated region; in the unsaturated zone the migration of water is relatively slow compared to the saturated zone (assuming the same material in both zones, which is the case at the site).

The water table was encountered in the boreholes at elevations ranging from 754 to 766 ft. (230 to 233 m) (Table 2.4-1; Figure 2.4-5). Table 2.4-1 only presents estimates of the water table, which indicate local variability but no trends. However, the longer term monitoring data provides additional information about the water table (Table 2.4-2). Based on this long term monitoring data, the groundwater flow direction is dominantly NNE-SSW (Figure 2.4-4) below the site, indicating that the flow regime is relatively stable. The water table fluctuation was a maximum of 2.2 ft. (0.67 m) during the monitoring period. This observation was corroborated by water table estimations from 1958 (Figure 2.4-6) at larger time scales. The consistency in water

table elevation levels over more than sixty years indicates that the water table and the hydraulic gradient do not vary significantly over long time periods.

To characterize the hydraulic conductivity of the sandy layers at the site, in-situ hydraulic slug tests were performed in the monitoring wells. Both falling and rising head tests were conducted. The tests are summarized in Table 2.4-3. The results of Advanced Aquifer Test Analysis Software (AQTESOLV) (Hydrosolve, 2011) hydraulic conductivity evaluations are presented in Table 2.4-4. The average conductivity was 0.0045 feet per second (ft./sec) (0.00137 m/s) based on the empirical/analytical method of Bouwer and Rice (Bouwer and Rice, 1976). The arithmetic mean of the AQTESOLV hydraulic conductivity values from on-site slug tests is 0.0045 ft./sec. The geometric mean of the AQTESOLV hydraulic conductivity values from on-site slug tests is 0.0041 ft./sec. Since the calculated arithmetic mean of the hydraulic conductivity values was found to be more conservative than the calculated geometric mean of the hydraulic conductivity values, the arithmetic mean of the hydraulic conductivity values was used to calculate the expected advective travel times provided in Table 2.4-12.

Because the density of sand increases with depth, it is likely that results of well test interpretations are upper bounds for lower sand layers. A hydraulic conductivity of 0.004 ft./sec (0.00122 m/s) is considered to be an appropriate estimate for the sand deposits. This value is very close to the value reported by Gaffield et al. based on the calibration procedure of their analytic element model (457 ft./day=0.0052 ft./sec) (Gaffield et al., 2002). Based on this conductivity estimate and the hydraulic gradients, the Darcy flux is 2.06×10^{-6} ft./sec and 3.07×10^{-6} ft./sec (6.28×10^{-7} and 9.36×10^{-7} m/s) in east-west (EW) and north-south (NS) direction, respectively (hydraulic conductivity [k] =0.004 ft./sec [0.0012 m/s]; gradient is calculated as the average hydraulic gradient presented in Figure 2.4-5). This flux rate is two orders of magnitude higher than that assumed by Gaffield et al. (Gaffield et al., 2002) for infiltration (12.7 in/yr = 3.35×10^{-8} ft./sec [1.02×10^{-8} m/s]). The higher flux rate indicates that a significant part of the recharge to the groundwater beneath the site is coming from off site.

Since groundwater moves from higher groundwater level areas to low level areas, groundwater usually discharges to surface water (lake, river, etc.). The Janesville area is drained entirely by the Rock River and its tributaries. Based on long-term monitoring data, the groundwater flow direction is dominantly NNE-SSW (Figure 2.4-4) below the site.

2.4.2 FLOODS

This subsection identifies historical flooding (defined as occurrences of abnormally high water stage or overflow from a stream, floodway, lake, or coastal area) at the site.

2.4.2.1 Rock River Flows

The Rock River and the unnamed tributary stream are subject to flooding throughout the year; however, the largest potential for flooding occurs during the spring runoff. These floods are the result of combined precipitation and rain-on-snow events. Peak flows occurring during winter months when temperatures are low can also result in ice jam events. A USGS gauge on the Rock River is located approximately 2.5 mi. (4.0 km) to the west of the site (Figure 2.4-1). The portion of the Rock River basin contributing to the site is approximately the same as the basin contributing to the USGS gauge site (i.e., the site is not significantly upstream or downstream of the gauge location relative to the basin area). Flows recorded at the gauge are therefore applicable and closely represent analogous conditions at the site and do not need to be scaled

up or down to reflect a shift in the basin location. Based on available USGS flow data, March is a common month for floods in the Rock River (USGS, 2012a and FEMA, 2008).

The USGS web-based flow data were reviewed for the gauge site near Afton, located just across the river from the airport and just southwest of the site. This site has a period of record of nearly 100 years dating back to 1914 and is an applicable flow record of the Rock River near the site.

Measurements at the USGS gauge show a flow rate of about 10,000 to 13,000 cubic feet per second (cfs) (283 to 368 cubic meters per second [m^3/sec]) for the peak historical flood events, with the maximum flow rate being 16,700 cfs (473 m^3/sec) observed in June 2008. Based on this record, the flows of 10,000 to 13,000 cfs (283 to 368 m^3/sec) correspond approximately to the 10-year to 50-year events (FEMA, 2008). The peak flow of 16,700 cfs (473 m^3/sec) is generally consistent with the 100-year flood levels along the Rock River (Janesville, 2008 and FEMA, 2008). The flood level at the USGS gauge at Afton during the 2008 flood was approximately 755 ft. (230 m) in elevation (FEMA, 2008).

2.4.2.2 Flood Record Details and Elevations

The Federal Emergency Management Agency (FEMA) completed a flood hazard assessment for Rock County in August 2008 that looked at existence and severity of flood-related hazards, including the areas around the site. The study included the Rock River where it passes by the site (at approximately river mile 172 upstream from the confluence with the Mississippi River) and the unnamed tributary stream located just to the south of the site (Figure 2.4-1).

FEMA completed hydrologic and hydraulic analyses for the Rock River and the unnamed tributary stream to estimate flow magnitudes for various recurrence interval flood events and to estimate the water surface elevations for corresponding flood events. Table 2.4-5 provides a summary of flows for the Rock River for the reach from Janesville (river mile 178) to Afton near the USGS gauge (river mile 172), located just across the river from the site and the airport. Elevations are reported as an approximate range, based on the FEMA 2008 flood profiles, with the higher elevation corresponding to the upstream end of the reach at Janesville and the lower elevation at the downstream end near the USGS gauge at Afton. Table 2.4-6 provides a similar summary for the unnamed tributary to the Rock River for the reach between US 51 and Prairie Road just to the south of the site. The range of reported elevations is similarly derived from the FEMA 2008 flood profiles. Channel bottom elevations are based on surveys that supported the FEMA 2008 studies.

FEMA estimated the 100-year flood level as approximately 755 ft. (230 m) for the location of the USGS gauge at Afton (Table 2.4-5), which correlates well with the gauge flows and corresponding observed flood levels during the 2008 flood at the same location (FEMA, 2008). The estimated 500-year flood level is 756 ft. (230.4 m) (FEMA, 2008) (Table 2.4-5). The results show that the 100-year and 500-year floodwater surface elevations for the Rock River are well below the 825 ft. ground floor elevation of the main production facility and the waste staging and shipping building for the full reach of the Rock River extending from Janesville downstream and around the site through Afton (Table 2.4-5). Similarly, the 100-year and 500-year floodwater surface elevations for the unnamed tributary to the Rock River, for the reach just south of the site (Table 2.4-6), are well below the facility ground floor elevation.

2.4.2.3 Effect of Local Intense Precipitation

The effect of the local probable maximum precipitation (PMP) on the areas adjacent to safety-related structures of the facility, including the drainage from the roofs of the structures, was evaluated. The maximum water levels due to local PMP were estimated near the safety-related structures of the facility based on the site topographic survey map.

All elevations in this subsection are referenced to the NAVD 88.

A drainage system designed to carry runoff from the site up to a 100-year precipitation event consists of conveying water from roofs, as well as runoff from the site and adjacent areas, to peripheral ditches. The facility is surrounded by berms with interior ditches along the berms. The plant site is graded such that the high point of grade is set at Elevation 827 ft. (252.1 m). The grade around the structures slopes towards the peripheral ditches. The storm water drains into the peripheral ditches. A plan showing the delineated off-site drainage area is presented in Figure 2.4-11. Peripheral diversion swales and berms north and east of the site are provided to divert the off-site runoff around the facility area. During a local PMP event, the storm water drainage system is conservatively assumed to be not functional. No active surface water drainage waterway exists which flows towards the site. PMP runoff from the off-site area northeast of the site flows towards the site. The off-site area is relatively flat.

The finished site grade elevation is approximately 825 ft. (251.46 m), and the top of the finished foundation elevation is at least 4 inches (in.) above grade; therefore, water will not infiltrate the door openings in the case of a local PMP event.

The site is designed to withstand the effects of a local probable maximum precipitation (PMP) 100-year event. The PMP values and intensities are provided in Table 2.4-7. The values were determined from the 100-year rainfall intensity-duration-frequency curve for Madison, Wisconsin (WDOT, 1979) (Figure 2.4-10).

The effect of the PMP event on the areas adjacent to safety-related structures of the facility, including the drainage from the roofs of the structures, was evaluated. The maximum water levels due to local PMP were determined near the safety-related structures of the facility based on site topographic survey maps.

The site is protected from PMP flooding by a developed drainage channel on the north and east sides of the site and an existing drainage channel east and southeast of the site (Figure 2.4-11) (Figure 2.4-12). Off-site runoff approaches the site from the north or northeast (Figure 2.4-11).

The developed drainage channel on the north and east sides of the facility directs off-site runoff away from the facility. Off-site runoff that flows from the north towards the site is captured by the channel which directs flow to an uncontrolled sub-basin on the west side of the site (Figure 2.4-11). The runoff flow rate was calculated as 42 cfs. The upstream bank elevation of the channel is 827 ft. The channel is approximately 1100 ft. long with a 0.8% slope. In the event of a 100-year storm, the water surface elevation at the upstream end of the channel reaches a maximum height of 826.3 ft., which is below the bank height.

Off-site runoff that flows from the northeast towards the site is captured by an existing channel southeast of the site that flows to an unnamed tributary approximately one mile south of the site (Figure 2.4-1) (Table 2.4-6). The unnamed tributary flows east-to-west and meets the Rock River

approximately two miles south of the site. To determine the maximum water depth in the existing channel from PMP drainage, runoff from the entire 91 acre site was conservatively evaluated as conveyed by the existing channel. The runoff flow rate was calculated as 197 cfs. The maximum surface water elevation in the existing channel from a 100-year storm does not rise above the elevation of the banks. The water reaches an elevation of 826 ft. at the upstream end, below its bank elevation of 827 ft., and has an elevation of 818.5 ft. on its downstream end (south of the site), below its downstream bank elevation of 819.5 ft.

Stormwater inside the site boundary (e.g., paved areas) is directed to a stormwater management system (Figure 2.4-11). The facility design includes two infiltration cells that collect site runoff for the purpose of controlling total suspended solids (Figure 2.4-11). Infiltration cell #1 collects drainage, and at 810 ft. elevation, flows via a spillway to infiltration cell #2. The infiltration cells have a peak water surface elevation of 810 ft. during a 100-year storm event and will not pose a site flooding concern.

Site low points surrounding the production facility were conservatively analyzed for maximum flood depth from the 100-year PMP event (Figure 2.4-12). The maximum depth in all low points from impounded water is below the ground floor elevations of the main production facility and waste staging and shipping building, with margin.

PMP runoff flow rates for channel drainage were calculated using the Soil Conservation Service (SCS) methodology. Runoff, Q_{in}, for the 100-year storm event:

$$Q_{in} = \frac{(P - 0.2S)^2}{(P + 0.0S)^2} \qquad \text{Equation 2.4-1}$$

Where:

- Q is the Runoff (in.)
- P is the Rainfall (in., 24-hour period)
- S is the Potential maximum retention after runoff beings (in.)

$$S = \frac{1000}{CN} - 10 \qquad \text{Equation 2.4-2}$$

Where:

- CN is the Runoff Curve Number

$$q_p = q_u \times A_m \times Q_{in} \times F_p \qquad \text{Equation 2.4-3}$$

Where:

- q_p is the Peak Discharge (cfs)
- q_u is the Unit Peak Discharge (csm/in.)
- A_m is the Drainage area (mi^2)
- Q_{in} is the Runoff (inches)
- F_p is the Pond and Swamp Adjustment Factor

PMP runoff flow rates for evaluating site impounded areas were calculated using the Rational Dekalb method:

$$Q_{100} = C \times I \times A \qquad \text{Equation 2.4-4}$$

Where:

- Q_{100} is the 100-year event runoff in cubic feet per second (cfs)
- C is the Runoff coefficient
- I is the Intensity in inches/hour (in./hr)
- A is the Area, in acres

2.4.2.4 River or Stream Flooding

The PMF is calculated in Subsection 2.4.3 and corresponds to a flow of 133,000 cfs (3766 m^3/sec) on the Rock River. The main production facility ground elevation is at approximately 825 ft. (251 m) NAVD 88, which is approximately 51 ft. (15 m) above the calculated PMF shown in Table 2.4-9. The vertical separation between the PMF water level and the facility ground elevation precludes potential inundation at the site and provides sufficient margin to prevent wind generated waves from reaching the site. Inundation and wind induced waves are not a credible threat to the facility.

As discussed in Subsection 2.4.2.8, seismically induced dam failure is not a credible risk for creating flooding greater than that calculated for the PMF.

Ice jams were considered as part of the PMF. Given the substantial vertical margin between the site elevation and the PMF elevation, ice jams are not a credible threat to the facility.

2.4.2.5 Surges

The site is not adjacent to a sea coast subject to hurricanes. Consequently, surge due to probable maximum hurricane (PMH) is not a credible threat to the facility. Similarly, PMH wind and maximum windstorm-induced (non-hurricane) wave action is also not applicable to the site. Given the substantial margin that exists between the facility ground floor and the PMF elevation, surges due to wave action on the Rock River are not a credible threat.

2.4.2.6 Seiches

The site is approximately 63 mi. (101 km) from the nearest large body of water (Lake Michigan) (USGS, 1971). Consequently, meteorologically induced seiches in inland lakes, coastal harbors, and embayments are not a credible threat to the facility. The maximum seiche reported for Lake Michigan (Hughes, 1965) is approximately 2 to 4 ft. (0.6 to 1.2 m) high.

2.4.2.7 Tsunami

Tsunami hazards would theoretically originate from Lake Michigan, located approximately 63 mi. (101 km) to the east of the site. The elevation of the lake in the Kenosha area is approximately 580 ft. (177 m) (USGS, 2012b), which is approximately 245 ft. (75 m) below the ground floor elevation of the facility. While large waves may be generated in Lake Michigan, it is not a credible scenario that this wave would be greater than 245 ft. and then maintain any appreciable height over the more than 60 mi. (96 km) to the site. Therefore, the risk of tsunami is not credible, including seismic, hillslope failure, and submarine landslide generated tsunami-like waves.

2.4.2.8 Seismically Induced Dam Failures (or Breaches)

Potential dam failures affecting the site are addressed in Subsection 2.4.4. Seismic risks for the site are covered in Section 2.5. As described in Subsection 2.4.4, dam failures induced by any source (including operating basis earthquake [OBE]) will not cause flooding that would reach the ground floor elevation. Failure of dam structures coincident with runoff, surge, or seiche floods would also not reach the site elevation, even considering a 25-year flood event.

2.4.2.9 Flooding Caused by Landslides

Seismically induced flooding typically is the result of landslides (above or below water) that cause flood waves. As discussed in Section 2.5, the site is not subject to significant seismic hazards. The site is also not adjacent to a body of water subject to flooding caused by landslides. Dams upstream of the site that could be affected by landslides are addressed in Subsection 2.4.4. Dam failures induced by landslides will not cause flooding that could reach the facility ground floor elevation. Similarly, landslide-induced dam failure or overtopping would not produce runoff, surge, or seiche floods that could reach the site.

2.4.2.10 Effects of Ice Formation in Water Bodies

The large vertical separation between the PMF elevation and the ground elevation at the site is assumed to preclude the potential for impacts from ice jams at the site. Ice effects on water bodies are described in more detail in Subsection 2.4.7.

The estimation of the PMF at the site incorporates the assumed magnitude of the probable maximum flood event, which includes consideration of the occurrence of historical ice jam derived flood events along with all other historical flood events. As such, the estimated PMF flood elevation includes the maximum estimated water level from ice jam events. The PMF elevation is 51 ft. (15 m) below the facility ground floor elevation, and therefore there is not a credible scenario under which an ice jam derived flood event would impact the site.

2.4.2.11 Combined Events Criteria

The PMF (133,000 cfs [3766 m^3/sec]) is seven times greater than the 500-year flood as stated by FEMA (Table 2.4-9). This indicates that the PMF based on the NRC Regulatory Guide 3.40 and 1.59 approach considers multiple combined events with an effective probability of less than 1/500 (0.2 percent) (USNRC, 1977a; USNRC, 1977b).

Even for this extreme event, however, the river elevation would only reach 774 ft. (235 m), which is 51 ft. (15 m) below the site ground elevation of approximately 825 ft. (251 m) (Table 2.4-9).

2.4.3 PROBABLE MAXIMUM FLOOD ON STREAMS AND RIVERS

This subsection defines the probable maximum flood (PMF) that will be used to establish the design basis flood level, and determine if any structures, systems, and components require flood protection.

2.4.3.1 Probable Maximum Flood Estimates

The PMF for the site is estimated using procedures developed by the NRC in Regulatory Guides 3.40 and 1.59, and by referencing U.S. Army Corps of Engineers data (USNRC, 1977a; USNRC, 1977b; USACE, 1984). The NRC provides alternative and simplified methods for estimating PMF events to address planning studies, to provide an initial basis for understanding the order of magnitude for the PMF at a given site, for smaller scale sites, and for sites where little information is available.

The second revision to Regulatory Guide 1.59, Design Basis Floods for Nuclear Power Plants (USNRC, 1977a), was used to estimate the PMF for a given site based on the corresponding drainage area, for sites in the eastern portion of the United States. The NRC guidelines provide isolines that are enveloped PMF estimates for the eastern United States based on PMF estimates in identified river basins (with known drainage basin area, runoff, and PMF peak discharges) to estimate the PMF in a targeted basin by using Creager curves (Regulatory Guide 1.59, USNRC, 1977a). Creager curves were developed based on estimated PMF peak flows based on basin size and historical flood data from around the world. Furthermore, the NRC document includes PMF estimates for the Rock River at a location downstream of the site (Regulatory Guide 1.59, USNRC, 1977a).

The following comparisons of available PMF information were considered in the review of the PMF at the site:

- Direct-Ratio Area-Adjusted PMF
  - Uses the ratio of drainage areas at Janesville (Afton Gage), 3340 sq. mi. (8651 sq. km) to the drainage area published in Regulatory Guide 1.59 at Byron, Illinois, 8000 sq. mi. (20,720 sq. km).
- Area-Adjusted PMF for Area Downstream of Indianford Dam plus Indianford Dam Spillway Capacity
  - Uses the Creager formula to estimate the PMF of the contributing drainage area downstream of Indianford Dam by using the 'C' value estimated from the PMF at Byron, Illinois published in Regulatory Guide 1.59.
  - Assumes discharge from Indianford is the maximum spillway capacity of 8000 cfs (227 m^3/sec), as published by the WDNR (WDNR, 2012a), but does not consider the effects of dam overtopping and/or failure.
  - This method attempts to account for the impact of Lake Koshkonong.
- Area-Adjusted PMF using Creager Formula with Total Drainage Area
  - Uses the Creager formula to estimate the PMF of the total contributing drainage area at Janesville (Afton Gage) by using the 'C' value estimated from the PMF at Byron, Illinois published in Regulatory Guide 1.59.
  - This method neglects the effects of Lake Koshkonong.
- Downstream PMF at Byron, Illinois
  - Does not adjust for drainage area and uses the PMF flow for a contributing drainage area over twice the size as represented for Janesville.
  - This method is highly conservative.

Based on the NRC simplified approach for estimating the PMF, and by using only the isolines from the nomographs provided in the guidelines, the envelope for the PMF for the drainage area corresponding to the site and location would be between approximately 250,000 and 500,000 cfs (7079 and 14,158 m^3/sec) (Regulatory Guide 1.59). The NRC document also publishes the peak

flows from the NRC-accepted PMF estimates that were normalized to produce the isolines published in the document (Regulatory Guide 1.59). An estimate for the PMF of the Rock River at Byron, Illinois (located downstream of the site) is published with a peak discharge of 308,000 cfs (8721 m^3/sec) for a contributing drainage area of 8000 sq. mi. [20,719 sq. km]. Therefore, this estimate of PMF is considered more representative of the contributing basin characteristics than using the isolines. Considering that the contributing basin area to the site (i.e., 3340 sq. mi. [8650 sq. km]) is less than the contributing basin area on the Rock River at Byron, Illinois (i.e., 8000 sq. mi. [20,719 sq. km]), the PMF peak flow for the Rock River near the site should be less than the 308,000 cfs (8721 m^3/sec) estimated at Byron. The estimated PMF for the site is 133,000 cfs (3766 m^3/sec). The PMF value was calculated based on the methods as described above and as summarized in Table 2.4-9 and Table 2.4-10.

The PMF estimates, using the methods as outlined above, are provided in Table 2.4-9. Parameters used in these calculations are summarized in Table 2.4-10.

The PMF flows (Table 2.4-9) were used in a hydraulic calculation at a cross-section of the Rock River and adjacent floodplain at the USGS Afton gauging station, located adjacent the site and referenced previously in this subsection (Figure 2.4-13). The calculation estimated water surface elevations for the 100- and 500-year recurrence interval flows, as well as the established PMF flow values. The corresponding water surface elevations correlated closely to the FEMA established flood levels for the 100- and 500-year flood events.

2.4.3.2 Design Bases for Flooding in Streams and Rivers

The estimated PMF for the site corresponds to a flow of 133,000 cfs (3766 m^3/sec) on the Rock River. The PMF value was calculated based on the methods as described in Subsection 2.4.3.1 and as summarized in Tables 2.4-9 and 2.4-10. The corresponding flood elevation on the Rock River is 774 ft. (235 m), which is below the ground floor elevation of the facility. Therefore, the site is not affected by this flood. The flood design basis for the facility is discussed in Section 3.3.

2.4.4 POTENTIAL DAM FAILURES

The Rock River has two dams located upstream of the site (Table 2.4-11). The Centerway Dam is located in the city of Janesville (Figure 2.4-9) (Figure 2.4-14). The dam is not designed or operated as a flood control structure, and therefore, it has limited impoundment (FEMA, 2008). As such, the dam does not represent a potential hazard to downstream reaches of the river channel from increased release or modification to flood flow or in response to planned or unplanned operational flow.

The Indianford Dam is located approximately 25 river mi. (40 km) upstream of the site and approximately 20 river mi. (32 km) upstream of Janesville (Figure 2.4-9) (Figure 2.4-14). The Indianford Dam impounds Lake Koshkonong, which is a naturally occurring lake that has been artificially increased in level and size by the Indianford Dam, creating a lake with a surface area of about 16.3 sq. mi. (42.2 sq. km). The maximum depth of Lake Koshkonong is 7 ft. (2.1 m) (WDNR, 2012b). The contributing drainage area upstream of the lake outlet at the Indianford Dam is approximately 2560 sq. mi. (6630 sq. km), or approximately 77 percent of the contributing drainage area of the Rock River basin at the site location. The Indianford Dam is run-of-river, only increases the lake level by 5 to 6 ft. (1.5 to 1.8 m), and is tailwater controlled. The available storage capacity of the lake could be a significant mitigating factor during any flood event. As such, the size of Lake Koshkonong is expected to produce an attenuating effect on potential

floods during peak storms, while the size of the Indianford Dam is relatively small and would be backwatered (due to the tail-water control) during any peak event, again focusing any flood attenuation benefits on the lake itself.

2.4.4.1 Flood Waves from Severe Breaching of an Upstream Dam

Based on the potential dam failure discussed in Subsection 2.4.4, there is no credible scenario in which flood waves resulting from a dam breach or failure, including those due to hydrologic failure as a result of overtopping for any reason, would be routed to the site and would result in a water surface elevation that may result in flooding of safety-related structures, systems and components.

The dams upstream of the site on the Rock River are low, small and tail-water controlled, effectively mitigating the potential for causing flood waves in the event they were breached.

2.4.4.2 Domino-Type or Cascading Dam Failures

Based on the discussion in Subsection 2.4.4, there is no credible scenario in which successive failures of several dams in the path to the plant site caused by failure of an upstream dam due to plausible reasons, such as probable maximum flood, landslide-induced severe flood, earthquakes, or volcanic activity, would affect the highest water surface elevation at the site under the cascading failure conditions.

2.4.4.3 Dynamic Effects on Structures

Based on the discussion in Subsection 2.4.4, dynamic effects of dam failure-induced flood waves on safety-related structures, systems and components is not a credible scenario.

2.4.4.4 Loss of Water Supply Due to Failure of a Downstream Dam

Due to facility design, a safety-related water supply is not required. Therefore, the facility would not be influenced by failure of a downstream dam. All water for facility operation is supplied by the City of Janesville public water supply system. Therefore, low water considerations are not applicable.

2.4.4.5 Effects of Sediment Deposition and Erosion

Due to the facility design, the effects of sediment deposition or erosion during dam failure-induced flood waves that may result in blockage or loss would not influence the function of safety-related structures, systems and components.

2.4.4.6 Failure of On-site Water Control or Storage Structures

No significant levees, dikes, or engineered water storage facilities are required for this facility which could induce flooding at the site.

2.4.5 PROBABLE MAXIMUM SURGE AND SEICHE FLOODING

2.4.5.1 Probable Maximum Hurricane

The site is not adjacent to a sea coast subject to hurricanes. Consequently, surge due to probable maximum hurricane (PMH) is not a credible threat to the facility.

2.4.5.2 Seiche and Resonance

Seiche and surge flooding are related to the oscillation of the water surface in an enclosed or semi-enclosed body of water that is initiated by an external cause (USNRC, 2011). These flood hazards pertain to sites along the edge of lakes and large bodies of water. The site is not adjacent to open bodies of water or lakes. The site is 2 mi. (3.2 km) from the Rock River, and 63 mi. (101 km) from the nearest large body of water (Lake Michigan). The record high seiche on Lake Michigan occurred on June 26, 1954 (at Chicago). This wave was 2 to 4 ft. (0.6 to 1.2 m) high (Hughes, 1965), significantly less than the difference in elevation between the Rock River and the site. Thus, no hazards are expected to exist from seiche or surge flooding.

Additionally, the likelihood that a flood wave could be generated in the Rock River that is greater than the flood conditions addressed in the previous discussion of the PMF is highly unlikely. As such, and in the event that a seiche or surge or seismically induced flood event could occur, its flood characteristics would be far smaller in size and nature than what was estimated for the PMF and would not impact the site.

2.4.5.3 Wave Runup

The site is not located near a large body of open water. As such, wind-induced wave runup under PMH or probable maximum wind storm (PMWS) winds are expected to be less than those for the PMF. As such, the PMH and PMWS induced wave runup is not considered a credible hazard. The only body of water near the site is the Rock River. Even during a peak event of flooding, such as the PMF, the river is located at least 2 mi. (3.2 km) laterally away from the site and has approximately 38 to 64 ft. (12 to 20 m) of vertical separation between the PMF water level and the ground floor elevation at the site (Table 2.4-9). As such, wave runup that may originate from the PMF inundated area is not expected to pose a threat to the site.

2.4.5.4 Effects of Sediment Erosion and Deposition

Sediment erosion and deposition during storm surge and seiche-induced waves that may result in blockage or loss of function of safety-related structures, systems and components is not a credible scenario.

2.4.6 PROBABLE MAXIMUM TSUNAMI HAZARDS

This subsection provides the geohydrological design basis developed to ensure that any potential hazards to the safety-related structures, systems and components due to effects of a probable maximum tsunami are considered in the plant design.

2.4.6.1 Historical Tsunami Data

Historical tsunami data, including paleotsunami mappings and interpretations, regional records and eyewitness reports, and more recently available tide gauge and real-time bottom pressure gauge data, are not available for the site. The site has not been subjected to tsunami forces due to its inland location.

2.4.6.2 Probable Maximum Tsunami

As noted in Subsection 2.4.2.7, tsunami hazards would originate from Lake Michigan, located approximately 63 mi. (101 km) to the east of the site. While a large wave generated in Lake Michigan is possible, it is not a credible scenario that it would be greater than 230 ft. (670 m) in height and maintain any appreciable height over the more than 60 mi. (97 km) to the site. This suggests the risk of tsunami is correspondingly not credible. The probable maximum tsunami (PMT) is, therefore, not applicable to this site.

2.4.7 ICE EFFECTS

The hydrometeorological design basis is developed in this subsection to ensure that safety-related facilities and water supply are not affected by ice-induced hazards.

2.4.7.1 Historical Ice Accumulation

Historical ice accumulations (e.g., ice jams, wind-driven ice ridges, floes, frazil ice formation, etc.) on the Rock River are reported in the U.S. Army Corps of Engineers' Ice Jam Database (USACE, 2012). A total of 133 events are recorded for the Rock River.

2.4.7.2 High and Low Water Levels

The potential effects of ice-induced high or low flow levels are assumed to be addressed within the bounds of the PMF estimates provided in Subsection 2.4.3.1. Ice effects on high water levels are not considered to present a threat to the site. Ice-induced high flow levels would be less than 774.1 ft. (235 m) (Table 2.4-9). This is 51 ft. (15 m) below the site ground elevation of 825.1 ft. (251 m). The separation of 51 ft. (15 m) ensures that ice-induced high flow levels or low flow levels do not represent a credible threat to the facility.

2.4.7.3 Ice Sheet Formation

The potential of a surface ice-sheet reducing the volume of available liquid water in safety-related water reservoirs is not applicable to the facility because safety-related water requirements do not include a surface water reservoir that is exposed to the environment.

2.4.7.4 Ice-Induced Forces and Blockages

The potential for ice-produced forces on, or blockage of, safety-related facilities is minimal at the site, due to its location 2 mi. (3.2 km) from the Rock River and 63 mi. (101 km) from the nearest large body of water (Lake Michigan).

2.4.8 COOLING WATER CANALS AND RESERVOIRS

Canals and reservoirs used to transport and impound water supplied to the safety-related structures, systems and components are not included in the design of the facility.

2.4.9 CHANNEL DIVERSIONS

No river channel diversions are included in the design of the facility.

2.4.10 GROUNDWATER CONTAMINATION CONSIDERATIONS

This subsection describes groundwater conditions as they pertain to potential contamination at the site.

2.4.10.1 Contamination Effects on Local and Regional Groundwater

Water level maps (Figure 2.4-4) indicate that groundwater flow directions are NNE-SSW.

2.4.11 ACCIDENTAL RELEASES OF RADIOACTIVE LIQUID EFFLUENTS IN GROUND AND SURFACE WATERS

The hydrogeological characteristics of the site are evaluated in this subsection to support safety analyses described in Chapter 13.

2.4.11.1 Alternate Conceptual Models

Meyer et al. defined the conceptual model as "a hypothesis or interpretation about the behavior of the system to be modeled and of the connection between the components of the system" (USNRC, 2004). The site is underlain by simple alluvial and glacial geology. No alternative conceptual model is applicable.

2.4.11.2 Pathways

As discussed in Subsection 2.4.1.4, accidentally released radioactive contaminants are assumed to migrate along the following pathway:

a. Unsaturated zone
b. Saturated zone
c. Discharge at Rock River and its tributaries

In the unsaturated zone the dominant direction of contaminant migration is downward, driven by gravity and capillary forces.

Preliminary estimates can be made on advective particle travel times between the site and the potential discharge points, based on field measurements and available field information. The velocity of groundwater can be calculated by using the well-known Darcy Law (Bear, 1972):

$$q = k \times \frac{\Delta h}{\Delta l} \qquad \text{Equation 2.4-5}$$

Where:

- q is the Flux
- k is the Hydraulic conductivity Rainfall (in., 24-hour period)
- Δh is the Difference of head
- Δl is the Distance

However, water moves only through a portion of space (between the grains of the soil); therefore, q has to be divided by porosity to get water velocity:

$$v = \frac{q}{n} \qquad \text{Equation 2.4-6}$$

Where:

- n is the Porosity
- v is the Velocity

By knowing the distance between the source and the discharge point, an estimate can be made. This calculation is conservative in the following ways:

- Particles were released at the groundwater table, so the unsaturated zone had not been considered in the calculations due to the limited information available.
- The model is one-dimensional, so three-dimensional development of contaminant plume had not been modeled; pathways run straight from the site to the discharge points or areas.
- Important transport processes (adsorption, dispersion, diffusion, decay, dilution) were not involved in the calculations – only advective travel times have been estimated.
- Homogeneous, high conductivity values have been assigned to the model, no parameter heterogeneity has been considered.
- No dilution is considered along the bed of the Rock River and within the groundwater system.

Based on these assumptions, the calculation travel times and concentrations bound those that would be involved in an actual event.

A summary of parameters used for advective travel time estimations in the saturated zone is presented in Table 2.4-12. The calculations have been carried out for assumed release locations west and south to the Rock River, and to water supply wells MF461 and UJ792, identified as the nearest off-site features applicable for groundwater pathways. Using Equations 2.4-5 and 2.4-6, Table 2.4-12 provides advective groundwater travel times for two conservative cases: Expected hydraulic conductivity and porosity, and Conservative hydraulic conductivity and porosity. 30 percent effective transport porosity is used for the Expected cases. Typical 20 percent porosity in Rock County, WI, stated by Gaffield et al. (Gaffield et al., 2002) is not consistent with site-specific soil conditions described in Subsection 2.5.2.3. Yu C., et al., Data Collection Handbook to Support Modeling Impacts of Radioactive Material in Soil (USDOE, 1993), provided arithmetic mean effective porosity values of 30 percent, 32 percent, and 33 percent for coarse, medium, and fine sand, respectively, which are more typical of the subsurface conditions at the site; therefore, 30 percent porosity is used to calculate expected advective travel times. The conservative cases utilize a 10 percent porosity value. Note that all cases use very conservative

assumptions. The river release location uses channel base, and well assumes the maximum reported drawdown.

Bounding estimates for travel time through the unsaturated zone, or vadose zone, were determined based on the estimated travel distance (thickness) of the vadose zone and the estimated velocity of groundwater travel through the vadose zone. For vertical flow, the travel distance is calculated as the thickness of the vadose zone. The thickness of the vadose zone can be estimated as the difference between the surface and water elevations in boreholes drilled at the site, provided in Table 2.4-1. Estimates of vadose zone thickness are provided in Table 2.4-13. A reasonable representative vadose zone thickness for travel time calculations can be taken as the minimum measured vadose zone thickness of 50 ft. As described in Subsection 2.4.1.4, water table fluctuation at the site can be estimated to be two feet. A lower bound vadose zone thickness was estimated as the minimum measured vadose zone thickness (50 ft.) minus three times the estimated water table fluctuation (two feet), or 44 ft. An upper bound vadose zone thickness was estimated as the maximum measured thickness (65 ft.) plus three times the estimated water table fluctuation (two feet), or 71 ft. As described above, the velocity of groundwater can be calculated using Darcy's Law. The effective hydraulic conductivity for vadose zone transport was derived by applying a characteristic curve to the measured hydraulic conductivity values provided in Table 2.4-12 to adjust for the effect of water saturation. An effective gradient of 100 percent for vadose zone transport was assumed. Bounding estimates for travel time through the vadose zone are provided in Table 2.4-14.

There are four test wells within the property boundary for the facility which were used for monitoring groundwater in support of the initial hydrological assessment of the site. During the site selection characterization, some preliminary analysis of advective travel times in groundwater were performed, as described in Subsection 2.4.11.2 and Table 2.4-12.

Liquid effluent is not routinely discharged from the RCA. Liquid radioactive wastes generated at the facility are generally solidified and shipped to a disposal facility. Radioactive liquid discharges from the SHINE facility to the sanitary sewer are infrequent and made in accordance with 10 CFR 20.2003 and 10 CFR 20.2007. There are no piped liquid effluent pathways from the RCA to the sanitary sewer. Sampling is used to determine suitability for release. Ramps at the entrances to the RCA limit the release of unplanned water discharges in the RCA, such as from a cooling water system rupture or firefighting hose discharge. Therefore, accident radioactive releases from the facility are limited to releases via the airborne pathway.

There are no accidental radioactive liquid discharges from the RCA. Groundwater monitoring is conducted by the radiological environmental monitoring program at test wells south and west of the site (see Subsection 11.1.7).

2.4.11.3 Characteristics that Affect Transport

In transport calculations, the following processes are considered:

- Advective transport
- Dispersion
- Dilution
- Sorption
- Decay
- Diffusion

Estimates of advective travel times are presented in Table 2.4-12. Since the hydraulic gradient does not vary significantly based on a one-year monitoring data set (Figure 2.4-5), it can be assumed that advective travel times at the site will not change significantly with water level fluctuation.

Field characteristics or targeted measurements on dispersion are not available. Based on the literature the longitudinal dispersivity and transversal dispersivity can be assumed to be 10 percent and 1 percent of the model dimension, respectively (Kinzelbach, 1986). Although the correlation between the model extension and longitudinal dispersivity is not linear, the above ratios are frequently used in hydrogeological models. Assuming about 10,000 ft. (3048 m) between source and sink, the longitudinal and transversal dispersivity are 1000 and 100 ft. (305 and 30 m). Note that the rate of dispersion depends also on the variations in groundwater velocity; a variation in hydraulic gradient (seasonal, climatic), hydraulic conductivity (heterogeneity, grain size, etc.) or porosity (gradation, heterogeneity, grain size, etc.). Two types of dilution must be considered at the site: dilution in the groundwater, and dilution in the Rock River and other discharge points. It is important to note that dilution is highly dependent on the water balance. Increased precipitation may result in temporarily intensified flow either below the ground or on the ground.

Table 2.4-1 – Water Table in the Boreholes Drilled at the Site[a]

Borehole Number	Surface Elevation (ft.)	Surface Elevation (m)	Water Elevation (ft.)	Water Elevation (m)
G11-01	818.90	249.60	753.9	229.8
G11-02	822.09	250.57	763.6	232.8
G11-03	824.69	251.37	765.7	233.4
G11-04	821.65	250.44	763.2	232.6
G11-05	824.33	251.37	(b)	(b)
G11-06	825.65	251.66	(b)	(b)
G11-07	826.13	251.80	761.2	232.0
G11-08	824.52	251.31	765.5	233.3
G11-09	824.77	251.39	(b)	(b)
G11-10	825.96	251.75	761.0	232.0
SM-GW 1A	825.56	251.63	763.6	232.8
SM-GW 2A	819.01	249.63	762.0	232.3
SM-GW 3A	827.09	252.10	764.6	233.1
SM-GW 4A	811.50	247.35	761.5	232.1

a) Elevations are in NAVD 88.
b) Measurements are obscured by drilling fluids.

Table 2.4-2 – Monitoring Results in SM-GW-1A, SM-GW-2A, SM-GW-3A and SM-GW-4A Wells

Collection date	SM-GW-1A elevation ft. (m)	SM-GW-2A elevation in ft. (m)	SM-GW-3A elevation in ft. (m)	SM-GW-4A elevation in ft. (m)	Hydraulic gradient E-W	Hydraulic gradient N-S
10/26/2011	765.50 (233.32)	764.20 (232.93)	765.22 (233.24)	764.42 (233.00)	0.05%	0.08%
11/16/2011	765.38 (233.29)	764.09 (232.89)	765.09 (233.20)	764.32 (232.96)	0.05%	0.08%
12/13/2011	765.24 (233.25)	764.00 (232.87)	764.97 (233.16)	764.18 (232.92)	0.05%	0.08%
1/9/2012	765.16 (233.22)	763.91 (232.84)	764.88 (233.14)	764.80 (233.11)	0.05%	0.08%
2/13/2012	764.96 (233.16)	763.74 (232.79)	(msmt. unreliable)	763.90 (232.84)	N/A	0.08%
3/12/2012	764.85 (233.13)	763.63 (232.75)	764.59 (233.05)	763.80 (232.81)	0.05%	0.08%
4/16/2012	764.71 (233.08)	763.51 (232.72)	764.42 (233.00)	763.66 (232.76)	0.05%	0.08%
5/22/2012	764.43 (233.00)	763.28 (232.65)	764.12 (232.90)	763.51 (232.72)	0.04%	0.07%
6/12/2012	764.20 (232.93)	763.02 (232.57)	763.84 (232.82)	763.07 (232.58)	0.05%	0.07%
7/16/2012	763.52 (232.72)	762.25 (232.33)	762.97 (232.55)	762.64 (232.45)	0.02%	0.08%
8/15/2012	763.30 (232.65)	762.00 (232.26)	762.90 (232.53)	762.31 (232.35)	0.04%	0.08%
9/18/2012	763.01 (232.57)	761.74 (232.18)	762.62 (232.45)	762.04 (232.27)	0.04%	0.08%

Table 2.4-3 – Summary of Slug Tests for Monitoring Wells SM-GW-1A, SM-GW-2A, and SM-GW-3A

Well	Test	Test Head[a] Ho (ft.)	Initial Head[b] H (ft.)	Well Coordinate[c] Easting (ft.)	Well Coordinate[c] Northing (ft.)	Aquifer Thickness[c],[d] (ft.)	Depth to top of well screen[c] (ft.)	Length of well screen[e] (ft.)	Transducer Depth (ft.)
GW-1A	Slug In #1	7.540	7.110	W 492655.35	N 248568.86	100+	50	20 (6.94)	69
GW-1A	Slug Out #1	6.866	7.110	W 492655.35	N 248568.86	100+	50	20 (6.94)	69
GW-1A	Slug In #2	7.610	7.110	W 492655.35	N 248568.86	100+	50	20 (6.94)	69
GW-1A	Slug Out #2	6.857	7.110	W 492655.35	N 248568.86	100+	50	20 (6.94)	69
GW-2A	Slug In #1	6.539	5.695	W 492635.32	N 246973.23	100+	50	15 (8.51)	66
GW-2A	Slug Out #1	5.284	5.695	W 492635.32	N 246973.23	100+	50	15 (8.51)	66
GW-2A	Slug In #2	6.467	5.695	W 492635.32	N 246973.23	100+	50	15 (8.51)	66
GW-2A	Slug Out #2	5.151	5.695	W 492635.32	N 246973.23	100+	50	15 (8.51)	66
GW-2A	Slug In #3	6.662	5.695	W 492635.32	N 246973.23	100+	50	15 (8.51)	66
GW-2A	Slug Out #3	5.335	5.695	W 492635.32	N 246973.23	100+	50	15 (8.51)	66
GW-3A	Slug In #1	5.843	5.346	W 493372.93	N 247753.86	100+	55	15 (5.50)	70
GW-3A	Slug Out #1	5.108	5.346	W 493372.93	N 247753.86	100+	55	15 (5.50)	70
GW-3A	Slug In #2	6.188	5.346	W 493372.93	N 247753.86	100+	55	15 (5.50)	70
GW-3A	Slug Out #2	5.092	5.346	W 493372.93	N 247753.86	100+	55	15 (5.50)	70

a) Head measured in Troll data logger during test conducted on 12/22/11. “Test head Ho” is the disturbed head due to slug insertion or removal.
b) Head measured in Troll data logger during slug test conducted on 12/22/11. “Initial Head H” is the head before testing, and also depth from the phreatic surface to piezometer.
c) Well coordinates, aquifer thickness, depth to top of well screen and length of well screen were determined from well completion records.
d) Total thickness of aquifer is expected to be over 100 ft. (30 m), including aquifer below bottom of well.
e) Length of well screen: Total Length (Saturated Length).

Table 2.4-4 – Permeabilities Evaluated from Bouwer and Rice (1976) Method, AQTESOLV, and the Average, Standard Deviation of the Results for All of the Tests and Slug-in, Slug-out Tests

Borehole	Test Number	Test Type	k (ft/sec)	k (m/sec)
GW-1A	1	In	0.0029	.0009
GW-1A	1	Out	0.0037	.0011
GW-1A	2	In	0.0037	.0011
GW-1A	2	Out	0.0027	.0008
GW-2A	1	In	0.0078	.0024
GW-2A	1	Out	0.0034	.0010
GW-2A	2	In	0.0041	.0012
GW-2A	2	Out	0.0030	.0009
GW-2A	3	In	0.0038	.0012
GW-2A	3	Out	0.0020	.0006
GW-3A	1	In	0.0053	.0016
GW-3A	1	Out	0.0081	.0025
GW-3A	2	In	0.0083	.0025
GW-3A	2	Out	0.0043	.0013
Average		In	0.0051	.0016
Standard Deviation		In	0.0021	.0001
Average		Out	0.0039	.0012
Standard Deviation		Out	0.0020	.0006
Average			0.0045	.0014
Standard Deviation			0.0021	.0006
Median			0.0037	.0011

Table 2.4-5 – Summary of FEMA Flood Information for the Rock River

R[(a)]	P[(b)]	Peak Discharge in (cfs [m^3/sec])	Bottom of Channel in (ft. [m])	Water Surface Elevation in from Janesville to Afton, Respectively[(c)] (ft. [m])
10	0.10	10,900 (308.7)	Approx. 738 to 748 (224.9 to 228.0)	Approx. 758.5 to 752 (231.2 to 229.2)
50	0.02	14,500 (410.6)		Approx. 760 to 754 (231.6 to 229.8)
100	0.01	16,000 (453.1)		Approx. 761 to 755 (232.0 to 231.1)
500	0.002	19,000 (538)		Approx. 762 to 756 (232.3 to 230.4)

a) R = Recurrence interval.
b) P = Annual probability.
c) Elevations are approximate, in NAVD 88. Channel bottom elevations are based on FEMA (2008). Results reported for the reach from Janesville to Afton near the USGS gauge.

Table 2.4-6 – Summary of FEMA Flood Information for the Unnamed Tributary to the Rock River

R[(a)]	P[(b)]	Peak Discharge in (cfs [m^3/sec])	Bottom of Channel (ft. [m])	Water Surface Elevation from Highway 51 to Prairie Road[(c)] (ft. [m])
10	0.10	2,255 (63.9)	Approx. 753 to 770 (229.5 to 234.7)	Approx. 758.5 to 774.5 (231.1 to 236.0)
50	0.02	3,473 (98.3)		Approx. 759.5 to 775.5 (231.4 to 236.3)
100	0.01	4,205 (119.1)		Approx. 760 to 776 (231.6 to 233.5)
500	0.002	5,813 (164.6)		Approx. 761 to 777 (232.0 to 236.8)

a) R = Recurrence interval.
b) P = Annual probability.
c) Elevations are approximate, in NAVD 88. Channel bottom elevations are based on FEMA (2008).

Table 2.4-7 – 100-Year PMP Values and Intensities at the SHINE Site[(a)]

PMP Duration (minutes)	5	15	30	60	120	180	360	720	1440
PMP Value (inches)	0.67	1.5	2.25	3	3.8	4.5	4.8	5.4	6
PMP intensity (inches/hr)	8	6	4.5	3	1.9	1.5	0.8	0.45	0.25

a) The values presented in this table are used for determination of water levels at the safety-related structure resulting from the local PMP.

Reference: Figure 2.4-11, PMP Rainfall Intensity-Duration-Frequency Curve.

Table 2.4-8 – Design Precipitation 24-Hour Storm Accumulations

Return Interval	Precipitation Accumulation (in.)	Precipitation Accumulation (centimeters)
2-Year	2.9	7.4
10-Year	4.1	10.4
100-Year	6.0	15.2

Reference: Rock County, 2004

Table 2.4-9 – Summary of PMF Estimates for the SHINE Site[a]

Event	Source	Flow in cfs (m^3/sec)	River Elevation ft. (m)	
			FEMA[b]	Golder[b]
100-year	FEMA 2008	16,000 (453)	761 (232)	760.6 (231.8)
500-year	FEMA 2008	19,000 (538)	762 (232)	761.3 (232.0)
Direct-Ratio Area-Adjusted PMF	Regulatory Guide 1.59	129,000 (3,653)	--	774.0 (235.9)
Area-Adjusted PMF for Area Downstream of Indianford Dam plus Indianford Dam Spillway Capacity	Regulatory Guide 1.59/ WDNR, 2012b	133,000 (3,766)	--	774.3 (236.0)
Area-Adjusted PMF using Creager Formula with Total Drainage Area	Regulatory Guide 1.59	227,000 (6,427)	--	782.4 (238.5)
Downstream PMF at Byron	Regulatory Guide 1.59	308,000 (8,721)	--	786.7 (239.8)

a) The elevation of the facility site is approximately 825 ft. (251 m). Assuming a PMF peak flow of about 130,000 cfs, over approximately 38-64 ft. (1-20m) of freeboard is available at the site location.
b) Elevation data are in NAVD 88.

Table 2.4-10 – Parameters for PMF Calculations

Parameter	Value	Units	Basis
Drainage Area at Janesville (Afton Gauge)	3,340 (8,650)	sq. mi. (sq. km)	FEMA, 2008
Drainage Area at Byron	8,000 (20,720)	sq. mi. (sq. km)	USNRC, 1977b
Drainage Area at Indianford Dam	2,560 (6,630)	sq. mi. (sq. km)	FEMA, 2008
Drainage Area at Indianford Dam (downstream)	780 (2,020)	sq. mi. (sq. km)	FEMA, 2008
PMF at Byron	308,000 (8,721)	cfs (m^3/sec)	USNRC, 1977b
C-Max for Craeger Formula	36.4	-	Back calculated from PMF at Byron
Craeger Formula and PMF Equations			USNRC, 1977b

Table 2.4-11 – Dams Near the SHINE Site

Dam No.	Name	Ref No.	Owner	(Lat/Long)	Hydraulic height (ft. [m])	Structure height (ft. [m])	Impoundment Area (ac. [ha])	Normal Storage Vol (ac-ft)	Max. Storage Col (ac-ft)	Upstream Drainage Area (sq. mi [sq. km])	Discharge Through Primary Spillway (cfsm^3/sec])	Total Discharge Through All Spillways (cfs [m^3/sec])	Date of Last Inspection	Crest Length (ft. [m])	Primary Spillway Width (ft. [m])	WI State Hazard Classification[a]
1	Indian Ford	60 8	Rock Koshkonong Statutory Lake District	- 89.089076, 42.803356	6 (1.8)	13 (4.0)	10460[b] (4,233)	53,000 [b]	107,000 [b]	2,597 (6,718)	8,000 (226)	8,000 (226)	3-May-11	500 (152)	277 (84)	LOW
2	Centerway	73 3	North American Hydro Utility Company	- 89.026121, 42.684865	9 (2.7)	14 (4.3)	800 (323)	1,900	6,000	3,235 (9,379)	12,150 (344)	12,150 (344)	9-Oct-09	325 (99)	273 (83)	LOW

a) Definitions of dam hazards: "High Hazard Dams" mean a large dam the failure of which would probably cause loss of human life. "Low Hazard Dam" means a large dam the failure of which would probably not cause significant property damage or loss of human life.
b) Controls the outlet from Lake Koshkonong, which is essentially the impoundment for the dam.

Reference: WDNR, 2012a.

Table 2.4-12 – Summary of Parameters Used for Advective Travel Time Estimations (Sheet 1 of 2)

Model Version	Permeability and Porosity Assumptions	Coordinates for Source at SHINE Facility[a]		Coordinates of Assumed Release Location[b]		Distance (ft. [m])	Head at Assumed Source[c] (ft. [m]) NAVD-88)	Head at Assumed Release Location[d] (ft. [m]) NAVD-88)	Effective Transport Porosity[e] (%)	Hydraulic Conductivity[f] (ft./sec [m/s])	Adjective Travel Time[g] (yrs)
		Easting[h] (ft.)	Northing[h] (ft.)	Easting[h] (ft.)	Northing[h] (ft.)						
Pathway to Rock River (West)	Expected	2,230,850.4	229,066.1	2,219,924.1	228,944.5	10,927 (3,331)	766 (233.5)	738 (224.9)	30	0.0045 (0.0014)	9.0
Pathway to Rock River (West)	Conservative	2,230,850.4	229,066.1	2,219,924.1	228,944.5	10,927 (3,331)	766 (233.5)	738 (224.9)	10	0.0083 (0.0025)	1.6
Pathway to Rock River Tributary (South)	Expected	2,230,850.4	229,066.1	2,230,990.7	216,461.9	12,605 (3,842)	766 (233.5)	753 (229.5)	30	0.0045 (0.0014)	26
Pathway to Rock River Tributary (South)	Conservative	2,230,850.4	229,066.1	2,230,990.7	216,461.9	12,605 (3,842)	766 (233.5)	753 (229.5)	10	0.0083 (0.0025)	4.7
Pathway to Nearest Well “Receptor” (MF461)	Expected	2,230,850.4	229,066.1	2,228,697.7	230,882.0	2,816 (858)	766 (233.5)	754 (229.8)	30	0.0045 (0.0014)	1.4
Pathway to Nearest Well “Receptor” (MF461)	Conservative	2,230,850.4	229,066.1	2,228,697.7	230,882.0	2,816 (858)	766 (233.5)	754 (229.8)	10	0.0083 (0.0025)	0.3
Pathway to Low Head DNR Well “Receptor” (UJ792)	Expected	2,230,850.4	229,066.1	2,229,329.0	227,819.4	1,967 (600)	766 (233.5)	660 (201)	30	0.0045 (0.0014)	0.1
Pathway to Low Head DNR Well “Receptor” (UJ792)	Conservative	2,230,850.4	229,066.1	2,229,329.0	227,819.4	1,967 (600)	766 (233.5)	660 (201)	10	0.0083 (0.0025)	0.01

Table 2.4-12 – Summary of Parameters Used for Advective Travel Time Estimations (Sheet 2 of 2)

Model Version	Permeability and Porosity Assumptions	Coordinates for Source at SHINE Facility[a]		Coordinates of Assumed Release Location[b]		Distance (ft. [m])	Head at Assumed Source[c] (ft. [m]) NAVD-88)	Head at Assumed Release Location[d] (ft. [m]) NAVD-88)	Effective Transport Porosity[e] (%)	Hydraulic Conductivity[f] (ft./sec [m/s])	Adjective Travel Time[g] (yrs)
		Easting[h] (ft.)	Northing[h] (ft.)	Easting[h] (ft.)	Northing[h] (ft.)						
Pathway to Nearest Pre-1988 Well "Receptor" (RO3284)	Expected	2,230,338.0	228,321.4	2,229,329.0	227,819.4	1,127 (343)	766 (233.5)	761 (232.0)	30	0.0045	0.5
Pathway to Nearest Pre-1988 Well "Receptor" (RO3284)	Conservative	2,230,338.0	228,321.4	2,229,329.0	227,819.4	1,127 (343)	766 (233.5)	761 (232.0)	10	0.0083	0.1

a) SHINE source coordinate calculated as center of site.
b) Release coordinates for Rock River (West) and South) are calculated assuming a straight line from the SHINE facility.
c) Head at SHINE facility based on maximum head measured during monitoring period (Figure 2.4-5).
d) Head at Rock River (West) and Rock River Tributary (South) release locations based on channel bottom (Tables 2.4-1 and 2.4-2). Head at Well MF461 calculated based on minimum head reported in WDNR, 2012b.
e) Low (Conservative) transport porosity value from Gaffield et al, 2002. High (Expected) transport velocity from US DOE, April 1993, Table 3.2 (see Subsection 2.4.11.2).
f) Hydraulic conductivity based on the average hydraulic conductivity from slug tests (Table 2.4-4). Conservative case is highest hydraulic conductivity from slug tests. Note that arithmetic average hydraulic conductivity is more conservative than geometric mean hydraulic conductivity.
g) Advective travel time calculated from Darcy's Law (Bear, 1972).
h. WI State Plane South Zone NAD83 (HARN)

Table 2.4-13 – Thickness of Vadose Zone

Borehole Number	Surface Elevation[(a)] (ft.)	Water Elevation[(a)] (ft.)	Thickness of Vadose Zone (ft.)
G11-01	818.90	753.9	65.00
G11-02	822.09	763.6	58.49
G11-03	824.69	765.7	58.99
G11-04	821.65	763.2	58.45
G11-05	824.33	(b)	(b)
G11-06	825.65	(b)	(b)
G11-07	826.13	761.2	64.93
G11-08	824.52	765.5	59.02
G11-09	824.77	(b)	(b)
G11-10	825.96	761.0	64.96
SM-GW 1A	825.56	763.6	61.96
SM-GW 2A	819.01	762.0	57.01
SM-GW 3A	827.09	764.6	62.49
SM-GW 4A	811.50	761.5	50.00
Maximum Thickness of Vadose Zone			**65.00**
Minimum Thickness of Vadose Zone			**50.00**
Average Thickness of Vadose Zone			**60.12**

a) Elevations are NAVD 88.
b) Measurements obscured by drilling fluids.

Table 2.4-14 – Vadose Zone Advective Travel Time

Vadose Zone Thickness ft.	Assumption	Soil Hydraulic Conductivity[a] ft./s (m/s)	Unsaturated Water Content[b] (%)	Relative Permeability (%)	Effective Transport Porosity[c] (%)	Gradient (%)	Advective Travel Time (years)
44	Upper Bound [Less Conservative]	0.002	20%	1%	40%	100%	2.8E-2
44	Expected [Mean]	0.0045	40%	10%	30%	100%	9.3E-4
44	Lower Bound [More Conservative]	0.0083	70%	40%	10%	100%	4.2E-5
50	Upper Bound [Less Conservative]	0.002	20%	1%	40%	100%	3.2E-2
50	Expected [Mean]	0.0045	40%	10%	30%	100%	1.1E-3
50	Lower Bound [More Conservative]	0.0083	70%	40%	10%	100%	4.8E-5
71	Upper Bound [Less Conservative]	0.002	20%	1%	40%	100%	4.5E-2
71	Expected [Mean]	0.0045	40%	10%	30%	100%	1.5E-3
71	Lower Bound [More Conservative]	0.0083	70%	40%	10%	100%	6.8E-5

a) Expected and lower bound values are based on the values from Table 2.4-13. The upper bound value was approximated as 50% of the mean value.
b) Estimated from values reported in Domenico and Schwartz (1997).
c) Expected and lower bound values are based on values provided in Table 2.4-13. The upper bound value was estimated based on maximum values anticipated for sandy soils.

Figure 2.4-1 – SHINE Site in Relation to Rock River

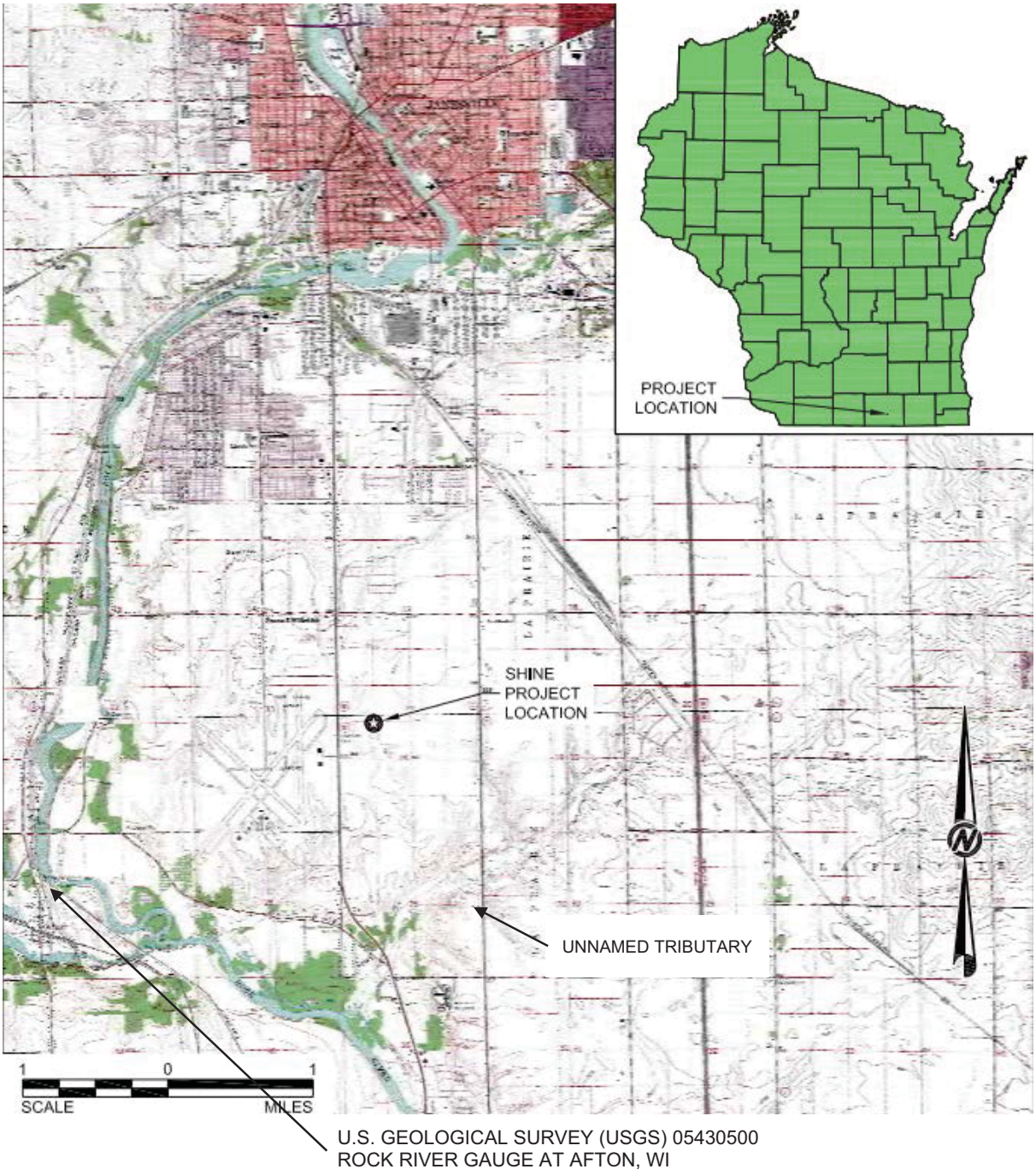

Figure 2.4-2 – Schematic of the Flow System in Rock County

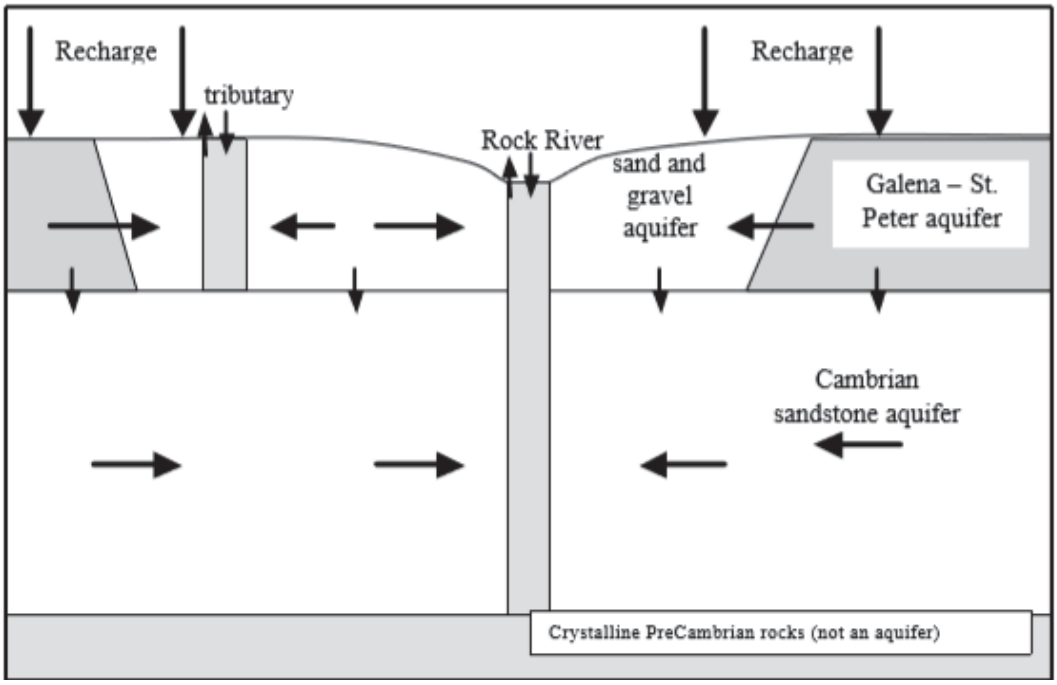

NOTES

1) Arrows indicate the potential flow directions
2) Arrow size indicates the relative magnitude of flow

Gaffield, et. al., 2002

Figure 2.4-3 – SHINE Site Groundwater Monitoring Wells

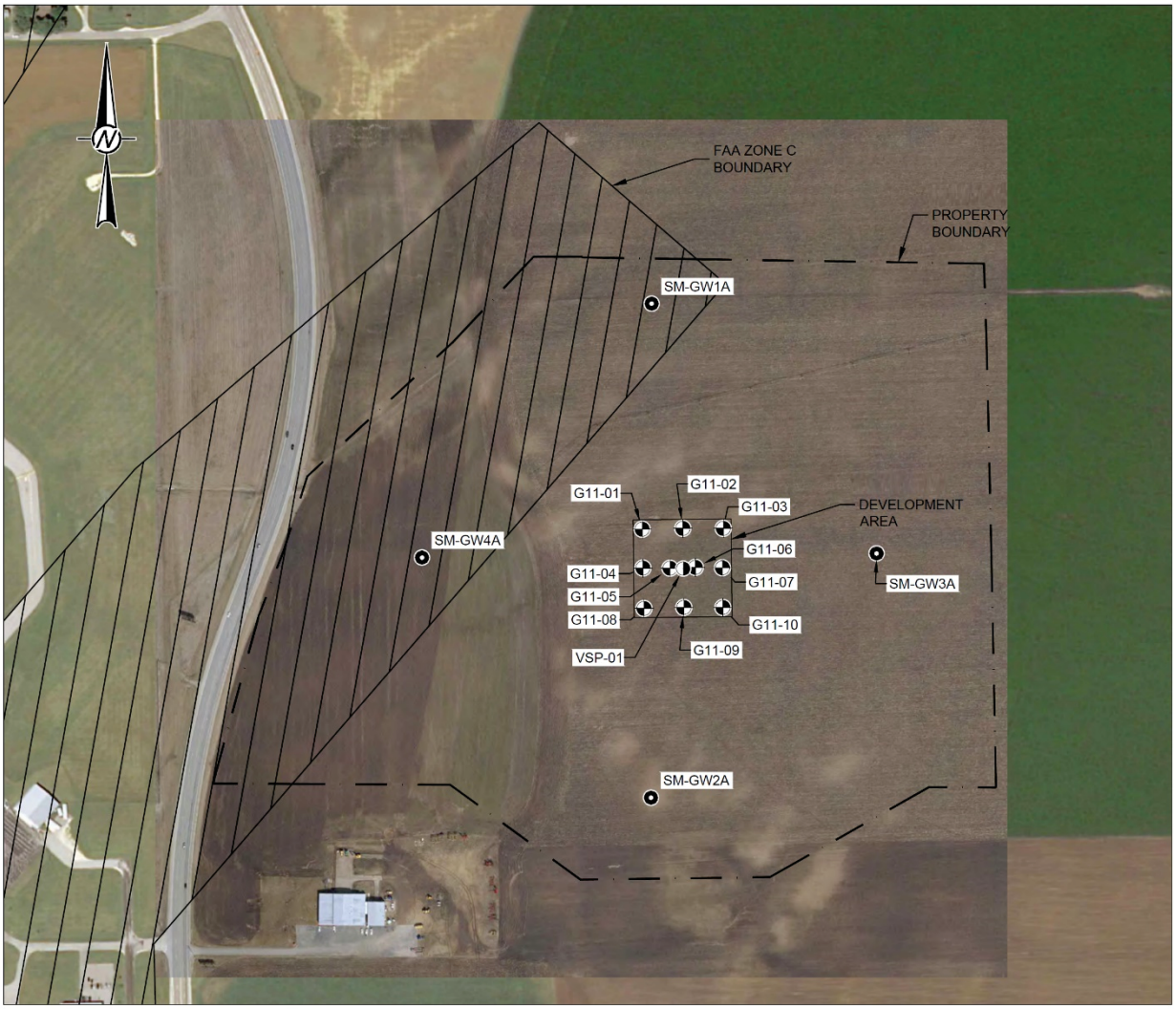

Notes

1.) Borehole and well locations as surveyed by Ayers Associates on November 11, 2011.

Figure 2.4-4 – Simplified Groundwater Table Contours Based on Measured Groundwater Elevations in Monitoring Wells

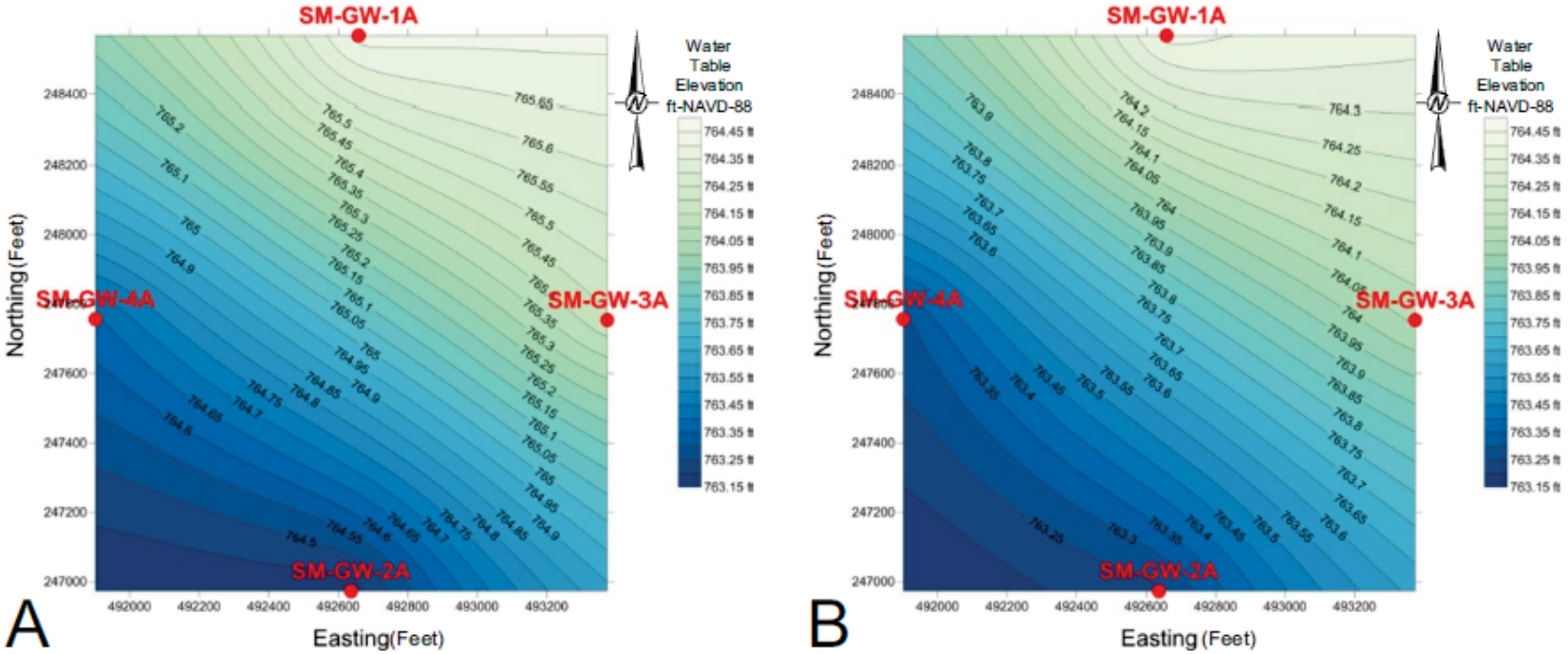

NOTES

1.) PLOT A BASED ON MEASUREMENTS FROM 10/26/2011.
2.) PLOT B BASED ON MEASUREMENTS FROM 06/12/2012.
3.) MAPS ARE JUST FOR VISUALIZATION PURPOSES. MAPS HAVE BEEN GENERATED BY SURFER DEFAULT PARAMETERS OF KRIGING

Figure 2.4-5 – SHINE Site Monitored Hydraulic Gradients

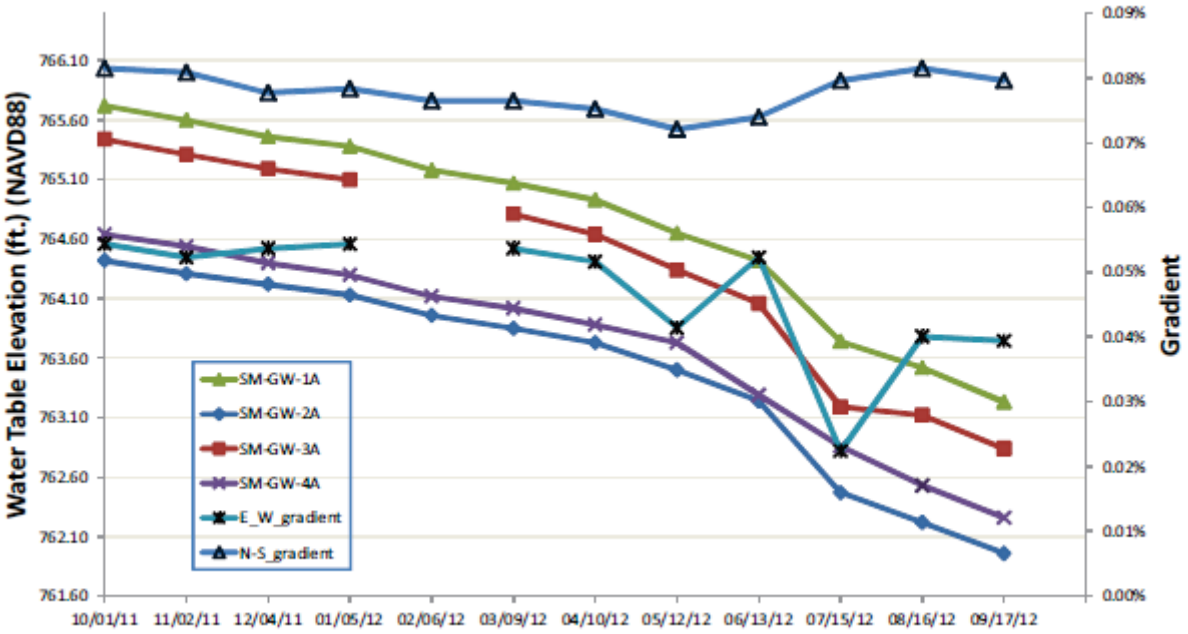

Figure 2.4-6 – Piezometric Water Table Surface from 1958

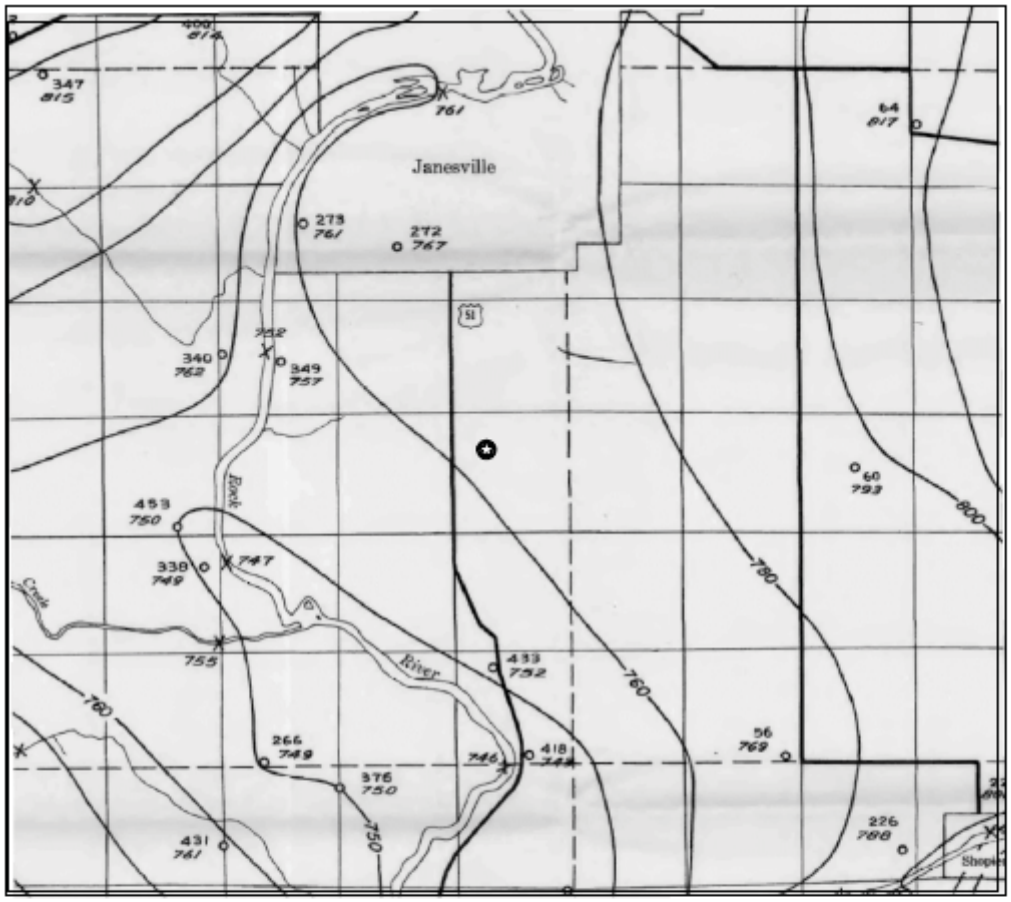

LEGEND

SHINE SITE

REFERENCE

1.) LEROUX, 1963.

Figure 2.4-7 – Groundwater Elevation Contours (Static State)

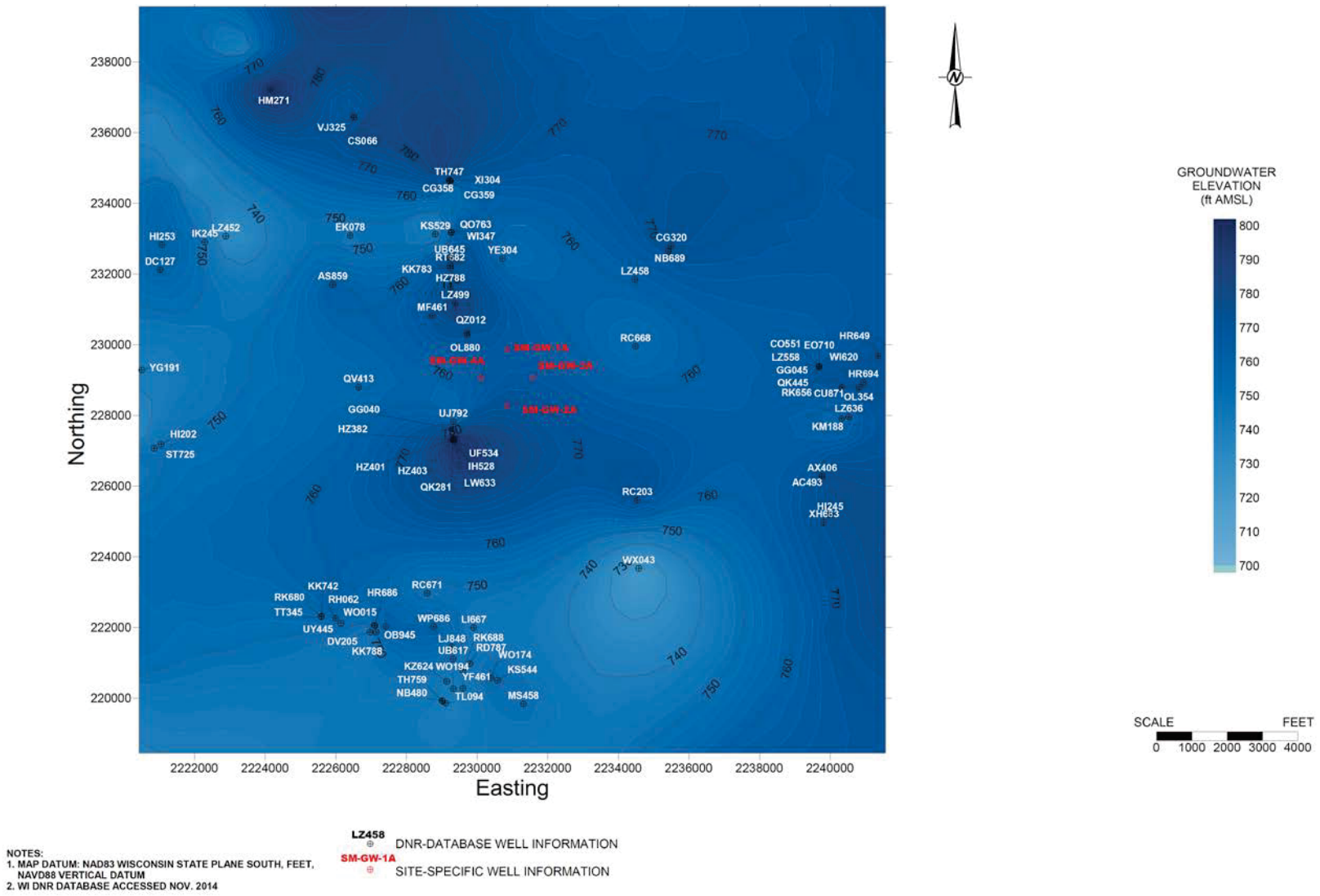

Figure 2.4-8 – Groundwater Elevation Contours (Pumping State)

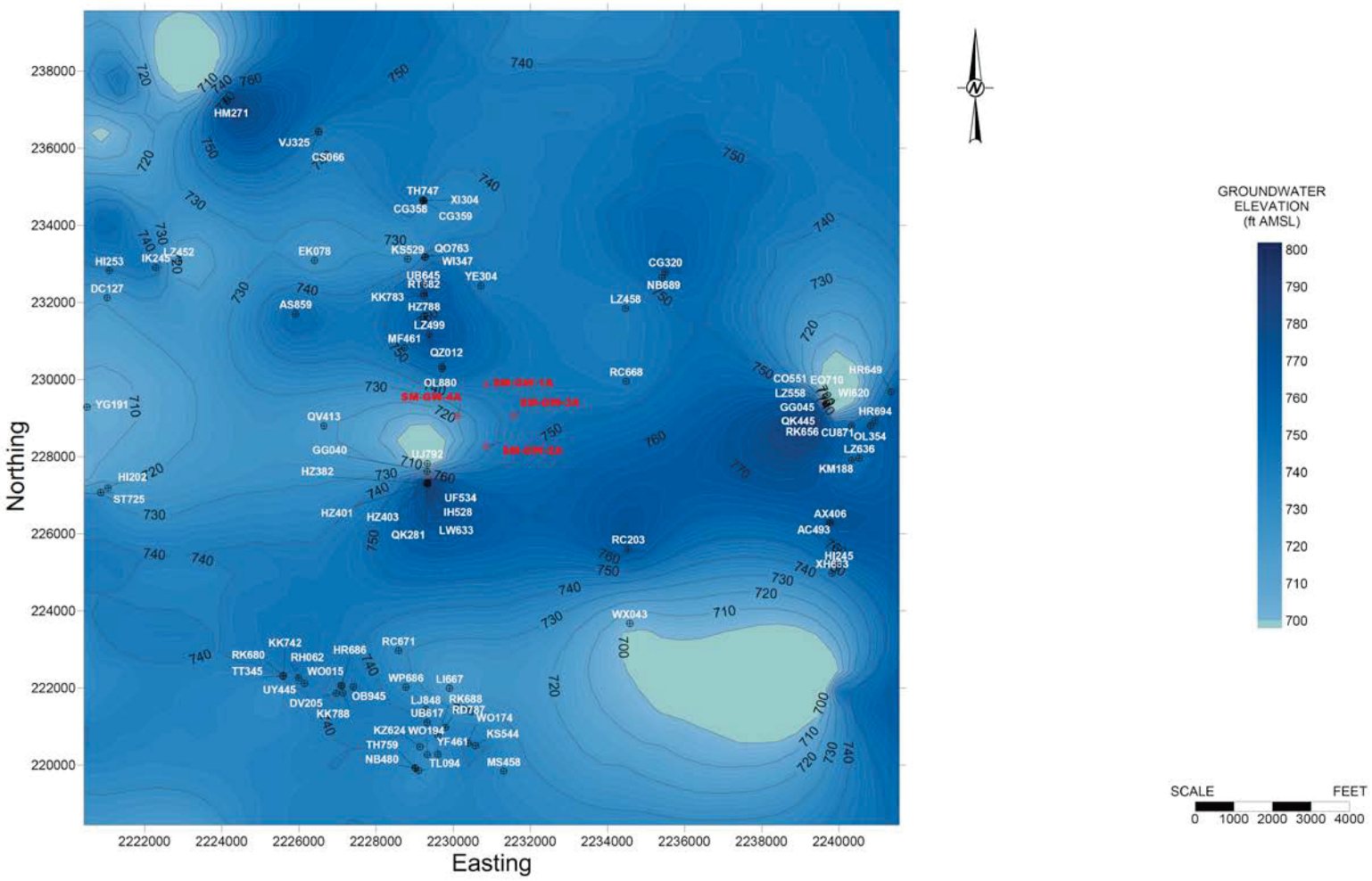

NOTES:
1. MAP DATUM: NAD83 WISCONSIN STATE PLANE SOUTH, FEET, NAVD88 VERTICAL DATUM
2. WI DNR DATABASE ACCESSED NOV. 2014

LZ458 DNR-DATABASE WELL INFORMATION

SM-GW-1A SITE-SPECIFIC WELL INFORMATION

Figure 2.4-9 – SHINE Site Vicinity Hydraulic Features

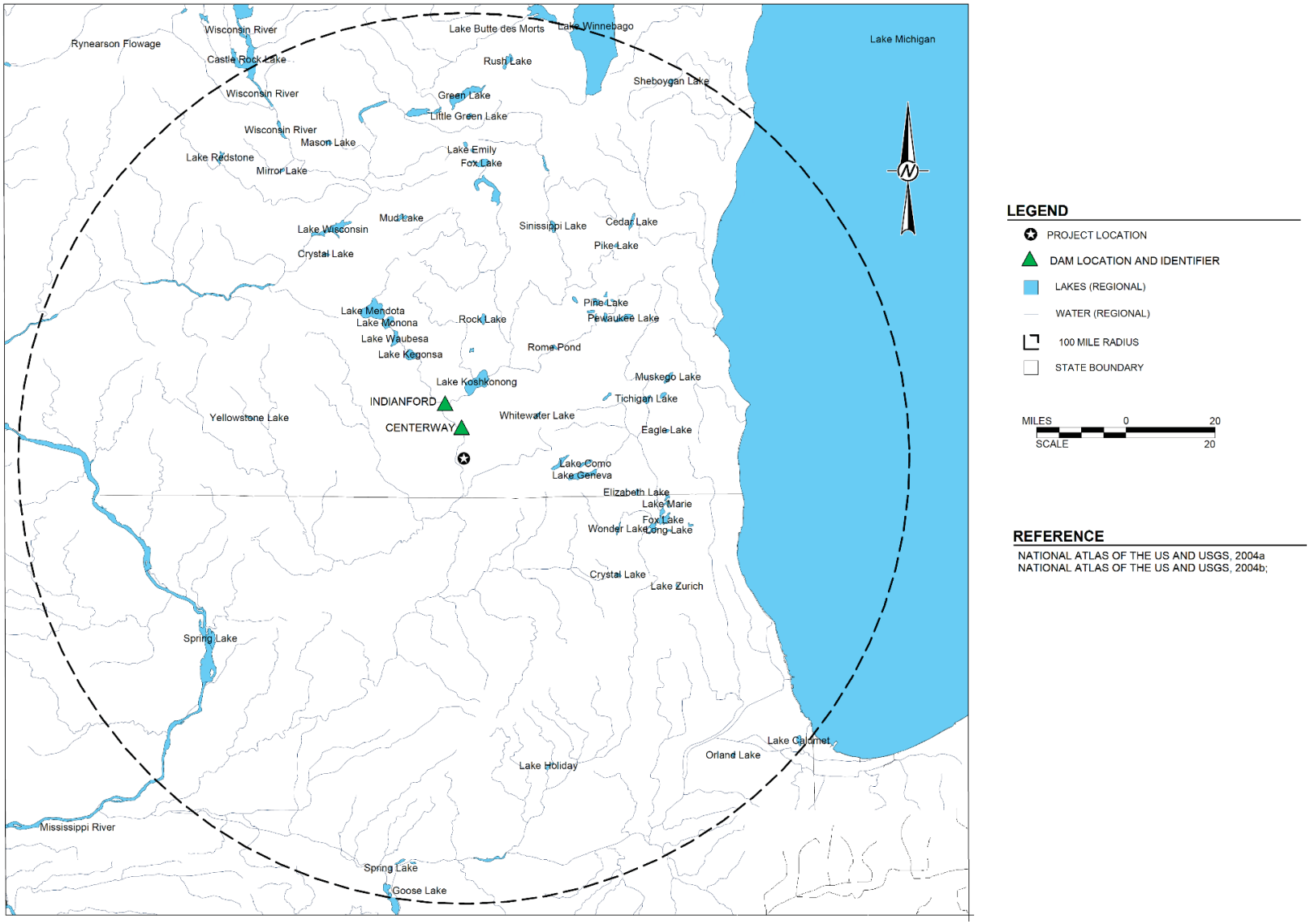

Figure 2.4-10 – PMP Rainfall Intensity - Duration - Frequency Curve[(a)]

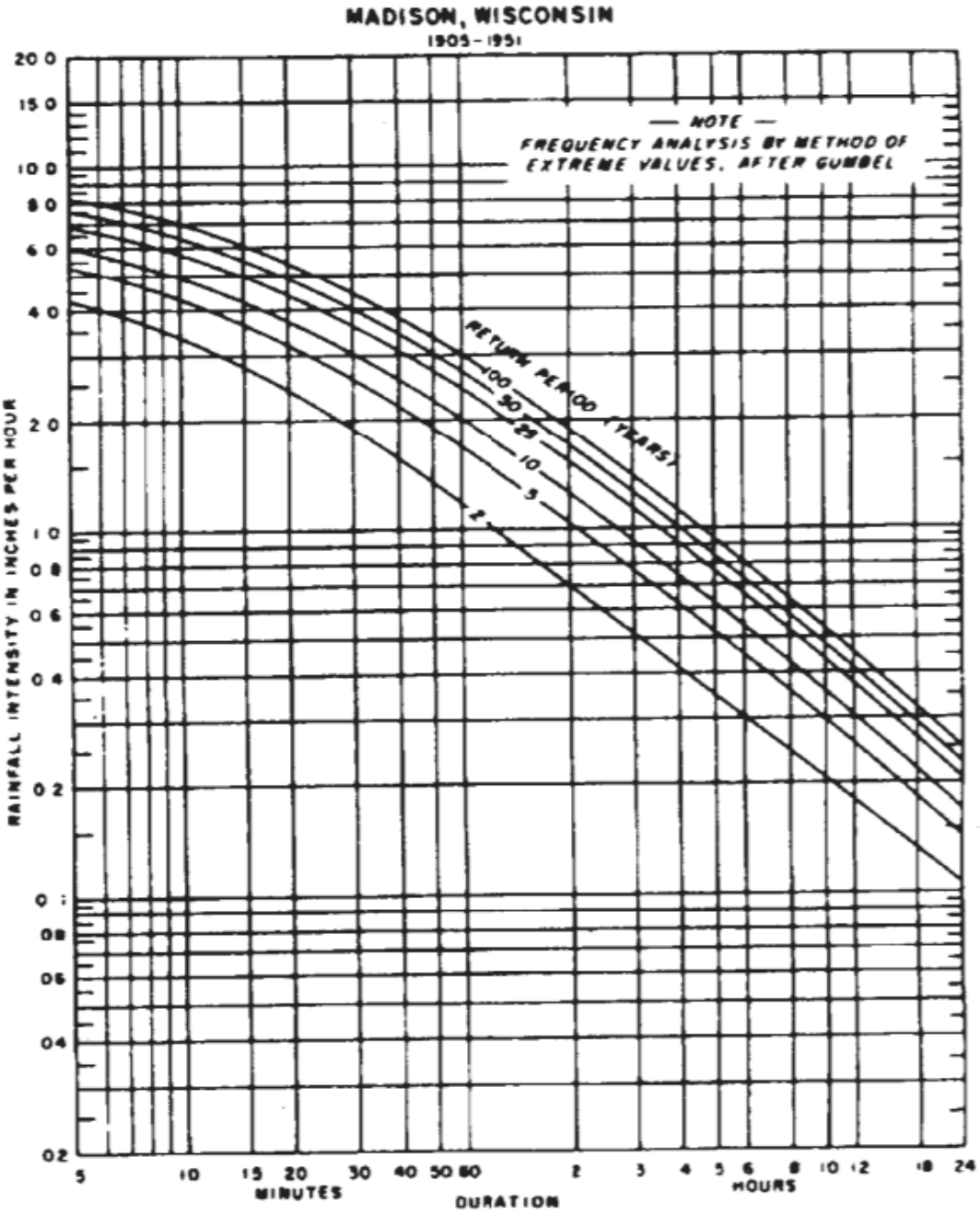

a) State of Wisconsin Department of Transportation, Facilities Development Manual, Chapter 13, Drainage, Attachment 5.4, Rainfall Intensity-Duration-Frequency Curves

Figure 2.4-11 – PMP Site Drainage Area

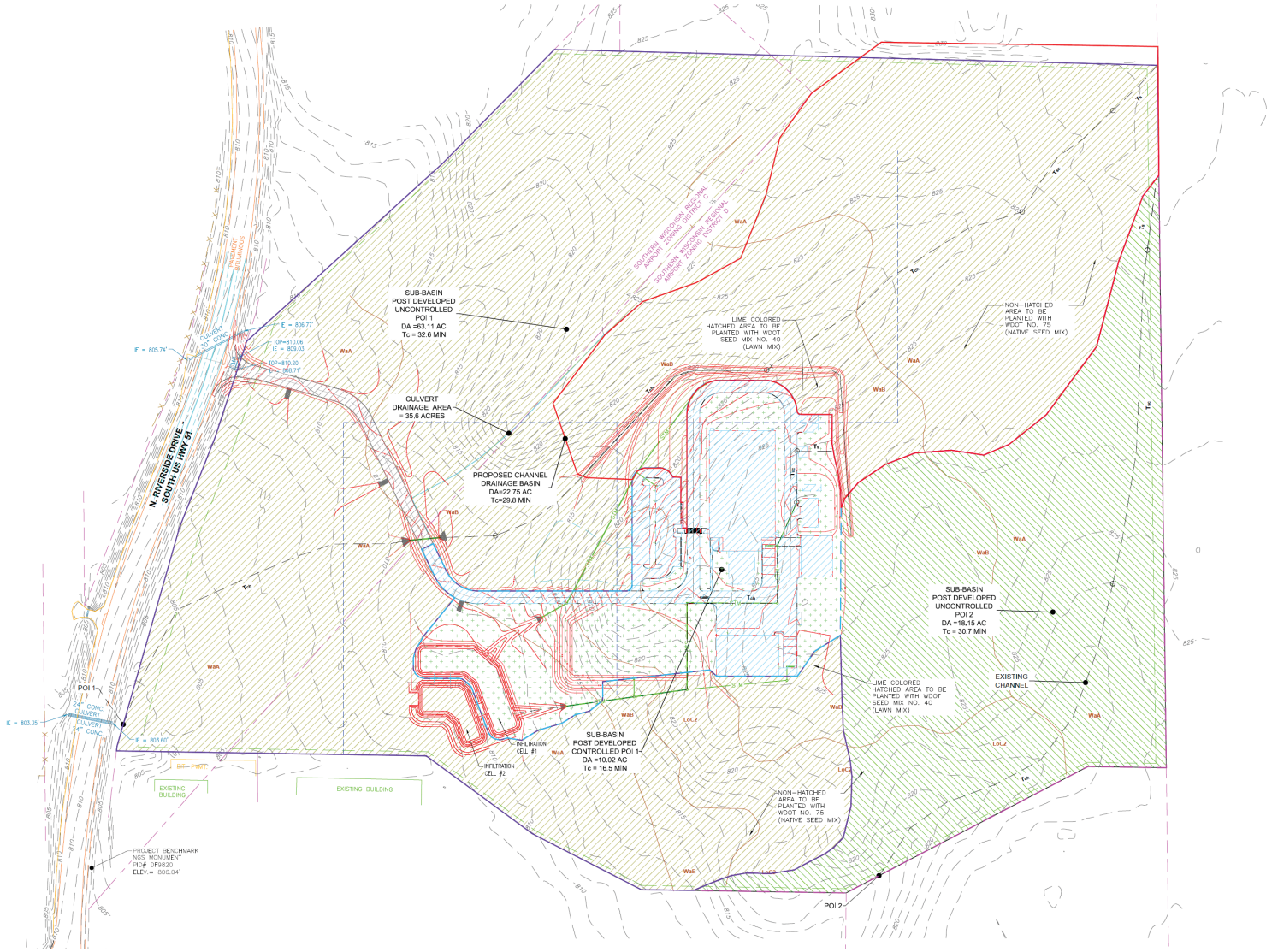

Figure 2.4-12 – PMP 100-Year Event Facility Drainage[a]

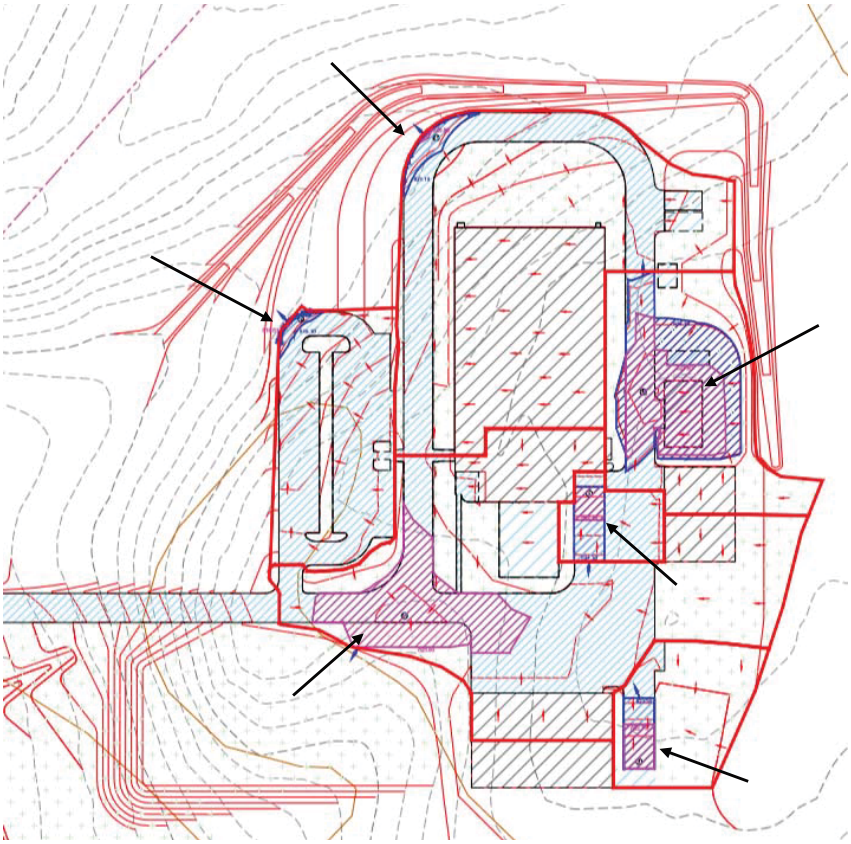

a. Figure displays location of (six) localized low points subject to impoundment if drainage is assumed blocked. Surface elevation of impounded areas during a 100-year PMP event remain below the ground floor elevation of the main production facility and waste staging and shipping building.

Figure 2.4-13 – Rock River Cross-Section Used in PMF Calculation

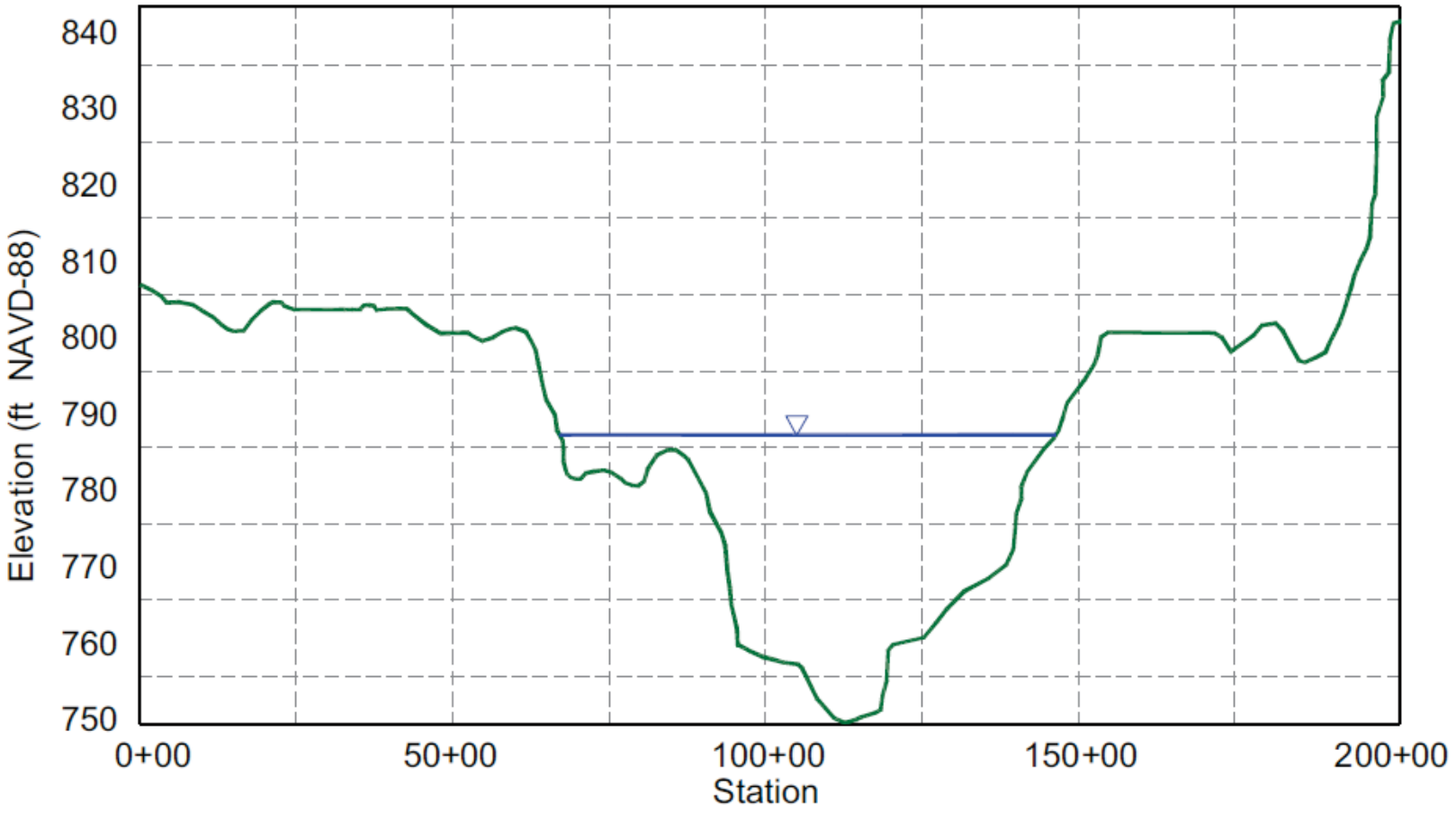

REFERENCE

1.) USGS, 2012b.

Figure 2.4-14 – Dam Locations in Vicinity of SHINE Site

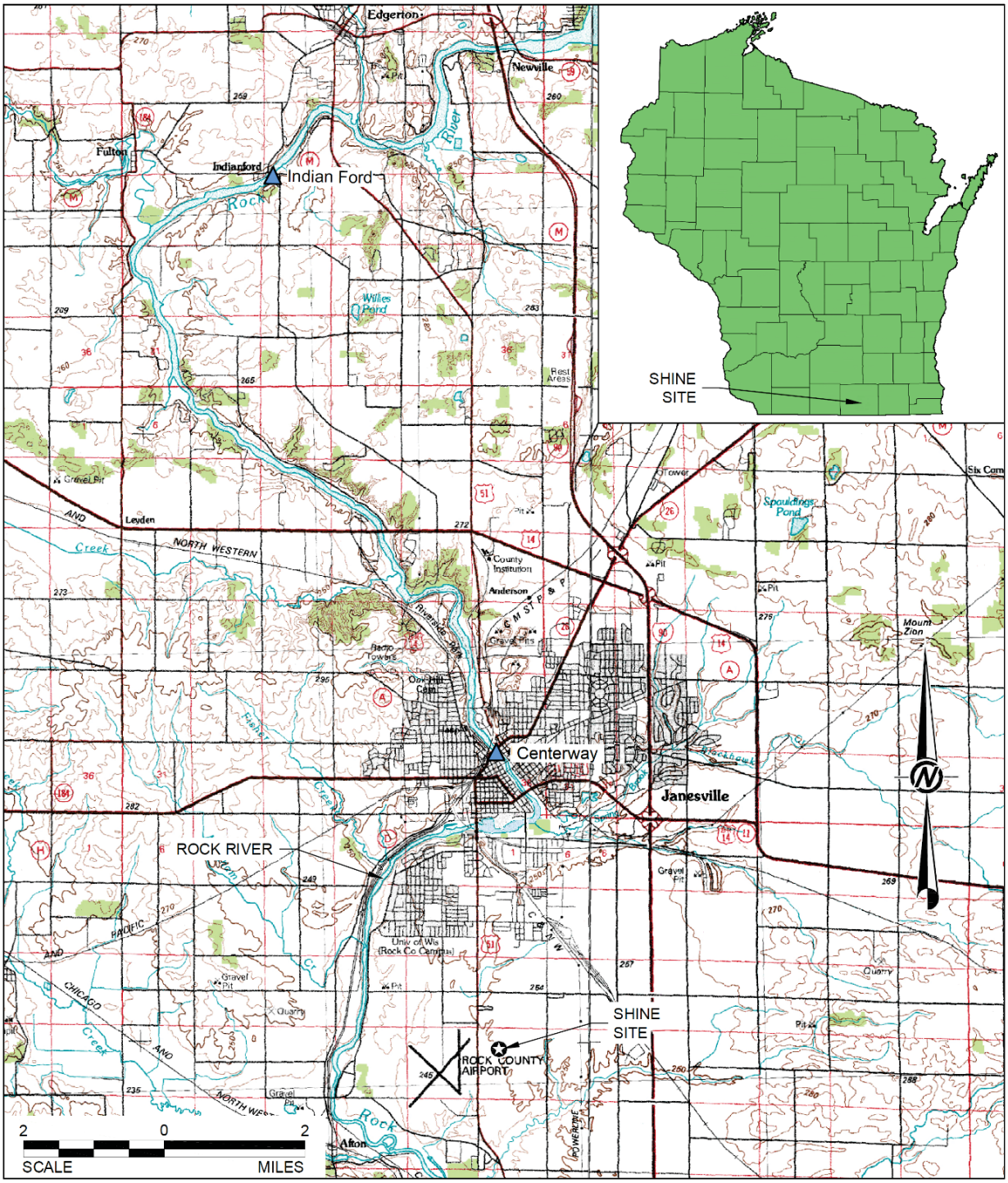

LEGEND

SHINE SITE

DAM LOCATION AND IDENTIFER

2.5 GEOLOGY, SEISMOLOGY, AND GEOTECHNICAL ENGINEERING

This section provides information on the geology, seismology, and geotechnical characteristics of the site.

The site is located in Rock County, on the south side of the city of Janesville, Wisconsin as shown on Figure 2.5-1. The site has historically been cultivated for agricultural crops. The surface topography of the site area slopes gently to the southwest towards the north-south flowing Rock River located 2 mi. (3.2 km) to the west. The ground surface across the 91.27 acre site decreases in elevation by about 23 ft. (7 m) from the northeast to the southwest. Surveyed levels indicate grades ranging from elevation 827 to 804 ft. (252.1 to 245.1 m) NAVD 88.

2.5.1 REGIONAL GEOLOGY

This subsection provides summary descriptions of the geologic units, their origins, structure, and tectonic development in the region surrounding the site. The regional geology descriptions are based on a review of relevant, readily available, peer reviewed, published reports and maps, and where available, records and unpublished reports from federal and state agencies. Several unpublished reports and student theses, local field trip guides, and conference papers have also been reviewed. Information on the site conditions has been acquired from these same sources and from site specific geotechnical field investigations.

The regional summary includes a description of the following major geologic characteristics within about 200 mi. (322 km) of the site (Figure 2.5-2):

- Regional physiography and geomorphology.
- Tectonic provinces and structures within the basement rocks.
- Bedrock geology including stratigraphy, lithology, and structure.
- Magnetic and gravity geophysical anomalies.
- Surficial geology and glacial history.

The evaluation of regional geology and tectonics does not focus strongly on the regional tectonic provinces because in this part of North America they are based largely on basement terranes unrelated to the present tectonic setting of a geologically-stable continental interior. Rather, this regional geological analysis focuses on identifying the major geologic and geophysical structures of the region, and an evaluation of any evidence that these structures may represent potential seismogenic sources and/or capable faults that have been the source of historical earthquakes or could generate future large earthquakes. In Subsection 2.5.2, the geologic setting, structural geology, geologic history and soil conditions of the site are described in greater detail.

The geologic units and structures that comprise the regional geology of Wisconsin preserve a record of several phases of continental accretion and deformation, sedimentary erosion and deposition, and in the Quaternary period (last 1.8 million years), glacial and post-glacial processes that have resulted in the present-day landscape. These are described in further detail below.

For this section, the SHINE region is defined as the area within a 200 mi. (322 km) radius of the site. For the assessment of the capability of the mapped faults, the definition of capable as set out in Appendix A of 10 CFR 100: a capable fault is a fault with at least one of the following:

a. Movement at or near the ground surface at least once within the past 35,000 years or movement of a recurring nature within the past 500,000 years.
b. Macro seismicity instrumentally determined with records of sufficient precision to demonstrate a direct relationship with the fault.
c. A structural relationship to a capable fault according to characteristics noted in a. and b. above such that movement on one could be reasonably expected to be accompanied by movement on the other.

The 10 CFR 100 definition of capable identifies faults that are considered capable of being the source of moderate to large earthquakes in the future. Evidence for the existence of capable faults is based on a geomorphic expression of surface fault rupture in surficial sediments that range in age from present day to 35,000 and/or 500,000 years old, instrumental evidence for the alignment of hypocenters that could indicate a subsurface fault; and in the case where these types of evidence are lacking, a structural relationship with a known capable fault (i.e., a fault is parallel or offsets similarly aged rocks by the same amount as the capable fault).

2.5.1.1 Physiography and Geomorphology

Southern and central Wisconsin are located within the Central Lowland Province of the Interior Plains Division of the United States (USGS, 2003), one of many geomorphic or physiographic regions of the United States as defined by the general texture of the surface terrain, rock type, and geologic structure and history. The regions represent a three-tiered classification of the United States by division, province, and section.

Figure 2.5-2 shows the boundaries of the three physiographic sections of the Central Lowland Province that surround and include the site. The south central portion of Wisconsin is located within the Till Plains — a region of predominantly Illinoian age glacial deposits (formed 310,000 to 128,000 years ago). To the west is the Wisconsin Driftless section — a region of unglaciated terrain. To the east is the Eastern Lake section that contains the most recent topography formed in association with the deposition of glacial advance deposits that surround present-day Lake Michigan.

The present day physiography of the Central Lowland Province and the three sections described above have been influenced by processes associated with Pleistocene (1.8 million years to 10,000 years ago) glacial erosion and deposition, and the subsequent post glacial erosional and deposition as described by Fullerton et al. and Attig et al. (Fullerton et al., 2003 and Attig et al., 2011). Glacial processes in this part of Wisconsin were part of the widespread glaciations that affected the entire northern portion of the continent. Although the most recent episode of widespread glacial advance in Wisconsin (late Wisconsin Glaciation) occurred from approximately 31,000 years ago to about 11,000 years ago, and covered much of the state, the immediate area of the site was not covered by glacial ice during this most recent glaciation episode.

2.5.1.2 Tectonic Provinces, Basement Rocks and Major Geologic Structures

The major tectonic provinces and geologic structures surrounding the site preserve a record of major geologic events occurring over about the last 2.6 billion years (Ga) of geologic history. Figure 2.5-3 (left) is a generalized summary of the major older (Archean and Paleoproterozoic-2.6 to 1.6 Ga) geologic provinces, structures and phases of major crustal deformation (orogens). Figure 2.5-3 (right) summarizes the same information but for the relatively younger Meso- to

Neo-late Proterozoic time (1.6 to 0.542 Ga). The tectonic chronological overview below is drawn from the studies of Charpentier, R.R. (1987); Howell, P.D., and van der Pluijm, B. (1990); Sims, P.K., and Carter, L.M.H. (1996); Braschayko, S.M. (2005); Sims et al. (2005); Schulz, K.J., and Cannon, W.F. (2007); Whitmeyer, S.J., and Karlstrom, K.E. (2007); Cannon et al. (2008); Garrity, C.P., and Soller, D.R. (2009); and Hammer et al. (2011).

In Wisconsin and the surrounding region, the geologic age of the tectonic provinces and structures generally decrease from north to south. The geologic provinces are inferred to represent several stages of continental expansion that occurred by processes of continental accretion and intrusions of igneous rock (e.g., granite); and continental rifting related to partial continental breakup.

The Superior or Southern Province of the Canadian Shield in northern Wisconsin forms part of the Archean craton that preserves rocks ranging in age from approximately 2.6 to 2.75 Ga. In the northern Wisconsin and Lake Superior region, the Superior Province (Figure 2.5-3) consists of gneiss, amphibolites, granite, and metavolcanic rock types.

The Penokean Orogen (Figure 2.5-3) in northern Wisconsin represents two phases of accretion to the southern margin of the Canadian Shield in this part of North America. Approximately 1.86 to 1.84 Ga ago, the Pembrine-Wausau terrane, a volcanic arc, accreted to the Canadian Shield along an east-northeast-trending suture zone. Then approximately 1.84 to 1.82 Ga, the Marshfield terrane, composed of Archean crust, accreted to the Pembrine-Wausau terrane.

The processes of continental accretion continued as the Yavapai Province, included in the Central Plains Orogen (Figure 2.5-3) of southern Wisconsin, accreted to the Penokean Orogen terranes at approximately 1.76 to 1.72 Ga. The Yavapai Province represents an assemblage of oceanic volcanic arc rocks as inferred by the abundance of rhyolite and granite rocks preserved within the Province. In southern Wisconsin, quartzite deposits with an approximate age of 1.7 Ga were deposited as the siliceous rhyolite and granite rocks were eroded and deposited in local sedimentary basins.

Following the accretion of the Yavapai Province, the Mazatzal Province of southern Wisconsin and northern Illinois accreted to the Yavapai Province at approximately 1.69 to 1.65 Ga. Accretion occurred along a northeast-striking (northwest vergent) suture zone (Figure 2.5-3). The Mazatzal Province rocks, included in the Central Plains Orogen, represent volcanic and related sedimentary rocks that formed at the then active continental margin. Intrusion of granite-rhyolite rocks into the Penokean Orogen terranes, and Yavapai and Mazatzal Provinces along the southern Wisconsin border region and in northern Wisconsin, occurred at approximately 1.48 to 1.35 Ga.

At approximately 1.1 to 1.2 Ga, a period of continental breakup resulted in the development of the Mid-Continent Rift (Figure 2.5-3). While the rifting ultimately failed to fully break up this part of the North American continent, it left a major geologic and geophysical region known as the Mid Continent Rift (MCR). The MCR can be traced north from Michigan up through Lake Superior, then southwest through northern Wisconsin and the Midwest of the United States (Figure 2.5-3). Rocks associated with the MCR include flood basalt, rhyolite, sandstone, and gabbroic assemblages. In addition, several northeast-striking normal faults developed in southern Wisconsin as part of intracontinental extension within the Marshfield terrane, Yavapai and Mazatzal Provinces, 1 Ga old quartzite deposits, and 1.48 to 1.35 Ga old granite-rhyolite rocks.

During the Paleozoic Era, the Michigan Basin formed and accumulated substantial thicknesses of Cambrian to Pennsylvanian sedimentary deposits (540 to 300 million years [Ma] ago). The Michigan Basin is one of several basins in the Midwest of North America that contain predominantly Paleozoic sedimentary rocks underlain by Precambrian basement rock units. Models for the formation of the Michigan Basin include post-rifting thermal subsidence, tectonic reactivation of pre-existing crustal structures, and regional subsidence influenced by the active Appalachian Orogeny farther east. As shown on Figure 2.5-4, three major structures that controlled the western margin of the Michigan Basin are present in Wisconsin - the Wisconsin Dome in northern Wisconsin, the north-trending Wisconsin Arch in the southern portion of the state and trending into northern Illinois, and the northwest-trending Kankakee Arch in northern Illinois and Indiana.

2.5.1.3 Bedrock Geology

The regional Proterozoic basement rocks are parts of the Marshfield, Penokean, Yavapai, and Mazatzal Provinces/terranes (Figure 2.5-3), as well as local quartzite and granite-rhyolite intrusive rocks that, in general, are overlain by Paleozoic marine sedimentary rocks. The following discussion of regional bedrock for the project region, including stratigraphy and lithology, is based on geological maps prepared by Mudrey et al. (Muedry et al., 1982) and Garrity and Soller (Garrity, C.P. and Soller, D.R., 2009). Figure 2.5-5 shows the mapped bedrock geology of the project region.

The oldest rocks in the project region occur in the north (Figure 2.5-5), consisting of isolated Early Proterozoic quartzite and felsic volcanic rocks, and the Middle Proterozoic Wolf River Batholith. The oldest Phanerozoic sedimentary rocks generally occur in the northwest, but are also locally present where younger bedrock units have been eroded away, or where the older bedrock has been locally uplifted along major faults. Cambrian sedimentary rocks composed of sandstone, dolomite, and shale represent the oldest Phanerozoic bedrock units. Flanking the eastern and southern margins of the Cambrian bedrock units are Ordovician shale, dolomite, and sandstone, with additional limestone and conglomerate units. The Ordovician units are in turn flanked to the south and east by Silurian dolomite. Along the southern portion of the project area, Upper Devonian and Pennsylvanian limestone, sandstone, and clay rocks have been mapped. Upper Devonian and Lower Mississippian carbonate, sandstone, and shale rocks are preserved along the eastern portion of the project area.

2.5.1.4 Structural Geology

This subsection provides a summary of the regional structural geology in terms of known and/or mapped major faults and folds within approximately 200 miles of the site. To assist in the understanding of the summary, the description commences with structures mapped in Wisconsin and then continues clockwise through Michigan, Indiana, Illinois, Missouri, Iowa, and Minnesota. Additionally, the development of regional structural basins and arches is described. Basement faults mapped in Rock County are discussed separately in Subsection 2.5.6, where they are evaluated in terms of being capable faults per 10 CFR 100, Appendix A.

The amount and quality of information on the precise fault locations are variable. Information on the history of structural development and the time since last displacement is also highly variable. Because most of the mapped faults are covered by glacial and glacial outwash sediments deposited during multiple continental ice sheet advances and retreats, fault locations and offsets have typically been evaluated from subsurface investigations (e.g., groundwater borehole logs,

magnetic and gravity anomalies, seismic reflection/refraction surveys). The current scientific consensus is that faults mapped within the basement and bedrock within 200 miles of the site are not capable faults. This consensus is based on:

- Published interpretations of the structural geologic development that indicates that most of the basement and bedrock faults formed and accumulated displacement during the Paleozoic Era;
- Regional and fault-specific studies for groundwater exploration that indicate that the larger faults (e.g., Waukesha fault) have no evidence for offset of the Quaternary glacial sediments;
- Paleoliquefaction features that appear limited to the Wabash Valley and New Madrid areas having possible sources located more than about 200 miles from the site; and
- Similar studies of faults and fault activity undertaken for two nuclear safety analyses in Wisconsin and Illinois completed in the last 10 years (Exelon, 2006a).

Most of the fault and fold structures in geologic maps appear to have been active during the early to middle Paleozoic Era, as judged by the varying vertical offsets of the Paleozoic bedrock units. A few of the mapped faults (e.g., Northern Wisconsin faults) appear to have been active in pre-Paleozoic time because they affect only the older basement rocks. In the absence of a Paleozoic sedimentary cover, however, these basement faults may also be similar in age to those that offset the Paleozoic sedimentary rocks farther south.

Because much of eastern Wisconsin and Illinois were ice-covered (glaciated) until late into the Wisconsin glaciation period, only those faults that have ruptured to the ground surface in the last 11,000 years have the potential to preserve surface traces. Similarly, in southeast Wisconsin and western Illinois, much of the land surface was ice-covered from Illinoian glaciation, so only those faults that have moved since the last glaciation period have the potential to preserve surface traces. Only those faults mapped within the driftless section of western Wisconsin, southeast Minnesota, and northeast Iowa that have not been glaciated in the Quaternary Period have the potential to preserve faults scarps showing surface evidence for repeated movement in the last 500,000 years.

Liquefaction features within the Wabash Valley suggest at least seven Holocene earthquakes and one late Pleistocene earthquake have occurred. Individual earthquakes are recognized from the timing of liquefaction features, the regional pattern of liquefaction effects, and geotechnical testing results. Although the fault or faults that may have generated the Wabash Valley liquefaction features have not been identified, the liquefaction features appear to have originated from earthquakes centered in southern Indiana and Illinois, more than 200 miles from the SHINE site.

Accordingly, with the exception of unidentified possible faults beneath the Wabash Valley, the faults mapped within 200 miles of the site are not capable faults. The fault or fault sources of the multiple earthquakes that generated the Wabash Valley liquefaction features are yet to be identified. Once identified, however, these fault(s) would be considered as capable as defined in 10 CFR 100.

2.5.1.4.1 Northern Wisconsin Faults

In northern Wisconsin, several faults are associated with the Archean and Proterozoic magmatic terranes and Penokean Orogen (Figure 2.5-4) (Sims, P.K., and Schultz, K.J., 1996). The

northwest-trending, southwest-vergent Eau Pleine Shear Zone, approximately 78 mi. (125 km) long, separates the Pembrine-Wausau terrane from the Marshfield terrane. The Wolf River Batholith is bounded by high-angle normal faults along the western and southern boundaries - the western boundary fault is approximately 61 mi. (98 km) long, has a northeast strike, and a western downthrown block; the southern boundary fault is approximately 34 mi. (54 km) long, has a northeast strike, with the southern block downthrown. The location of the March 14, 1900 E[**M**] 2.32 earthquake epicenter may have been located on or near a fault in the magmatic terranes or Penokean Orogen. Based on the lack of confirmed Quaternary movement, that faults within the Archean and Proterozoic magmatic terranes and Penokean Orogen are not considered to be capable faults.

2.5.1.4.2 Waukesha Fault

The Waukesha fault of southeastern Wisconsin is a northeast-striking normal fault (southeast side down) mapped within the Silurian and possibly Ordovician sedimentary rock units (Mudrey et al., 1982) (Figure 2.5-4). Fault length estimates range from 38.5 mi. (62 km) to 133 mi. (214 km), with multiple strands or splays possible (Braschayko, S.M., 2005). There is no known evidence that the Waukesha fault or associated minor faults have Pleistocene or post-Pleistocene displacement (Exelon, 2006a). The Waukesha fault and associated faults have no evidence that they are capable faults.

2.5.1.4.3 Madison Fault

The Madison fault is mapped as an east-striking, approximately 8-mi. long (13 km) fault by Mudrey et al. (Mudrey et al., 1982) (Figure 2.5-4). From Exelon (Exelon, 2006a), two fault segments of the Madison fault are inferred: a northern segment with north side downthrown 40 to 75 ft. (12.2 to 23 m), and a southern segment with south side downthrown 85 to 125 ft. (26 to 38 m). Both fault segments lack evidence for Pleistocene or post-Pleistocene displacement. Fault segments associated with the Madison fault show no evidence that they are capable faults.

2.5.1.4.4 Structures Associated with the Mineral Point and Meekers Grove Anticlines

Located in the southwestern corner of Wisconsin, plus adjacent portions of Iowa and Illinois, the Upper Mississippi Valley mining district contains folds with southeast-, east- and northeast trending fold axes. These folds include the Mineral Point and Meekers Grove anticlines, and Galena syncline (Exelon, 2006a and Exelon, 2006b) (Figure 2.5-4). The northeast striking Mifflin fault is approximately 10 mi. (16 km) long and is located on the northeast limb of the Mineral Point anticline (DPC, 2010). The Mifflin fault has at least 65 ft. (20 m) of vertical separation (northeast side down) and about 1000 ft. (305 m) of strike-slip separation, with the most recent fault movement estimated to have occurred from 330 Ma to 240 Ma (DPC, 2010). The last movement on the Mineral Point and Meekers Grove anticlines is estimated by Exelon as Late Paleozoic in age (Exelon, 2006a). The Mifflin fault, and Mineral Point and Meekers Grove anticlines are, therefore, not considered to be capable faults.

Major faults within the bedrock of Michigan have not been identified by Garrity and Soller (Garrity, C.P. and Soller, D.R., 2009). The potential for capable faults in these areas is not considered further.

2.5.1.4.5 Royal Center Fault

The Royal Center fault in northwestern Indiana is an approximately 57-mi. (92 km) long fault (Figure 2.5-4). The fault has a northeast strike, and the southeast block is downthrown approximately 100 ft. (Exelon, 2006a and Exelon, 2006b). Estimates for the timing of most recent movement include Post-Middle Devonian and Pre-Pleistocene (Exelon, 2006a). The Royal Center fault is, therefore, not considered to be a capable fault.

2.5.1.4.6 Saint Charles Lineament (SCL)

The Saint Charles Lineament (SCL) is a northeast-trending structure that can be traced for more than 932 mi. (1500 km). The SCL has been interpreted from geochemical and geophysical signatures that extend from southwest Ontario, Canada to southeast Oklahoma (Harrison, R.W., and Schultz, A., 2002 and Exelon, 2006a). While there are several structural interpretations for the SCL, it is generally characterized as forming a boundary between Proterozoic basement bedrock units. Paleozoic bedrock strata appear not to be disrupted by the SCL.

In Alton, Illinois, about 15 miles (24 km) north of St. Louis, Missouri, a set of conjugate strike-slip faults of probable Late Mississippian to Early Pennsylvanian age occur in association with the SCL. The faults do not displace the overlying Pleistocene loess unit. Harrison and Schultz summarize two lines of "weak and non-definitive" evidence for possible neotectonic activity along the SCL: (a) structural control of the Missouri River that could be related to the presence of faults or other bedrock structures, and (b) tilting of possible Miocene-age gravels above the Pennsylvanian bedrock that could have been caused by differential displacements along the SCL (Harrison, R.W., and Schultz, A., 2002).

Since 1974, seven earthquakes of magnitude 2.5 or less have been recorded in regions surrounding the SCL. Four epicenters appear to be located near the SCL and three additional epicenters could possibly be related to the SCL. Based on the lack of confirmed Quaternary movement and the limited evidence of historic earthquake activity, the SCL is not considered to be a capable fault. Four of the earthquakes have magnitudes less than body-wave magnitude (mb) 2.0, and three are between mb 2.0 and mb 2.5.

None of the seven earthquakes are listed in the composite earthquake catalog developed for the Central and Eastern United States Seismic Source Characterization for Nuclear Facilities (CEUS-SSC). Since the seven earthquakes are not in the CEUS-SSC catalog, they were considered not of a large enough magnitude or well enough located to indicate neotectonic activity along the SCL. The seven referenced earthquakes do not suggest ongoing activity on the SCL and are not listed in Table 2.5-1. Additionally, because there is no evidence that any of these earthquakes were felt, they are not included Table 2.5-3.

2.5.1.4.7 Faults in the Chicago area and Cook County Faults

In northeastern Illinois (Figure 2.5-4), a northwest-striking fault zone with Precambrian basement down thrown to the southwest by 900 ft. (274 m) has been mapped in the Chicago area by Exelon and DPC (Exelon, 2006a and DPC, 2010). The most recent fault offset may be pre-middle Ordovician in age. An additional interpretation by DPC suggests that the Precambrian basement is not offset and a fault may not be present (DPC, 2010). An additional 25 minor faults have been identified in the subsurface rocks of Cook County. The location and existence of these faults is based on the interpretation of subsurface seismic reflection data. The interpretations

indicate up to 55 ft. (17 m) of vertical displacement on faults dated as post-Silurian and pre-Pleistocene in age (DPC, 2010) (Figure 2.5-4). None of these faults has evidence of displacement of the present-day ground surface. Available evidence indicates that the Chicago area and Cook County faults are not capable faults.

2.5.1.4.8 The Sandwich Fault Zone

The Sandwich fault zone in northern Illinois is a northwest-striking, approximately 85-mi. long (137 km), normal fault system with a generally down-to-the-northeast sense of vertical displacement, and up to approximately 330 ft. (100 m) of vertical separation (Kolata et al., 2005 and DPC, 2010) (Figure 2.5-4). There are also anticlines mapped with fold axes parallel to the fault system (Exelon, 2006b). The most recent fault movement is constrained to post-Silurian time and pre-Pleistocene (DPC, 2010), or post-Pennsylvanian and pre-Pleistocene (Exelon, 2006a). Based on felt intensities, the earthquakes of May 26, 1909 and January 2, 1912 might be related to the Sandwich fault zone within the Precambrian basement (Larson, T.H., 2002 and Exelon, 2006a). However, the lack of surface rupture in the last 35,000 years, and lack of microearthquake activity associated with the fault suggests that the Sandwich fault is not a capable fault.

2.5.1.4.9 La Salle Anticlinorium

The La Salle anticlinorium is a northwest-trending series of open folds in northern Illinois that extend for 230 mi. (370 km) along the eastern flank of the Illinois Basin (DPC, 2010) (Figure 2.5-4). Faults may be present on the west flank of the anticlinorium and exhibit pre--Cretaceous movement (DPC, 2010). The major movement of the fold belt is post-Mississippian (Exelon, 2006a). Larson suggested that three historic earthquakes in 1881, 1972, and 1999 may have been generated on faults associated with the northwest-trending Peru monocline that is part of the La Salle anticlinorium (Larson, T.H., 2002). Larson suggests that these moderate earthquakes may indicate that some faults within this larger Paleozoic structure could be in the process of reactivation within the present-day stress field (Larson, T.H., 2002). The lack of surface rupture in the last 35,000 years, however, and a lack of microearthquake activity associated with the faults related to the folds suggest that the faults associated with the La Salle anticlinorium are not capable faults.

2.5.1.4.10 Wabash Valley Liquefaction Features

The northern boundary of the Wabash Valley liquefaction features region is located approximately 170 mi. (274 km) south of the site (Figure 2.5-4). Studies of paleoliquefaction features indicate that at least seven Holocene earthquakes and one late Pleistocene earthquake may have generated on the order of **M** 7.5 earthquakes (Obermeier, S.F., and Crone, A.J., compilers, 1994). Faults associated with the Wabash Valley liquefaction features are capable faults.

2.5.1.4.11 Peoria Folds

Located in central Illinois, the Peoria folds (Figure 2.5-4) include a series of 16 synclines and anticlines that generally trend to the east-northeast (Nelson, W.J., 1995; Exelon, 2006a and Exelon, 2006b). The anticlines include the Astoria, Farmington, Littleton, Bardolph, Brereton, St. David, Sciota, Seville, and Versailles folds. The synclines include the Bryant, Bushnell, Canton, Elmwood, Fairview, Ripley, and Table Grove folds. These folds range in length from

approximately 5 mi. (8 km) to 29 mi. (46 km), and have an eastward plunge along with the regional easterly dip. The folds generally have less than 100 ft. (30 m) of structural relief. The major movement and development age for the fold system is estimated as Mississippian and Pennsylvanian (Exelon, 2006a). Based on the lack of confirmed Quaternary movement, the Peoria folds are not related to capable faults.

2.5.1.4.12 Southeast Iowa Folds

In southeastern Iowa, near the state borders with Missouri and Illinois (Figure 2.5-4), a series of five northwest-trending anticlines that range in length from 42 mi. (67 km) to 68 mi. (109 km) have been mapped by Exelon (Exelon, 2006a and Exelon, 2006b). The folds are the Oquawka, Sperry, Burlington, Skunk River, and Bentonsport anticlines. The folds appear to have formed in the Mississippian Epoch of the Carboniferous Period more than 320 Ma (Exelon, 2006a). Based on the lack of any evidence for fold development into the Quaternary Period, these five anticlines in southeast Iowa are not related to capable faults.

2.5.1.4.13 Plum River Fault Zone

In northern Illinois and eastern Iowa, the Plum River fault zone is an approximately 150-mi. long (241 km), east-northeast-striking fault and fold system (DPC, 2010 and Witzke et al., 2010) (Figure 2.5-4). The faults have en echelon segments with 100 to 400 ft. (30 to 122 m) of vertical, down-to-the-north separation. Exelon recognizes synclines and anticlines that are parallel to the fault system (Exelon, 2006b). The last movement on the fault zone is constrained to have occurred between post-middle Silurian and pre-middle Illinoian time (DPC, 2010). No evidence of Quaternary activity has been identified on the Plum River fault zone by Exelon (Exelon, 2006a). Based on the lack of confirmed Quaternary movements, the faults associated with the Plum River fault zone are not considered to be capable faults.

2.5.1.4.14 Amana Fault Zone

To the west of the Plum River fault zone, the Amana fault zone is a northeast-trending fault mapped for a length of approximately 20 mi. (32 km) (Figure 2.5-4). Witzke et al. (2010) indicate that the Amana fault zone is a continuation of the Plum River fault zone, but with an opposite sense of vertical separation (south-side block down). Exelon designates the Amana fault zone as a separate fault segment from the Plum River fault zone (Exelon, 2006b). Based on the similarity in strike and geologic setting with the Plum River fault zone, the Amana fault zone is not considered a capable fault.

2.5.1.4.15 Iowa City-Clinton Fault Zone

To the south of the Plum River fault zone, the Iowa City-Clinton fault zone follows a similar east-northeast strike to that of the Plum River fault zone (Witzke et al., 2010) (Figure 2.5-4). The Iowa City-Clinton fault zone has a south-side-down sense of vertical separation. The Iowa City-Clinton fault zone has not been mapped in Illinois (Kolata et al., 2005). There is no known evidence for displacement during the Quaternary Period along mapped traces of the Iowa City-Clinton fault zone. Based on similar geometries and physiographic settings for both fault zones, the faults associated with the Iowa City-Clinton fault zone are not considered to be capable faults.

2.5.1.4.16 Southeast Minnesota Faults

Jirsa et al. mapped several faults in the southeast corner of Minnesota (Figure 2.5-4) (Jirsa et al., 2011). In Wabasha and Goodhue Counties, northwest-, northeast-, and north-trending faults extend up to 10 mi. (16 km) in length. The faults are located in the Minnesota River Valley subprovince — a region of the Archean southern Superior Province. The faults offset Upper Cambrian and Lower Ordovician sedimentary rocks. In Houston County, northwest-, northeast-, and east-trending faults extend up to 9 mi. (14 km) in length. The faults are located within the Yavapai Province and displace Middle and Upper Cambrian and Lower Ordovician sedimentary rocks. In Mower County, north to northwest-trending faults extend up to 11 mi. (18 km) in length. The faults are located within the MCR and displace Middle and Upper Devonian sedimentary rocks. DPC completed a study of facility site characteristics at a boiling water reactor south of Genoa, Wisconsin (DPC, 2010). They concluded that faults within a 200 mi. (322 km) radius of the site are at least pre-Pleistocene in age and, therefore, are not capable faults. They note that the closest mapped fault to the Genoa project site of any size is the Mifflin fault. While faults in Wabasha, Goodhue, Houston and Counties in Minnesota from Jirsa et al. (2011) are not specifically mentioned in DPC (2010), the faults in the southeast corner of Minnesota are not considered to be capable faults.

2.5.1.4.17 Michigan Basin

The faults and folds described above have developed during the formation and development of a series of regional basins, arches, and domes (Figure 2.5-4). The Michigan Basin contains Cambrian to Pennsylvanian sedimentary deposits (540 Ma to 300 Ma). The Illinois Basin is located to the southwest of the site. The last known major tectonic movements occurred in the Michigan Basin in the early to late Proterozoic (Exelon, 2006a). The Wisconsin Dome is located in the northern portion of Wisconsin, to the west of the Michigan Basin (Heyl et al., 1978). Separating the basins and domes are several structural arches. The Wisconsin Arch trends south from the Wisconsin Dome and had its last major tectonic movements in the early to late Paleozoic (Exelon, 2006a). The Kankakee Arch in northern Illinois forms the southwestern margin of the Michigan Basin (Howell, P.D., and van der Pluijm, B., 1990), and had its last major tectonic movements in the Ordovician to Pennsylvanian (Exelon, 2006a). The Mississippi River Arch to the west of the Illinois Basin had its last major tectonic movements in the post-early Pennsylvanian (Exelon, 2006a). Faults within the Michigan Basin are not considered to be capable.

2.5.1.5 Regional Magnetic and Gravity Geophysical Anomalies

Maps and interpretations of geophysical magnetic and gravity anomalies have been used by others to summarize the geologic interpretations of the regional geological history and structure. Much of the published literature focuses on areas in central and northern Wisconsin, such as the MCR, Penokean fold belt, and Wolf River Batholith (e.g., Klasner et al., 1985 and Chandler, V.W., 1996). In this section, the regional patterns of two major potential field geophysical anomalies are evaluated for additional information on the location and seismic potential of major regional structures.

Five principal sources of magnetic anomaly data are available for review: the magnetic anomaly map of North America (NAMAG, 2002); subsequent interpretation of Precambrian basement (Sims et al., 2005); the Earth magnetic anomaly grid (Maus et al., 2009); the Wisconsin

composite aeromagnetic map (Daniels, D.L., and Snyder, S.L., 2002); and a magnetic anomaly map of Illinois (Daniels et al., 2008).

Figure 2.5-6 is the magnetic anomaly map from Maus et al., 2009 with interpretation of Precambrian basement structures from Sims et al., 2005. The magnetic anomalies have been interpreted by Sims et al. to illustrate the major tectonic features such as the MCR and major basement faults (Sims et al., 2005). Sims et al. also infer several northeast-striking ductile shear zones (faults in the mid to lower crust) and northwest-striking high-angle faults (Sims et al., 2005). They suggest that these basement structures are of late Paleoproterozoic-Mesoproterozoic age (1.76 to 1.70 Ga), and were the result of northwest-southeast shortening of the crust at that time. These shear zones probably bound the 1.76 to 1.65 Ga belt of rhyolite quartz arenite to the north of the site. To the south of this belt of siliceous rocks, the Eastern granite-rhyolite province (1.5 to 1.4 Ga) is preserved and continues into Illinois. The site is located within the Eastern granite rhyolite province. Figure 2.5-7 is a large-scale map of uninterpreted magnetic anomalies of Wisconsin and northern Illinois (Maus et al., 2009).

Three principal sources of gravity anomaly data are available for the region: the Bouguer gravity anomaly map of the conterminous United States presented by Kucks, R.P. (1999), the Bouguer gravity anomaly map of Wisconsin prepared by Daniels, D.L. and Snyder, S.L. (2002), and a Bouguer gravity anomaly map of Illinois (Daniels et al., 2008). Interpretation of the gravity maps suggests that the southern margin of the central Wisconsin gravity low is possibly the northeast-trending shear zone that marks the boundary between the rhyolite-quartz arenite belt and Eastern granite-rhyolite province. Figures 2.5-8 and 2.5-9 are uninterpreted regional Bouguer gravity anomaly maps, and cover most of Wisconsin and northern Illinois, respectively. These maps show the MCR as a strong positive anomaly because it is a region of dense volcanic and igneous rocks surrounded by lower-density sedimentary rocks. The Wolf River Batholith is interpreted by Chandler (1996) to be the source of the large negative gravity anomaly in central Wisconsin.

Details of the composite aeromagnetic and Bouguer gravity anomalies in southern Wisconsin are provided in Figure 2.5-10 and Figure 2.5-11 respectively, to expand the discussion of regional geophysical anomalies and to include an evaluation of potential karst features at the site.

The major structure observed from the geophysical anomalies provided in Figure 2.5-10 and Figure 2.5-11 is the northeast-striking Waukesha fault, identified from structural contours of the Precambrian basement rocks. Structural contours indicate up to 1500 ft. of vertical separation across the Waukesha fault. Based on three-dimensional modeling of aeromagnetic and gravity anomalies, a total vertical separation of approximately 500 to 1100 m at the Waukesha fault is inferred.

A review of the geophysical anomaly maps for southern Wisconsin indicates the following:

- Smaller faults and folds within the Paleozoic Era are not resolvable in the aeromagnetic anomaly map (Figure 2.5-10).
- The offset across the basement rocks at the Waukesha fault can reasonably be resolved in the Bouguer gravity anomaly map (Figure 2.5-11).
- Smaller faults and folds within both the basement and bedrock rocks are not readily apparent in the Bouguer gravity anomaly map (Figure 2.5-11).

Based on the above discussion, the available regional magnetic and Bouguer gravity anomalies in southern Wisconsin are suitable only for identifying the major regional fault structures with large vertical separations.

Karst features are a hazard to development because it not only presents a pathway for rapid movement of groundwater, but also it may cause surface subsidence as overlying soils collapse into open fractures. In addition to surface observations that indicate the presence of karst features, geophysical imaging techniques are used to detect the presence of existing subsurface voids with the potential for collapse. Electrical resistivity tomography has proven to be an effective method to detect past or incipient sinkholes.

The Wisconsin Geological and Natural History Survey (WGNHS) do not have electrical resistivity tomography data or interpretations for the site. While the WGNHS have reports of small sinkholes (less than five ft in diameter and less than five ft in depth) in parts of Rock County, they are not aware of property damage or significant issues surrounding the presence of these sinkholes. WGNHS do not have any reports of sinkholes at the SHINE site. Because the site is in the Rock River Valley and has several hundred feet of sediment overlying the bedrock, it is very unlikely that a sinkhole will form near the site.

The site has little topographic relief and lacks any geomorphic evidence of differential subsidence that may indicate past or ongoing solution of any subsurface carbonate rocks and formation of karst features.

Based on the available evidence, there is a very low probability that karst features are present within the carbonate bedrock below the site.

2.5.1.6 Surficial Geology and Glacial History

The surficial geology of the region is controlled principally by processes associated with the advance and retreat of Pleistocene glaciers, and processes such as erosion and sedimentation that followed the retreat of glacial ice (post-glacial). Several major periods of Pleistocene ice advance are recognized in northern North America. These Pleistocene glaciations are known as the pre-Illinoian, Illinoian (also referred to as pre-Wisconsin), and Wisconsin (Roy et al., 2004) glaciations. Figure 2.5-12 is a map of the surficial geology of the region as modified from Fullerton et al., 2003. Figure 2.5-13 indicates the estimated thickness of overburden and drift for Wisconsin and northern Illinois (Piskin, K., and Bergstrom, R.E., 1975 and WGNHS, 1983). The following summary is based on physiographic divisions from the USGS (2003), and summaries of the surficial geology and glacial history described by USDA SCS (1974); Fullerton et al. (2003); WGNHS (2004); Clayton, L. and Attig, J.W. (1997); and MLRA (2012).

The oldest known landform in the project region is the unglaciated Wisconsin Driftless section of the Central Lowland Province. The Wisconsin Driftless section contains relatively rugged, fluvially-dissected topography with about 600 ft. (180 m) of topographic relief. Based on its geomorphology and lack of preserved glacial deposits, the Wisconsin Driftless section has not been glaciated. In Dane County, Wisconsin, the Driftless section comprises near-horizontal Paleozoic sedimentary rocks that are locally mantled by Pleistocene deposits of windblown (eolian) and hillslope sediments.

Landforms composed of glacial deposits that formed during the Illinoian and Wisconsin Glaciations are present within the region. During the Wisconsin Glaciations, the Laurentide Ice

Sheet flowed south and comprised several ice lobes, including the Green Bay and Lake Michigan ice lobes that flowed over the region. Glacial till was deposited from these ice lobes and as basal and end moraines. Sand and gravel were transported from the edges of the glacial ice across the surrounding region to form extensive glacial outwash fan surfaces. Fine-grained sediments (silt and clay) were deposited within proglacial lakes near the ice margins and within the outwash plain. The maximum extent of the Wisconsin Glaciation ice occurred approximately 30,000 years ago. Ice was absent from the area of the state of Wisconsin beginning around 11,000 years ago (Attig et al., 2011). Alluvial and wind processes reworked the glacial deposits during the Holocene Epoch (last 10,000 years) during and following ice retreat.

With the retreat and almost complete melting of the Laurentide ice sheet, land surfaces of North America experienced a period of adjustment (known as glacial isostatic adjustment [GIA]) that continues to the present day. In GIA, slow movements occur in the highly viscous mantle in response to the loading and unloading of the Earth's surface. In North America, GIA is still causing vertical movements of the land surface because of the removal of significant volumes of ice more than 10,000 years ago. Based on Global Positioning System (GPS) measurements, Sella et al. established a hinge line in the Great Lakes vicinity; north of the line, uplift from GIA is still occurring (e.g., 10 millimeters per year [mm/yr] of present day uplift at Hudson Bay, Canada), while south of the line subsidence of up to 2 mm/yr is continuing at present (Sella et al., 2007). The site is located to the south of the hinge line. Based on the GIA model of Sella et al. (2007), Wisconsin has 0 to 2 mm/yr of ongoing subsidence caused by the melting of ice more than 10,000 years ago. This subsidence is, however, regional in nature and not expected to result in any differential movements at the site.

2.5.2 SITE GEOLOGY

This subsection is a summary of the geologic setting, stratigraphy and structure within about a 5 mi. (8 km) radius of the site.

2.5.2.1 Stratigraphy and Depth to Bedrock

As described in Subsection 2.5.1, the Precambrian basement rocks form geologic terranes that were accreted to the North American continent prior to about 1.48 to 1.35 Ga. During the Paleozoic Era, the site region was part of a large continental marine basin, the Michigan Basin, where deposits of shallow marine sediments accumulated over many millions of years. The development of the Wisconsin Arch within the Michigan Basin formed long wavelength, open regional folds within the Cambrian through Ordovician sedimentary rocks.

The bedrock geology units mapped in the vicinity of the project site (Figure 2.5-5) are the Ordovician Period Prairie du Chien Group (dolomite with some sandstone and shale), Ancell Group (sandstone with minor limestone, shale, and conglomerate), and Sinnippee Group (dolomite with some limestone and shale). From Mudrey et al., the Ordovician sedimentary rock sequence is approximately 200 ft. (60 m) thick, and underlain by an estimated 1000 ft. (300 m) of Cambrian age sedimentary rock, that in turn overlies the Precambrian basement rocks (Mudrey et al., 1982).

The surficial geology of Rock County (Figure 2.5-12) consists of the Wisconsin-age Jonestown moraine to the north. This moraine was formed at the margins of the Green Bay ice lobe. The remainder of the county contains Illinoian-age ground moraine deposits that in places were dissected by southward flowing Late Wisconsin outwash streams. The stream valleys now

contain Late Wisconsin- and possibly Holocene-age glaciofluvial outwash deposits (Fullerton et al., 2003 and RCGIS, 2012). The Green Bay ice lobe also produced paleo-lakes Yahara and Scuppernong with outflow that extended through the Rock River drainage basin (Clayton, L., and Attig, J.W., 1997).

Based on the geologic maps of Mudrey et al. and Cannon et al., the bedrock beneath the site is Cambrian-age sandstone that contains some dolomite and shale beds (Figure 2.5-5) (Mudrey et al., 1982 and Cannon et al., 1999). These sedimentary rocks were deposited in the Michigan Basin and then were gently deformed within the Wisconsin Arch. Bedrock units overlie Archean and Proterozoic volcanic and associated basement rocks that were intruded by a 1.48 to 1.35 Ga granite-rhyolite intrusive episode (Whitmeyer, S.J., and Karlstrom, K.E., 2007). The basement rock units are part of the Yavapai or Mazatzal Province/terrane (Figure 2.5-3).

Two estimates of depth to bedrock at the site are available: an estimate of 200 to 300 ft. (60 to 90 m) from WGNHS, 1983, and an estimate of 100 to 300 ft. (30 to 90 m) from Mudrey et al., 1982. Site geotechnical drilling investigations extended to a maximum depth of 221 ft. (67.4 m) below ground surface (bgs) and did not encounter bedrock. Accordingly, the depth to bedrock at the site is more than 221 ft. (67.4 m) bgs.

2.5.2.2 Structural Geology

The site is located near the axis of the Wisconsin Arch (Charpentier, R.R., 1987) (Figure 2.5-4). Despite the presence of the Arch, cross sections from Mudrey et al. (1982), suggest that the Cambrian and Ordovician sedimentary rock units beneath the site probably have very shallow to horizontal dips. These observations indicate little or no net deformation beneath the site over about the last 500 million years.

2.5.2.3 Site Soil Conditions

Soil mapping at and surrounding the site shows that it is located on the Warsaw and Lorenzo well-drained, loamy soils. Topsoil layers of the Warsaw and Lorenzo soil units are underlain by stratified sand and gravel at depths of approximately 10 to 40 in. (0.25 to1 m) (USDA SCS, 1974 and RCGIS, 2012). The sand and gravel units are inferred to result from deposition of fluvio-glacial sediments on glacial outwash plains and deposition during the construction and erosion of local fluvial terraces.

The subsurface conditions encountered at the site were evaluated by extending 15 boreholes beneath the site. In general terms, the site soil conditions comprise about 1 ft. (0.3 m) of topsoil and crop residue overlying relatively clean, fine- to coarse-grained sand with occasional gravel layers. Based on three deeper boreholes, these soil conditions extend to 180 to 185 ft. (54.9 to 56.4 m) bgs. Below the sand is a 10 to 18 ft. (3.0 to 5.5 m) thick layer of clayey silt that is underlain by sand or silty sand to the borehole termination depth of 221 ft. (67.4 m) bgs. Bedrock was not encountered beneath the site.

2.5.2.4 Non-Seismic Geological Hazards

Available reports and maps that describe geologic hazards associated with landslides, land subsidence, karst features, and swelling clays were reviewed for the site and its surrounding region in Rock County, Wisconsin.

Based on the landslide overview map of the conterminous United States (Radbruch-Hall et al., 1982 and Godt, J.W., and Radbruch-Hall, D.H., 1997), the site is located in a zone of low landslide incidence that is defined as less than 1.5 percent of area subjected to the effects of landslides. The Rock County Hazard Mitigation Plan (Vierbicher, 2010) indicates that "…no significant landslides have been reported in Rock County in recent years." The lack of landslide potential is consistent with the low gradient (less than 7 ft. [2.1 m] elevation change) of the site, and the unsaturated nature of the poorly-graded sands within 50 ft. (15.2 m) of the ground surface.

The Rock County Hazard Mitigation Plan also indicates that "subsidence has not been an issue in Rock County" and that the subsidence hazard is low (Vierbicher, 2010). The plan notes that under some conditions of agricultural tilling and pumping of groundwater a localized settlement and subsidence hazard may occur (Vierbicher, 2010).

Rock County contains carbonate bedrock susceptible to dissolution or karst formation (WGNHS, 2009). The Rock County Hazard Mitigation Plan (Vierbicher, 2010) indicates that no significant sinkholes have been reported in Rock County in recent years. The plan indicates a potential for karst features to form in the county, particularly in the eastern third of the county that lies to the east of the site. No evidence for karst or karst-related subsidence was observed at the site.

The swelling clays map of the conterminous United States prepared by Olive et al. has the site located in a unit identified as containing little or no swelling clay (Olive et al., 1989). The Rock County Hazard Mitigation Plan (Vierbicher, 2010) provides no information on the presence of soils with high shrink-swell potential, expansive soils, or swelling clays. Geotechnical investigations found no evidence of highly-plastic clays in any of the samples obtained during the subsurface investigation. Hazards from swelling or expansive clays are considered to be minimal at the site.

2.5.3 SEISMICITY

This subsection describes the history of recorded and felt earthquakes in southern Wisconsin-northern Illinois based on online earthquake catalogs and databases, and peer-reviewed publications on specific earthquake events.

2.5.3.1 Historic Earthquakes

A project-specific catalog of historic earthquakes was developed for the site by searching several earthquake databases and published references on the location and intensity of historic earthquakes. The following earthquake databases and references were reviewed in the initial phase of catalog development:

- Worldwide Advanced National Seismic System (ANSS) Composite Catalog (ANSS, 2012): The catalog is created by merging the master earthquake catalogs from contributing ANSS institutions and then removing duplicate solutions for the same event.
- USGS/NEIC 1973 to Present Preliminary Determination of Epicenters Catalog (PDE) (USGS, 2012d): The catalog includes earthquakes located by the U.S. Geological Survey National Earthquake Information Center (NEIC).
- Significant U.S. Earthquakes (USHIS) 1568-1989 (USGS, 2012d): The catalog is from the NEIC based on Stover, C.W. and Coffman, J.L. (1993).

- Eastern, Central, and Mountain States of the United States, 1350-1986 (SRA) (USGS, 2012d): The catalog is from the NEIC based on Stover et al. (1984).
- National Center for Earthquake Engineering Research (NCEER) Group (NCEER, 2012): Catalog of central and eastern United States earthquakes from 1627 to 1985 (Armbruster, J. and Seeber, L., 1992).
- U.S. Geological Survey reports on central United States earthquakes and earthquake information by state: Bakun, W.H. and Hopper, M.G. (2004); Dart, R.L., and Volpi, C.M. (2010); Stover, C.W. and Coffman, J.L. (1993); Wheeler, R.L. (2003); Wheeler et al. (2003) and USGS (2012f).
- Review of significant Canadian earthquakes from 1600 to 2006 (Lamontagne et al., 2008) and Natural Resources Canada earthquake information (Natural Resources Canada, 2012).
- Centennial Catalog (Engdahl, E.R.,and Villaseñor, A.,2002): A global catalog of earthquakes from 1900 to 2008.

Because of numerous inconsistencies within and between various earthquake databases and references (e.g., different epicenter locations for a given earthquake), a second phase of review was undertaken based on the Central Eastern United States earthquake catalog (CEUS-SSC) (CEUS-SSC, 2012). This earthquake catalog was compiled as part of studies to develop a new seismic source characterization model for the Central and Eastern United States. The catalog contains records of earthquakes documented from 1568 to 2008.

The regional earthquake catalogs which make up the CEUS-SSSC catalog may individually show epicenters for additional events not covered in Table 2.5-1. While some of these events may be real, they are unreliably recorded earthquakes, and others may result from mine explosions, earthquakes triggered by deep fluid injection and/or hydraulic fracturing of near-surface rocks, or other non-tectonic processes. In the development of this section, SHINE relied upon the analysis of earthquake records used to create the comprehensive earthquake catalog for the CEUS-SSC project. Therefore, while the U.S. Geological Survey-hosted database includes additional earthquake epicenters, SHINE included only those earthquakes that have passed the robust screening process used to prepare the CEUS-SSC catalog in Table 2.5-1.

Earthquakes from various magnitude scales were recalculated to a uniform magnitude scale using moment magnitude (**M**). Based on the uncertainty of assessment, the recalculated magnitudes for historic earthquakes are termed expected moment magnitude (E[**M**]) in the CEUS-SSC catalog (CEUS SSC, 2012). The primary benefits of using the CEUS-SSC (2012) catalog to develop the project-specific SHINE catalog include: a) using a single earthquake database that has been compiled and reviewed under uniform procedures; and b) obtaining uniform earthquake magnitudes for the project-specific database with E[**M**] values (CEUS-SSC, 2012).

The project-specific catalog was developed based on the CEUS-SSC catalog that contains 58 records of historic earthquakes with epicenters located within about 200 mi. (322 km) of the site (CEUS-SSC, 2012 and 2015). The project-specific catalog is listed in Table 2.5-1 and includes earthquake magnitudes ranging from E[**M**] 2.32 to 5.15. Four earthquake events are assigned depths of 5 km (3.1 mi.) or 10 km (6.2 mi.), with the remaining depths assigned a depth of 0 km (0 mi.). The October 22, 1909 and October 17, 1913 earthquake epicenters have the same latitude and longitude coordinates.

In the project-specific catalog, the largest earthquake is the May 26, 1909 E[**M**] 5.15 event located approximately 85 mi. (137 km) southeast of the site. The largest earthquake since the 1970s is the June 28, 2004 E[**M**] 4.13 event located approximately 82 mi. (132 km) south of the site. The closest earthquake epicenter to the site is the December 7, 1933 E[**M**] 3.03 event located approximately 21 mi. (34 km) to the northwest.

The project-specific catalog indicates that in general, the region surrounding the site has a historic record of relatively infrequent, small to moderate earthquakes that is typical of much of the central and eastern United States.

2.5.3.2 Felt Intensities

In addition to recorded earthquake epicenters, information is also available on how earthquake shaking has been experienced by people located in Janesville and other communities near the site. The experience of earthquake shaking and a qualitative assessment of damage is measured on the Modified Mercalli Intensity scale (MMI). Table 2.5-2 provides a description of MMI levels of intensity, referenced from USGS, 2000. While the quality of the measurements is highly variable depending on the skills of the observer and the quality of local engineered and non-engineered structures, the MMI scale nevertheless provides a reasonable estimate of the occurrence of moderate and large earthquakes that occurred before the development of a network of earthquake recording instruments.

The National Geophysical Data Center (NGDC) of the NOAA developed the National Earthquake Intensity Database (NEID), which is a collection of records of damage and felt reports from more than 23,000 U.S. earthquakes (NEID, 2012). The database contains information regarding the coordinates of earthquake epicenters, estimated magnitudes, and focal depths, names and coordinates of reporting cities (or localities), reported intensities, and the distance from a city (or locality) to the epicenter. Earthquakes listed in the NGDC database date from 1638 to 1985. From 1985 onward, the reports of earthquake shaking are maintained by the USGS.

Shaking intensity records from NEID of earthquakes within approximately 200 mi. (322 km) of the site contain reports from 12 earthquakes that occurred from 1928 to 1985 (NEID, 2012). A composite dataset is listed in Table 2.5-3, and consists of the earthquake location and expected moment magnitude from the CEUS-SSC database, plus the event MMI values from the NEID database and other sources cited in Table 2.5-3 (CEUS-SSC, 2012 and NEID, 2012). The 12 earthquakes listed in Table 2.5-3 are shown in Figure 2.5-14. An estimated MMI value of V at the site accompanied the 1909 E[**M**] 5.15 earthquake located approximately 85 mi. (137 km) to the southeast, and accompanied the 1972 E[**M**] 4.08 earthquake located approximately 70 mi. (113 km) to south-southwest (Table 2.5-3).

Historic earthquake reports and isoseismal maps were reviewed for the central United States from 1568 to 1989 (Stover, C.W. and Coffman, J.L., 1993), 1827 to 1952 (Bakun, W.H. and Hopper, M.G., 2004), and United States earthquake information by state and territory (USGS, 2012f). In addition, a summary of significant Canadian earthquakes from 1600 to 2006 (Lamontagne et al., 2008 and Natural Resources Canada, 2012) was also reviewed. Table 2.5-4 lists historic earthquakes with epicenters located more than 200 mi. (322 km) from the site where earthquake shaking was reported as felt or inferred to have been felt in the site area. As in Table 2.5-3, the composite dataset listed in Table 2.5-4 lists event location and estimated moment magnitude from the CEUS-SSC database, earthquake MMI values from Stover and Coffman, and estimated MMI values at the site from sources cited in the Table 2.5-4

(CEUS-SSC, 2012 and Stover, C.W. and Coffman, J.L., 1993). Depending on the level of detail in historical earthquake descriptions, the MMI value at the site had to be estimated for some earthquakes because only general felt intensity information for other earthquakes could be identified (e.g., "Felt in Wisconsin"). Figures 2.5-15 through 2.5-20 provide isoseismal maps from Stover and Coffman (Stover, C.W. and Coffman, J.L., 1993) and Bakun and Hopper (Bakun, W.H. and Hopper, M.G., 2004) for the more significant earthquakes listed in Table 2.5-4.

The MMI values for historic earthquakes within an approximate 200 mi. (322 km) radius of the site range from MMI II to MMI VII (Table 2.5-3). The largest MMI value (VII) recorded in the region was during the May 26, 1909 E[**M**] 5.15 earthquake. Figure 2.5-19 shows the isoseismal map from a detailed study of the 1909 earthquake by Bakun, W.H. and Hopper, M.G. (2004). The location of the estimated earthquake epicenter depends on the reference. For example, the 1909 event is located approximately 85 mi. (137 km) southeast of the site in CEUS-SSC, 2012 and Stover, C.W. and Coffman, J.L. (1993); and 68 mi. (109 km) south of the site according to the study of Bakun, W.H. and Hopper, M.G. (2004); and as depicted on Figure 2.5-19. For this report, the CEUS-SSC (2012) dataset is the primary dataset for epicenter locations for reasons discussed in Subsection 2.5.3.1. Thus, Figure 2.5-19 displays the felt intensity epicenter of the May 26, 1909 earthquake based on the location provided in CEUS-SSC (2012) and Stover, C.W. and Coffman, J.L. (1993).

Based on the review of felt intensity records for historic earthquakes (up to 1985), regional earthquakes have developed MMI values ranging from III to VII within approximately 200 mi. (322 km) of the site. At distances greater than 200 mi. (322 km) from the site, felt intensities of historic earthquakes (up to 1989) developed MMI values estimated at MMI I to V at the site. The maximum felt intensity experienced at the site in historical times corresponds only to moderate shaking (MMI V). MMI V intensity may have occurred at the site four times in approximately the last 200 years during earthquakes that occurred in 1811, 1886, 1909, and 1972.

2.5.4 MAXIMUM EARTHQUAKE POTENTIAL

The review of the regional geological stratigraphy, structure, and tectonics presented in Subsection 2.5.1 indicates that major geologic structures mapped in the region appear to have developed within a tectonic regime different from the present day. The long-term geologic history of the emplacement and metamorphism of regional basement rocks, analysis of the stratigraphy, and geologic structures mapped or inferred within the local sedimentary bedrock provide no positive evidence that they have experienced any significant tectonic movements in Quaternary time (over the last 1.8 million years). Most of the major geologic and geophysical structures are preserved in the pre-Phanerozoic basement rocks and appear related to major episodes of continental accretion and breakup before about 500 million years ago.

Several regional geologic structures appear to deform the Paleozoic rocks in the region: the Sandwich fault zone, the La Salle anticlinorium, several small and limited-length faults, and the regional Wisconsin and Kankakee Arches. The Wisconsin and Kankakee Arches are regional-scale, long wavelength tectonic features that appear related to crustal adjustment during and following the filling and development of the Michigan Basin more than 300 million years ago.

The bedrock faults, such as the Sandwich and Plum River fault zones, appear to have generated vertical offset of the Paleozoic rocks, indicating that the fault movements post-date the filling of the Michigan Basin. No evidence, however, is available to indicate that either of these faults has propagated upward into the Late Wisconsin sediments and/or to the ground surface. The lack of

a mapped surface trace for these faults indicates that there has been no surface displacement along the faults for perhaps 35,000 years. Based on the review of and interpretation of available literature and data, including NRC documents for other sites, the closest known capable faults to the site are part of the Wabash Valley liquefaction features located about 170 mi. (274 km) south of the site.

The pattern of historical seismicity for the region does not demonstrate a positive alignment of the few known epicenters that might indicate ongoing seismic activity and reactivation of these older structures by the present-day stress field. The epicenter of the E[**M**] 5.15 earthquake in 1909 estimated by Bakun and Hopper is, however, close to the mapped trace of the Sandwich fault that is mapped to offset the Paleozoic rocks of northern Illinois (Figure 2.5-5) (Bakun, W.H. and Hopper, M.G., 2004). It is not clear, however, whether this single, moderate-magnitude earthquake indicates Holocene reactivation of the Sandwich fault zone, or if the earthquake was generated by localized strain release on some other small-scale fault.

The review of historical earthquake records indicates that the maximum earthquake that has occurred during the last 200 years within 200 mi. (322 km) of the site is the E[**M**] 5.15 event. Well-studied historic earthquakes suggest that the strongest shaking experienced at the site is MMI V, with a maximum in the region of MMI VII. These values are typical for geologically stable, continental interior regions such as the central United States where infrequent, moderate magnitude earthquakes occur without a clear association with known geologic structures.

A 200-year historic earthquake record is generally considered too short a time period to estimate the longer term earthquake potential, particularly in regions where the larger earthquakes occur infrequently. To estimate the longer term earthquake shaking potential, the results of the disaggregation of the 2008 USGS National Seismic Hazard Model (Petersen et al., 2008) were calculated for return periods of 4975 to 19,900 years. Figures 2.5-21 through 2.5-25 show deaggregation results for 4975, 9950, and 19,900 years, respectively. The deaggregation plots for the longer return periods all indicate that the major contributor to seismic hazard are earthquakes with magnitudes between about **M** 5 and **M** 6. The PGA values for the longer return periods increase because the source earthquake has a higher probability of being closer to the site.

To assess the potential maximum magnitude that may impact the site and its immediate surroundings, the mean earthquake magnitude was estimated from the disaggregation of the 2008 USGS National Seismic Hazard Model (Petersen et al., 2008) for return periods of 4975, 9950 and 19,900 years, and a site located at 89.025 degrees west longitude and 42.624 degrees north latitude. The mean earthquake magnitudes for these long return period disaggregations are in a narrow range of about **M** 5.7 to 5.8. This magnitude range is about 0.5 to 0.6 magnitude units greater than the E[**M**] 5.15 maximum that is the largest historic earthquake magnitude to have occurred in the last 200 years within about 200 mi. (322 km) of the site. An **M** 5.8 earthquake can reasonably be regarded as the maximum potential earthquake magnitude to occur within the region.

2.5.5 VIBRATORY GROUND MOTION

This subsection presents an evaluation of the earthquake ground shaking expected at the site. Because most of the mapped faults, folds, and major known geological structures within 200 mi. (332 km) of the site are not considered to be seismically capable, the analysis of earthquake ground shaking at the site is based on interpolation of the national seismic hazard model. The

development of an earthquake ground motion design response spectrum follows the procedures set out in the structural codes and standards applicable to Wisconsin.

2.5.5.1 Earthquake Shaking Hazard Evaluation

Probabilistic seismic hazard analysis (PSHA) is commonly used to estimate expected levels of earthquake ground shaking for regions and for sites (e.g., McGuire, 2004). The PSHA method provides a probabilistic estimate (annual frequency of exceedance) for specified levels of earthquake ground motion. The earthquake ground motions can be reported as peak horizontal ground acceleration (PGA) estimates, as often required for foundation or slope stability analyses, or spectral accelerations (Sa = accelerations at a specified frequency), as commonly used in modern building codes and structural standards.

The USGS developed national probabilistic seismic hazard models in 1996, 2002, and 2008 (with minor updates in 2010), which all include Wisconsin (e.g., Petersen et al. 2008). Each update of the national probabilistic model and associated hazard maps has incorporated the latest information on fault locations and fault characteristics; historical earthquake locations, magnitudes and effects; and a range of ground motion prediction equations (GMPE) developed from earthquake records from the United States and around the world. The seismic hazard models can be used to estimate PGA and Sa values for any site in the conterminous United States (USGS, 2012e).

2.5.5.2 Earthquake Shaking Hazard Estimates

Probabilistic PGA estimates were acquired for the site based on the USGS 2008 national hazard model (USGS, 2012a) (Figures 2.5-21 through 2.5-25). For the site, the USGS 2008 model is limited to the estimation of hazard for outcropping, weak rock and hard rock sites with average shear-wave velocity profiles in the upper 100 ft. (30 m) of 760 m/s (2493 ft/sec) (soft rock and/or very stiff soil) or 2000 m/s (6562 ft/sec) (hard rock), respectively. The 760 m/s (2493 ft/sec) value was used to obtain PGA estimates for five return periods from 475 years to 19,900 years as listed in Table 2.5-5. The PGA values listed in Table 2.5-5 indicate a low to very low level of earthquake shaking hazard at the site.

2.5.5.3 2015 International Building Code Seismic Design Ground Motion Parameters

The Final ISG Augmenting NUREG-1537, Part 2, Section 6b.3 (USNRC, 2012) requires that the criticality accident alarm system (CAAS) be “designed to remain operational during credible events, such as a seismic shock equivalent to the site-specific, design-basis earthquake or the equivalent value specified by the Uniform Building Code.” In Wisconsin, the Uniform Building Code (UBC) has been superseded by the 2015 International Building Code (IBC) (IBC, 2015). Thus, seismic design parameters are discussed in terms of the 2015 IBC and associated standards rather than in terms of the UBC.

Seismic provisions within the 2015 IBC Chapter 16, Section 13, Earthquake Loads (IBC, 2015) and the ASCE 7-05 Standard, Chapter 11 (ASCE, 2005) are based on five-percent damped spectral accelerations for a maximum considered earthquake (MCE) with a return period of 2475 years (equivalent to a ground motion with a 2 percent probability of exceedance in 50 years). Spectral acceleration values for the MCE are for soil Site Class B (rock) site conditions (average shear wave velocity in the top 100 feet [30 m] between 2500 and 5000 ft/sec [760 to 1500 m/s]). For most sites, the short- (S_S) and long- (S_1) period spectral accelerations for rock

sites can be read from maps included with the IBC 2015 code, or they can be calculated from the online USGS Ground Motion Parameter Calculator and/ or U.S. Seismic “Design Maps” web application (USGS, 2012b).

In IBC, Site Class B soil conditions require modification for other soil site classes (Site Classes A, C, D, E, and F) by the application of the site coefficients F_a (site coefficient for 0.2 second period) and F_v (site coefficient for 1 second period). Soil-modified S_S becomes S_{MS} (maximum considered earthquake spectral response for 0.2 seconds modified for soil Site Class) and soil-modified S_1 become S_{M1} (maximum considered earthquake spectral response for 1 second period modified for soil Site Class) where $S_{MS} = S_S \times F_a$ and $S_{M1} = S_1 \times F_v$ (Equations 16-36 and 16-37 in IBC, 2009). The U.S. Seismic "Design Maps" web application (USGS, 2012b) indicates S_S and S_1 values of 0.129 g (gravitational acceleration) and 0.050 g, respectively (F_a and $F_v = 1$) for the MCE at the site. These values are slightly different than those obtained from the USGS 2008 national hazard maps because the 2009 IBC-ASCE 7-05 MCE values are based on the earlier 2002 USGS national hazard maps.

The site is a soil Site Class D site. When modified for a Site Class D site by application of the site coefficients F_a and F_Vv S_{MS} and S_{M1} values of 0.206 g and 0.119 g, respectively ($F_a = 1.6$ and $F_v = 2.4$) are obtained. The S_{MS} and S_{M1} values represent the MCE acceleration response spectral accelerations for the site as modified for the site soil conditions. These modified spectral acceleration values are then multiplied by two-thirds to develop the design acceleration response spectrum values of S_{DS} (design spectral response acceleration coefficient at short periods) and S_{D1} (design spectral response acceleration coefficient at 1-second period) for where $S_{DS} = S_{MS} \times 2/3$ and $S_{D1} = S_{M1} \times 2/3$ (Equations 16-38 and 16-39 from IBC, 2009). The S_{DS} and S_{D1} values are used to develop the design acceleration response spectrum suitable for structural analysis and design for the requirements of IBC 2015 and ASCE 7-05. Key parameters for the development of seismic design ground motions from the 2015 IBC-ASCE 7-05 seismic design procedures are listed in Table 2.5-6.

2.5.6 SURFACE FAULTING

The USGS Quaternary Fault and Fold Database of the United States, (USGS, 2012c) contains information on the location and activity of known or mapped Quaternary faults and folds in the United States. The database contains no record of Quaternary faults or folds within an approximate 200 mile (322 km) radius of the site. A review of site aerial photographs and Google Earth™ images found no evidence for geomorphic features that might indicate the presence of a fault with demonstrated surface rupture in the Quaternary within 5 mi. (8 km) of the site.

Two east-striking faults mapped within the Cambrian to Ordovician sedimentary bedrock have been identified in the subsurface of Rock County by Mudrey et al. (Mudrey et al., 1982). The Janesville fault (also named the Evansville fault) consists of an approximately 19-mi. long (31 km), east-striking fault with the north side downthrown (DPC, 2010), and located approximately 6 mi. (10 km) north of Janesville (Figure 2.5-5). This fault is identified as the predominant fault segment, with a second segment striking to the north (DPC, 2010). It is assumed that the estimated 70 ft. (21.3 m) of displacement for the downthrown side (Exelon, 2006a) of the Janesville fault is associated with the primary east-striking fault segment. There is no evidence of Pleistocene or post-Pleistocene activity on the Janesville fault (Exelon, 2006a). The Janesville fault is not considered to be a capable fault.

An unnamed, approximately 1.6-mi. long, (2.6 km) east-trending fault in the bedrock units underlying Rock County is located approximately 1.9 mi. (3.1 km) north of Janesville (Mudrey et al., 1982) (Figure 2.5-5). The type or amount of fault displacement has not been determined for this unnamed fault. Based on the unnamed fault's similar orientation and location with respect to the Janesville fault, the unnamed fault is also not considered to be a capable fault.

From the USGS Quaternary Fault and Fold Database of the United States (USGS, 2012c), the northern boundary of the Wabash Valley liquefaction features region is located approximately 170 mi. (274 km) south of the site (Figure 2.5-4). Liquefaction studies indicate that at least seven Holocene (10,000 years ago to present day) up to **M** 7.5 earthquakes and one late Pleistocene (130,000 years to 10,000 years) earthquake may have occurred in this region (Obermeier, S.F., and Crone, A.J., compilers, 1994). Surface faulting associated with future earthquakes is not anticipated to affect the site.

2.5.7 LIQUEFACTION POTENTIAL

2.5.7.1 Site Soil Conditions

Geotechnical engineering characteristics of the site were evaluated by a series of field investigations. Based on standard penetrometer test (SPT) blow counts (N-values) measured in 14 boreholes extended at the site, the density of the sand beneath the site increases with depth. In general, the sandy soils observed down to a depth of approximately 60 to 80 ft. (18.3 to 24.4 m) can be classified as "compact to dense" except close to the level of the water table encountered in the boreholes. Although no soil heave was observed during drilling operations, six of the 14 borings included one SPT classified as “loose” at or just below the observed water level. Below approximately 80 ft. (24.4 m), sandy soils are classified as “dense to very dense”.

The 10 to 18 ft. thick (3.1 to 5.5 m) stratum of clayey silt encountered at approximately 180 to 185 ft. (54.9 to 56.4 m) bgs in the three deeper borings can be classified as “hard”. Results from penetrometer tests measured by hand corroborate the SPT results.

Laboratory tests of the distribution of soil grain sizes for samples selected from the boreholes indicate that the soils can be geotechnically classified as “poorly-graded sand, with gravel and silt." Soil moisture contents in the upper 50 ft. (15.2 m) ranged from 2.0 to 11.3 percent, and moisture contents below this depth ranged from 9.5 to 25.4 percent. Soluble-sulfate in soil at sample depths between 10 and 40 ft. (3.0 to 12.2 m) bgs exhibited "negligible sulfate exposure" levels (less than 0.10 percent by mass). Other laboratory testing indicated that the clayey silt had liquid limits (LL) of 18 to 19, and plastic limits (PL) of 13 to 14.

2.5.7.2 Groundwater Level

Groundwater was encountered at the time of drilling in the boreholes extended at the site. Measured groundwater level elevations ranged from about 754 to 766 ft. (230 to 233 m), about 50 to 65 ft. (18.3 to 19.8 m) bgs. Groundwater levels can generally be expected to fluctuate seasonally and annually with changes in local and regional precipitation patterns. Analyses of the groundwater flow direction and gradient are provided in Subsection 2.4.1.4.

2.5.7.3 Liquefaction Assessment

The potential for soil liquefaction at the site was reviewed in accordance with Regulatory Guide 1.198, Procedures and Criteria for Assessing Seismic Soil Liquefaction at Nuclear Power Plant Sites (USNRC, 2003).

A qualitative review of the potential for soil liquefaction indicates that the soils at the site pose no potential liquefaction hazard to the project because:

a. Liquefaction occurs only in saturated or near-saturated soils. The soils at the site are unsaturated to a depth of about 58 to 65 ft. (17.7 to 19.8 m) below the ground surface and thus are not liquefiable. Soils below these depths are generally considered non-liquefiable (even under higher seismic loads) due to the high effective stress confining the soil.
b. Liquefaction occurs generally in loose soils. The relative densities of the sandy soils in the upper 100 ft. (30 m) are generally compact to dense, and are, therefore, considered non-liquefiable under the design seismic ground motions.
c. The seismic design ground motions associated with this low seismic hazard are of insufficient scale and duration; the resulting seismic cyclic stresses are not considered capable of producing excess pore water pressure and thus insufficient to trigger liquefaction.

To confirm the qualitative analysis, a deterministic liquefaction analysis was undertaken to assess the liquefaction hazard potential for the site soil conditions, and to evaluate the potential for surface settlement due to liquefaction. The analysis was based on the SPT N-values that were acquired during geotechnical field investigations in 14 boreholes advanced at the site.

Liquefaction triggering analysis was performed at a PGA value of 0.13 g. This PGA value was derived by scaling the 4975-year return period PGA from the national seismic hazard model by 1.6 to account for the soil Site Class D site soil condition. An **M** 5.8 earthquake was selected as the maximum potential earthquake. The depth to highest groundwater level was estimated at 30 ft. (9.1 m) bgs to represent conservatively the groundwater levels higher than measured at the site and estimated to exist during the 500-year flood event.

Results of both the qualitative and quantitative liquefaction analysis demonstrate that there is no potential for liquefaction to occur within the soils underlying the site. The factor of safety against liquefaction ranges from 2 to 30, and in most cases exceeds 3. The median factor of safety against liquefaction is 5.3. Factors of safety greater than 1.4 are considered “high”, and in those cases “soil elements would suffer relatively minor cyclic pore pressure generation” (NUREG/CR-5741) (USNRC, 2000).

2.5.8 CONCLUSIONS

Analysis of the long-term geologic history of the emplacement, metamorphism, and structural evolution of regional basement rocks; the stratigraphy and structure of the local sedimentary bedrock units, the glacial geology and geomorphology; and regional magnetic and gravity anomalies all indicate that the site is located within a region characterized by long-term tectonic stability. Analysis of the development and displacement history of 17 mapped fault and fault structures within 200 mi. (322 km) of the site found no evidence to indicate that these structures are capable faults as defined in Appendix A of 10 CFR 100. The closest known capable faults are

part of the Wabash Valley liquefaction features located about 170 mi. (274 km) south of the site, and the New Madrid seismic zone located about 400 mi. (644 km) south of the site.

The USGS Quaternary Fault and Fold Database of the United States, including the 2010 update (USGS, 2012c) contains no record of Quaternary faults or folds within an approximate 200 mi. (322 km) radius of the site. The Janesville fault, an approximately 19 mi. long (31 km) fault located approximately 6 mi. (10 km) north of Janesville (Figure 2.5-5), has no evidence of Pleistocene or post-Pleistocene activity. An unnamed, approximately 1.6 mi. long (2.6 km), east trending fault in the bedrock approximately 1.9 mi. (3.1 km) north of Janesville has a similar orientation to the Janesville fault, and is also considered not to be a capable fault. Surface faulting associated with future earthquakes is not anticipated to affect the site.

Geotechnical data collected from site-specific subsurface investigations show that the site has a very gentle gradient, and is underlain by more than 200 ft. (61.0 m) of dense to very dense sand, sandy silt and silty sand. The water table at the time of investigation was more than 50 ft. (15.2 m) bgs. Results of both a qualitative and quantitative liquefaction analysis demonstrate that there is no potential for liquefaction to occur within the soils underlying the site. The median factor of safety against liquefaction is 5.3, and ranges from 2 to 30. Geological hazards related to landslide occurrence, and other subsidence, karst formation and swelling clays are all considered to be insignificant at the site.

A project-specific earthquake catalog extracted from the CEUS-SSC (2012) catalog contains 58 records of historic earthquakes with epicenters located within about 200 mi. (322 km) of the site. Earthquake magnitudes range from E[**M**] 2.32 to 5.15. The largest recorded earthquake within 200 mi. (322 km) was the May 26, 1909 E[**M**] 5.15 event located approximately 85 mi. (137 km) southeast of the site. The closest earthquake epicenter to the site is the December 7, 1933 E[**M**] 3.03 event located approximately 21 mi. (34 km) to the northwest of the site. The MMI values from historic earthquakes within an approximate 200 mi. (322 km) radius of the site range from MMI III to MMI VII. The maximum felt intensity experienced at the site in historical times corresponds only to a moderate level shaking (MMI V). MMI V intensity may have occurred at the site four times in approximately the last 200 years during earthquakes that occurred in 1811, 1886, 1909, and 1972. The historical earthquake catalog indicates that in general, the region surrounding the site has an historic record of relatively infrequent, small to moderate earthquakes that is typical of much of the central and eastern United States.

National seismic hazard maps (USGS, 2012e) indicate that the site is located within one of the lowest seismic hazard regions in the conterminous United States. For example, a low hazard is illustrated by a PGA value of 0.19 g having a return period of more than 19,900 years. The low hazard is also reflected in the seismic parameters required for application of the 2009 IBC-ASCE 7-05 seismic design procedures. The site S_{MS} and S_{M1} values of 0.206 g and 0.119 g, respectively represent the MCE acceleration response spectral accelerations with a two percent probability of exceedance in the next 50 years (2475-year return period) for the site soil conditions. Regional earthquake hazard estimates, an estimated maximum potential earthquake of **M** 5.8 earthquake, and site-specific spectral accelerations required for application of the 2015 IBC-ASCE 7-05 seismic design procedures suggest that earthquake shaking should not be a major constraint for the development of facilities at the site.

Table 2.5-1 – Historic Earthquake Epicenters Located Within Approximately 200 Miles (322 km) of the SHINE Site
(Sheet 1 of 3)

Year[a]	Month[a]	Day[a][b]	Latitude (°N)[a]	Longitude (°W)[a]	Depth[a]	Expected Moment Magnitude (E[M])[a]	Distance to Site (km)[c]
1804	8	20	42.0	87.8	0	4.18	122
1804	8	24	42	89	0	4.12	69
1833	2	4	42.3	85.6	0	3.83	284
1861	12	23	42.09	87.98	0	2.98	105
1869	8	17	41.56	90.60	0	2.32	176
1876	5	22	41.29	89.51	0	3.31	154
1881	4	20	41.6	85.8	0	2.65	290
1881	5	27	41.3	89.1	0	4.44	147
1883	2	4	40.5	89.0	0	4.52	236
1883	2	4	42.3	85.6	0	4.73	284
1887	2	11	40.37	91.39	0	2.98	319
1889	3	3	40.5	89.0	0	2.65	236
1892	8	4	42.68	88.28	0	2.79	61
1893	12	20	41.62	85.95	0	3.96	278
1894	2	27	42.12	86.46	0	2.65	219
1894	11	9	42.12	86.46	0	2.65	219
1895	10	7	41.1	89.0	0	3.31	169
1897	6	6	43.33	91.51	0	3.01	217
1897	12	3	43.1	89.8	0	3.92	83
1897	12	3	42.4	90.4	0	3.31	116
1899	2	11	41.6	86.8	0	4.11	216
1899	2	11	43.35	85.40	0	2.67	306
1899	10	11	42.1	86.5	0	3.15	216
1900	3	14	45.5	89.5	0	2.32	322
1907	11	28	42.3	89.8	0	2.77	73
1909	5	26	41.6	88.1	0	5.15	137

Table 2.5-1 – Historic Earthquake Epicenters Located Within Approximately 200 Miles (322 km) of the SHINE Site
(Sheet 2 of 3)

Year[a]	Month[a]	Day[a][b]	Latitude (°N)[a]	Longitude (°W)[a]	Depth[a]	Expected Moment Magnitude (E[M])[a]	Distance to Site (km)[c]
1909	7	19	40.3	90.7	0	4.35	294
1909	10	22	41.8	89.7	0	2.98	107
1911	7	29	41.8	87.6	0	2.98	149
1912	1	2	42.3	89.0	0	4.38	36
1912	9	25	42.3	89.1	0	2.32	37
1913	10	17	41.8	89.7	0	3.38	107
1914	10	7	43.1	89.4	0	2.65	61
1921	2	26	39.85	88.93	0	2.32	308
1921	3	14	40	88	0	4.11	304
1922	7	7	43.8	88.5	0	4.1	137
1923	11	10	40.0	89.9	0	3.21	301
1925	1	26	42.5	92.4	0	2.62	277
1928	1	23	42	90	0	3.00	106
1933	12	7	42.9	89.2	0	3.03	34
1934	11	12	41.5	90.5	0	3.73	175
1938	2	12	41.6	87.0	0	3.69	202
1942	3	1	41.2	89.7	0	3.48	168
1944	3	16	42.0	88.3	0	2.61	92
1947	3	16	42.1	88.3	0	2.65	83
1947	5	6	43.0	87.9	0	3.53	101
1948	1	15	43.1	89.7	0	2.65	76
1948	4	20	41.7	91.8	0	2.65	251
1956	3	13	40.5	90.4	0	3.31	262
1956	7	18	43.6	87.7	0	2.65	153
1956	10	13	42.9	87.9	0	2.65	97
1957	1	8	43.5	88.8	0	2.32	99
1972	9	15	41.64	89.37	10	4.08	113
1978	2	16	39.80	88.23	5	2.38	321

Table 2.5-1 – Historic Earthquake Epicenters Located Within Approximately 200 Miles (322 km) of the SHINE Site
(Sheet 3 of 3)

Year[a]	Month[a]	Day[a][b]	Latitude (^{o}N)[a]	Longitude (^{o}W)[a]	Depth[a]	Expected Moment Magnitude (E[M])[a]	Distance to Site (km)[c]
1981	6	12	43.9	89.9	0	2.65	159
1985	9	9	41.848	88.014	5	2.91	120
1999	9	2	41.72	89.43	5	3.41	106
2004	6	28	41.44	88.94	5	4.13	132

a. Data from CEUS-SSC (2012).
b. Day is based on time with respect to Coordinated Universal Time (UTC), not local time.
c. Approximate Distance (ellipsoidal) earthquake epicenter to SHINE Janesville site estimated based on site location at 42.624136° N, 89.024875° W.

Table 2.5-2 – Modified Mercalli Intensity Scale

Level	Abbreviated Description
I	Not felt except by a very few under especially favorable conditions.
II	Felt only by a few persons at rest, especially on upper floors of buildings. Delicately suspended objects may swing.
III	Felt quite noticeably by persons indoors, especially on upper floors of buildings. Many people do not recognize it as an earthquake. Standing motor cars may rock slightly. Vibration similar to the passing of a truck. Duration estimated.
IV	Felt indoors by many, outdoors by a few during the day. At night, some awakened. Dishes, windows, doors disturbed; walls make cracking sound. Sensation like heavy truck striking building. Standing motor cars rocked noticeably.
V	Felt by nearly everyone; many awakened. Some dishes, windows broken. Unstable objects overturned. Pendulum clocks may stop.
VI	Felt by all, many frightened. Some heavy furniture moved; a few instances of fallen plaster. Damage slight.
VII	Damage negligible in buildings of good design and construction; slight to moderate in well-built ordinary structures; considerable damage in poorly built or badly designed structures; some chimneys broken.
VIII	Damage slight in specially designed structures; considerable damage in ordinary substantial buildings with partial collapse. Damage great in poorly built structures. Fall of chimneys, factory stacks, columns, monuments, walls. Heavy furniture overturned.
IX	Damage considerable in specially designed structures; well-designed frame structures thrown out of plumb. Damage great in substantial buildings, with partial collapse. Buildings shifted off foundations.
X	Some well-built wooden structures destroyed; most masonry and frame structures destroyed with foundations. Rail bent.
XI	Few, if any (masonry) structures remain standing. Bridges destroyed. Rails bent greatly.
XII	Damage total. Lines of sight and level are distorted. Objects thrown into the air.

Reference: USGS (2000).

Table 2.5-3 – Recorded Earthquake Intensities (Modified Mercalli Intensity – MMI) for Earthquakes Within Approximately 200 Miles (322 km) of the SHINE Site

			Earthquake					
Year[a]	Month[a]	Day[a][b]	Lat (°N)[a]	Long (°W)[a]	MMI[c]	Expected Moment Magnitude (E[M])[a]	Distance to Site (km)[d]	MMI at SHINE Janesville Site (Reported or Estimated)
1804	8	24	42	89	VI	4.12	69	-
1883	2	4	42.3	85.6	VI	4.73	284	-
1909	5	26	41.6	88.1	VII	5.15	137	V[e]
1909	7	19	40.3	90.7	VII	4.35	294	-
1912	1	2	42.3	89.0	III	4.38	36	Felt in Madison, Milwaukee[f]
1923	11	10	40.0	89.9	V	3.21	301	-
1928	1	23	42	90	IV	3.00	106	-
1942	3	1	41.2	89.7	IV	3.48	168	-
1972	9	15	41.64	89.37	VI	4.08	113	V[g]
1974	11	25	40.3	87.4	II	-	292	-
1985	9	9	41.848	88.014	V	2.91	120	-
1985	11	12	41.85	88.01	V	-	120	-

a. Data from CEUS-SSC (2012) source file; except 11/25/1974 and 11/12/1985 data from NEID (2012).
b. Day is based on time with respect to Coordinated Universal Time (UTC), not local time.
c. Maximum MMI for earthquake from NEID (2012) data.
d. Approximate distance (ellipsoidal) from earthquake epicenter to SHINE site estimated based on site location at 42.624136° N, 89.024875° W.
e. From Bakun and Hopper (2004).
f. From (USGS, 2012f), Wisconsin Earthquake History.
g. From NEID (2012) data for Janesville, Wisconsin (42.68° N, 89.02° W).

Table 2.5-4 – Recorded Earthquake Intensities (Modified Mercalli Intensity – MMI) for Earthquakes with Epicenters farther than 200 Miles (322 km) of the SHINE Site

				Earthquake				Distance to Site (km)[a]	MMI at Site (Reported or Estimated)
Year[b]	Month[a]	Day[a][c]	Location	Lat (°N)[a]	Long (°W)[a]	MMI[d]	(E[M])[a]		
1811	12	16	Arkansas	36	90	X	7.17	740	V[c]
1877	11	15	Nebraska	41	97	VII	5.50	686	Felt in Wisconsin[c]
1886	9	1	South Carolina	33.0	80.2	X	6.90	1319	II-III to IV[c]; V[f]
1891	9	27	Illinois	38.3	88.5	VII	5.52	482	I-III[e] (site is may be outside this iso-seismal)
1895	10	31	Missouri	37.82	89.32	VIII	6.00	534	IV[c]
1917	4	9	Illinois	37	90	VII	4.86	630	Felt in Wisconsin[c]
1925	3	1	Quebec	47.8	69.8	-	6.18	1611	III in Milwaukee and LaCrosse[g]
1935	11	1	Quebec	46.78	79.07	-	6.06	913	III[f]
1937	3	2	Ohio	40.488	84.273	VII	5.0Mfa	462	Felt in Milwaukee[g]
1937	3	9	Ohio	40.4	84.2	VIII	5.11	472	Felt in Milwaukee and Madison[g]
1939	11	23	Illinois	38.18	90.14	V	4.75	502	III[f]
1944	9	5	New York	45.0	74.7	VIII	5.71	1181	Felt in Wisconsin[g]
1968	11	9	Illinois	37.91	88.37	VII	5.32	526	I-III[c]; IV[f]
1974	4	3	Illinois	38.549	88.072	VI	4.29	460	I-III in southern Wisconsin[g]
1987	6	10	Illinois	38.713	87.954	VI	4.95	444	Felt in Wisconsin[c]

a. Data from CEUS-SSC (2012) source file: CEUS_EQ_Catalog_R0.shp; except 3/2/1937 data from Stover and Coffman(1993), Mfa (body-wave magnitude calculated from earthquake felt area).
b. Day is based on time with respect to Coordinated Universal Time (UTC), not local time.
c. From Stover and Coffman (1993).
d. Approximate distance (ellipsoidal) from earthquake epicenter to SHINE Site estimated based on site location at 42.624136° N, 89.024875° W.
e. From Bakun and Hopper (2004).
f. From NEID (2012) for Janesville, Wisconsin (42.68° N, 89.02° W).
g. From (USGS, 2012f), Wisconsin Earthquake History.

Table 2.5-5 – Probabilistic Estimates of PGA for Selected Return Periods at the SHINE Site for an Average Shear Wave Velocity (760 m/s) Site Class B[(a)]

Return Period (years)	PGA (g)
475	0.017
2,475	0.050
4,975	0.079
9,950	0.124
19,900	0.194

a. Parameters based on SHINE site location of 42.624°N, 89.025°W.

Table 2.5-6 – IBC-ASCE 7-05 Seismic Parameters for the SHINE Site[a][b][c]

Parameter	Value
S_S	0.129 g
S_1	0.050 g
Site Class	D
S_{MS}	0.206 g
S_{M1}	0.119 g
F_a	1.6
F_v	2.4
T_L	12 seconds

a. Parameters based on SHINE site location of 42.624136°N, 89.024875°W.
b. Parameters include the following: short period spectral response acceleration (S_S); 1-second spectral response acceleration (S_1); maximum considered earthquake spectral response for short period (S_{MS}); maximum considered earthquake spectral response for 1-second period (S_{M1}); site coefficient for short period (F_a); site coefficient for 1- second period (F_v) (IBC, 2015); and long-period transition period (T_L) (ASCE, 2005).
c. S_S and S_1 are for Site Class B; S_{MS} and S_{M1} are for Site Class D.

Figure 2.5-1 – Site Vicinity Map

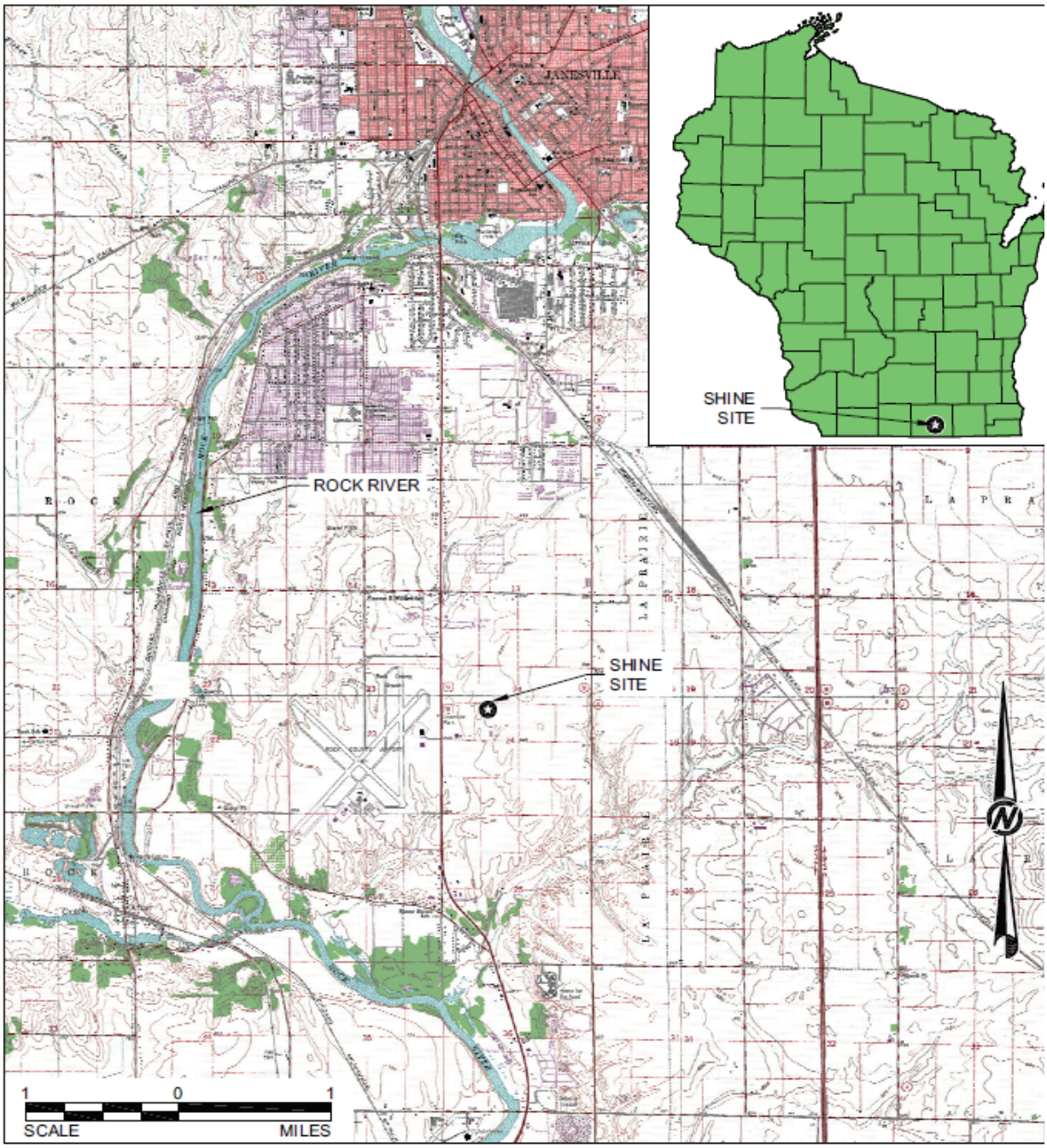

LEGEND

SHINE SITE

REFERENCES

WDNR, 2012

Figure 2.5-2 – Map of Physiographic Sections

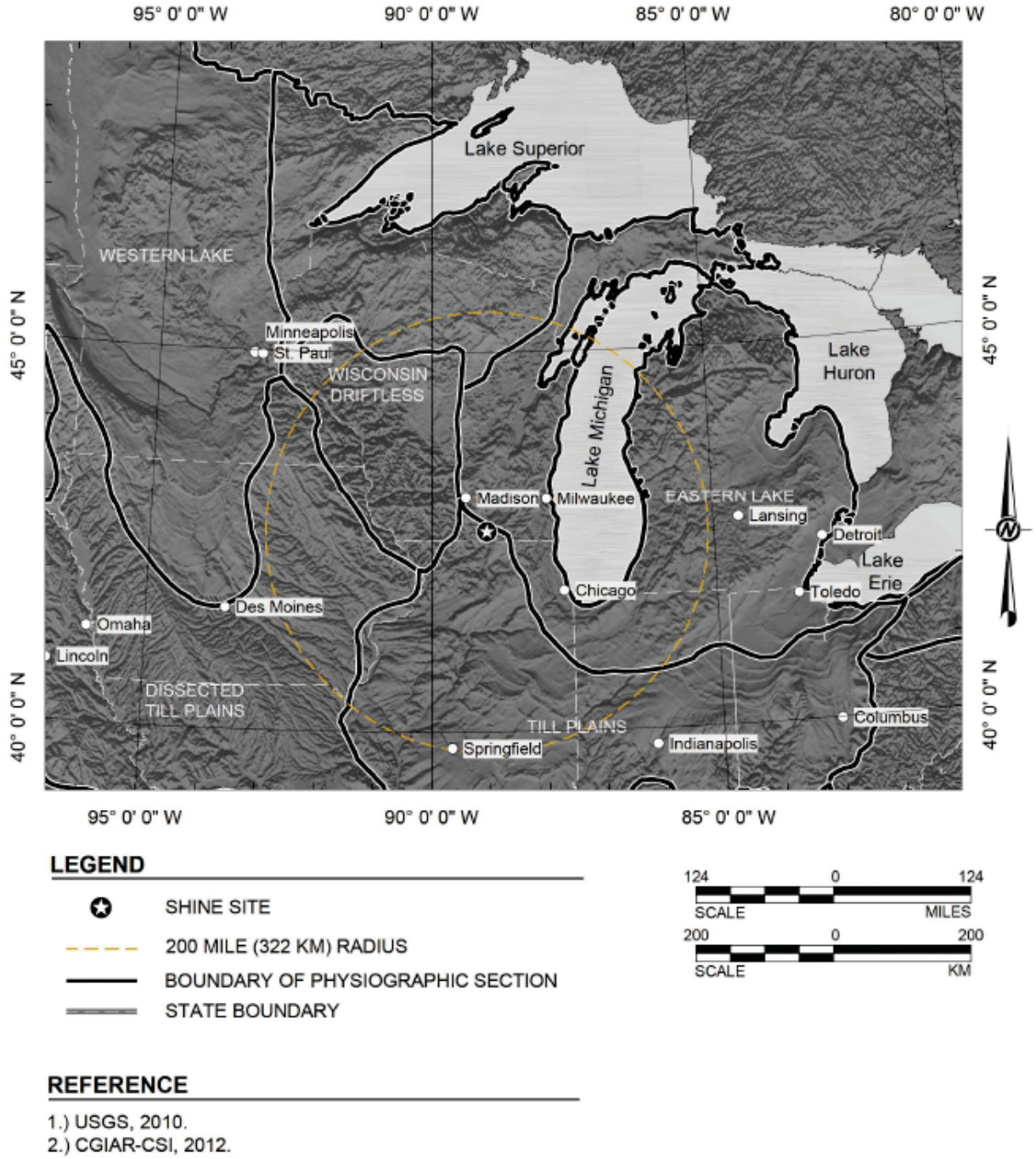

REFERENCE

1.) USGS, 2010.
2.) CGIAR-CSI, 2012.

Figure 2.5-3 – Tectonic Provinces Map

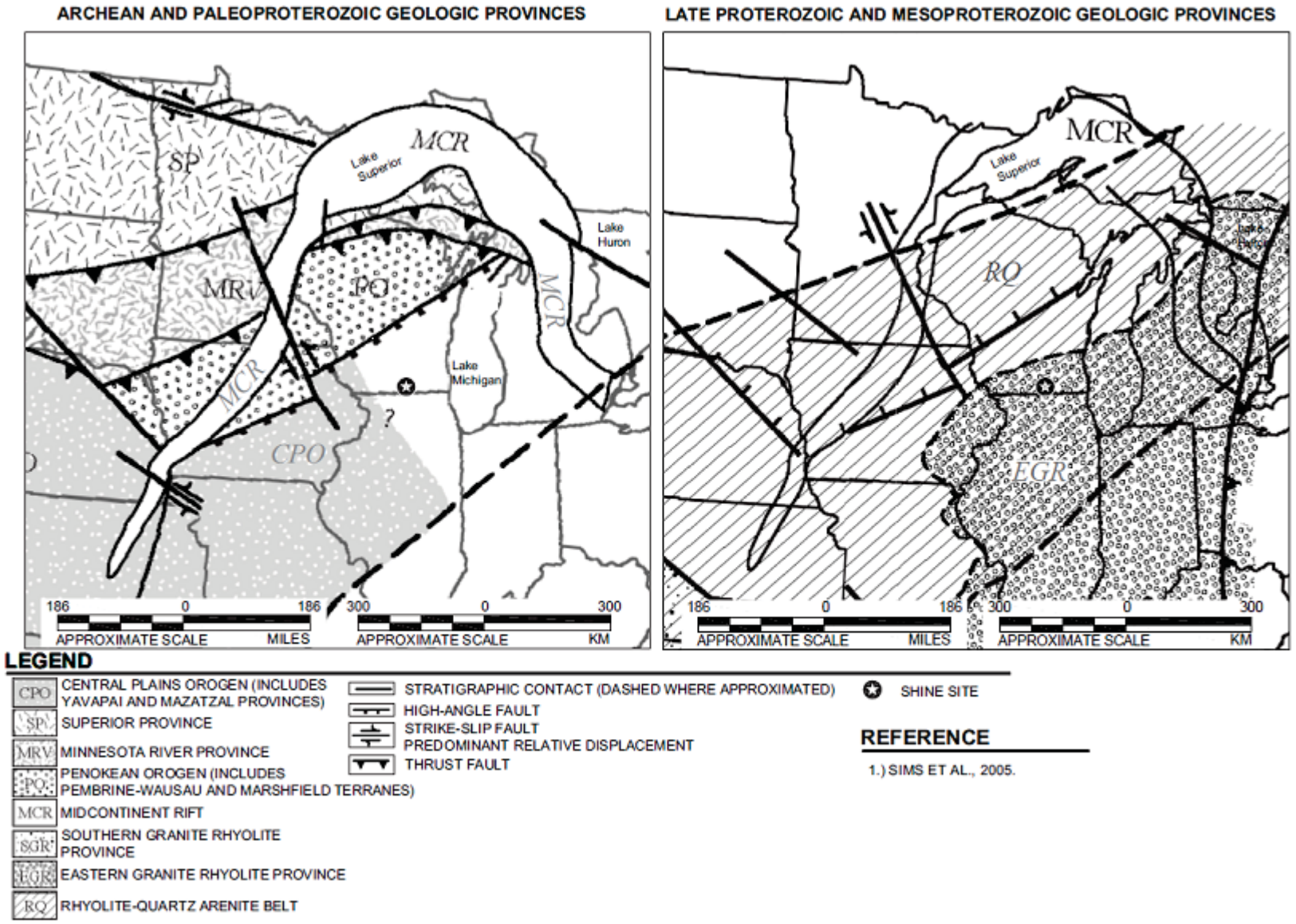

Figure 2.5-4 – Generalized Regional Structural Geologic Map

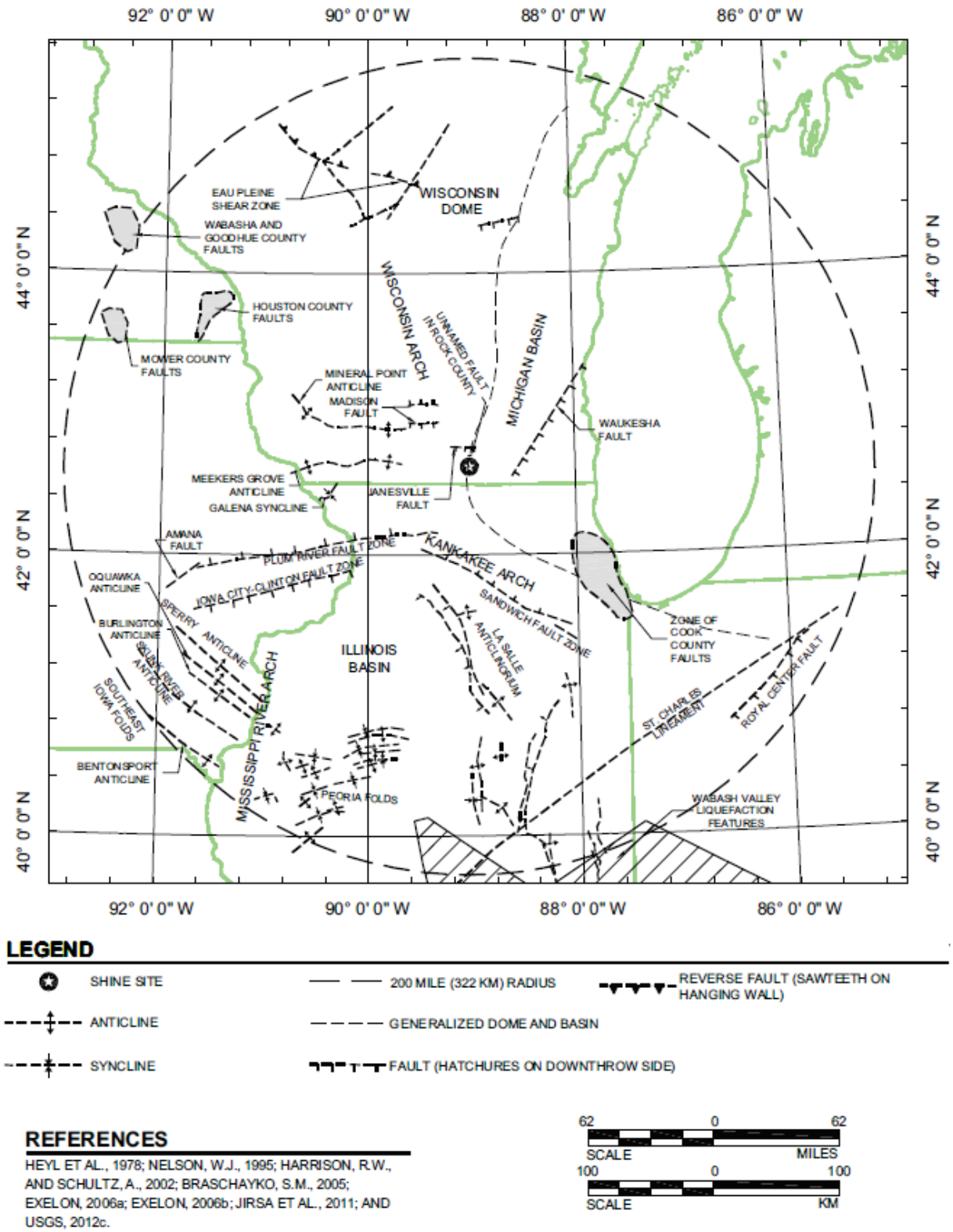

REFERENCES

HEYL ET AL., 1978; NELSON, W.J., 1995; HARRISON, R.W., AND SCHULTZ, A., 2002; BRASCHAYKO, S.M., 2005; EXELON, 2006a; EXELON, 2006b; JIRSA ET AL., 2011; AND USGS, 2012c.

Figure 2.5-5 – Generalized Regional Geologic Map

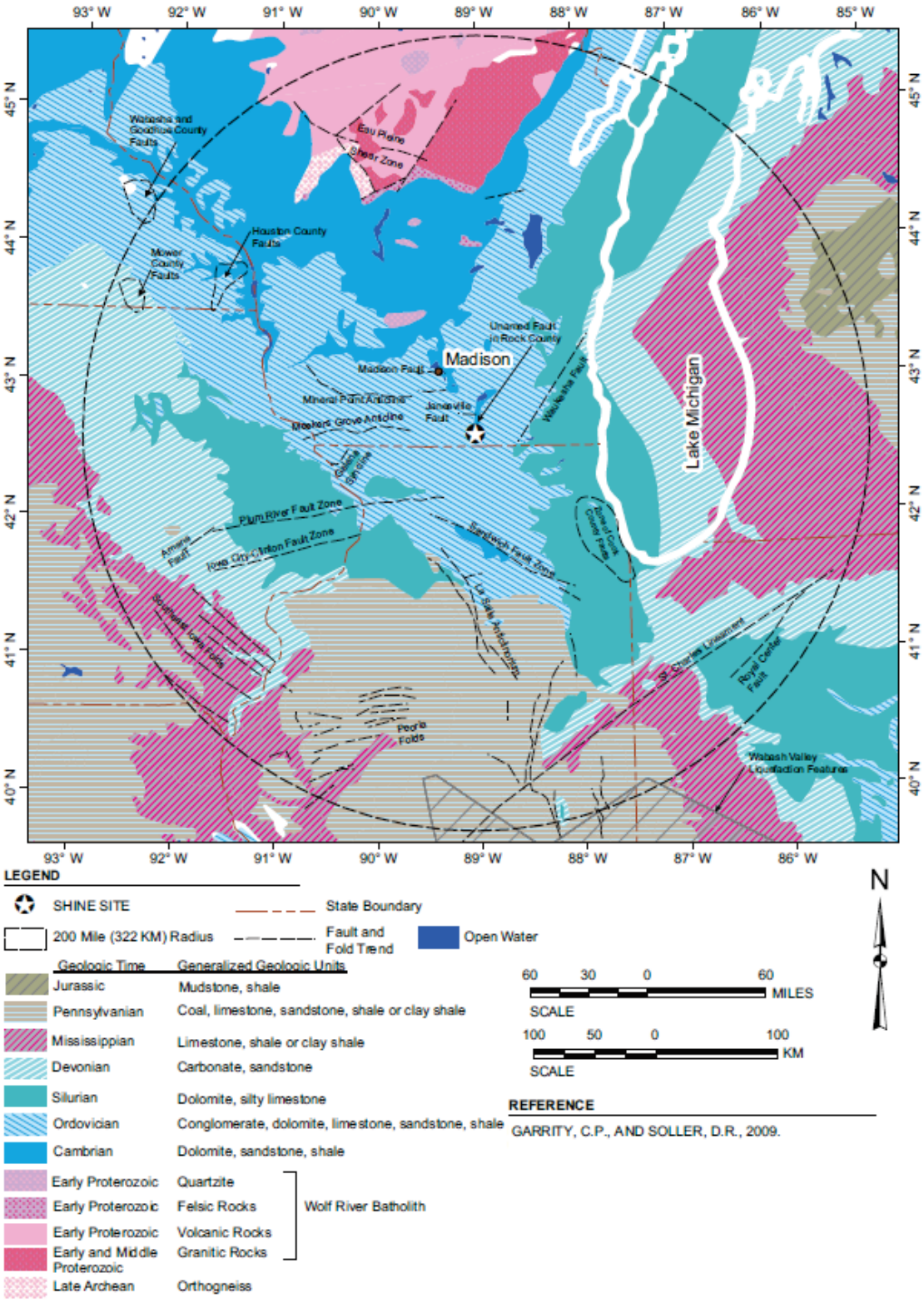

Figure 2.5-6 – Regional Magnetic Anomaly Map and Structural Interpretation

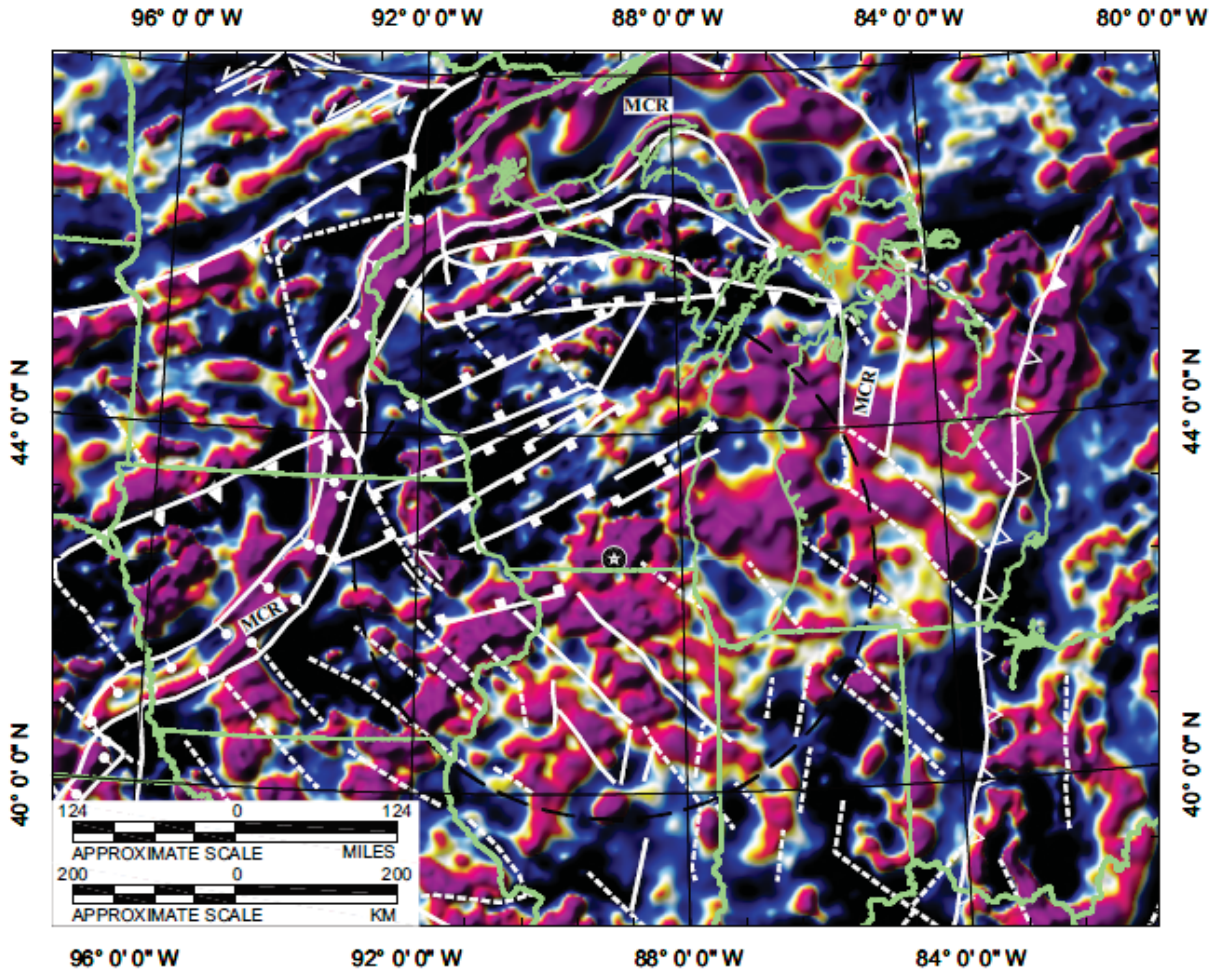

LEGEND

- SHINE SITE
- MCR MIDCONTINENT RIFT
- 200 MILE (322 KM) RADIUS
- HIGH-ANGLE FAULT - CHIEFLY TRANSCURRENT SHEARS AND FAULTS OF LATE PALEOPROTEROZOIC - MESOPROTERZOIC AGE, BUT INCLUDES FAULTS OF LATE ARCHEAN AGE IN NORTHERN MIDCONTINENT. ARROWS INDICATE RELATIVE DISPLACEMENT WHERE KNOWN. SOLID LINE, BASED CHIEFLY ON GEOLOGIC DATA; DASHED LINE, BASED CHIEFLY ON MAGNETIC DATA. NOTE: SAME DISTINCTION APPLIES TO STRUCTURES FOLLOWING:
- DUCTILE SHEAR ZONE; MAINLY OF LATE PALEOPROTEROZOIC AGE
- BOUNDARY OF MAJOR RIFT ZONE OF LATE MESOPROTEROZOIC (MIDCONTINENT RIFT) AND CAMBRIAN (REELFOOT RIFT) AGE
- THRUST FAULT OF MESOPROTEROZOIC (~1.1 Ga) AGE
- THRUST FAULT OF PALEOPROTEROZOIC AGE ASSOCIATED WITH SUTURE ZONES. SOLID LINE, BASED CHIEFLY ON GEOLOGIC DATA; DASHED LINE BASED CHIEFLY ON MAGNETIC DATA.

Total Intensity Anomaly
nT
-200 -150 -100 -50 0 50 100 150 200

REFERENCE

1.) MAUS ET AL., 2009.
2.) SIMS ET AL., 2005.

Figure 2.5-7 – Regional Magnetic Anomaly Map and Structural Interpretation

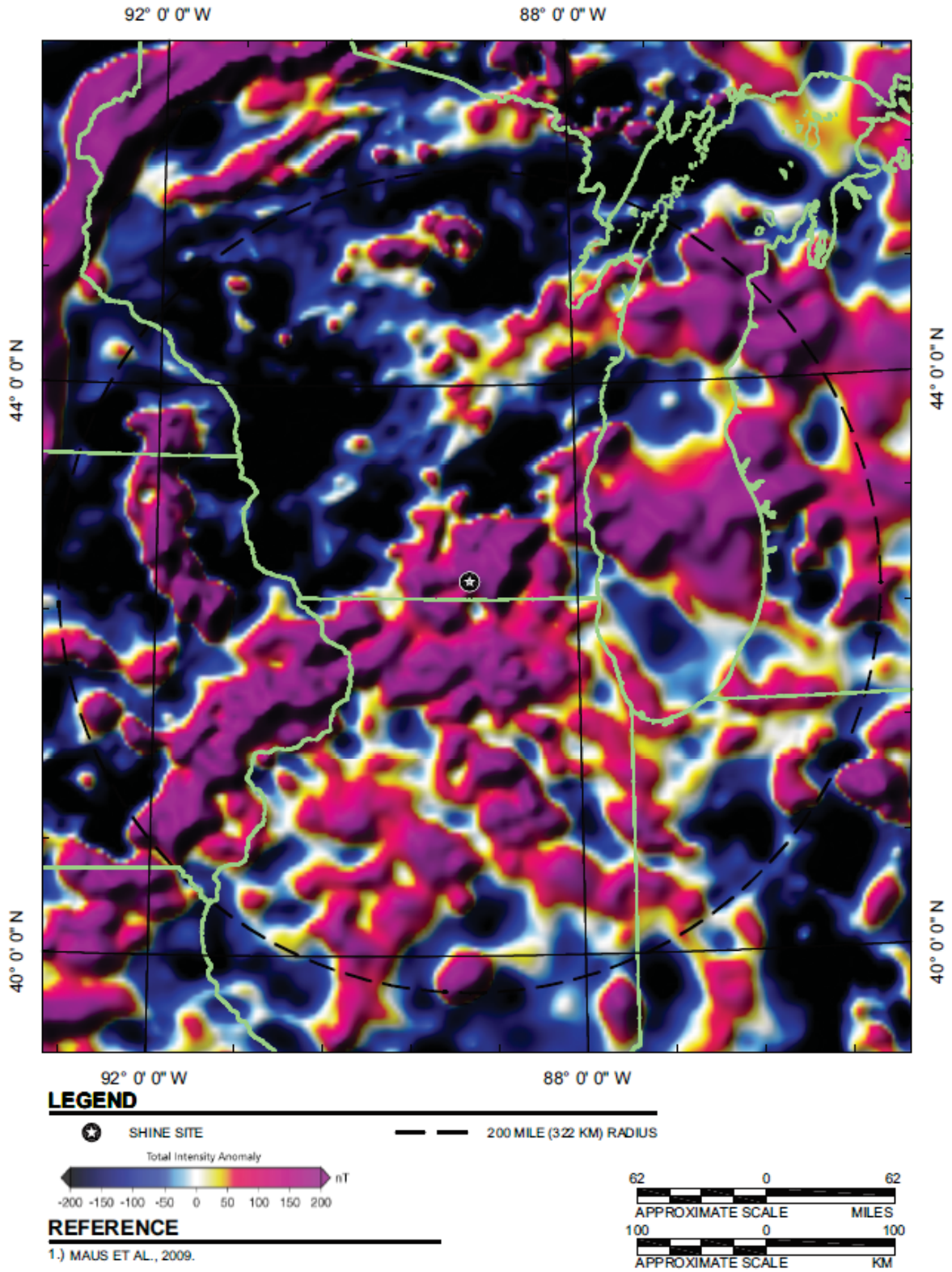

Figure 2.5-8 – Regional Bouguer Gravity Anomaly Map

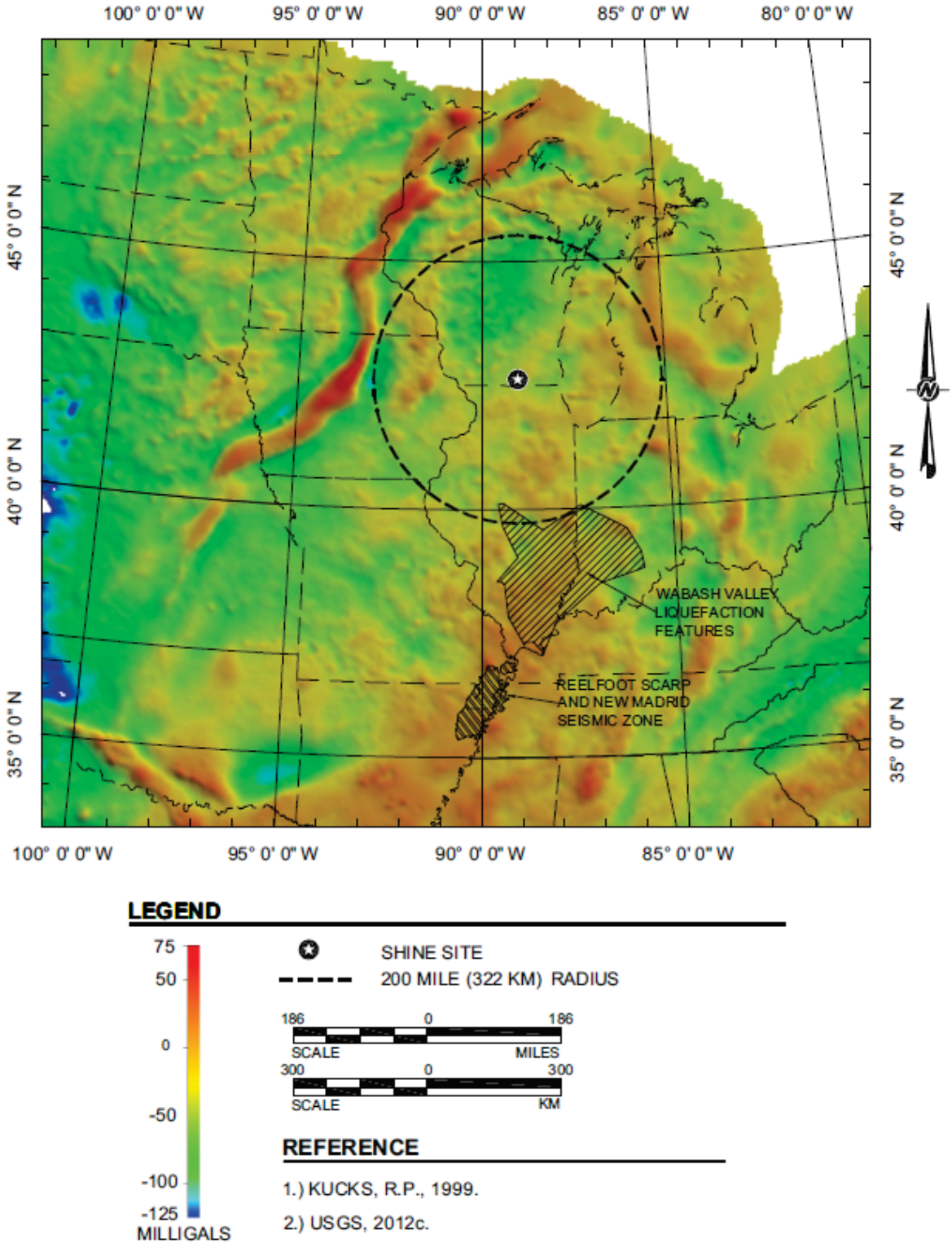

Figure 2.5-9 – Bouguer Gravity Anomaly Map of Wisconsin and Northern Illinois

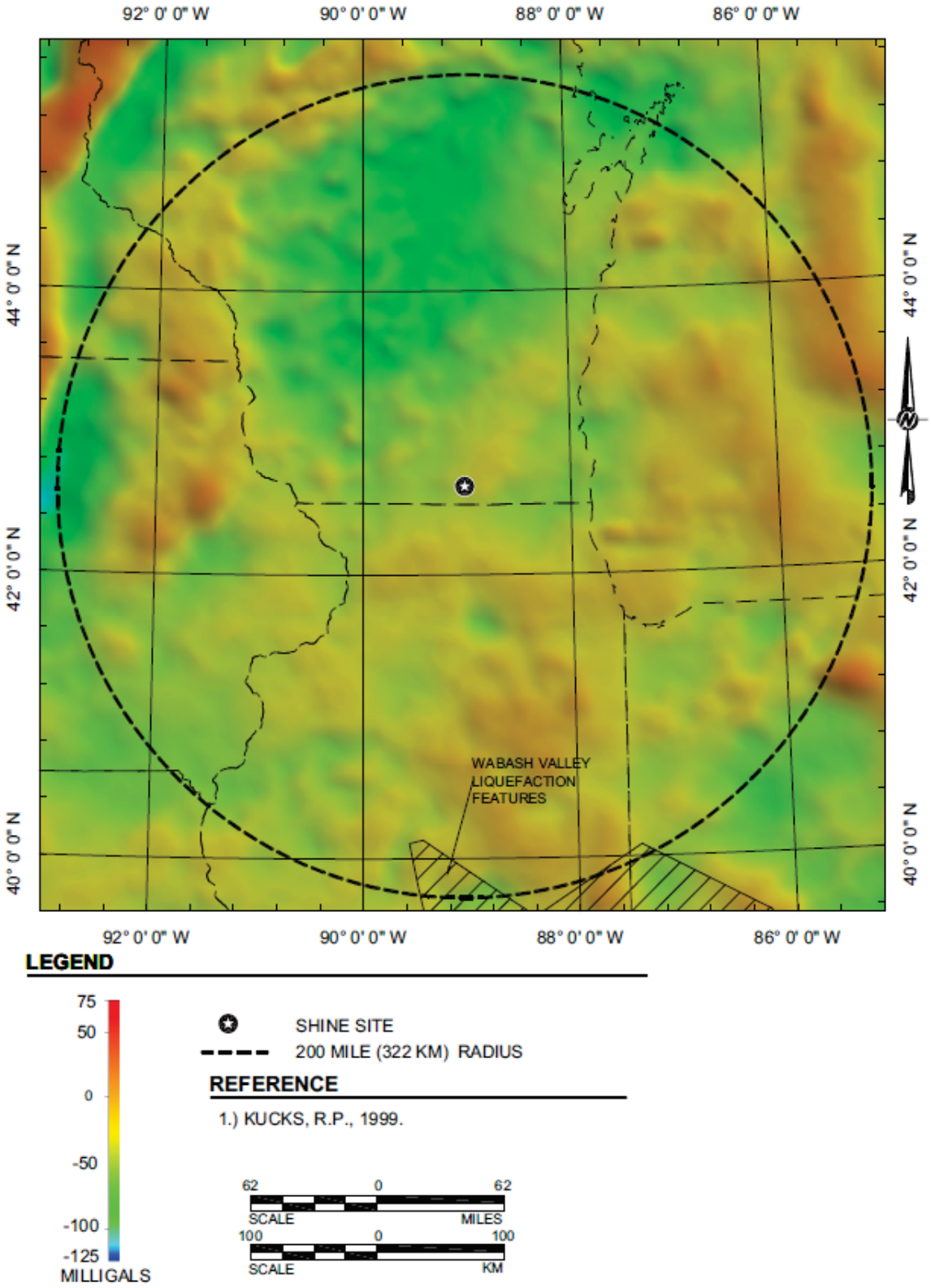

Figure 2.5-10 – Composite Aeromagnetic Anomalies and Main Geological Structures, Southern Wisconsin

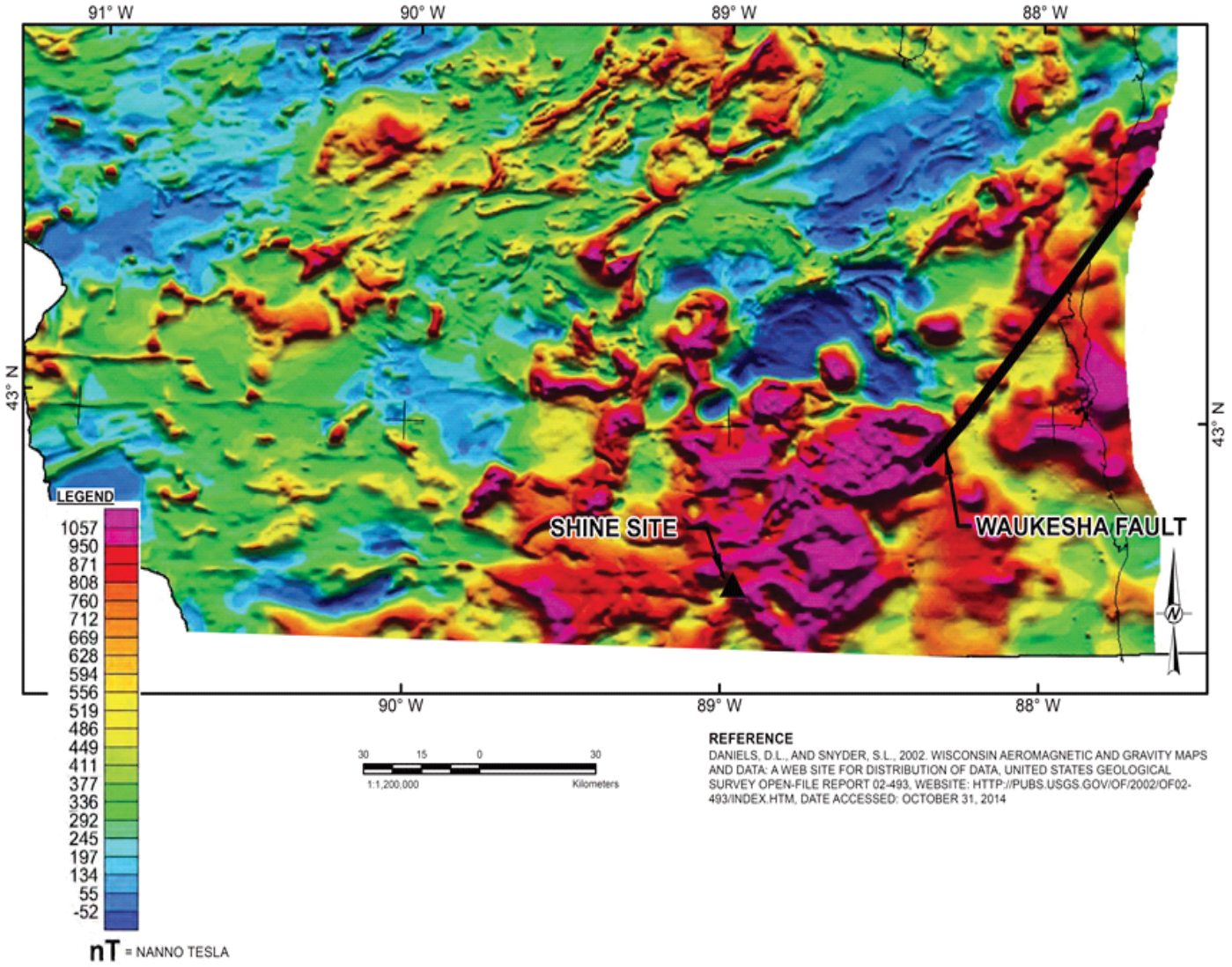

Figure 2.5-11 – Bouguer Gravity Anomalies and Main Geological Structures, Southern Wisconsin

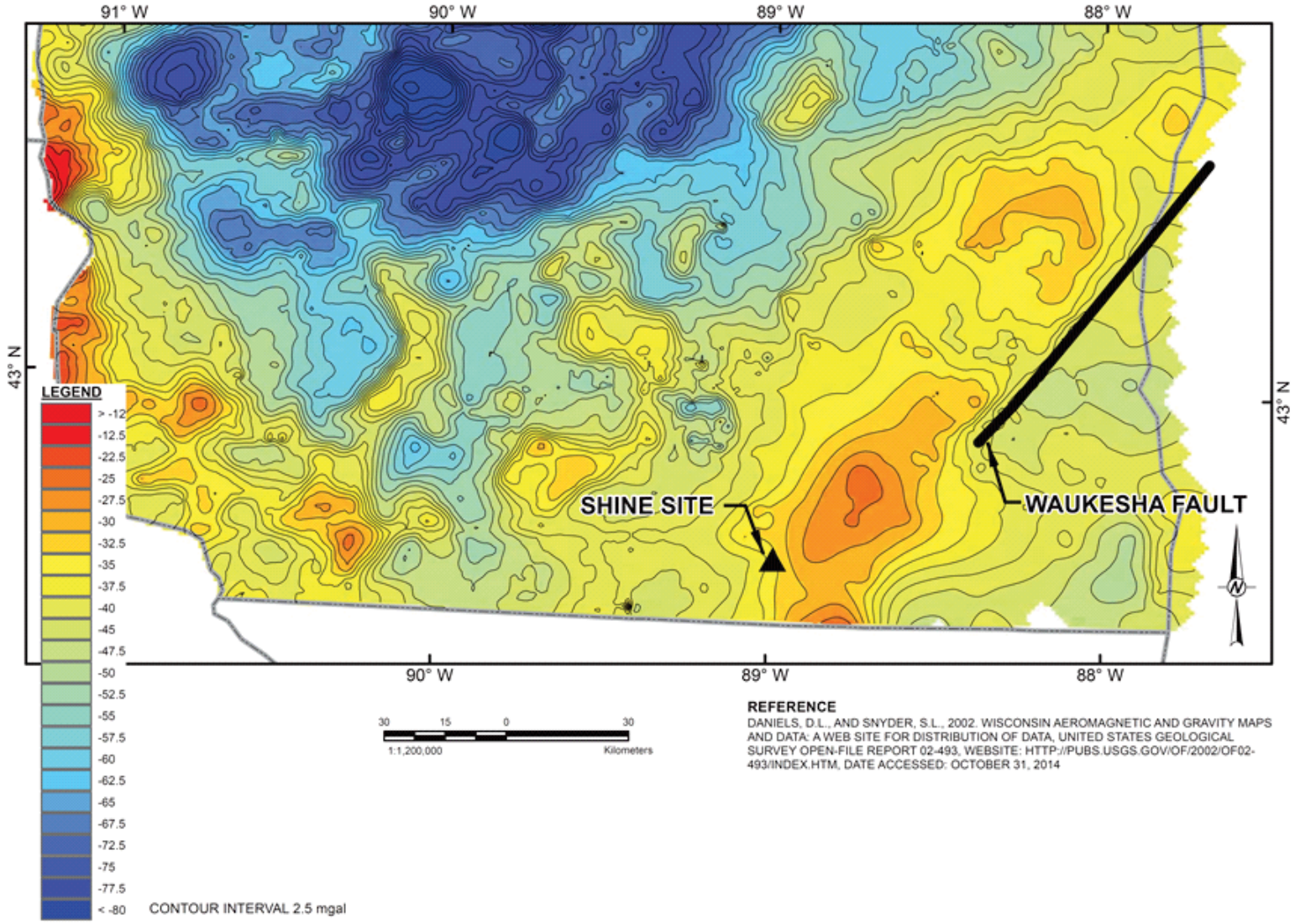

Figure 2.5-12 – Regional Surficial Geology Map

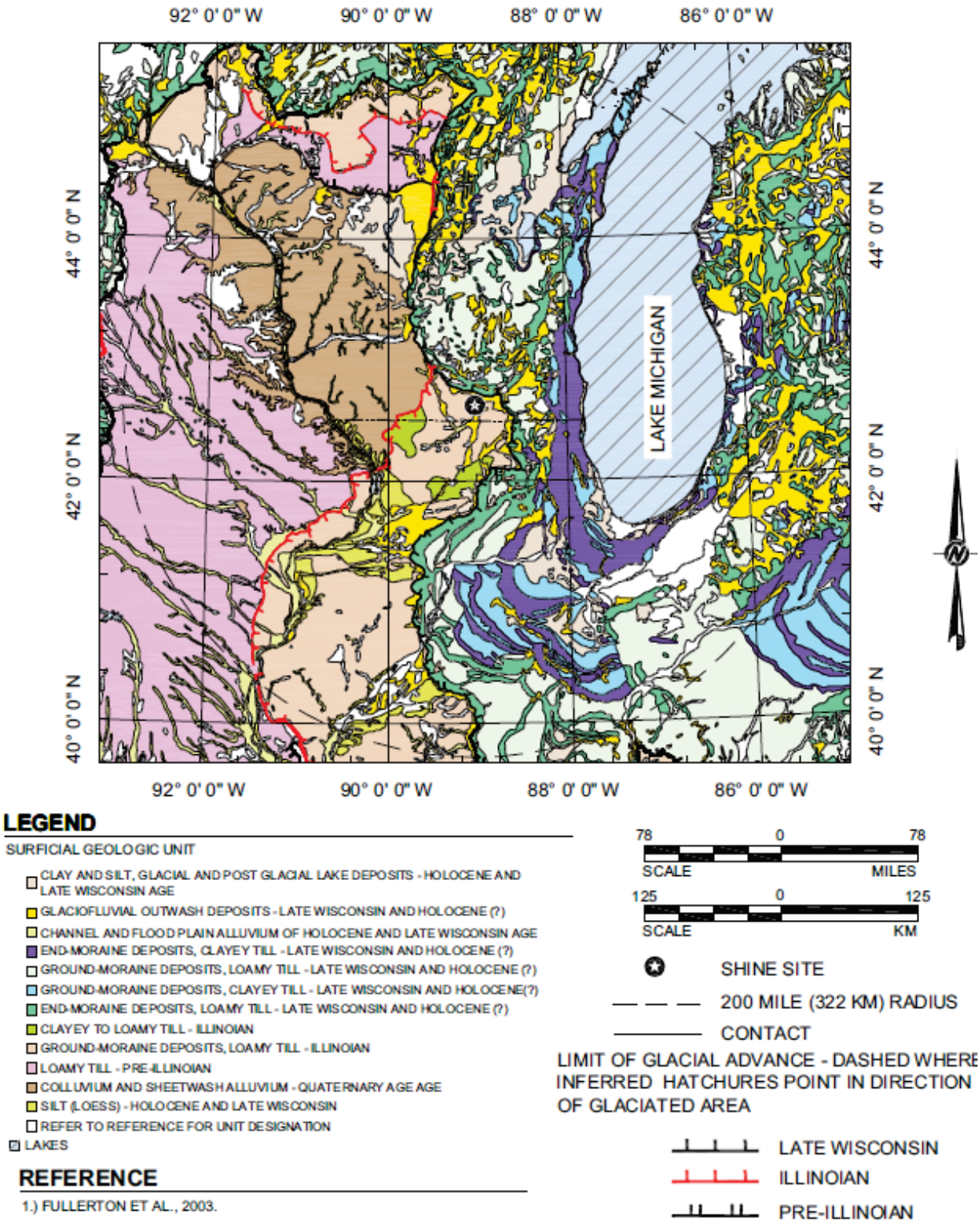

Figure 2.5-13 – Unconsolidated and Drift Thicknesses Map of Wisconsin and Northern Illinois

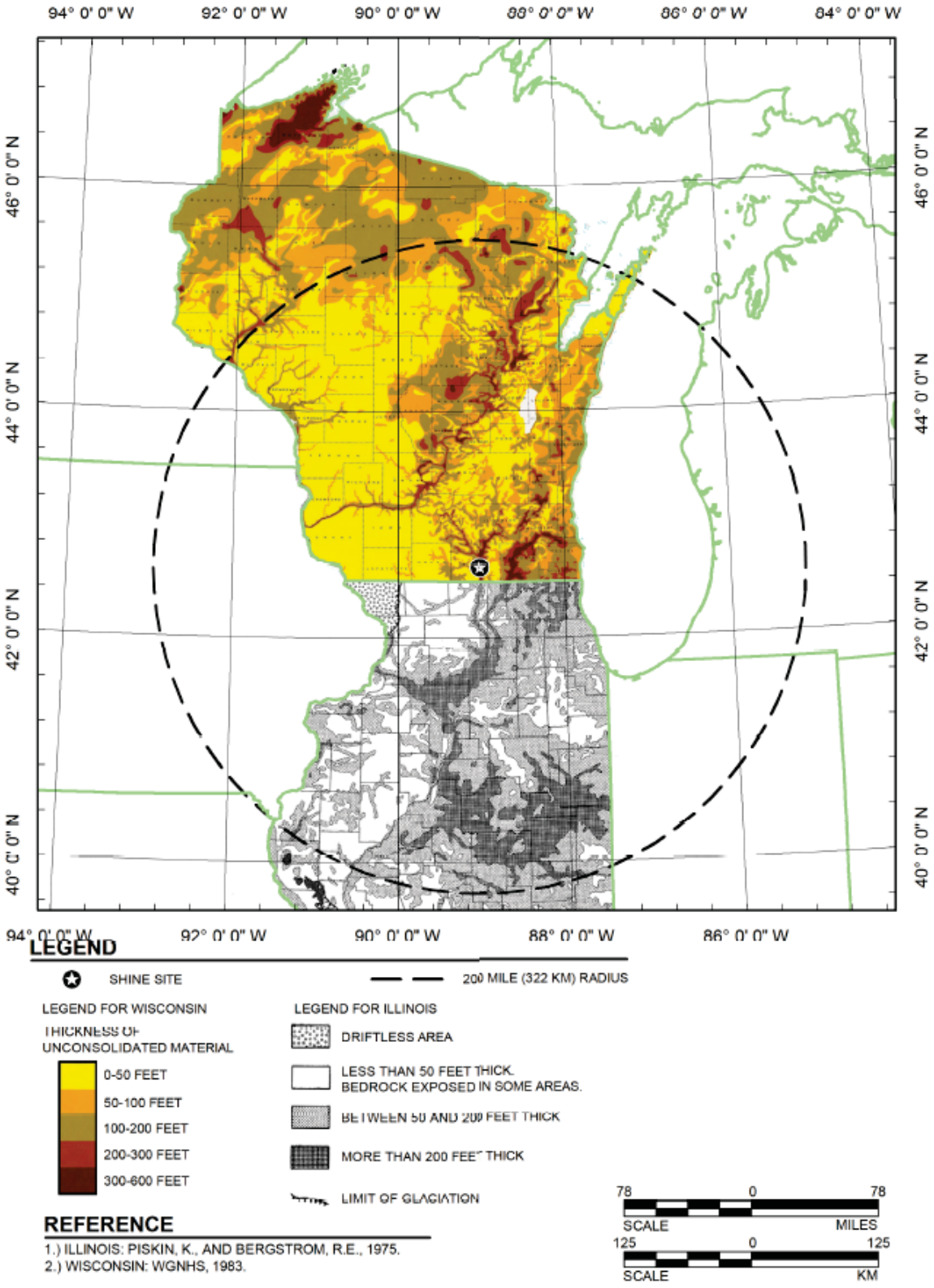

Figure 2.5-14 – Historical Earthquake Epicenters

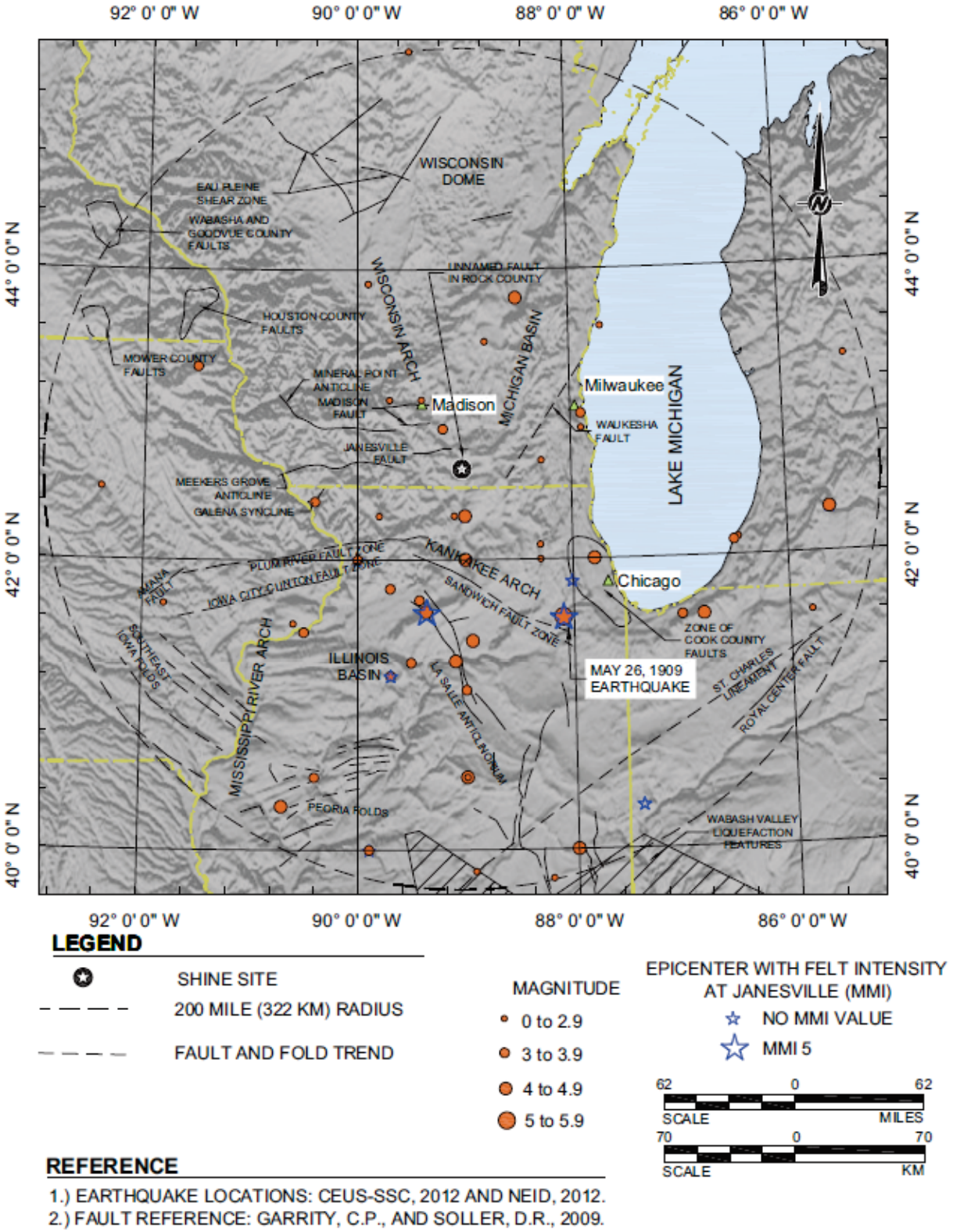

Figure 2.5-15 – Isoseismal Map December 16, 1811 Earthquake

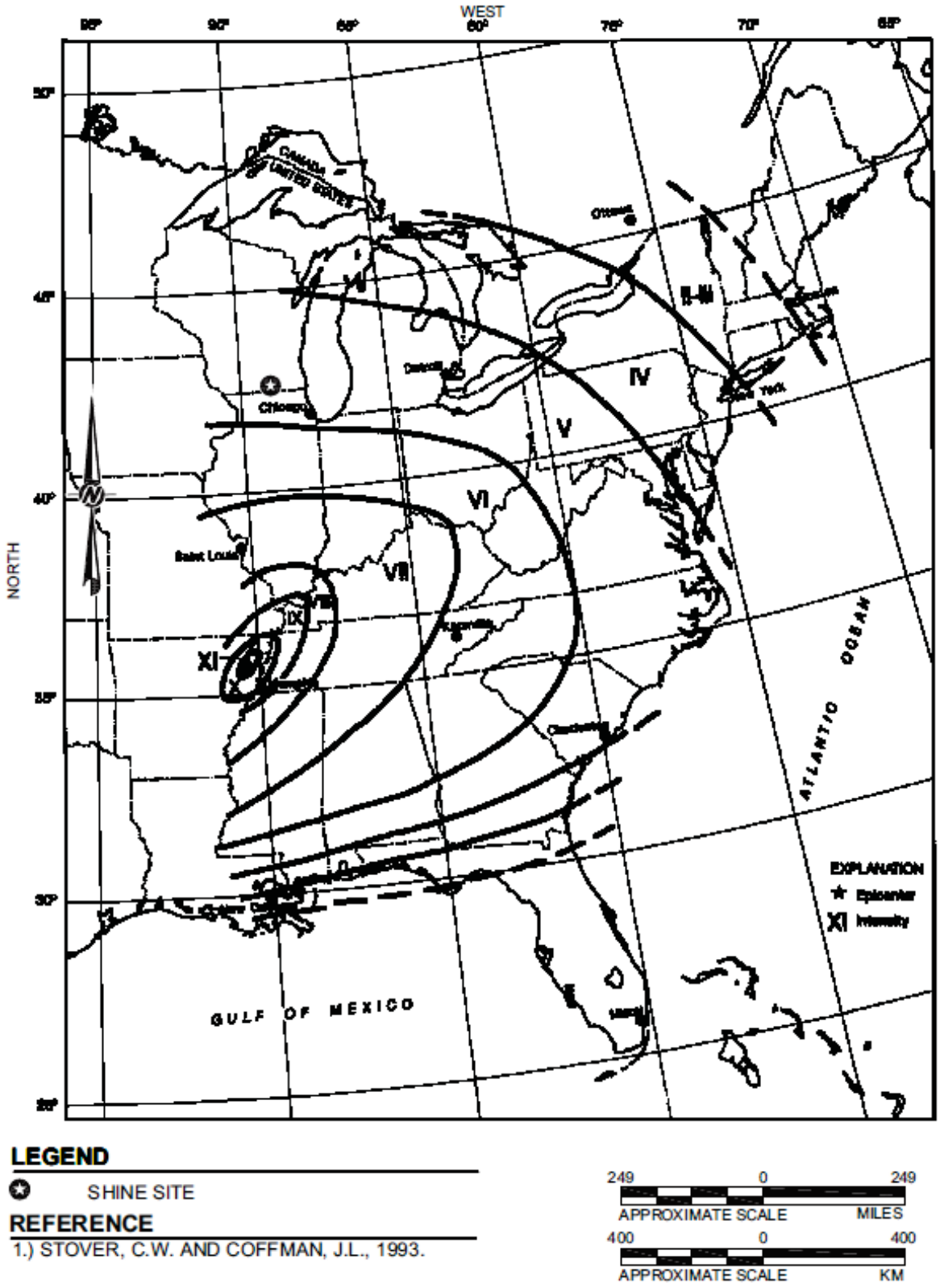

Figure 2.5-16 – Isoseismal Map September 01, 1866 Earthquake

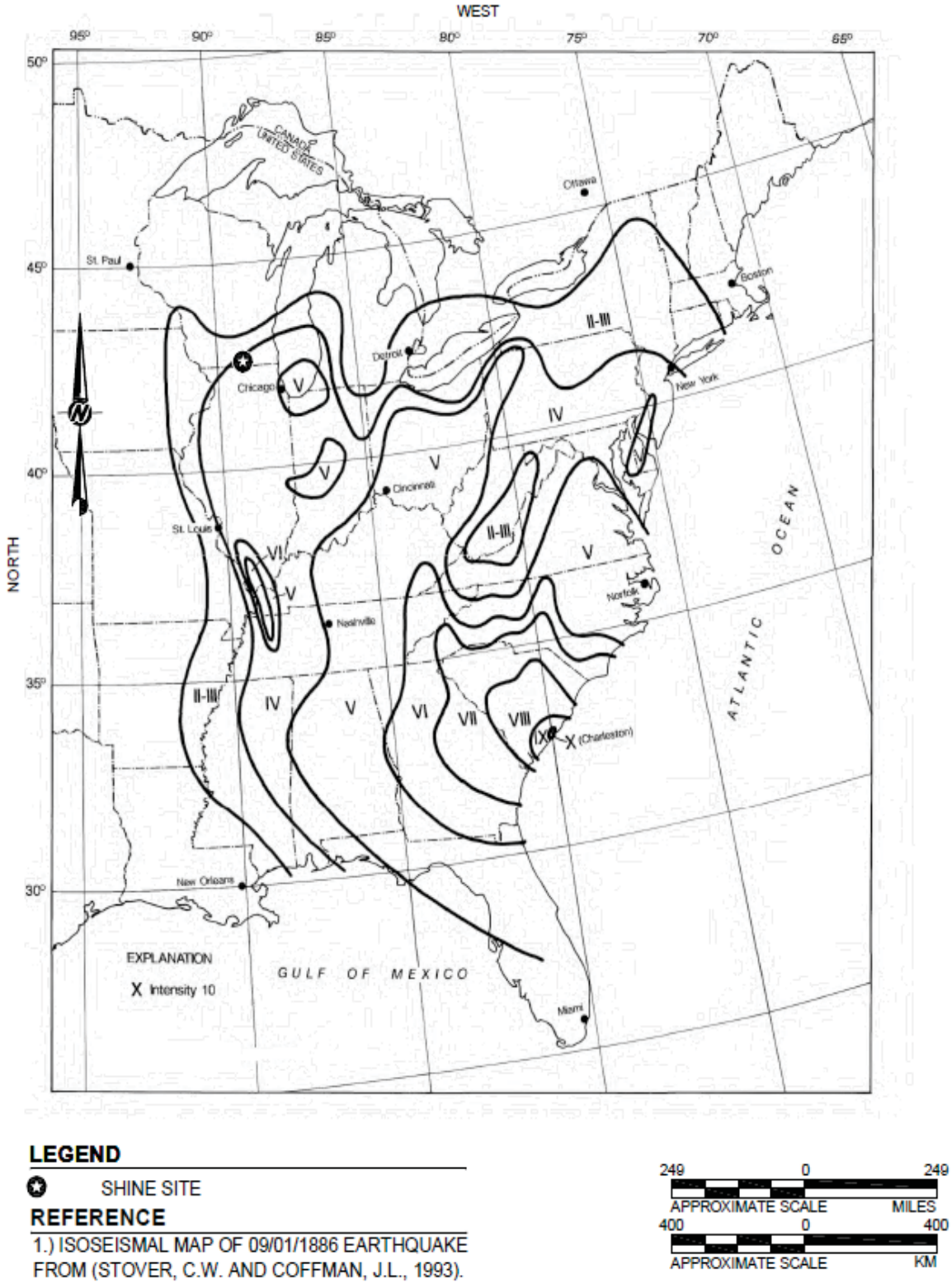

Figure 2.5-17 – Isoseismal Map September 27, 1891 Earthquake

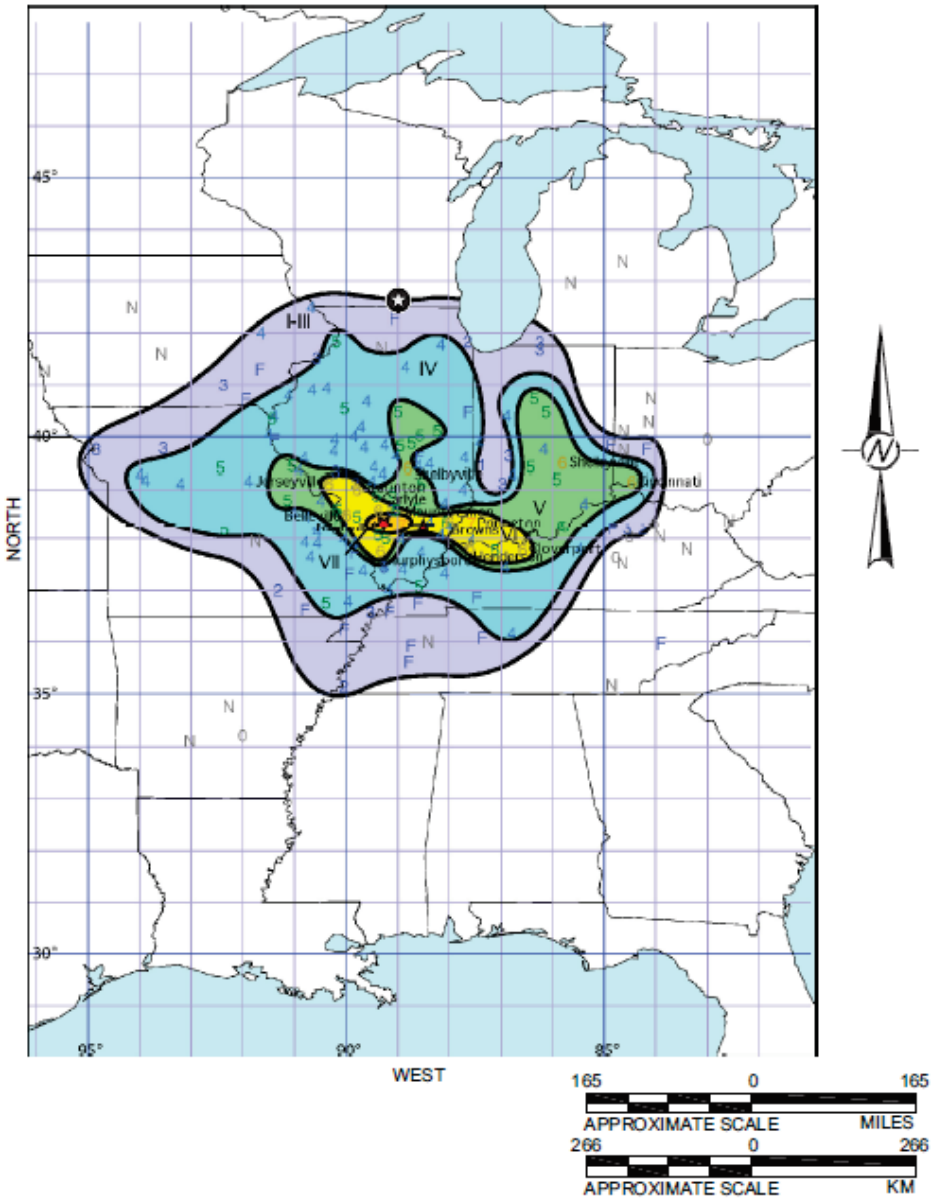

LEGEND

SHINE SITE

NUMBERS ARE MMI ASSIGNMENTS:

F - DENOTES THAT THE EVENT WAS FELT, BUT THAT THE INFORMATION IS NOT SUFFICIENT TO ASSIGN AN MMI.

O - DENOTES THAT THE EVENT WAS REPORTED AS NOT FELT.

N - DENOTES THAT THE EVENT WAS NOT MENTIONED AND IS PRESUMED "NOT FELT".

THE THICK BLACK ISOSEISMAL LINES ENCLOSE ISOSEISMAL AREAS.

THE EASTERN RED STAR IS STOVER AND COFFMAN'S (1993) EPICENTER LOCATION.

THE WESTERN RED STAR IS BAKUN AND HOPPER'S (2004) PREFERRED EPICENTER LOCATION.

REFERENCE

1.) BAKUN, W.H. AND HOPPER, M.G., 2004.

Figure 2.5-18 – Isoseismal Map October 31, 1895 Earthquake

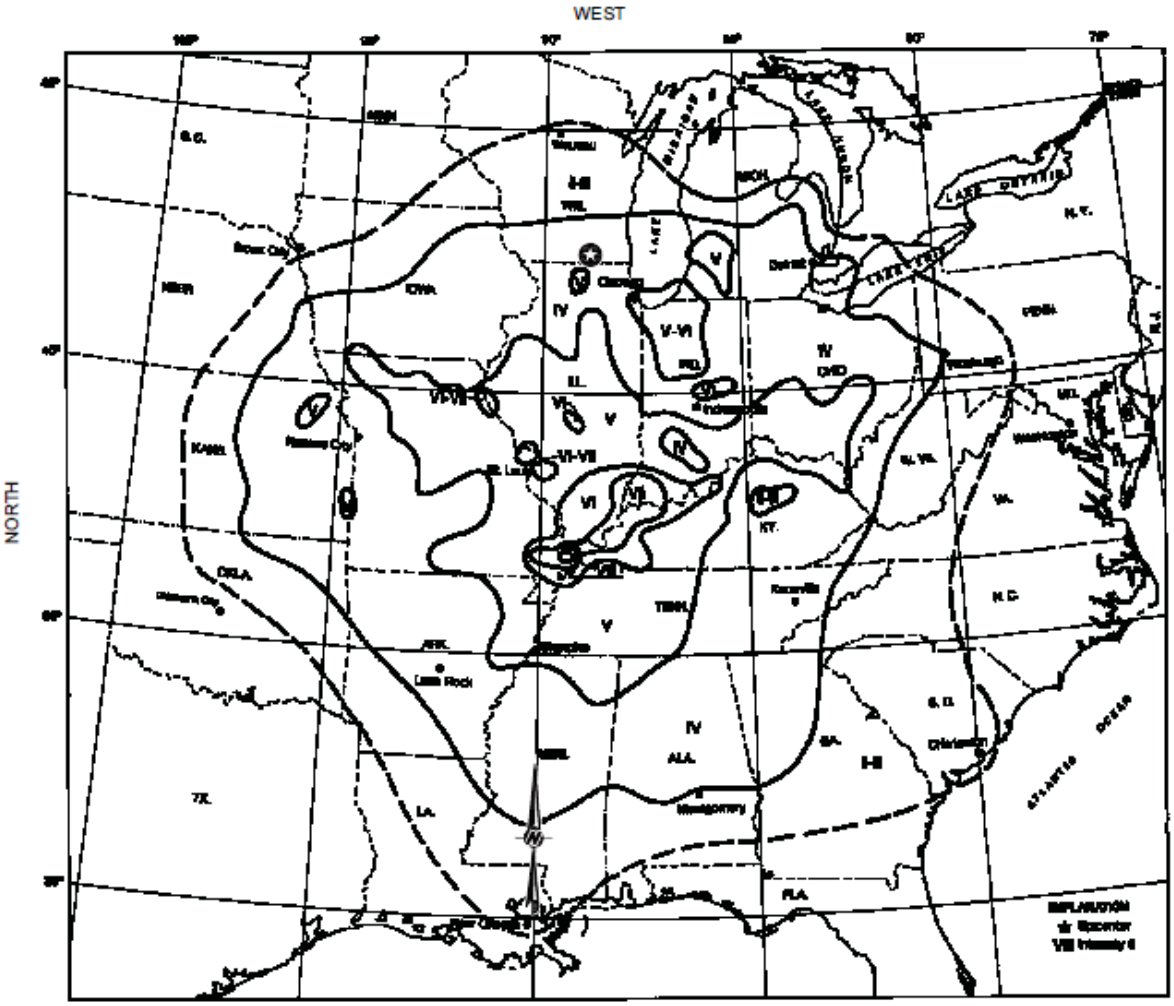

Figure 2.5-19 – Isoseismal Map May 26, 1909 Earthquake

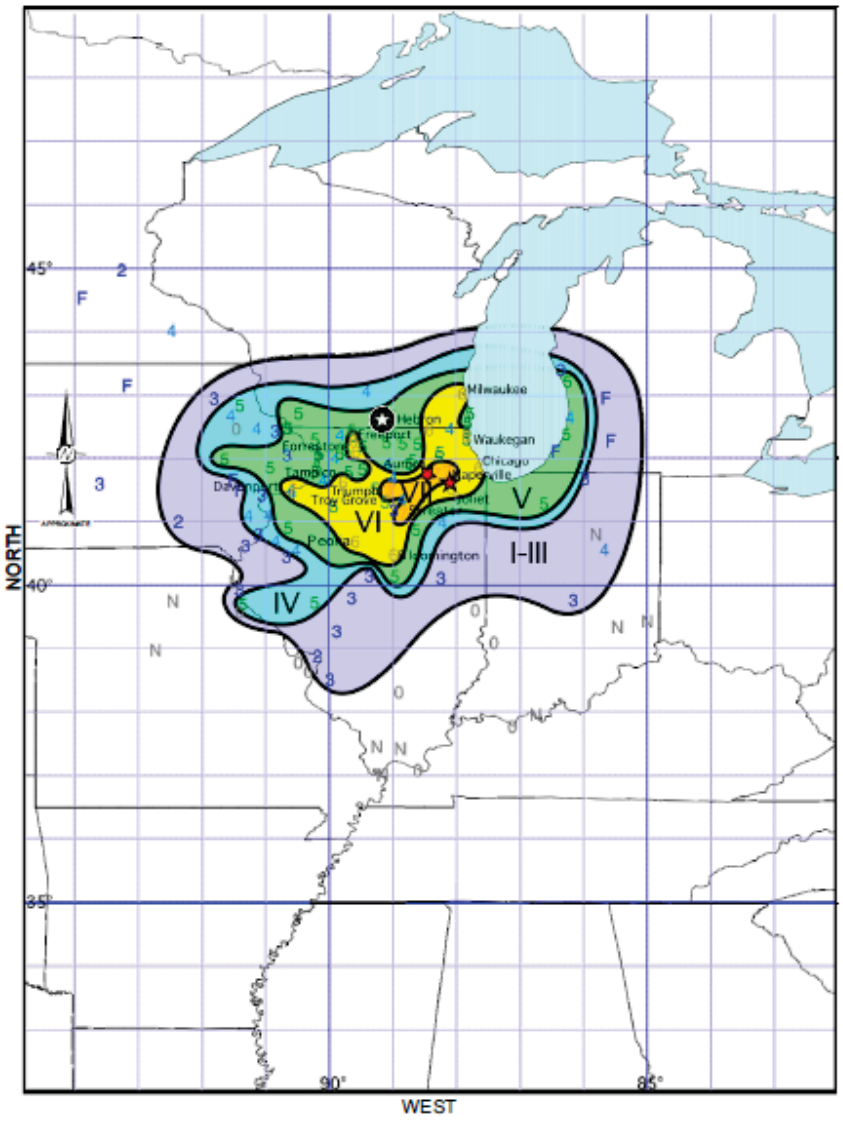

LEGEND

SHINE SITE

NUMBERS ARE MMI ASSIGNMENTS:

F - DENOTES THAT THE EVENT WAS FELT, BUT THAT THE INFORMATION IS NOT SUFFICIENT TO ASSIGN AN MMI.

O - DENOTES THAT THE EVENT WAS REPORTED AS NOT FELT.

N - DENOTES THAT THE EVENT WAS NOT MENTIONED AND IS PRESUMED "NOT FELT".

THE THICK BLACK ISOSEISMAL LINES ENCLOSE ISOSEISMAL AREAS.

THE EASTERN RED STAR IS STOVER AND COFFMAN'S (1993) EPICENTER LOCATION.

THE WESTERN RED STAR IS BAKUN AND HOPPER'S (2004) PREFERRED EPICENTER LOCATION.

REFERENCE

1.) BAKUN, W.H. AND HOPPER, M.G., 2004.

Figure 2.5-20 – Isoseismal Map November 09, 1968 Earthquake

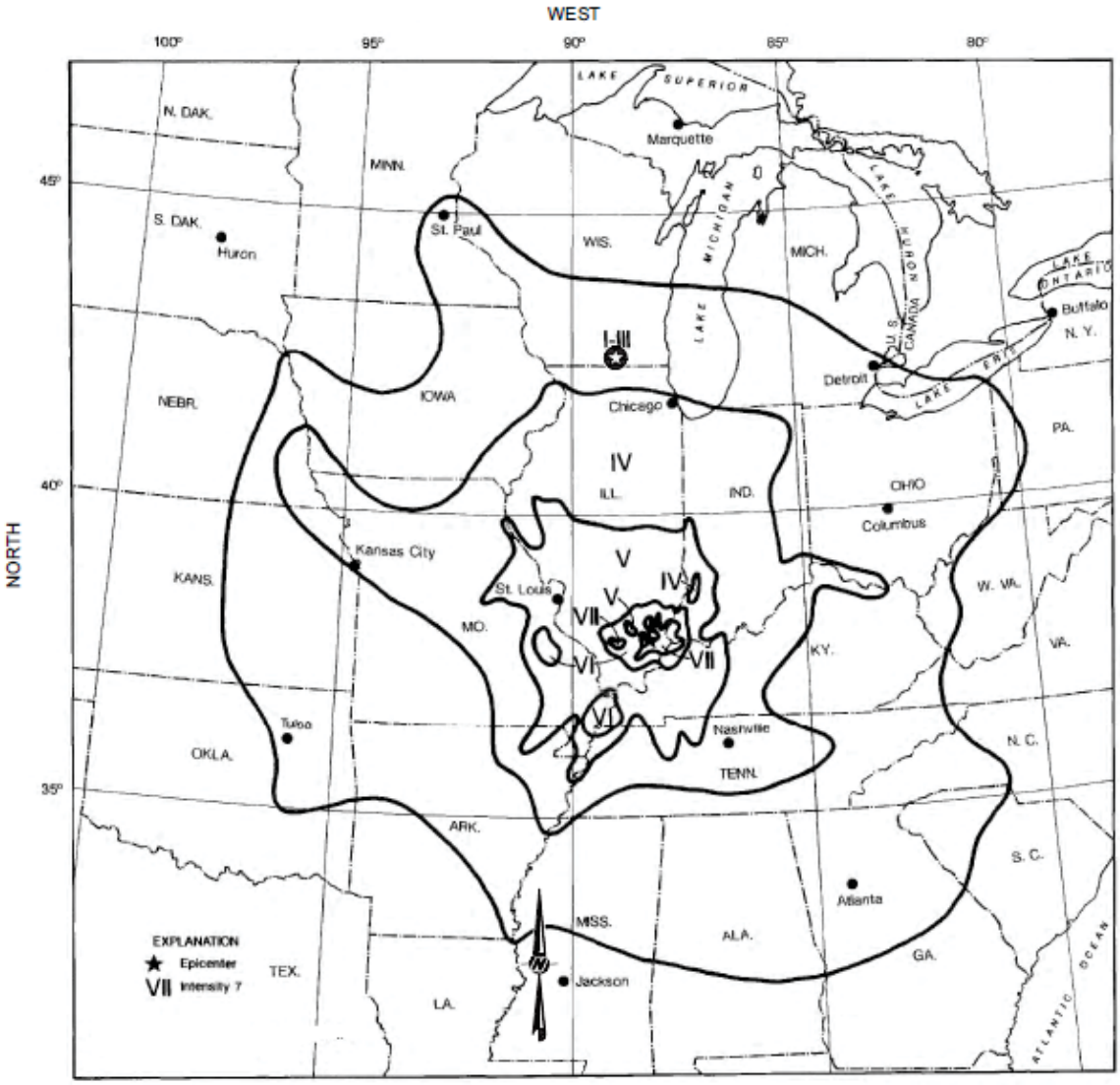

LEGEND

SHINE SITE

REFERENCE

1.) STOVER, C.W. AND COFFMAN, J.L., 1993.

193 0 193
APPROXIMATE SCALE MILES

310 0 310
APPROXIMATE SCALE KM

Figure 2.5-21 – Deaggregation of USGS 2008 PSHA Model for 475-Year Return Period PGA

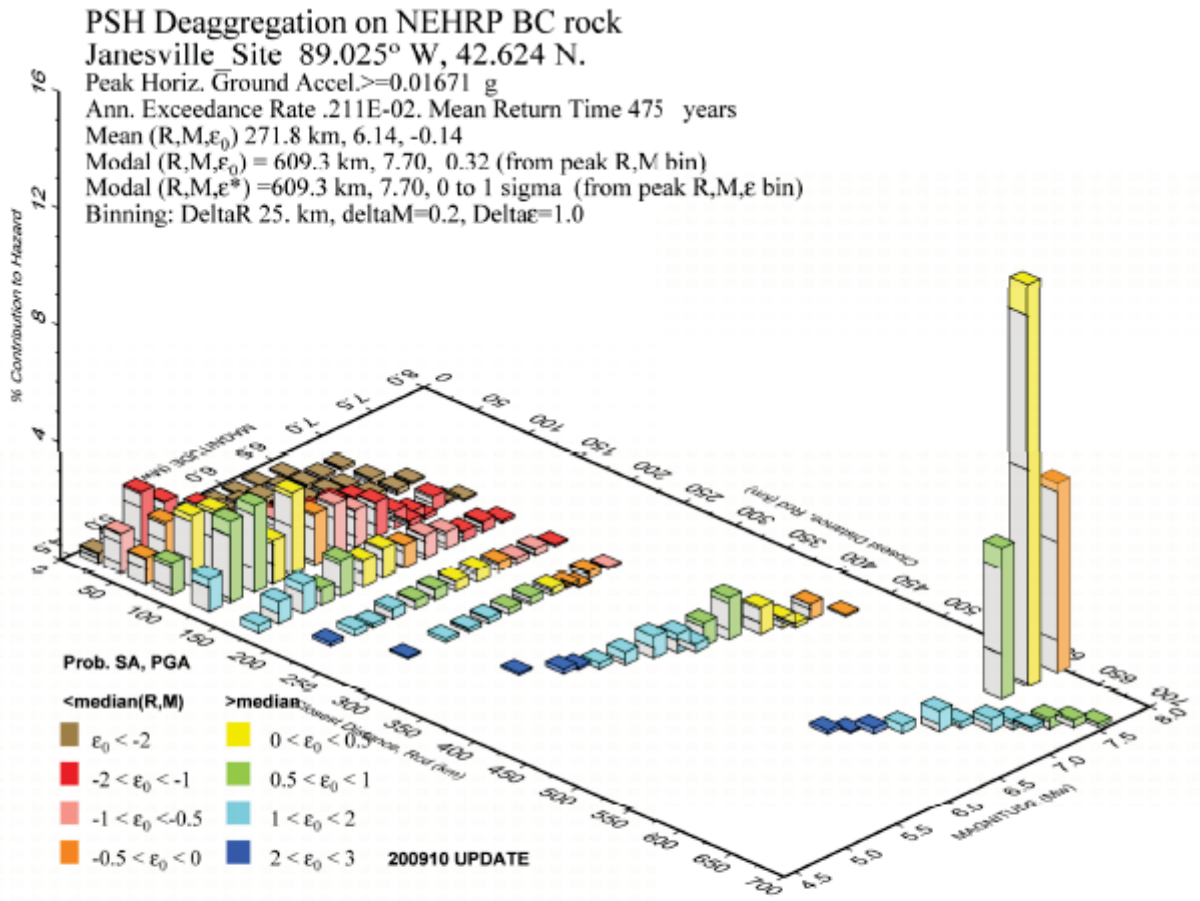

Distance (R), magnitude (M), epsilon (E0,E) deaggregation for a site on rock with average vs= 760. m/s top 30 m.
USGS CGHT PSHA2008 UPDATE Bins with lt 0.05% contrib. omitted

NOTE

1.) CALCULATION FOR SHINE SITE (42.624°N, 89.025°W) FROM THE 2008 USGS NATIONAL PSHA (V_s^{30} = 760 m/s, SITE CLASS BC).

REFERENCE

1.) USGS, 2012a.

Figure 2.5-22 – Deaggregation of USGS 2008 PSHA Model for 2,475-Year Return Period PGA

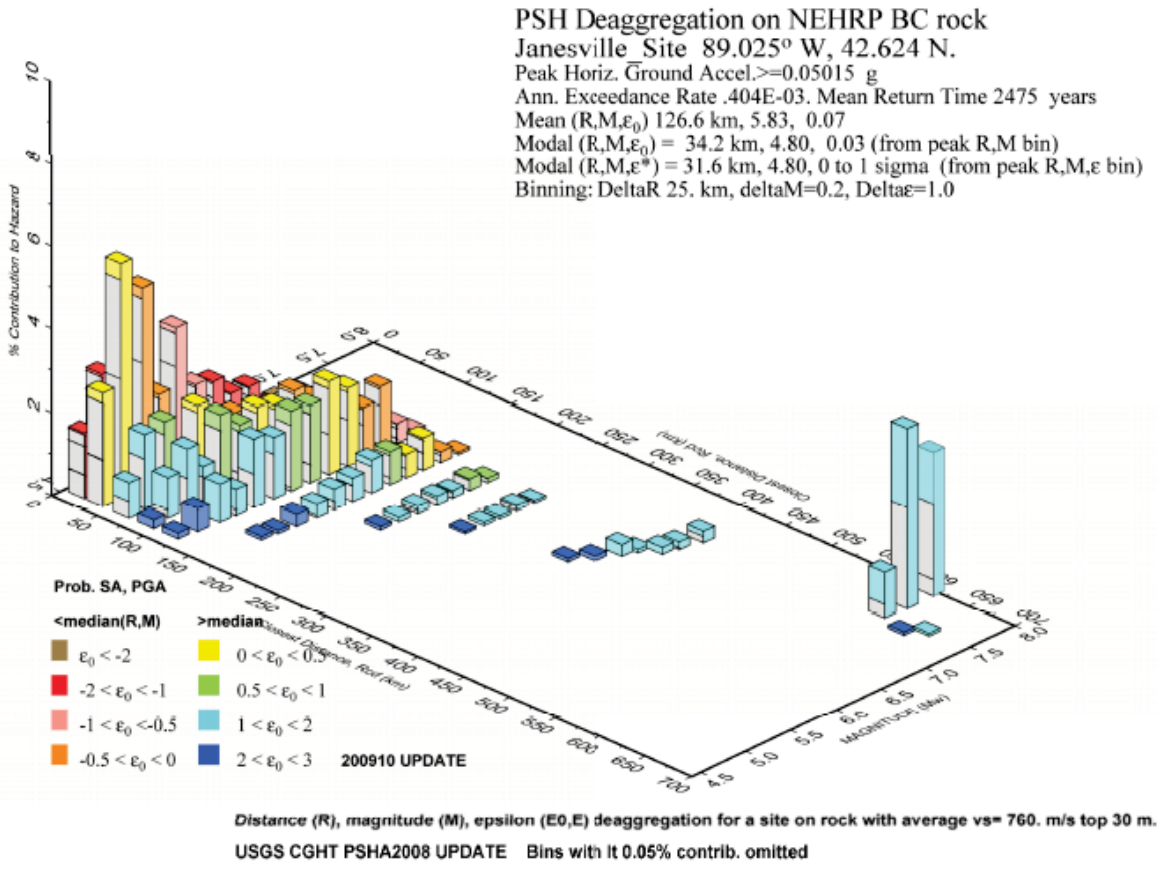

Distance (R), magnitude (M), epsilon (E0,E) deaggregation for a site on rock with average vs= 760. m/s top 30 m.

USGS CGHT PSHA2008 UPDATE Bins with lt 0.05% contrib. omitted

NOTE

1.) CALCULATION FOR SHINE SITE (42.624°N, 89.025°W) FROM THE 2008 USGS NATIONAL PSHA (V_s^{30} = 760 m/s, SITE CLASS BC).

REFERENCE

1.) USGS, 2012a.

Figure 2.5-23 – Deaggregation of USGS 2008 PSHA Model for 4,975-Year Return Period PGA

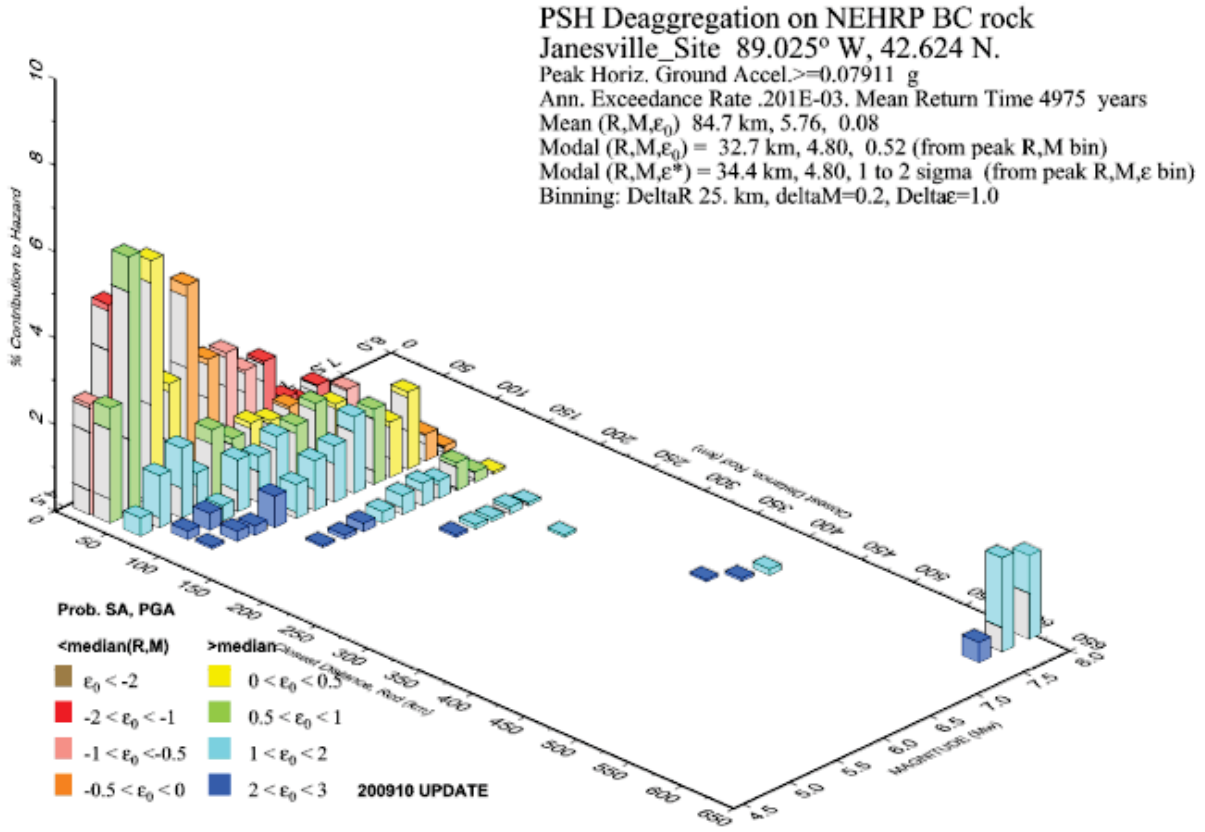

Distance (R), magnitude (M), epsilon (E0,E) deaggregation for a site on rock with average vs= 760. m/s top 30 m.
USGS CGHT PSHA2008 UPDATE Bins with lt 0.05% contrib. omitted

NOTE

1.) CALCULATION FOR SHINE SITE (42.624°N, 89.025°W) FROM THE 2008 USGS NATIONAL PSHA (V_s^{30} = 760 m/s, SITE CLASS BC).

REFERENCE

1.) USGS, 2012a.

Figure 2.5-24 – Deaggregation of USGS 2008 PSHA Model for 9,950-Year Return Period PGA

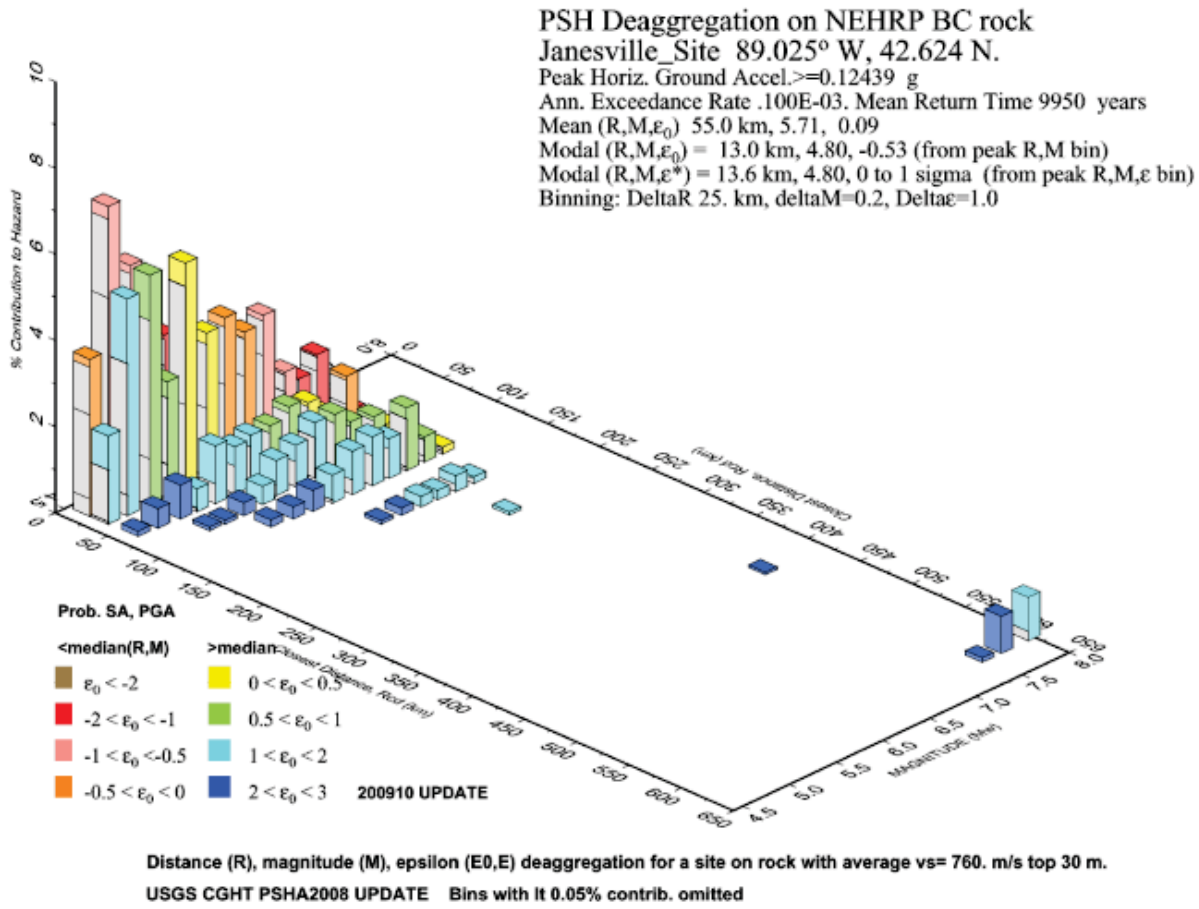

Distance (R), magnitude (M), epsilon (E0,E) deaggregation for a site on rock with average vs= 760. m/s top 30 m.
USGS CGHT PSHA2008 UPDATE Bins with lt 0.05% contrib. omitted

NOTE

1.) CALCULATION FOR SHINE SITE (42.624°N, 89.025°W) FROM THE 2008 USGS NATIONAL PSHA (V_s^{30}= 760 m/s, SITE CLASS BC).

REFERENCE

1.) USGS, 2012a.

Figure 2.5-25 – Deaggregation of USGS 2008 PSHA Model for 19,900-Year Return Period PGA

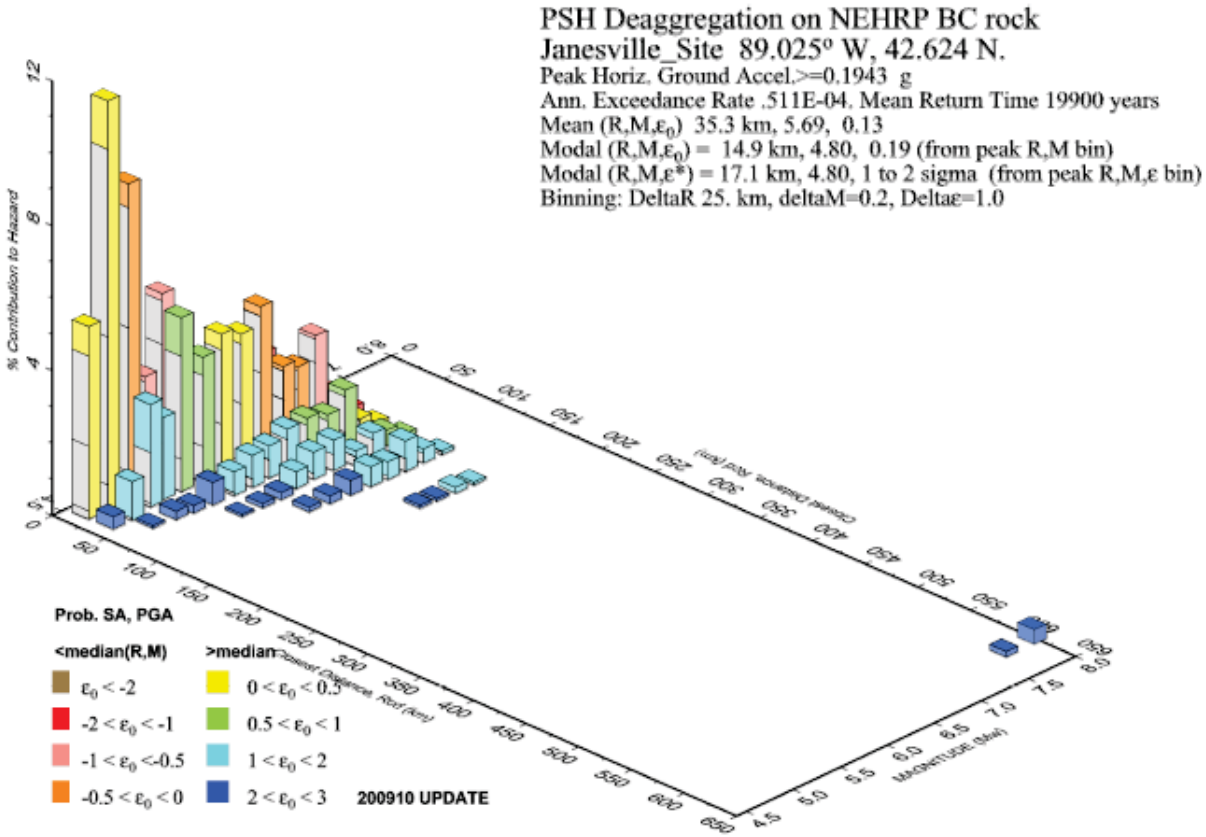

NOTE

1.) CALCULATION FOR SHINE SITE (42.624°N, 89.025°W) FROM THE 2008 USGS NATIONAL PSHA (V_s^{30}= 760 m/s, SITE CLASS BC).

REFERENCE

1.) USGS, 2012a.

2.6 REFERENCES

2.6.1 GEOGRAPHY AND DEMOGRAPHY

ANSI/ANS, 2015. Emergency Planning for Research Reactors, ANSI/ANS 15.16-2015, American National Standards Institute/American Nuclear Society, 2015.

City of Beloit, 2006. City of Beloit Parks and Open Space Plan, City of Beloit, 2006.

City of Beloit, 2018. City of Beloit Comprehensive Plan, City of Beloit. 2018.

City of Janesville, 2008. City of Janesville Park and Open Space Plan, City of Janesville, 2008.

City of Janesville, 2009. City of Janesville Comprehensive Plan, City of Janesville, 2009.

DOA, 2013. Projections for Wisconsin Counties, Components of Change by Decade: 2010-2040, Wisconsin Department of Administration (DOA), 2013.

ESRI, 2018. ArcGIS Pro version 2.2.12813

Greatschools, 2019. Data on Janesville Schools enrollment, Website: http://www.greatschools.org/, Date accessed: April 4, 2019.

Janesville Area Convention & Visitors Bureau, 2011. Website: http://www.janesvillecvb.com/, Date accessed: December 12, 2011.

Janesville Area Convention & Visitors Bureau, 2019. Website: http://www.janesvillecvb.com/, Date accessed: April 5, 2019.

Mercy Health System, **2011.** Website, http://www.mercyhealthsystem.org/body.cfm?id=7, Date accessed: December 2, 2011.

NAIP, 2010. USDA NAIP Imagery, Website: http://www.fsa.usda.gov/FSA/apfoapp?area=home&subject=prog&topic=nai, Date accessed: August 15, 2012.

Rock County Wisconsin Economic Development Alliance, 2019. Listing of Largest Employers, Website: https://www.rockcountyalliance.com/market-data/workforce/major-employers, Date accessed: April 4, 2019.

Schooltree, 2019. Data on Janesville Schools enrollment, Website: http://wisconsin.schooltree.org, Date accessed: April 4, 2019.

USCB, 2012. Census 2010 Summary File 1, Website: http://factfinder2.census.gov/faces/nav/jsf/pages/index.xhtml, Date accessed: February 1, 2012.

USCB, 2017. Rock County Quick Facts, United States Census Bureau, Website: https://www.census.gov/quickfacts/rockcountywisconsin, Date accessed: January 15, 2019

USCB TIGER, 2010. 2010 Census TIGER/Line Shapefiles, U.S. Census Bureau, Geography Division, Geographic Productions Branch, Website: http://www.census.gov/geo/www/tiger/tgrshp2010/tgrshp2010.html, Date accessed: August 15, 2012.

USGS, 1980. Rockford, Illinois; Wisconsin (Eastern U.S.) 1:250,000 Series (Topographic) Map, U.S. Geological Survey (USGS), Reston, Virginia 1980.

WDPI, 2018. 2017-2018 School Report Card Data Download File, Wisconsin Department of Public Instruction, 2018, Website: https://apps2.dpi.wi.gov/reportcards/, Date accessed: December 14, 2018.

Wisconsin Department of Health Services, 2019. Wisconsin Assisted Living Facilities, Website: https://www.dhs.wisconsin.gov/guide/rock.htm, Date accessed: April 3, 2019.

2.6.2 NEARBY INDUSTRIAL, TRANSPORTATION, AND MILITARY FACILITIES

Abitec Corporation, 2012. Website: http://www.abiteccorp.com/, Date accessed: April 9, 2012.

Abitec Corporation, 2015. Correspondence from Jay Gasser, Abitec Corporation Health and Safety Manager, to Catherine Kolb, SHINE Medical Technologies, January 23, 2015.

ACI, 2014. Code Requirements for Nuclear Safety-Related Concrete Structures & Commentary, ACI 349-13, American Concrete Institute, 2014.

Alliant Energy, 2012. Correspondence from Jesse OBrien, Alliant Energy, to Max Ross, Sargent & Lundy, June 21, 2012.

ALOHA, 2008. Computer Program: Areal Locations of Hazardous Atmospheres Version 5.4.1, Developed by EPA and NOAA, 2008.

ALOHA, 2013. Computer Program: Areal Locations of Hazardous Atmospheres Version 5.4.4, Developed by EPA and NOAA, 2013.

APO, 2019. Terminal Area Forecast Detail Report, Federal Aviation Administration, Office of Aviation Policy and Plans, 2019.

City of Beloit, 2015. Correspondence from Mike Tinder, City of Beloit Water Utility Supervisor, to Catherine Kolb, SHINE Medical Technologies, January 14, 2015.

City of Beloit, 2018. City of Beloit Comprehensive Plan, City of Beloit, 2018.

City of Janesville, 2009. City of Janesville Comprehensive Plan, City of Janesville, 2009.

City of Janesville, 2012. Correspondence from Vic Grassman, Economic Development Director, to Timothy Krause, Sargent & Lundy, April 13, 2012.

City of Janesville, 2015a. Correspondence from Craig Thiesenhusen, City of Janesville Water Utility Superintendent, to Catherine Kolb, SHINE Medical Technologies, January 26, 2015.

City of Janesville, 2015b. Correspondence from Joe Zakovec, City of Janesville Wastewater Superintendent, to Catherine Kolb, SHINE Medical Technologies, January 21, 2015.

Crop Production Services, 2012. Crop Production Services Home, Website: http://www.cpsagu.com, Date accessed: April 9, 2012.

DOE, 2006. Accident Analysis for Aircraft Crash into Hazardous Facilities, DOE-STD-3014-96, U.S. Department of Energy, October 1996, Reaffirmed May 2006.

Evonik Industries, 2012. Evonik Industries – Specialty Chemicals, Website: http://corporate.evonik.com/en/Pages/default.aspx, Date accessed: April 2012.

FEMA, 1989. Handbook of Chemical Hazard Analysis Procedures, Federal Emergency Management Agency, U.S. Department of Transportation, U.S. Environmental Protection Agency, 1989-626-095-10575.

Manta, 2012a. Crop Production Services, Website: http://www.manta.com/c/mmd2gbb/crop-production-service-inc, Date accessed: April 9, 2012.

Manta, 2012b. Janesville Jet Center, Website: http://www.manta.com/c/mmssbpk/janesville-jet-center, Date accessed: April 9, 2012.

Manta, 2012c. School District of Beloit Turner, Website: http://www.manta.com/c/mm7lwfm/school-district-beloit-turner, Date accessed: April 9, 2012.

NPMS, 2019. National Pipeline Mapping System. Website: https://www.npms.phmsa.dot.gov/, Date accessed: May 30, 2019.

Rock County, 2012. Correspondence from Shirley Connors, Rock County Emergency Management Agency, to Daniel Laubenthal, Sargent & Lundy, February 14, 2012.

USDOT, 2007. Flight Standards Information Management System (FSIMS), U.S. Department of Transportation (DOT), Federal Aviation Administration, Order 8900.1, Effective Date: 09/13/2007.

USDOT 2019a. Terminal Area Forecast (TAF) Report, U.S. Department of Transportation, Federal Aviation Administration, February 2019.

USDOT 2019b. Air Traffic Activity System (ATADS) Tower Operations Report, U.S. Department of Transportation, Federal Aviation Administration, April 2019.

USNRC, 1978. Evaluation of Explosions Postulated to Occur at Nearby Facilities and on Transportation Routes Near Nuclear Power Plants, Regulatory Guide 1.91, Revision 1, U.S. Nuclear Regulatory Commission, 1978.

USNRC, 1996. Guidelines for Preparing and Reviewing Applications for the Licensing of Non-Power Reactors, Format and Content, NUREG-1537, Part 1, U.S. Nuclear Regulatory Commission, 1996.

USNRC, 1999. Recommendations for Revision of Regulatory Guide 1.78, NUREG/CR-6624, U.S. Nuclear Regulatory Commission 1999.

USNRC, 2004. Fire Dynamics Tools: Quantitative Fire Hazard Analysis Methods for the U.S. Nuclear Regulatory Commission Fire Protection Inspection Program, NUREG-1805, U.S. Nuclear Regulatory Commission, 2004.

USNRC, 2010. Aircraft Hazards, NUREG-0800, Subsection 3.5.1.6, Revision 4, U.S. Nuclear Regulatory Commission, 2010.

Wisconsin DOT, 2007. Wisconsin Truckers Guide, Wisconsin Department of Transportation, 2007.

Wisconsin Emergency Management, 2011. Correspondence from Rebecca Slater, EPCRA Compliance Officer, to Bernie Mount, Sargent & Lundy, November 3, 2011.

2.6.3 METEOROLOGY

AFCCC, 1999. Engineering Weather Data, 2000 Interactive Edition, Air Force Combat Climatology Center, National Climatic Data Center, 1999.

AMS, 2012. Glossary of Meteorology, American Meteorological Society, 2012.

Arguez et al., 2012. A.A. Arguez and collaborators, NOAA's 1981-2010 U.S. Climate Normals An Overview. Bulletin of the American Meteorological Society, Vol. 93, No. 11, pp 1687-1697, 2012.

ASCE, 2006. Minimum Design Loads for Buildings and Other Structures, ASCE Standard ASCE/SEI 7-05 Including Supplement No. 1, American Society of Civil Engineers, 2006.

ASHRAE, 2017. 2017 ASHRAE Handbook – Fundamentals, American Society of Heating, Refrigerating and Air-Conditioning Engineers, Inc., IP edition. Chapter 14, American Society of Heating, Refrigerating and Air-Conditioning Engineers, Inc., 2017.

Changnon et al., 2004. Changnon, S. A., J. R. Angel, K. E. Kunkel, C. M. B. Lehmann, Climate Atlas of Illinois, Illinois State Water Survey, 2004.

Del Greco et al., 2006. S. A. Del Greco and collaborators, Surface Data Integration at NOAA's National Climatic Data Center: Data Format, Processing, QC and Product Generation, 86th AMS Annual Meeting, 29 January - 2 February, 2006.

EDS, 1968. Climatic Atlas of the United States, Environmental Data Service, U.S. Superintendent of Documents, U.S. Government Printing Office, 1968.

FAA, 1992. Non-Federal Navigational Aids and Air Traffic Control Facilities, Order 6700.20A, Federal Aviation Administration, 1992.

FAA, 2017. Automated Weather Observing Systems (AWOS) for Non-Federal Applications, Advisory Circular AC 150/5220-16E, Federal Aviation Administration, 2017.

IAEA, 1987. Siting of Research Reactors, Report IAEA-TECDOC-403, International Atomic Energy Agency, 1987.

Moran, J. M. and E. J. Hopkins, 2002. Wisconsin's Weather and Climate, The University of Wisconsin Press, 2002.

NCDC, 1952. Local Climatological Summary with Comparative Data, 1951, Madison, Wisconsin, National Climatic Data Center, 1952.

NCDC, 1953. Local Climatological Data with Comparative Data, 1952, Madison, Wisconsin, National Climatic Data Center, 1953.

NCDC, 1954. Local Climatological Summary with Comparative Data, 1953, Madison, Wisconsin, National Climatic Data Center, 1954.

NCDC, 1955. Local Climatological Summary with Comparative Data, 1954, Madison, Wisconsin, National Climatic Data Center, 1955.

NCDC, 1956. Local Climatological Summary with Comparative Data, 1955, Madison, Wisconsin, National Climatic Data Center, 1956.

NCDC, 1957. Local Climatological Summary with Comparative Data, 1956, Madison, Wisconsin, National Climatic Data Center, 1957.

NCDC, 1958. Local Climatological Summary with Comparative Data, 1957, Madison, Wisconsin, National Climatic Data Center, 1958.

NCDC, 1959. Local Climatological Summary with Comparative Data, 1958 Madison, Wisconsin, National Climatic Data Center, 1959.

NCDC, 1960a. Storm Data, November 1960, Volume 2 No. 11, National Climatic Data Center, 1960.

NCDC, 1960b. Local Climatological Summary with Comparative Data, 1959, Madison, Wisconsin, National Climatic Data Center, 1960.

NCDC, 1961a. Storm Data, September 1961, Volume 3 No. 9, National Climatic Data Center, 1961.

NCDC, 1961b. Local Climatological Summary with Comparative Data, 1960, Madison, Wisconsin, National Climatic Data Center, 1961.

NCDC, 1962. Local Climatological Summary with Comparative Data, 1961, Madison, Wisconsin, National Climatic Data Center, 1962.

NCDC, 1963. Local Climatological Summary with Comparative Data, 1962, Madison, Wisconsin, National Climatic Data Center, 1963.

NCDC, 1964. Local Climatological Summary with Comparative Data, 1963, Madison, Wisconsin, National Climatic Data Center, 1964.

NCDC, 1965. Local Climatological Summary with Comparative Data, 1964, Madison, Wisconsin, National Climatic Data Center, 1965.

NCDC, 1966. Local Climatological Summary with Comparative Data, 1965, Madison, Wisconsin, National Climatic Data Center, 1966.

NCDC, 1967a. Storm Data, April 1967, Volume 9 No. 4, National Climatic Data Center, 1967.

NCDC, 1967b. Storm Data, August 1967, Volume 9 No. 8, National Climatic Data Center, 1967.

NCDC, 1967c. Storm Data, January 1967, Volume 9 No. 1, National Climatic Data Center, 1967.

NCDC, 1967d. Local Climatological Summary with Comparative Data, 1966, Madison, Wisconsin, National Climatic Data Center, 1967.

NCDC, 1968. Local Climatological Summary with Comparative Data, 1967, Madison, Wisconsin, National Climatic Data Center, 1968.

NCDC, 1969. Local Climatological Summary with Comparative Data, 1968, Madison, Wisconsin, National Climatic Data Center, 1969.

NCDC, 1970a. Storm Data, October 1970, Volume 12 No. 10, National Climatic Data Center, 1970.

NCDC, 1970b. Local Climatological Summary with Comparative Data, 1969, Madison, Wisconsin, National Climatic Data Center, 1970.

NCDC, 1971a. Storm Data, November 1971, Volume 13 No. 11, National Climatic Data Center, 1971.

NCDC, 1971b. Local Climatological Summary with Comparative Data, 1970, Madison, Wisconsin, National Climatic Data Center, 1971.

NCDC, 1972. Local Climatological Summary with Comparative Data, 1971, Madison, Wisconsin, National Climatic Data Center, 1972.

NCDC, 1973. Local Climatological Summary with Comparative Data, 1972, Madison, Wisconsin, National Climatic Data Center, 1973.

NCDC, 1974. Local Climatological Summary with Comparative Data, 1973, Madison, Wisconsin, National Climatic Data Center, 1974.

NCDC, 1975a. Storm Data, June 1975 Volume 17 No. 6, National Climatic Data Center, 1975.

NCDC, 1975b. Local Climatological Summary with Comparative Data, 1974, Madison, Wisconsin, National Climatic Data Center, 1975.

NCDC, 1976. Local Climatological Summary with Comparative Data, 1975, Madison, Wisconsin, National Climatic Data Center, 1976.

NCDC, 1977. Local Climatological Summary with Comparative Data, 1976, Madison, Wisconsin, National Climatic Data Center, 1977.

NCDC, 1978. Local Climatological Summary with Comparative Data, 1977, Madison, Wisconsin, National Climatic Data Center, 1978.

NCDC, 1979. Local Climatological Summary with Comparative Data, 1978, Madison, Wisconsin, National Climatic Data Center, 1979.

NCDC, 1980a. Storm Data, June 1980, Volume 22 No. 6, National Climatic Data Center, 1980.

NCDC, 1980b. Local Climatological Summary with Comparative Data, 1979, Madison, Wisconsin, National Climatic Data Center, 1980.

NCDC, 1981. Local Climatological Summary with Comparative Data, 1980, Madison, Wisconsin, National Climatic Data Center, 1981.

NCDC, 1982. Local Climatological Summary with Comparative Data, 1981, Madison, Wisconsin, National Climatic Data Center, 1982.

NCDC, 1983. Local Climatological Summary with Comparative Data, 1982, Madison, Wisconsin, National Climatic Data Center, 1983.

NCDC, 1984a. Storm Data, June 1984 Volume 26 No. 6, National Climatic Data Center, 1984.

NCDC, 1984b. Local Climatological Summary with Comparative Data, 1983, Madison, Wisconsin, National Climatic Data Center, 1984.

NCDC, 1985. Local Climatological Summary with Comparative Data, 1984, Madison, Wisconsin, National Climatic Data Center, 1985.

NCDC, 1986. Local Climatological Summary with Comparative Data, 1985, Madison, Wisconsin, National Climatic Data Center, 1986.

NCDC, 1987. Local Climatological Summary with Comparative Data, 1986, Madison, Wisconsin, National Climatic Data Center, 1987.

NCDC, 1988a. Storm Data, May 1988, Volume 30 No. 5, National Climatic Data Center, 1988.

NCDC, 1988b. Local Climatological Summary with Comparative Data, 1987, Madison, Wisconsin, National Climatic Data Center, 1988.

NCDC, 1989. Local Climatological Summary with Comparative Data, 1988, Madison, Wisconsin, National Climatic Data Center, 1989.

NCDC, 1990. Local Climatological Summary with Comparative Data, 1989, Madison, Wisconsin, National Climatic Data Center, 1990.

NCDC, 1991a. Storm Data, March 1991, Volume 33 No. 3, National Climatic Data Center, 1991.

NCDC, 1991b. Local Climatological Summary with Comparative Data, 1990, Madison, Wisconsin, National Climatic Data Center, 1991.

NCDC, 1992a. Storm Data, June 1992, Volume 34 No. 6, National Climatic Data Center, 1992.

NCDC, 1992b. Local Climatological Summary with Comparative Data, 1991, Madison, Wisconsin, National Climatic Data Center, 1992.

NCDC, 1993. Local Climatological Summary with Comparative Data, 1992, Madison, Wisconsin, National Climatic Data Center, 1993.

NCDC, 1994. Local Climatological Summary with Comparative Data, 1993, Madison, Wisconsin, National Climatic Data Center, 1994.

NCDC, 1995. Local Climatological Summary with Comparative Data, 1994, Madison, Wisconsin, National Climatic Data Center, 1995.

NCDC, 1996a. International Station Meteorological Climate Summary, Ver. 4.0, National Climatic Data Center, 1996.

NCDC, 1996b. Local Climatological Summary with Comparative Data, 1995, Madison, Wisconsin, National Climatic Data Center, 1996.

NCDC, 1997. Local Climatological Summary with Comparative Data, 1996, Madison, Wisconsin, National Climatic Data Center, 1997.

NCDC, 1998a. Storm Data, June 1998, Volume 40 No. 6, National Climatic Data Center, 1998.

NCDC, 1998b. Local Climatological Summary with Comparative Data, 1997, Madison, Wisconsin, National Climatic Data Center, 1998.

NCDC, 1999a. Daily Weather Maps, Weekly Series, December 28 1998 – January 3, 1999, National Climatic Data Center, 1999.

NCDC, 1999b. Local Climatological Summary with Comparative Data, 1998, Madison, Wisconsin, National Climatic Data Center, 1999.

NCDC, 2000a. Storm Data, January 1999, Volume 41 No. 1, National Climatic Data Center, 2000.

NCDC, 2000b. Local Climatological Summary with Comparative Data, 1999, Madison, Wisconsin, National Climatic Data Center, 2000.

NCDC, 2001a. Climatography of the United States No. 20, 1971-2000, Arboretum Univ Wis, WI, National Climatic Data Center, 2001.

NCDC, 2001b. Climatography of the United States No. 20, 1971-2000, Arlington Univ Farm, WI, National Climatic Data Center, 2001.

NCDC, 2001c. Climatography of the United States No. 20, 1971-2000, Baraboo, WI, National Climatic Data Center, 2001.

NCDC, 2001d. Climatography of the United States No. 20, 1971-2000, Beaver Dam, WI, National Climatic Data Center, 2001.

NCDC, 2001e. Climatography of the United States No. 20, 1971-2000, Beloit, WI, National Climatic Data Center, 2001.

NCDC, 2001f. Climatography of the United States No. 20, 1971-2000, Brodhead, WI, National Climatic Data Center, 2001.

NCDC, 2001g. Climatography of the United States No. 20, 1971-2000, Charmany Farm, WI, National Climatic Data Center, 2001.

NCDC, 2001h. Climatography of the United States No. 20, 1971-2000, Dalton, WI, National Climatic Data Center, 2001.

NCDC, 2001i. Climatography of the United States No. 20, 1971-2000, DeKalb, IL, National Climatic Data Center, 2001.

NCDC, 2001j. Climatography of the United States No. 20, 1971-2000, Fond du Lac, WI, National Climatic Data Center, 2001.

NCDC, 2001k. Climatography of the United States No. 20, 1971-2000, Fort Atkinson, WI, National Climatic Data Center, 2001.

NCDC, 2001l. Climatography of the United States No. 20, 1971-2000, Hartford 2 W, WI, National Climatic Data Center, 2001.

NCDC, 2001m. Climatography of the United States No. 20, 1971-2000, Horicon, WI, National Climatic Data Center, 2001.

NCDC, 2001n. Climatography of the United States No. 20, 1971-2000, Lake Geneva, WI, National Climatic Data Center, 2001.

NCDC, 2001o. Climatography of the United States No. 20, 1971-2000, Lake Mills, WI, National Climatic Data Center, 2001.

NCDC, 2001p. Climatography of the United States No. 20, 1971-2000, Madison Dane Co AP, WI, National Climatic Data Center, 2001.

NCDC, 2001q. Climatography of the United States No. 20, 1971-2000, Marengo, IL, National Climatic Data Center, 2001.

NCDC, 2001r. Climatography of the United States No. 20, 1971-2000, Oconomowoc, WI, National Climatic Data Center, 2001.

NCDC, 2001s. Climatography of the United States No. 20, 1971-2000, Portage, WI, National Climatic Data Center, 2001.

NCDC, 2001t. Climatography of the United States No. 20, 1971-2000, Prairie du Sac 2 N, WI, National Climatic Data Center, 2001.

NCDC, 2001u. Climatography of the United States No. 20, 1971-2000, Rockford, IL, National Climatic Data Center, 2001.

NCDC, 2001v. Climatography of the United States No. 20, 1971-2000, Stoughton, WI, National Climatic Data Center, 2001.

NCDC, 2001w. Climatography of the United States No. 20, 1971-2000, Watertown, WI, National Climatic Data Center, 2001.

NCDC, 2001x. Climatography of the United States No. 20, 1971-2000, Wisconsin Dells, WI, National Climatic Data Center, 2001.

NCDC, 2001y. Local Climatological Summary with Comparative Data, 2000, Madison, Wisconsin, National Climatic Data Center, 2001.

NCDC, 2002a. Climate Atlas of the United States, Version 2.0 CD, National Climatic Data Center, 2002.

NCDC, 2002b. Division Normals and Standard Deviations of Temperature, Precipitation, and Heating and Cooling Degree Days, 1971-2000 (and previous normals periods), Section 1: Temperature, Climatography of the United States No. 85, National Climatic Data Center, 2002.

NCDC, 2002c. Division Normals and Standard Deviations of Temperature, Precipitation, and Heating and Cooling Degree Days, 1971-2000 (and previous normals periods), Section 2: Precipitation, Climatography of the United States No. 85, National Climatic Data Center, 2002.

NCDC, 2002d. Local Climatological Summary with Comparative Data, 2001, Madison, Wisconsin, National Climatic Data Center, 2002.

NCDC, 2003. Local Climatological Summary with Comparative Data, 2002, Madison, Wisconsin, National Climatic Data Center, 2003.

NCDC, 2004. Local Climatological Summary with Comparative Data, 2003, Madison, Wisconsin, National Climatic Data Center, 2004.

NCDC, 2005a. Data Documentation for Data Set 3280 (DSI-3280) Surface Airways Hourly, National Climatic Data Center, 2005.

NCDC, 2005b. Storm Data, August 2005, Volume 47 No. 8, National Climatic Data Center, 2005.

NCDC, 2005c. Local Climatological Summary with Comparative Data, 2004, Madison, Wisconsin, National Climatic Data Center, 2005.

NCDC, 2006a. Federal Climate Complex Data Documentation for Integrated Surface Data, National Climatic Data Center Air Force Combat Climatology Center Fleet Numerical Meteorology and Oceanography Detachment, 2006.

NCDC, 2006b. Local Climatological Summary with Comparative Data, 2005, Madison, Wisconsin, National Climatic Data Center, 2006.

NCDC, 2007. Local Climatological Summary with Comparative Data, 2006, Madison, Wisconsin, National Climatic Data Center, 2007.

NCDC, 2008a. Storm Data, January 2008 Volume 50 No. 1, National Climatic Data Center, 2008.

NCDC, 2008b. Local Climatological Summary with Comparative Data, 2007, Madison, Wisconsin, National Climatic Data Center, 2008.

NCDC, 2009. Local Climatological Summary with Comparative Data, 2008, Madison, Wisconsin, National Climatic Data Center, 2009.

NCDC, 2010. Local Climatological Summary with Comparative Data, 2009, Madison, Wisconsin, National Climatic Data Center, 2010.

NCDC, 2011a. NCDC Storm Event Database, National Climatic Data Center, Website: http://www4.ncdc.noaa.gov/cgi-win/wwcgi.dll?wwEvent~Storms, Date accessed: November 2011.

NCDC, 2011b. TD3505 - Airways Surface Observations, Surface weather observations in TD 3505 digital format from 2005-2010, for NWS-Madison, WI. National Climatic Data Center (NCDC), data purchased from NCDC, 2011.

NCDC, 2011c. TD3505 - Airways Surface Observations, Surface weather observations in TD 3505 digital format from 2005-2010, for NWS-Rockford, IL. National Climatic Data Center (NCDC), data purchased from NCDC, 2011.

NCDC, 2011d. TD3280 - Airways Surface Observations, Surface weather observations in TD 3280 digital format from 1948-2009, for NWS-Madison, WI. National Climatic Data Center (NCDC), data purchased from NCDC, 2011.

NCDC, 2011e. TD 3280 - Airways Surface Observations, Surface weather observations in TD 3280 digital format from 1973-2009, for NWS-Rockford, IL. National Climatic Data Center (NCDC), data purchased from NCDC, 2011.

NCDC, 2011f. 2010 Local Climatological Data, Annual Summary with Comparative Data, Madison, Wisconsin (KMSN), National Climatic Data Center, 2011.

NCDC, 2011g. TD3505 - Airways Surface Observations, Surface weather observations in TD 3505 digital format from 2005-2010, for Southern Wisconsin Regional Airport, Janesville, WI. National Climatic Data Center (NCDC), data purchased from NCDC, 2011.

NCDC, 2011h. 2010 Local Climatological Data, Annual Summary with Comparative Data, Rockford, Illinois (KRFD), National Climatic Data Center, 2011.

NCDC, 2011i. Climatological Data Annual Summary Illinois 2010, Volume 115, Number 13, National Climatic Data Center, 2011.

NCDC, 2011j. Climatological Data Annual Summary Wisconsin 2010, Volume 115, Number 13, National Climatic Data Center, 2011.

NCDC, 2012. Data File "anem_elev_inf" Referenced in Data Documentation for Data Set 6421 (DSI-6421) Enhanced Hourly Wind Station Data for the Contiguous United States National Climatic Data Center, 2012.

NCDC, 2014. Storm Data, June 2014, Volume 56 No. 6, National Climatic Data Center, 2014.

NCDC, 2018a. NCDC Storm Event Database, National Climatic Data Center, website: https://www.ncdc.noaa.gov/stormevents/, Date accessed: November 21, 2018.

NCDC, 2018b. TD3505 – Archive Data Server, National Climatic Data Center, data purchased from NCDC, 2018.

NCDC, 2019a. NCDC Summary of Monthly Normals 1981-2010. Madison Dane Co, Regional Airport. National Climatic Data Center, 2019.

NCDC, 2019b. 2018 Local Climatological Data, Annual Summary with Comparative Data, Madison, Wisconsin (KMSN), National Climatic Data Center, 2019.

NCDC, 2019c. 2018 Local Climatological Data, Annual Summary with Comparative Data, Rockford, Illinois (KRFD), National Climatic Data Center, 2019.

NCDC, 2019e. 2018 Local Climatological Data, Annual Summary with Comparative Data, Moline, Illinois (KMLI), National Climatic Data Center, 2019.

NCDC, 2019d. 2018 Local Climatological Data, Annual Summary with Comparative Data, Springfield, Illinois (KSPI), National Climatic Data Center, 2019.

NCDC, 2019f. Climatography of the United States, 2000-2018, Arboretum Univ Wis, WI, National Climatic Data Center, 2019.

NCDC, 2019g. Climatography of the United States, 2000-2018, Arlington Univ Farm, WI, National Climatic Data Center, 2019.

NCDC, 2019h. Climatography of the United States, 2000-2018, Baraboo, WI, National Climatic Data Center, 2019.

NCDC, 2019i. Climatography of the United States, 2000-2018, Beaver Dam, WI, National Climatic Data Center, 2019.

NCDC, 2019j. Climatography of the United States, 2000-2018, Beloit, WI, National Climatic Data Center, 2019.

NCDC, 2019k. Climatography of the United States, 2000-2018, Brodhead, WI, National Climatic Data Center, 2019.

NCDC, 2019l. Climatography of the United States, 2000-2018, Charmany Farm, WI, National Climatic Data Center, 2019.

NCDC, 2019m. Climatography of the United States, 2000-2007, Dalton, WI, National Climatic Data Center, 2019.

NCDC, 2019n. Climatography of the United States, 2000-2018, DeKalb, IL, National Climatic Data Center, 2019.

NCDC, 2019o. Climatography of the United States, 2000-2018, Fond du Lac, WI, National Climatic Data Center, 2019.

NCDC, 2019p. Climatography of the United States, 2000-2018, Fort Atkinson, WI, National Climatic Data Center, 2019.

NCDC, 2019q. Climatography of the United States, 2000-2018, Hartford 2 W, WI, National Climatic Data Center, 2019.

NCDC, 2019r. Climatography of the United States, 2000-2018, Horicon, WI, National Climatic Data Center, 2019.

NCDC, 2019s. Climatography of the United States, 2000-2018, Lake Geneva, WI, National Climatic Data Center, 2019.

NCDC, 2019t. Climatography of the United States, 2000-2018, Lake Mills, WI, National Climatic Data Center, 2019.

NCDC, 2019u. Climatography of the United States, 2000-2018, Marengo, IL, National Climatic Data Center, 2019.

NCDC, 2019v. Climatography of the United States, 2000-2018, Oconomowoc, WI, National Climatic Data Center, 2019.

NCDC, 2019w. Climatography of the United States, 2000-2018, Portage, WI, National Climatic Data Center, 2019.

NCDC, 2019x. Climatography of the United States, 2000-2008, Prairie du Sac 2 N, WI, National Climatic Data Center, 2019.

NCDC, 2019y. Climatography of the United States, 2000-2018, Stoughton, WI, National Climatic Data Center, 2019.

NCDC, 2019z. Climatography of the United States, 2000-2018, Watertown, WI, National Climatic Data Center, 2019.

NCDC, 2019aa. Climatography of the United States, 2000-2018, Wisconsin Dells, WI, National Climatic Data Center, 2019.

NCDC, 2019ab. Data file "ISH-HISTORY.TXT" Integrated Surface Database Station History, April, 2019, National Climatic Data Center, 2019.

NLSI, 2014. Vaisala 10-Year Flash Density Map – U.S. (2005-2014), National Lightning Safety Institute, 2014.

NOAA, 1999. Julian X.L. Wang and J.K. Angell, Air Stagnation Climatology for the United States (1948-1998). National Oceanic and Atmospheric Administration (NOAA), Air Resources Laboratory, Environmental Research Laboratories, Office of Oceanic and Atmospheric Research, 1999.

NPS, 2011. Class I Area Locations, National Park Service, U.S. Department of Interior, 2011.

Rand McNally, 1982. Goode's World Atlas, 16th edition, Rand McNally & Company, 1982.

Rand McNally, 2005. Goode's World Atlas, 21st edition, Rand McNally & Company, 2005.

Rock County, 2012. County Facts, Rock County, Wisconsin, 2012.

Stern, et al. 1984. Stern, A.C., R.W. Boubel, D.B. Turner, D.L. Fox, Fundamentals of Air Pollution, Academic Press, 1984.

Trewartha, G. T., 1954. An Introduction to Climate, McGraw-Hill Book Company, 1954.

Trewartha, G. T., 1961. The Earth's Problem Climates, The University of Wisconsin Press, 1961.

Turner, D.B, 1964. A Diffusion Model for an Urban Area, Journal of Applied Meteorology, Vol. 3, pp 83-91, 1964.

U.S. Census Bureau, 2007. County and City Data Book: 2007, U.S. Census Bureau, 2007.

USDA, 1998. Rural Utilities Service Summary of Items of Engineering Interest, U.S. Department of Agriculture (USDA), 1998.

USDOC, 1978. Probable Maximum Precipitation Estimates, United States East of the 105th Meridian, National Oceanic and Atmospheric Administration, U.S. Department of the Army Corps of Engineers, U.S. Department of Commerce, Hydrometeorological Report No. 51, 1978.

USEPA, 1990. Prevention of Significant Deterioration Workshop Manual, Prevention of Significant Deterioration and Nonattainment Area Permitting, U.S. Environmental Protection Agency, Office of Air Quality Planning and Standards, 1990.

USEPA, 1999. "PCRAMMET.FOR", FORTRAN program, version 99169. U.S. Environmental Protection Agency, Technology Transfer Networks Support Center for Regulatory Atmospheric Modeling, 1999.

USEPA, 2015. Code of Federal Regulations, Title 40 – Parts 50, 51, 52, 53 and 58 National Ambient Air Quality Standards for Ozone, U.S. Environmental Protection Agency, 2015.

USEPA, 2018. Environmental Protection Agency - Code of Federal Regulations, Title 40 – Part 81 – Additional Air Quality Designations for the 2015 Ozone National Ambient Air Quality Standards, 2018.

USEPA, 2019. Non-Attainment Status for Each County by year in Wisconsin as of March 31, 2019, U.S. Environmental Protection Agency, 2019.

USGS, 1980. Rockford, Illinois; Wisconsin (Eastern U.S.) 1:250,000 Series (Topographic) Map, U.S. Geological Survey, 1980.

WDNR, 2013. Air Monitoring Network Plan 2013, Wisconsin Department of Natural Resources, 2013.

WISDOT, 2017. Geotechnical Manual, Chapter 2 Geology of Wisconsin, Section 3 Glacial Geology, Wisconsin Department of Transportation, March 1, 2017.

2.6.4 HYDROLOGY

Bear, 1972. Dynamics of Fluids in Porous Media, Elsevier, 1972.

Bouwer, H. and R.C. Rice, 1976. A Slug Test Method for Determining Hydraulic Conductivity of Unconfined Aquifers with Completely or Partially Penetrating Wells, Water Resources Research, Vol. 12, No. 3, pp. 423-428, 1976.

Domenico and Schwartz, 1997. Physical and Chemical Hydrogeology, 2nd Edition, John Wiley & Sons, 1997.

FEMA, 2008. Flood Insurance Study: Rock County, Wisconsin and Incorporated Areas, Flood Insurance Study Number 55105CV001A, Two volumes, Federal Emergency Management Agency, 2008.

Gaffield et. al., 2002. Delineation of Zones of Contribution for Municipal Wells in Rock County, Wisconsin: Final report – Madison, Wisconsin Geological and Natural History Survey, 2002.

Hughes, 1965. The Prediction of Surges in the Southern Basin of Lake Michigan, Monthly Weather Review, Vol. 93, No. 5, pg. 292-296, 1965.

Hydrosolve, 2011. AQTESOLV User Documentation, Hydrosolve, Inc., 2011.

Kinzelbach, 1986. Groundwater Modeling (An introduction with sample programs in BASIC), Elsevier, 1986.

LeRoux, 1963. Geology and Ground-Water Resources of Rock County Wisconsin, Geological Survey Water-Supply Paper 1619-X, U.S. Government Printing Office, 1963.

Rock County, 2004. Rock County Storm Water Management Ordinance, Chapter 28 of the Rock County Code of Ordinances, 2004.

USACE, 1984. Probable Maximum Flood Estimation – Eastern United States, TP-100, U.S. Army Corps of Engineers, Hydrologic Engineering Center, 1984.

USACE, 2012. CRREL Ice Jam Database, U.S. Army Corps of Engineers, Website: https://rsgis.crrel.usace.army.mil/icejam, Date accessed: September 10, 2012.

USDOE, 1993. Data Collection Handbook to Support Modeling Impacts of Radioactive Material in Soil, U.S. Department of Energy, 1993.

USGS, 1971. Map of Racine, Wisconsin; Michigan; Illinois; Location Diagram for NK 16-5, U.S. Geological Survey, 1971.

USGS, 2012a. Stormwater Data, U.S. Geological Survey, Website: http://waterdata.usgs.gov/nwis/sw, Date accessed: 2012.

USGS, 2012b. Elevation Data, U.S. Geological Survey, Website: http://www.usgs.gov/pubprod, Date accessed: 2012.

USNRC, 1977a. Design Basis Floods for Nuclear Power Plants, Regulatory Guide 1.59, Revision 2, U.S. Nuclear Regulatory Commission, 1977.

USNRC, 1977b. Design Basis Floods for Fuel Reprocessing Plants and for Plutonium Processing and Fuel Fabrication Plants, Regulatory Guide 3.40, Revision 1, U.S. Nuclear Regulatory Commission, 1977.

USNRC, 1996. Guidelines for Preparing and Reviewing Applications for the Licensing of Non-Power Reactors, Format and Content, NUREG-1537, Part 1, U.S. Nuclear Regulatory Commission, 1996.

USNRC, 2004. Combined Estimation of Hydrogeologic Conceptual Model and Parameter Uncertainty, NUREG/CR-6843 (PNNL-14534), U.S. Nuclear Regulatory Commission, 2004.

USNRC, 2011. Design-Basis Flood Estimation for Site Characterization at Nuclear Power Plants in the United States of America, NUREG/CR-7046 (PNNL-20091), U.S. Nuclear Regulatory Commission, 2011.

Vierbicher, 2010. Rock County Hazard Mitigation Plan Update. Prepared by Vierbicher in cooperation with the Rock County Emergency Management and Rock County Planning Economic and Community Development Agency, 2010.

WDNR, 2012a. Dam Safety database, Wisconsin Office of Dam Safety, Wisconsin Department of Natural Resources, Website: http://dnr/wi.gov/topic/dams/, Date accessed: 2012.

WDNR, 2012b. Well Inventory, Wisconsin Department of Natural Resources, Website: http://prodoasext.dnr.wi.gov/inter1/spinvent$.startup, Date accessed: August 8, 2012.

WDNR, 2012c. Lake Koshkonong, Wisconsin Department of Natural Resources (WDNR), Website: http://dnr.wi.gov/lakes/lakepages/LakeDetail.aspx?wbic=808700, Date accessed: November 19, 2012.

WDOT, 1979. Facilities Development Manual, Chapter 13, Drainage, Attachment 5.4, Rainfall Intensity-Duration-Frequency Curves, Madison, WI (1905-1951), Wisconsin Department of Transportation, 1979.

WGNHS, 2009. Map data, University of Wisconsin-Extension Geological and Natural History Survey, Website: https://wgnhs.wisc.edu/maps-data/maps/, Date accessed: 2009.

2.6.5 GEOLOGY, SEISMOLOGY, AND GEOTECHNICAL ENGINEERING

ANSS, 2012. Advanced National Seismic System ANSS Catalog Search, Northern California Earthquake Data Center, Website: http://quake.geo.berkeley.edu/cnss/catalog-search.html, Date accessed: January 9, 2012.

Armbruster, J. and Seeber, L., 1992. NCEER-91 Earthquake Catalog for the United States, National Center for Earthquake Engineering Research, Website: http://folkworm.ceri.memphis.edu/catalogs/html/cat_nceer.html, Date accessed: January 27, 2012.

ASCE, 2005. Minimum Design Loads for Buildings and Other Structures (7-05), American Society of Civil Engineers, 2005.

Attig, J.W., Bricknell, M., Carson, E.C., Clayton, L., Johnson, M.D., Mickelson, D.M., and Syverson, K.M., 2011. Glaciation of Wisconsin, Educational Series 36 [fourth edition], Wisconsin Geological and Natural History Survey, 2011.

Bakun, W.H. and Hopper, M.G., 2004. Catalog of Significant Historical Earthquakes in the Central United States, Open-File Report 2004-1086, U.S. Geological Survey, 2004.

Braschayko, S.M., 2005. The Waukesha Fault and Its Relationship to the Michigan Basin: A Literature Compilation, Open-File Report 2005-05, Wisconsin Geological and Natural History Survey, 2005.

Cannon, W.F., LaBerge, G.L., Klasner, J.S., and Schulz, K.J., 2008. The Gogebic Iron Range - A Sample of the Northern Margin of the Penokean Fold and Thrust Belt, Professional Paper 1730, U.S. Geological Survey, 2008.

Cannon, W.F., Kress, T.H., and Sutphin, D.M., 1999. Digital Geologic Map and Mineral Deposits of the Lake Superior Region, Minnesota, Wisconsin, Michigan, Open File Report 97-455 (Version 3), U.S. Geological Survey, 1999.

CEUS-SSC, 2012. Central Eastern United States – Seismic Source Characterization for Nuclear Facilities, U.S. Nuclear Regulatory Commission, U.S. Department of Energy, Electric Power Research Institute, 2012.

CGIAR-CSI, 2012. STRM 90 m Digital Elevation Database V4.1, Consortium for Spatial Information, Website: http://www.cgiar-csi.org/data/elevation/item/45-srtm-90m-digital-elevation-database-v41, Date accessed: April 27, 2012.

Chandler, V.W., 1996. Gravity and Magnetic Studies Conducted Recently, in: Sims, P.K., and Carter, L.M.H, (eds.), Archean and Proterozoic Geology of the Lake Superior Region, U.S.A., Professional Paper 1556, U.S. Geological Survey, 1996.

Charpentier, R.R., 1987. A summary of petroleum plays and characteristics of the Michigan basin, Open File Report 87-450R, U.S. Geological Survey, 1987.

Clayton, L., and Attig, J.W., 1997. Pleistocene Geology of Dane County, Wisconsin, Bulletin 95, Wisconsin Geological and Natural History Survey, 1997.

Crone, A.J., and Schweig, E.S., compilers, 1994. Fault number 1023, Reelfoot scarp and New Madrid seismic zone, United States Geological Survey Quaternary fault and fold database of the United States, U.S. Geological Survey, Website: http://earthquakes.usgs.gov/regional/qfaults, Date accessed: April 23, 2012.

Daniels, D.L., and Snyder, S.L., 2002. Wisconsin Aeromagnetic and Gravity Maps and Data, Open-File Report 02-493, U.S. Geological Survey, 2002.

Daniels, D.L., Kucks, R.P., and Hill, P.L., 2008. Illinois, Indiana, and Ohio Magnetic and Gravity Maps and Data, U.S. Geological Survey, 2008.

Dart, R.L., and Volpi, C.M., 2010. Earthquakes in the Central United States, 1699-2010, General Information Product 115, scale 1:250,000, U.S. Geological Survey, 2010.

DPC, 2010. La Crosse Boiling Water Reactor - Decommissioning Plan Revision, November 2010, Dairyland Power Cooperative, 2010 (ML110190592).

Engdahl, E.R., and Villaseñor, A., 2002. Global Seismicity: 1900–1999, in: Lee, W.H.K., Kanamori, H., Jennings, P.C., Kisslinger, C., (eds.), International Handbook of Earthquake and Engineering Seismology, Part A, Chapter 41, Academic Press, 2012.

Exelon, 2006a. Site Safety Analysis Report for Exelon Generation Company, LLC Clinton Early Site Permit, Appendix B - Seismic Hazards Report, Cover to Chapter 2, Revision 4, U.S. Nuclear Regulatory Commission Accession Number ML061100308, Exelon Generation Co, LLC.

Exelon, 2006b. Site Safety Analysis Report for Exelon Generation Company, LLC Clinton Early Site Permit, Appendix B - Seismic Hazards Report. Chapter 4 Figure 4.2-1 to Chapter 6, Revision 4, U.S. Nuclear Regulatory Commission Accession Number ML061100310, Exelon Generation Co, LLC.

Fullerton, D.S., Bush, C.A., and Pennell, J.N., 2003. Map of surficial deposits and materials in the eastern and central United States (east of 102 degrees West longitude), Geologic Investigation Series I-2789, Version 1.0, U.S. Geological Survey, 2003.

Garrity, C.P., and Soller, D.R., 2009. Database of Geologic Map of North America - adapted from the map by J.C. Reed, Jr. and others 2005, U.S. Geological Survey, 2009.

Godt, J.W., and Radbruch-Hall, D.H., 1997. Landslide Overview Map of the Conterminous United States, Digital Compilation of Landslide Overview Map of the Conterminous United States, Dorothy H. Radbruch-Hall, Roger B. Colton, William E. Davies, Ivo Lucchitta, Betty A. Skipp, and David J. Varnes, 1982, Open-File Report 97-289, U.S. Geological Survey, 1997.

Hammer, P.T.C., Clowes, R.M., Cook, F.A., Vasudevan, K., and van der Velden, A.J., 2011. The big picture: A lithospheric cross-section of the North American continent, doi: 10.1130/GSATG95A.1, GSA Today, 2011.

Harrison, R.W., and Schultz, A., 2002. Tectonic Framework of the Southwestern Margin of the Illinois Basin and Its Influence on Neotectonism and Seismicity, Seismological Research Letters, 2002.

Heyl, A.V., Broughton, W.A., and West, W.S., 1978. Geology of the Upper Mississippi Valley Base-Metal District, Information Circular Number 16, University of Wisconsin-Extension Geological and Natural History Survey, 1970 (Revised 1978).

Howell, P.D., and van der Pluijm, B., 1990. Early history of the Michigan basin: Subsidence and Appalachian tectonics, Geology, 1990.

IBC, 2015. International Building Code, International Code Council, Inc., 2015.

Jirsa, M.A., Boerboom, T.J., Chandler, V.W., Mossler, J.H., Runkel, A.C., Setterholm, D.R., 2011. Geologic Map of Minnesota-Bedrock Geology, State Map Series S-21, scale 1:500,000, Minnesota Geological Survey, 2011.

Klasner, J.S., King, E.R., and Jones, W.J., 1985. Chapter 21, Geologic Interpretation of Gravity and Magnetic Data for Northern Michigan and Wisconsin, in: Hinze, W.J., (ed.), The Utility of Regional Gravity and Magnetic Anomaly Maps, doi: 10.1190/1.0931830346.ch21, Society of Exploration Geophysicists, 1985.

Kolata, D.R., Denny, F.B., Devera, J.A., Hansel, A.K., Jacobson, R.J., Lasemi, Z., McGarry, C.S., Nelson, W.J., Norby, R.D., Treworgy, C.G., and Weibel, C.P., 2005. Bedrock Geology of Illinois, Illinois Map 14, scale 1:500,000, Illinois State Geological Survey, 2005.

Kucks, R.P., 1999. Isostatic gravity anomaly grid for the conterminous US, Mineral Resource On-Line Spatial Data, Digital Data Series DDS-9, U.S. Geological Survey, Website: http://tin.er.usgs.gov/gravity/isostatic, Date accessed: December 18, 2011.

Lamontagne, M., Halchuk, S., Cassidy, J.F., and Rogers, G.C., 2008. Significant Canadian Earthquakes of the Period 1600-2006, doi: 10.1785/gssrl.79.2.211, Seismological Research Letters, 2008.

Larson, T.H., 2002. The Earthquake of 2 September 1999 in Northern Illinois: Intensities and Possible Neotectonism, Seismological Research Letters, 2002.

Maus, S., Barckhausen, U., et al., 2009. EMAG2: Earth Magnetic Anomaly Grid (2-arc-minute resolution), Website: http://geomag.org/models/emag2.html, Date accessed: April 23, 2012.

McGuire, 2004. Seismic Hazard and Risk Analysis, Earthquake Engineering Research Institute, MNO-10, 2004.

MLRA, 2012. Land Resource Regions and Major Land Resource Areas of the United States, the Caribbean, and the Pacific Basin, MLRA Explorer Custom Report K – Northern Lake State Forest and Forage Region, 95B – Southern Wisconsin and Northern Illinois Drift Plain, United States Department of Agriculture Natural Resources Conservation Service, Website: http://www.cei.psu.edu/mlra, Date accessed: January 16, 2012.

Mudrey, Jr., M.G., Brown, B.A., and Greenberg, J.K., 1982. Bedrock Geologic Map of Wisconsin, scale 1:1,000,000, University of Wisconsin-Extension Geological and Natural History Survey, 1982.

NAMAG, 2002. North American Magnetic Anomaly Group, Bankey, V., Cuevas, A., Daniels, D., Finn, C.A., Hernandez, I., Hill, P., Kucks, R., Warner Miles, W., Pilkington, M., Roberts, C., Roest, W., Rystrom, V., Shearer, S., Snyder, S., Sweeney, R., and Velez, J., Magnetic Anomaly Map of North America, Version 1.0, U.S. Geological Survey, 2002.

Natural Resources Canada, 2012. Important Canadian Earthquakes, Natural Resources Canada, Website: http://earthquakescanada.nrcan.gc.ca/historic-historique/map-carte-eng.php, Date accessed: January 16, 2012.

NCEER, 2012. NCEER Catalog Search, National Center for Earthquake Engineering Research, Center for Earthquake Research and Information, University of Memphis, Website: http://folkworm.ceri.memphis.edu/catalogs/html/cat_nceer.html, Date accessed: April 5, 2012.

NEID, 2012. Earthquake Intensity Database Search 1638-1985, National Geophysical Data Center, National Oceanic and Atmospheric Administration, Website: http://www.ngdc.noaa.gov/hazard/int_srch.shtml#eqcoord, Date accessed: January 10, 2012.

Nelson, W.J., 1995. Structural Features in Illinois, Department of Natural Resources, Illinois State Geological Survey, 1995.

Obermeier, S.F., and Crone, A.J., compilers, 1994. Fault number 1024, Wabash Valley liquefaction features, Quaternary fault and fold database of the United States, U.S. Geological Survey, Website: http://earthquakes.usgs.gov/regional/qfaults, Date accessed: April 23, 2012.

Olive, W.W., Chleborad, A.F., Frahme, C.W., Schlocker, J., Schneider, R.R., and Schuster, R.L., 1989. Swelling Clays Map of the Conterminous United States, Miscellaneous Investigations Series Map I-1940, 1 sheet, scale 1:7,500,000, U.S. Geological Survey, 1989.

Petersen, M., Frankel, A., Harmsen, S., Mueller, C., Haller, K., Wheeler, R., Wesson, R., Zeng, Y., Boyd, O., Perkins, D., Luco, N., Field, E., Wills, C., and Rukstales, K., 2008. Documentation for the 2008 Update of the United States National Seismic Hazard Maps, Open-File Report 2008–1128, U.S. Geological Survey, 2008.

Piskin, K., and Bergstrom, R.E., 1975. Glacial Drift in Illinois: Thickness and Character, Illinois State Geological Survey, 1975.

Radbruch-Hall, D.H., Colton, R.B., Davies, W.E., Lucchitta, I., Skipp, B.A., and Varnes, D.J., 1982. Landslide Overview Map of the Conterminous United States, Professional Paper 1183, U.S. Geological Survey, 1982.

RCGIS, 2012. Rock County Geographic Information System, Rock County, State of Wisconsin, Website: http://68.249.68.135/Rock/viewer.htm?Title=Rock%20County%20GIS%20Map%20Viewer, Date accessed: January 16, 2012.

Roy, M., Clark, P.U., Barendregt, R.W., Glassman, J.R., and Enkin, R.J., 2004. Glacial stratigraphy and paleomagnetism of late Cenozoic deposits of the north-central United States, doi: 10.1130/ B25325.1, Geological Society of America Bulletin, 2004.

Schulz, K.J., and Cannon, W.F., 2007. The Penokean orogeny in the Lake Superior region, doi: 10.1016/j.precamres.2007.02.022, Precambrian Research, 2007.

Sella, G.F., Stein, S., Dixon, T.H., Craymer, M., James, T.S., Mazzotti, S., and Dokka, R.K., 2007. Observation of glacial isostatic adjustment in ‘‘stable’’ North America with GPS, doi: 10.1029/2006GL027081, Geophysical Research Letters, 2007.

Sims, P.K., and Carter, L.M.H., 1996. Archean and Proterozoic Geology of the Lake Superior Region, U.S.A., 1993, Professional Paper 1556, U.S. Geological Survey, 1996.

Sims, P.K., and Schulz, K.J., 1996. Wisconsin Magmatic Terranes, in: Sims, P.K., and Carter, L.M.H, (eds.), Archean and Proterozoic Geology of the Lake Superior Region, U.S.A., 1993, Professional Paper 1556, U.S. Geological Survey, 1996.

Sims, P.K., Saltus, R.W., and Anderson, E.D., 2005. Preliminary Precambrian basement structure map of the continental United States - an interpretation of geologic and aeromagnetic data, Open-File Report 2005-1029, Version 1.0, U.S. Geological Survey, 2005.

Stover, C.W. and Coffman, J.L., 1993. Seismicity of the United States, 1568-1989 (Revised), Professional Paper 1527, U.S. Geological Survey, 1993.

Stover, C.W., Reagor, B.G., and Algermissen, S.T., 1984. United States Earthquake Data File, Open-File Report 84-225, U.S. Geological Survey, 1984.

USDA SCS, 1974. Soil Survey of Rock County, Wisconsin, United States Department of Agriculture Soil Conservation Service, in cooperation with University of Wisconsin Department of Soil Science, Wisconsin Geological and Natural History Survey, and the Wisconsin Agricultural Experiment Station, 1974.

USGS, 2000. The Severity of an Earthquake, United States Geological Survey Unnumbered Series, General Interest Publication, U.S. Geological Survey, 2000.

USGS, 2003. A Tapestry of Time and Terrain: The Union of Two Maps – Geology and Topography, U.S. Geological Survey, 2003.

USGS, 2010. Physiographic divisions of the conterminous U.S., U.S. Geological Survey, Website: http://water.usgs.gov/GIS/metadata/usgswrd/XML/physio.xml, Date accessed: April 25, 2012.

USGS, 2012a. 2008 Interactive Deaggregations (Beta), U.S. Geological Survey, Website: https://geohazards.usgs.gov/deaggint/2008, Date accessed: April 5, 2012.

USGS, 2012b. Java Ground Motion Parameter Calculator, U.S. Geological Survey, Website: http://earthquake.usgs.gov/hazards/designmaps/javacalc.php, Date accessed: April 5, 2012.

USGS, 2012c. Quaternary Fault and Fold Database of the United States, 3 November 2010 update, United States Geological Survey, Website: http://earthquake.usgs.gov/hazards/qfaults, Date accessed: April 5, 2012.

USGS, 2012d. Rectangular Area Earthquake Search for United States Geological Survey/ National Earthquake Information Center (Preliminary Determination of Epicenters (PDE) since 1973), Significant United States Earthquakes (1568 - 1989), and Eastern, Central and Mountain States of United States (1350 - 1986) catalogs, U.S. Geological Survey, Website: http://earthquake.usgs.gov/earthquakes/eqarchives/epic/ epic_rect.php, Date accessed: January 9, 2012.

USGS, 2012e. Seismic Design Maps and Tools for Engineers, U.S. Geological Survey, Website: http://earthquake.usgs.gov/hazards/designmaps, Date accessed: April 5, 2012.

USGS, 2012f. United States Earthquake Information by State/Territory, Wisconsin Earthquake History, U.S. Geological Survey, Website: http://earthquake.usgs.gov/earthquakes/states, Date accessed: January 26, 2012.

USNRC, 2000. Technical Bases for Regulatory Guide for Soil Liquefaction, NUREG/CR-5741, U.S. Nuclear Regulatory Commission, 2000.

USNRC, 2003. Procedures and Criteria for Assessing Seismic Soil Liquefaction at Nuclear Power Plant Sites, Regulatory Guide 1.198, U.S. Nuclear Regulatory Commission, 2003.

USNRC, 2012. Interim Staff Guidance Augmenting NUREG-1537, Part 2, "Guidelines for Preparing and Reviewing Applications for the Licensing of Non-Power Reactors: Standard Review Plan and Acceptance Criteria," for Licensing Radioisotope Production Facilities and Aqueous Homogeneous Reactors, Interim Staff Guidance Augmenting NUREG-1537, Part 2, U.S. Nuclear Regulatory Commission, 2012.

Vierbicher, 2010. Rock County Hazard Mitigation Plan Update, prepared by Vierbicher in cooperation with the Rock County Emergency Management and Rock County Planning Economic and Community Development Agency, 2010.

WGNHS, 1983. Thickness of Unconsolidated Material in Wisconsin, University of Wisconsin-Extension Geological and Natural History Survey, 1983.

WGNHS, 2004. Landscapes of Wisconsin, Wisconsin Geological and Natural History Survey, 2004.

WGNHS, 2009. Karst and Shallow Carbonate Bedrock in Wisconsin, Wisconsin Geological and Natural History Survey, 2009.

Wheeler, R.L., 2003. Earthquakes of the Central United States, 1795-2002 – Construction of the earthquake catalog for an outreach map, Open-File Report 03-232, U.S. Geological Survey, 2003.

Wheeler, R.L., Omdahl, E.M., Dart, R.L., Wilkerson, G.D., and Bradford, R.H., 2003. Earthquakes in the Central United States —1699–2002, Geologic Investigations Series I-2812, Version 1.0, 1 sheet, scale 1:250,000, U.S. Geological Survey, 2003.

Whitmeyer, S.J., and Karlstrom, K.E., 2007. Tectonic model for the Proterozoic growth of North America, doi: 10.1130/GES00055.1, Geosphere, 2007.

Wisconsin DNR, 2012. Wisconsin DNR WebView, Wisconsin Department of Natural Resources, Date accessed: April 13, 2012.

Witzke, B.J., Anderson, R.R., and Pope, J.P., 2010. Bedrock Geologic map of Iowa, Open File Map 2010-01, scale 1:500,000, Iowa Geological and Water Survey, 2010.